Exploring the fundamentals of solar photovoltaic technology and its modelling

Chapter · January 2016

CITATIONS
8

READS
333

4 authors:

Amevi Acakpovi
Accra Technical University
105 PUBLICATIONS **501** CITATIONS
SEE PROFILE

Mathias Michael
Accra Technical University
12 PUBLICATIONS **92** CITATIONS
SEE PROFILE

Nana Yaw Asabere
Accra Technical University
61 PUBLICATIONS **712** CITATIONS
SEE PROFILE

Japhet Honvo
2 PUBLICATIONS **8** CITATIONS
SEE PROFILE

Renewable Energy Systems

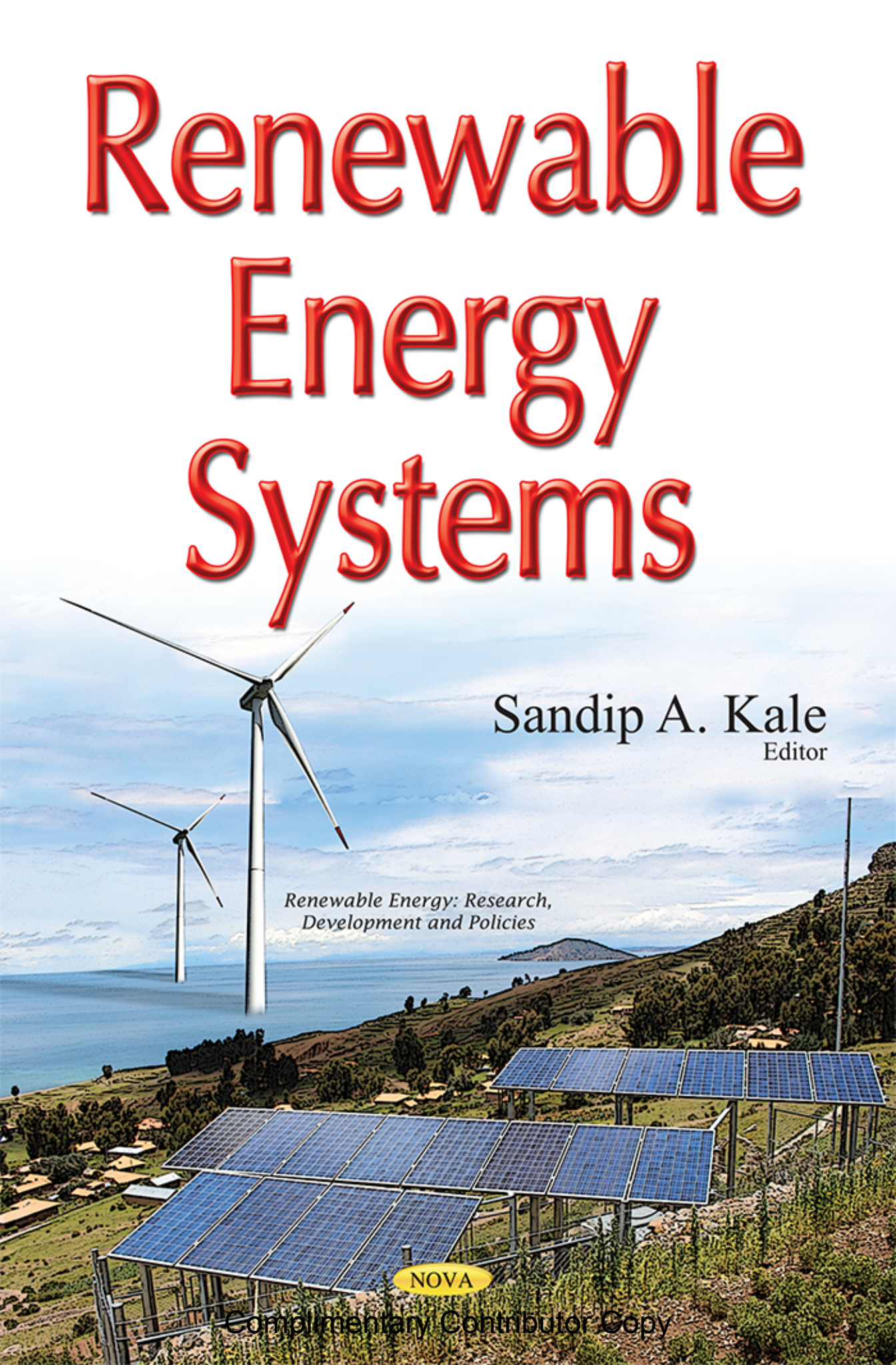

Sandip A. Kale
Editor

Renewable Energy: Research, Development and Policies

NOVA

RENEWABLE ENERGY SYSTEMS

RENEWABLE ENERGY: RESEARCH, DEVELOPMENT AND POLICIES

Additional books in this series can be found on Nova's website under the Series tab.

Additional e-books in this series can be found on Nova's website under the e-book tab.

RENEWABLE ENERGY: RESEARCH, DEVELOPMENT AND POLICIES

RENEWABLE ENERGY SYSTEMS

SANDIP A. KALE
EDITOR

nova publishers
New York

Library of Congress Cataloging-in-Publication Data

ISBN: 978-1-53610-441-7 (eBook)

Published by Nova Science Publishers, Inc. † New York

CONTENTS

Preface		**vii**
Chapter 1	Exploring the Fundamentals of Solar Photovoltaic Technology and its Modelling *Amevi Acakpovi, Mathias Bennet Michael, Nana Yaw Asabere and Japhet Honvo*	**1**
Chapter 2	Emerging Solar PV Technologies: A Paradigm Shift *Sarita Baghel and Nandini Sharma*	**39**
Chapter 3	Study of Performance Analysis of Modern Materials for Transparent Thin Film Solar Cells *Abhishek S. Oswal, Mahasidha R. Birajdar, Mohammed Hussien Rady and Sandip A. Kale*	**53**
Chapter 4	Performance Evaluation of a Domestic Passive Solar Food Dryer *Collins N. Nwaokocha, Oguntola J. Alamu, Olayinka Adunola, Solomon O. Giwa and Adeyemi A. Adeala*	**67**
Chapter 5	Different Techniques for Prediction of Wind Power Generation *Azim Heydari and Farshid Keynia*	**85**
Chapter 6	Performance Evaluation of Wind Farm Clusters –A Methodological Approach *D. G. Rajakumar, N. Nagesha and M. C. Mallikarjune Gowda*	**101**
Chapter 7	Dynamic Analysis of a Weak Grid Supplied from Diesel and Wind Generator *A. N. Safacas and E. C. Tsimplostephanakis*	**115**
Chapter 8	Structural Analysis of Multistorey Vertical Axis Wind Turbine Using Finite Element Method *Abhijeet M. Malge and Prashant M. Pawar*	**147**
Chapter 9	Physical Properties of Biodiesel: Density and Viscosity *Narayan Gaonkar and R. G. Vaidya*	**163**

Chapter 10 Investigation on a Low Heat Rejection Engine Using Neem Kernel Oil and Its Methyl Ester as Fuel **181**
Basavaraj M. Shrigiri, Omprakash D. Hebbal and K. Hema Chandra Reddy

Chapter 11 Renewable Energy Conversion and Waste Heat Recovery Using Organic Rankine Cycles **195**
Alberto Benato, Anna Stoppato and Alberto Mirandola

Chapter 12 Renewable Energy Technologies in Nigeria: Challenges and Opportunities for Sustainable Development **225**
Sunday O. Oyedepo and Philip.O. Babalola

About the Editor **259**

Index **261**

PREFACE

Renewable energy is contributing significantly to fulfill the continuously increasing energy demand of the world due to huge technological developments in order to make human life more prosperous and sustainable. The renewable energy sector has become an integral source of energy production in many countries. Research in the field of renewable energy has to play a vital role if the potential of renewable energy is to be fully exploited. Efficient and cost-competitive systems, durability, power control, effective performance measurement systems are expected from researchers and scientists. Solar, wind and bio energy are the majorly contributing renewable energy sources and uncompromisingly moving towards mature stage in order to build surety of power for the future. This book is intended to explore some recent developments in the field of these renewable energy sources. This book comprises of twelve chapters authored by authors from nine countries.

Solar energy is the basic source of renewable energy and has huge potential to meet the energy demand of the world. First four chapters are on solar energy. Solar photovoltaic emerges as the most widely used technology to harness sunlight. The first chapter presents the basic concepts of solar energy and photovoltaic cells, modules, array with their characteristics and provides a technique for modeling PV cell operation under Matlab/Simulink. For decades crystalline silicon based solar cells have dominated the PV market. The second chapter presents various aspects of perovskites, multi-junction concentrator photovoltaic, quantum dot photovoltaic and grapheme as an alternative to conventional silicon based solar cells. The material of a transparent thin film is reasonably important to achieve better performance. The recent transparent thin film materials such as Ga-doped ZnO thin film, W-doped In2O3 thin film, ZnMgO/ITO multilayer thin film and CdTe thin film are studied and their performance is compared in the third chapter. In addition to solar PV, solar thermal energy is also preferred in many developing countries for various applications. The next chapter deals with development and performance evaluation of a domestic passive solar food dryer.

Wind energy is another main grown-up renewable energy source. Next four chapters are dedicated to wind energy. Two new methods: MGDM neural network combined with a Particle Swarm Optimization algorithm and MGDM neural network combined with Genetics Algorithm are used to predict wind power are presented in the fifth chapter. Subsequently, next chapter includes a methodological approach for performance evaluation of wind farm clusters. In chapter seven a detailed analysis of the dynamic behavior of a weak hybrid power system supplied by a diesel and a wind generator is presented. The last chapter on the wind

energy presents a structural analysis of multi-storey vertical axis wind turbine using finite element method.

Chapter number nine is an informative chapter presents characteristic physical properties such as density and viscosity of biodiesels. The models and equations which describe the variation of density and viscosity of biodiesel as a function of temperature and blend percent are reviewed in this chapter. Tenth chapter has investigated performance of a low heat rejection engine using neem kernel oil and its methyl ester as fuel.

Eleventh chapter presents a renewable energy conversion and waste heat recovery using organic Rankine cycles. Last chapter presents various challenges and opportunities for sustainable development for implementation of renewable energy technologies in Nigeria.

I envision the use of this book for the researchers and students engaged in the field of renewable energy. I am thankful to authors for contributing in this book and reviewers for valuable reviews and suggestions.

Sandip A. Kale
Editor

In: Renewable Energy Systems
Editor: Sandip A. Kale
ISBN: 978-1-53610-423-3

Chapter 1

EXPLORING THE FUNDAMENTALS OF SOLAR PHOTOVOLTAIC TECHNOLOGY AND ITS MODELLING

Amevi Acakpovi[1,*], Mathias Bennet Michael[2], Nana Yaw Asabere[3] and Japhet Honvo[4]

[1,2]Electrical/Electronic Engineering Department, Accra Polytechnic, Accra, Ghana
[3]Computer Science Department, Accra Polytechnic, Accra, Ghana
[4]Department of Electrical Engineering, Polytechnic Montreal, Montreal, Canada

ABSTRACT

Despite the progressive adoption of solar technology as a reliable alternative power supply, there is a lack of expertise in handling solar systems installation and even understanding the basic concepts on the operation of solar photovoltaic technology. This chapter presents the basic concepts of solar energy and the availability of the solar resource; it also describes the concept of PV cells, modules, array with their characteristics and provides a technique for modelling PV cell operation under Matlab/Simulink. Furthermore, the chapter explains essential parameters to consider when selecting a PV module for a specific application. This chapter demystifies the myth on solar photovoltaic technology and provides all needed information on the basics of solar technology and its modelling in a very simple manner.

Keywords: photovoltaic, PV cell module and array, PV cell modelling, characteristics of PV modules

* Corresponding Author E-mail: acakpovia@gmail.com.

1. INTRODUCTION

Understanding the basis of photovoltaic (PV) systems is necessary for their acceptance, integration and adoption in developing countries. The low integration of PV systems in Africa can account for the major power crisis the African region is currently suffering. It is known that Sub-Saharan Africa faces chronic power supply problems which are related to aging plants with low maintenance and also over-reliance on hydropower plants(International Bank for Reconstruction and Development and The World Bank, 2010). It is estimated that the total generation capacity of 48 Sub-Saharan countries is 68 gigawatts which is barely lower than Spain's generation capacity (World Bank, 2008). More than 30 African countries are currently experiencing power shortages that hinder economic growth(International Renewable Energy Agency, 2012). It is however amazing to realize the inexhaustible potential of solar that exists in Africa. In Germany for instance, a total of 38.5 TWh of energy was generated in 2015 and this contributes to 7.5% of Germany's net electricity consumption (Wirth, 2016).

There is a total lack of awareness on the generation capacity and benefits that follow the installation of solar plants in Africa. Even though, few countries are now investing in solar PV technology, the basic concepts underpinning the wide use and maintenance of solar PV technology remains unrevealed to many. The integration of solar PV in new buildings in Ghana for instance is still not totally embraced despite the power shortages due to reliance on National Grid. There are deficiencies in technical skills needed to design and install PV systems and this is due to lack of institutions running curricula on PV systems.

With regard to all the problems listed above, this chapter is written to raise awareness on the basics of PV solar systems. It presents the solar resource available on our planet and a definition of common terms used in solar engineering. It is helpful for a beginner engineer or a layman who wants to understand how solar PV system work, how to select solar modules for specific applications and interpret clear solar module datasheets. It also provides an interesting approach for researchers in modelling the behaviour of a PV cell both analytically and by simulation. It is a rich material that actually responds to most questions asked on PV systems in general. This chapter is not a complete training manual that makes one a designer or technician of PV systems. It is still important to undertake a full training for one to qualify as a PV systems Engineer.

2. BASICS OF SOLAR ENERGY

The solar energy available on earth is very abundant and inexhaustible but very limited portion of this energy is actually used. The reasons may be related to lack of adequate technology to exploit the solar energy with high efficiency. Despite the drive to increase the conversion efficiency of solar energy added to advancement in nanotechnology, average conversion efficiencies are still clustered around 20 to 27%. Therefore, how solar energy is estimated and converted? This section provides some essential basics of solar energy including solar radiation and its data, irradiance, irradiation, sun path diagram, sun location determination, tilting of solar module and determination of magnetic North and true North.

2.1. Solar Radiation

Among the existing sources of energy available, the sun is seen as original source of all other forms of energy on our planet. Sun radiations can be received directly on earth and used in various forms. Additionally, sun radiations can be converted into other forms of energy including wind energy, coal and oil to mention few (Stapleton and Neill, 2012). The energy generated by the sun can be explained by a nuclear fusion, a reaction in which two or more atomic nuclei collide to produce one or more different atomic nuclei and subatomic particles which can be neutrons or protons. The energy generated from the fusion reaction is subsequently transferred to the solar system.

Sun energy is primarily emitted to the solar system as radiation. This radiation is emitted in many forms including high energy radiation such as microwaves, visible light and infrared (or heat energy) as shown in Figure 1 below. Solar power generation is mostly concerned with the visible part of the solar spectrum (Molleo, 2012).

Peeters (1979) asserted that a substantial amount of the solar radiation that arrives to the earth is reflected back due to clouds and gases. The reflected portion of the solar radiation back into space is known as the Albedo of the atmosphere (Figure 2).In other terms; Albedo signifies the level of reflectivity that occurs at the earth surface. Surfaces that may behave as mirror are likely to produce a high level of reflectivity and therefore an increasing albedo; these include ice, snow top etc. On the contrary, water can absorb the radiation better than ice and is also less reflective. Consequently, vast waters like oceans and rivers that are not dominated by ice absorb more solar radiation.

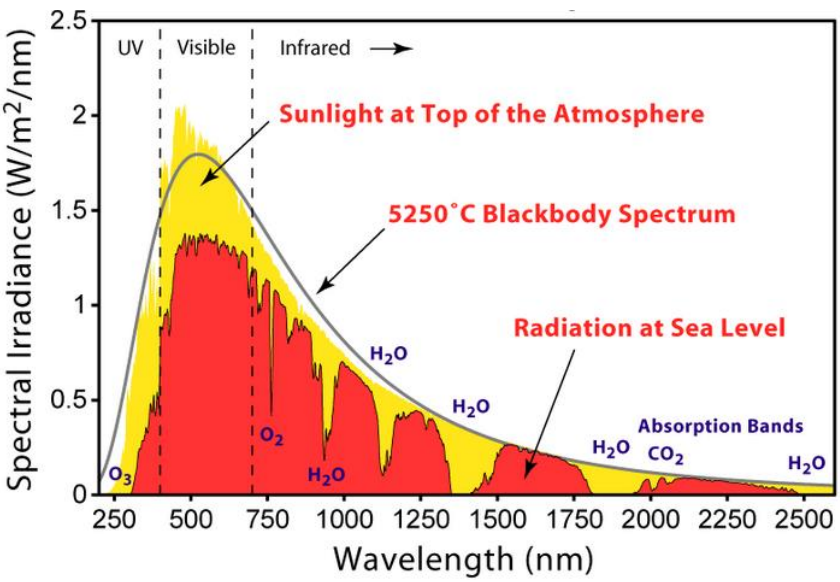

Figure 1. Solar Radiation Spectrum on Earth. (American Society for Testing and Materials (ASTM) Terrestrial Reference Spectra, 2013).

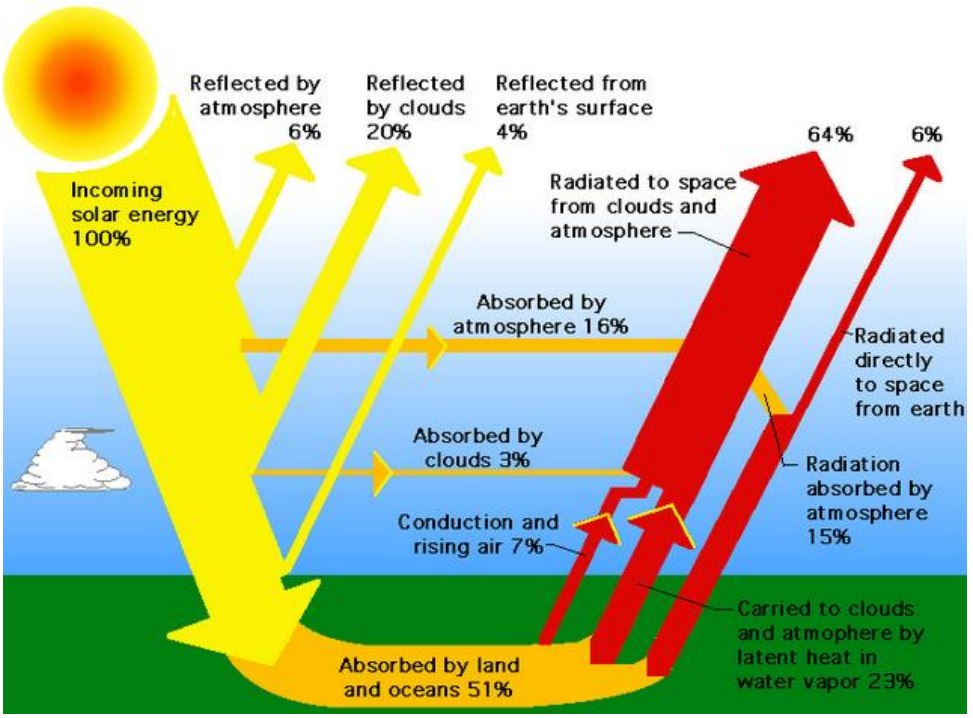

Figure 2. Earth Energy Budget(Earth's Energy Budget).

As depicted in Figure 2, the incoming solar radiation that reaches the Earth's atmosphere is divided into two categories. One, that passes directly through the planet's surface, known as direct radiation and the second one that is scattered or absorbed and re-emitted within the atmosphere. This scattered radiation is known as diffuse radiation and is not usually as intense as direct radiation. For instance, on a sunny day diffuse radiations will contribute only 10% of visible light.

As a result of the atmosphere's effects in scattering and absorbing radiation, the greater the amount of atmosphere that the radiation needs to go through to reach the earth, the lower the level of solar radiation may become at the surface of the Earth.

The spectral composition of the radiation reaching the Earth is slightly altered by the gases through which it passes. In particular, water and CO_2in the atmosphere almost completely absorb some wavelength. One indication of the relative distance that radiation must travel through in the atmosphere to reach a given location is the air mass. The air mass, mostly noted AM, is defined as,

$$AM = \frac{1}{\cos(\theta)} \tag{1}$$

where, θ represents the angle illustrated in Figure 3 below. Beyond the earth's atmosphere, the air mass is referred to as air mass zero (AM=0). AM 1 corresponds to the sun being directly overhead.

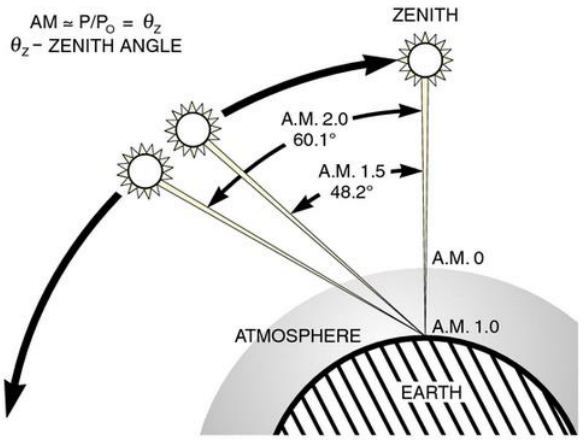

Figure 3. Examples of how Air Mass is calculated(Iqbal, 1983).

The *photovoltaic effect* is the generation of electrical energy in the form of voltage or current in a material that is exposed to light and it can be classified as a physical and chemical phenomenon. Solar panels also called solar modules are made of silicon in wafers, cells using a multi-layered deposition method. The silicon is electrically set up to allow the photo-electric effect to produce electricity. Solar modules are often referred to generically as 'PV' (i.e., photovoltaic).

The Standard Test Conditions, known as STC are conditions under which solar module outputs are rated. STC is defined by the following:

Air Mass = 1.5
Solar Radiation =1000w/m^2
Cell Temperature = 25^{o}C

Remark: Cell temperature does not refer to ambient temperature.

2.2. Solar Radiation Data

One important aspect of solar energy is to effectively use the solar radiation data from the area where the solar system will be installed. In Ghana, radiation data is available from the Ghana meteorological Agency (http:/www.meteo.gov.gh) or it might be supplied by the solar module supplier. The National Aeronautical Space Administration (NASA) in the USA also provides world-wide data on the web: available from the following web site: http://eosweb.larc.nasa.gov/sse/. Ganoe et al.(2014) described the RETScreenPlus Software, developed by Ministry of Energy in Canada as "a Windows-based energy management software tool that allows project owners to easily verify the ongoing energy performance of their facilities". The RETScreenPlus Software provides comprehensive and effective data on renewable energies that are used worldwide for renewable energy design. Some important data include wind speed, altitude, latitude, solar radiation, average temperature etc. An extract of data from the RETScreen software is presented in Figure 4 below.

Country - region		Ghana		
Province / State				
Climate data location	*See map*	Tema		
Latitude		°N	5.6	
Longitude		°E	0.0	**Source**
Elevation		m	15	NASA
Heating design temperature		°C	22.2	NASA
Cooling design temperature		°C	28.8	NASA
Earth temperature amplitude		°C	5.4	NASA

Month	Air temperature	Relative humidity	Daily solar radiation - horizontal	Atmospheric pressure	Wind speed	Earth temperature	Heating degree-days 18 °C	Cooling degree-days 10 °C
	°C	%	kWh/m²/d	kPa	m/s	°C	°C-d	°C-d
January	26.1	76.1%	5.78	100.5	2.9	28.0	0	500
February	26.4	78.4%	6.09	100.4	3.2	28.3	0	460
March	26.5	82.3%	5.94	100.4	3.2	28.3	0	510
April	26.6	83.5%	5.72	100.4	2.8	28.3	0	497
May	26.5	83.9%	5.32	100.5	2.5	28.1	0	511
June	25.7	83.1%	4.71	100.7	2.6	26.8	0	470
July	24.6	82.6%	5.20	100.8	3.5	25.3	0	451
August	24.2	82.8%	5.31	100.8	3.7	24.9	0	441

Figure 4. RETScreen Plus Data Provided for the Location Tema-Ghana. (RETScreenPlus Software, 2013).

Solar radiation tables are often developed based on the measurement or direct and diffuse irradiation each hour, recorded as hourly irradiation (W/m^2,giving the total daily irradiation (kWh/m^2 or MJ/m^2). The sun of direct and diffuse irradiation gives global irradiation, which is then used to calculate the Peak Sun Hours(PSH) as detailed above.

There will be variations in the available irradiation directly related to the tilt angle of the solar array. However, due to Kenya's location on the equator, tilting the panel to the latitude will have a minimal impact on the yield of the panels. It is recommended that the panels be tilted 15^o south in order to facilitate self-cleaning. Figure 5 below shows the distribution of solar irradiation pattern in Ghana.

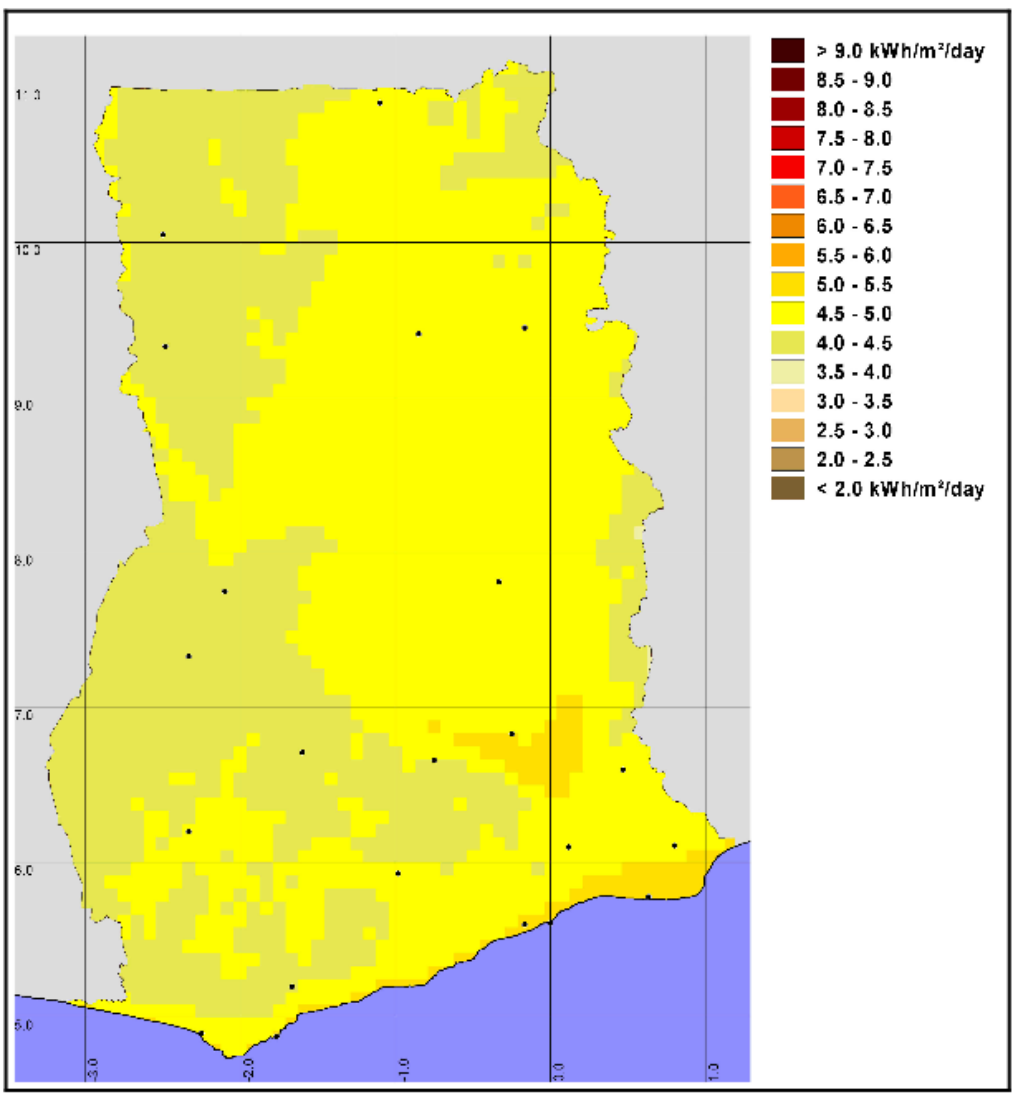

Figure 5. Solar Irradiation Map in Ghana(Schillings et. al., 2004).

2.3. Irradiance

The received energy from the Sun per unit area is called irradiance. Irradiance is manifested as electromagnetic radiation for measurable wavelength that falls on a unit area. Irradiance is measured by considering an orthogonality to sun radiations and the measurement may be done in space or at the surface of the Earth's after scattering and atmospheric absorption (Greg, 2016). Sun's energy reaches the earth's atmosphere at a peak value of 1.367kW/m^2; this is recognized as the solar constant (Basu, 2001). As discussed previously, this energy decreases as it passes through the atmosphere reaching approximately 1kW/m^2 at the sea level. The amount of solar power available per unit area is known as irradiance. Solar parameters are summarized in Table 1 below.

Table 1. Summary of solar parameters

Parameter	Symbol	Quantity and Unit
Irradiance	G	kW/m^2, W/m^2
Solar constant	Gsc	1.367 kW/m^2, 1,367W/m^2
Peak value at sea level	Go	1.0 kW/m^2, 1,000W/m^2
Nominal Value	-	0.8 kW/m^2, 800W/m^2

Irradiance is measured by a device called pyrometer or by using a reference cell (high quality).

2.4. Irradiation and Peak Sun Hours

The total amount of radiant solar energy received per unit area for a given period of time is defined as Irradiation. It can be estimated on daily, monthly or annually basis. Energy is expressed in Joules (J). It is also expressed in terms of Mega Joules (MJ) especially for big quantity of energy. The conversion factor from solar energy to irradiation (kWh: kilowatt-hours) is:

$$1\,kWh = 3.6MJ \tag{2}$$

$$1\,MJ = \frac{1}{3.6}MJ \tag{3}$$

Daily irradiation is commonly called daily Peak Sun Hours (PSH). Boxwell (2012) defines "peak sun hours" as the solar insolation received by a particular location with the assumption that the sun irradiation is at its apex for some hours. More precisely, the number of daily PSH consists of the number of hours for which a power rate of 1kW/m^2, would produce an equal amount of energy to the total energy originally received for that day.

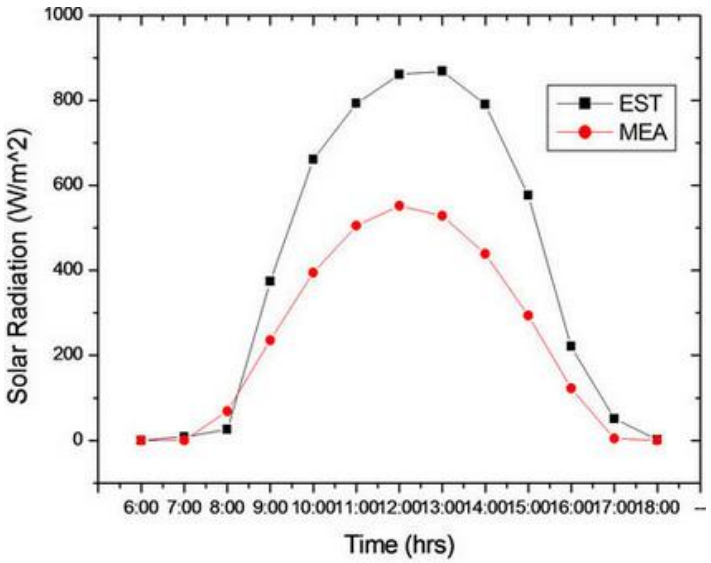

Figure 6. Schematic representation of Peak Sun Hours.

Assuming the solar radiation on a horizontal surface is 30 MJ/m^2 for a day and we want to determine the number of PSH. We first need to convert MJ to kWh.

This means that 30MJ/m^2 would be equal to:

$$30 \cdot \frac{MJ}{m^2} \times \frac{1kWh}{3.6MJ} = 8.33kWh/m^2 \tag{4}$$

The PSH of 8.33 means a sun radiation of 1kW/m^2 falling on the selected site for a duration of 8.33 hours which is equivalent to the accrued energy in the day with varying irradiation at the same site. Figure 6 shows a typical variation of irradiation through a day.

2.5. Sunpath Diagram

Sun paths at any latitude and any time of the year can be determined from a two-dimensional surface in a sunpath diagram (Figure 7 and 8). This diagram can be used to determine the position of the sun at any time of the day and for any day in the year. Two different projections are used to locate the position of the sun: cylindrical projection and polar projection. The most usual form used in the industry is the polar projection known as the stereographic projection. The stereographic projection implies a projection of a sphere onto a plane. This type of projection covers the entire sphere, at the exception of one point, i.e., the projection point.

The sunpath diagram is composed of:

- The azimuth angles that are represented on the circumference of the diagram. In some diagrams it is marked showing 0^o to 360^o relative to TRUE NORTH while in other diagrams just the four compass directions.

- The altitude angles, represented by concentric circles;
- Sunpath lines from east to west for different dates in the year;
- Time of the lines crossing the sun path lines;
- Location information that refers to latitude.

Sunpath diagrams can be used to calculate the amount of shading at a particular site, and also the time of year that this shading will occur.

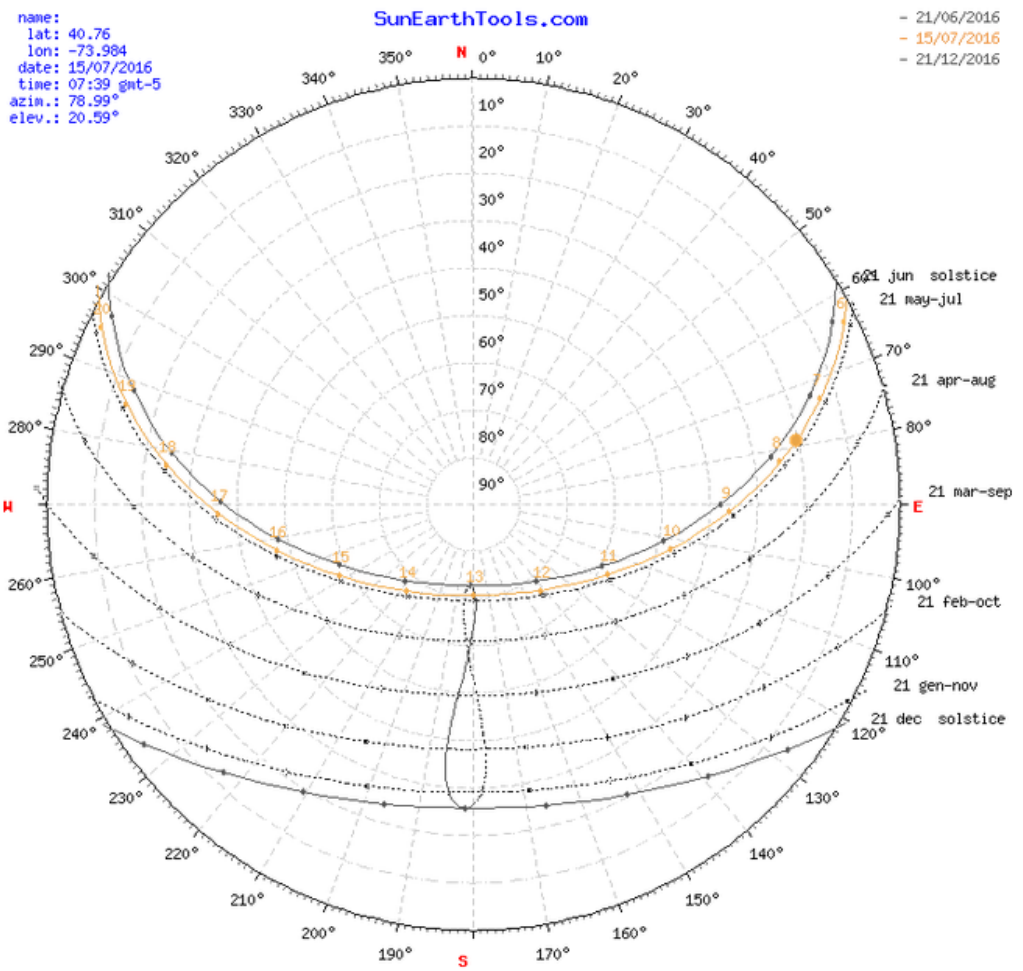

Figure 7. Example of a sunpath diagram (Mahdavinejad et al., 2014).

2.6. Determination of Sun Location

The Sun location can be accurately determined with the knowledge of two angles:

- Altitude (Y) the angle between the sun and the horizon (in degrees).

- Azimuth (α) the angle between north and the sun's position. Similar to using a compass where the direction being faced is measured as a number of degrees from North. The altitude and azimuth of the sun are constantly changing throughout the day and year as the Earth rotates on its axis (day/night).

a. Altitude

The angle between the sun and horizontal (or ground) is referred to as altitude and is always an angle between 0◦and 90◦. The sun is higher in the sky in periods of equinox and lower in the sky during solstice periods due to the natural angle between the Earth and the sun as the Earth orbits the sun throughout the year.

b. Azimuth

The sun moves from East to West across the sky through the day. The angle between North and the point of the compass where the sun is positioned is called the azimuth angle. In general, the azimuth is measured clockwise going from 0◦ (true North) to 359◦. East is 90◦, south is 180◦ and west is 270◦. Azimuth and altitude are important for describing where the sun is in the sky, and to help ensure that the PV array is installed so it can produce as much electricity as possible. In the diagram below (Figure 9), altitude and azimuth are shown along with the points of the compass.

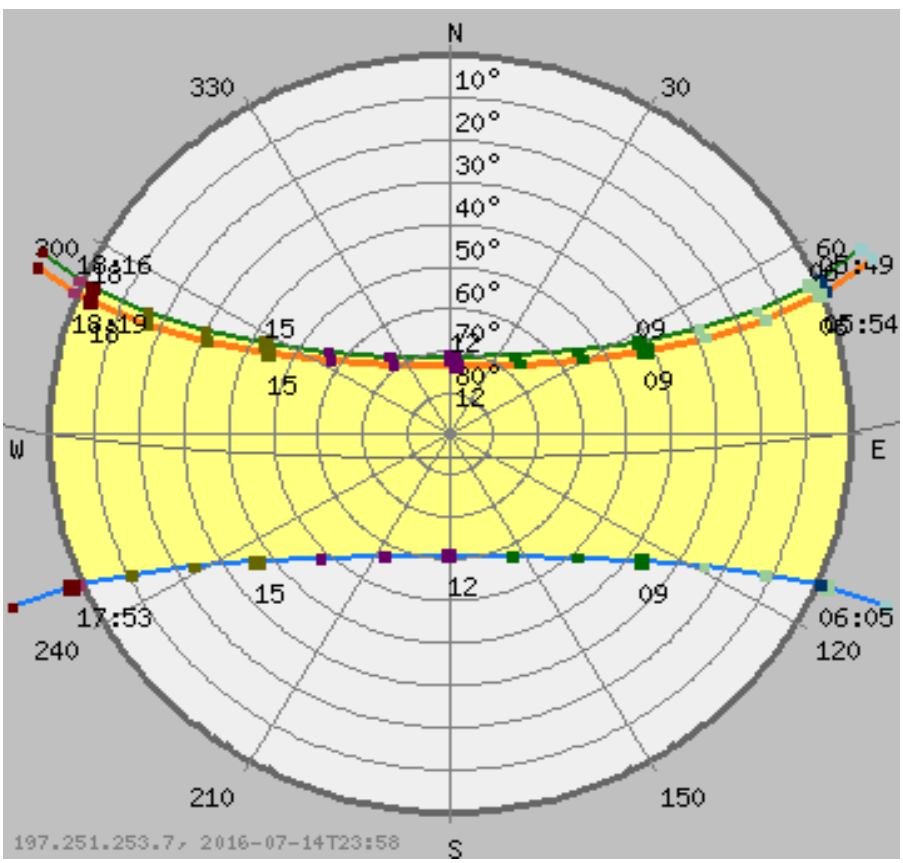

Figure 8. Example of a sunpath diagram (GAISMA).

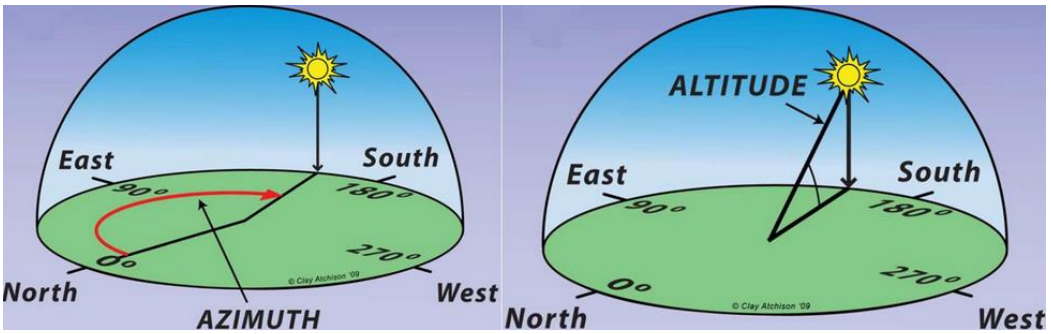

Figure 9. Altitude and Azimuth Angles (Atchison, 2015).

c. Solar Altitude

As a consequence of the earth rotating around the sun as illustrated in Figure 10, the sun appears to move between the Tropic of Capricorn (25.45°s) in the southern Hemisphere. When the sun is over either of the tropics, it is known as solstice and when the sun is over the equator is known as equinox.

The sun reaches the Tropic of cancer at the northern solstice (June 21st) and the Tropic of Capricorn at the southern solstice (December 22nd). The sun crosses the equator at the equinoxes in March 21st and September 23rd, this means that the altitude of the sun at solar noon varies a total of 64.9◦ during the calendar year. The formula for calculating the altitude of the sun when it is over the equator for specified latitude is:

$$\gamma^t = 90^o - latitude\left(\deg rees\right) \tag{5}$$

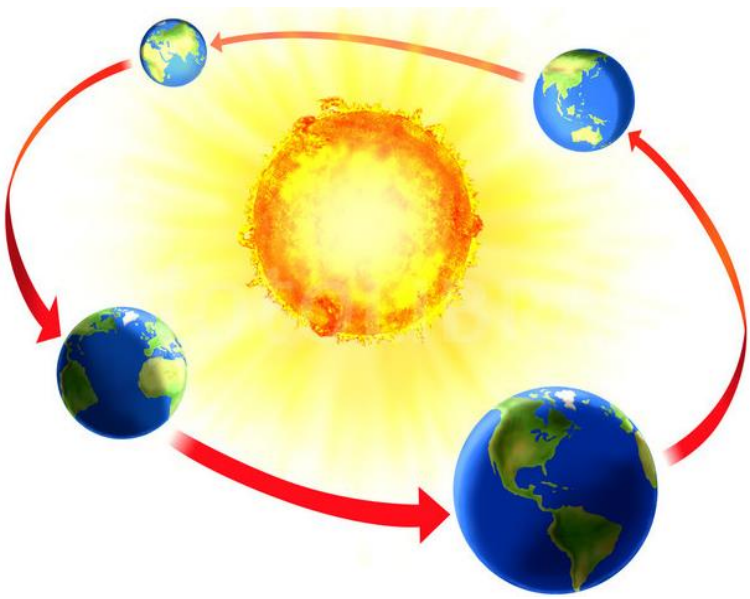

Figure 10. Earth rotation around the Sun(Earth orbit around the sun).

The formula for calculating the altitude of the sun when it is over the tropics i.e., either the tropic of cancer or the tropic of Capricorn is given below.

$$\gamma^t = 90^o - latitude(\deg rees) \pm 23.45 \quad (6)$$

Whether to use the + or – is dependent on the hemisphere (northern or southern) where you are located and over which "tropic" (either Cancer or Capricorn) you want to determine the sun's altitude. When applying this formula it is assumed that you are facing the equator, for example, facing South in the Northern Hemisphere.

As a rule of thumb, when the latitude is in the same hemisphere as the tropic you add 23.45◦ and when the latitude is in the opposite hemisphere as the tropic yousubtract23.45◦. For instance, a location is at 5.3◦N. therefore the latitude of the sun when it is over the tropic and the equator is as follows:

Equator (March 21st and September 23rd)

$$\gamma^t = 90^o - latitude(\deg rees) = 90 - 5.3 = 84.7^o$$

Tropic of Capricorn (December 22nd)

$$\gamma^t = 90^o - latitude(\deg rees) - 23.45 = 90 - 5.3 - 23.45 = 61.25^o$$

Tropic of Cancer (June 22nd)

$$\gamma^t = 90^o - latitude(\deg rees) + 23.45 = 90 - 5.3 - 23.45 = 61.25^o$$

The altitude of the sun should be expressed as a number below 90◦, and therefore it should be 71.85◦ (180◦ - 108.15◦) facing south in this case.

The importance of knowing the sun's actual position in the sky can be related to the positioning of solar modules because it is necessary to determine any obstacles that can shade the modules. Figure10 gives an example of the sun's position in the sky for Accra. In the tropics it is important to remember that the sun can be in both the Northern and the Southern skies as shown in Figure 11. For location on the equator, the sun spends an equal amount of time in both hemispheres. If you are in the tropics it is important to determine the amount of time, and at what time of the year, the sun is in the northern and southern directions. This is to ensure that objects like trees and building will not shade the solar modules.

Near the equator, the sun is in the southern part of the sky at solar noon during late September to mid-March. In Accra for example, for the period from late-March to late-September, the sun will actually be in the northern part of the sky. Therefore you will need to look for potential obstacles that could cause shading in both the southern and northern direction.

Table 2 provides information on altitude of the sun for various latitudes in the northern hemisphere tropics (i.e., Ghana). This table provides the altitude at the two solstices and also indicates when the sun is in the northern sky with respect to the latitude. This can help locate possible obstacles that will shade the modules at various times of the year.

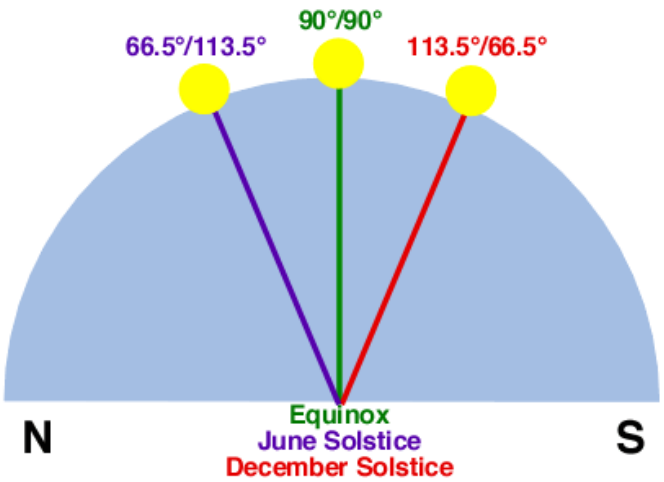

Figure 11. Solar Altitude for Accra at equinox and solstices (Petersen et al., 2015).

2.7. Tilting Solar Modules

The positioning of solar modules should be done in a way that the amount of radiation collected is as large as possible. To achieve this, when, the solar modules should be tilted at an angle to the horizontal (β deg) such that there is a 90◦ angle between the sun (at solar noon) and the solar module as shown in Figure 12.

To adjust a module perpendicularly in the direction of the sun continuously, a solar tracking system will be required. The tracking system actually tracks the sun rays and moves the solar panel to position them perpendicularly all the time. The only disadvantage is the fact that this system can be expensive. The usual solution is therefore to install the system at an angle which will provide the highest annual yield. The module should therefore be installed at an angle that is orthogonal to the sun radiations at solar noon. In other terms, the angle must be equal to the latitude of the site. To summarize, maximum annual energy yield can be obtained only if modules are tilted at an angle equal to the latitude of the site. However, due to Ghana's position near the equator a minimum of 10º tilt is recommended to allow for passive cleaning.

Table 2. Solar altitudes for different latitudes in the Northern Hemisphere

Latitude	Altitude of the sun at Solstices	
	22nd June	22nd December
5◦N	71.55◦N	61.55◦S
3◦N	69.55◦N	63.55◦S
1◦N	67.55◦N	65.55◦S
1◦S	65.55◦N	67.55◦S
3◦S	63.55◦N	69.55◦S
5◦S	61.55◦N	71.55◦S

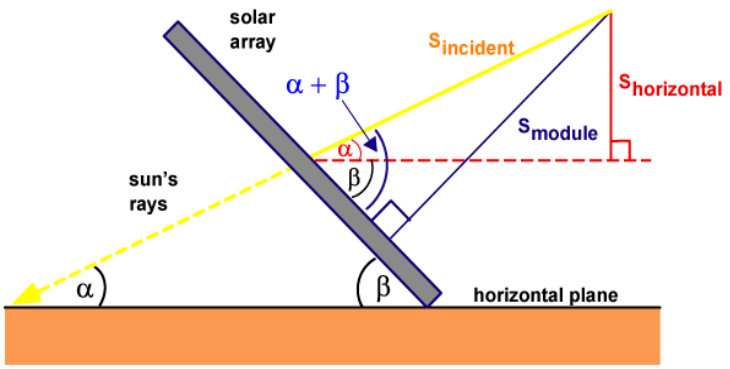

Figure 12. Location of solar module perpendicularly to Sun's radiation (Solar radiation on a tilted surface).

This does not take into account the influence of any shading (i.e., Building, trees etc.). Another way to calculate the ideal tilt is to use the altitude of the sun and the following formula:

$$Module\_Tilt(\beta) = 180^o - 90^o \pm altitude\_of\_sun \quad (7)$$

For instance if the average altitude of the sun in Tamale, (latitude 9.5) is 86◦N, the optimal module tilt at this location can be determined as follow

$$Module\_Tilt(\beta) = 180^o - 90^o - 86 = 4^o(North)$$

Hence the optimal tilt for a PV module in Tamale is 4◦ north. However, to maintain self-cleaning it should be tilted to 10º - 15 south.

In the tropics the sun can be either north or south of the solar module. Whether you point your solar module to the South or to the North is dependent on the exact latitude of the location. The closer to the equator you are, the more time the sun spends equally in both the northern and southern part of the sky. In general, installer in southern hemisphere will still point their modules north, while those in the northern hemisphere will point their modules south.

2.8. Magnetic North and True North

The existence of the earth's magnetic field explains the attraction exerted by the earth on any suspended magnet. The North end of a compass needle will deviate as a result of this attraction and the direction obtained is called Magnetic North. Solar modules must be placed in line with true North (or Geographic North), which indicates the direction between a point on the surface of the earth and the North Pole. Though magnetic and true north should in theory be the same direction, quite often, there is a difference between the two due to deviation in the magnetic flux lines at different places on earth. Figure 13 provides an illustration.

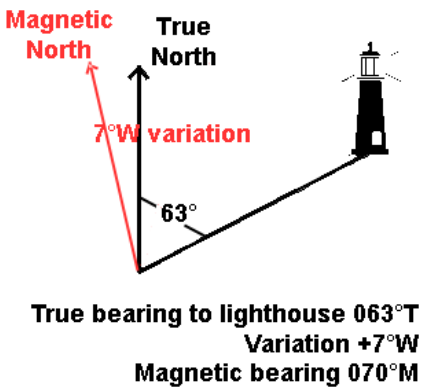

Figure 13. True North, Magnetic North and Magnetic Deviation(Navigation on chart work).

For example, in Accra the magnetic deviation is approximately 3ºWest. That means that True North is approximately 3ºWest of the compass north. Other examples are Kumasi, 4.49º W. Tamale, 3.1º W, Takoradi 4º W etc. However, any deviation has the potential to affect the annual system yield if not taken into account. Always take into account magnetic deviation when possible.

3. Solar Electricity

Energy generated from the sun through photovoltaic effect is in the form of electricity and is subjected to normal laws of electric circuits. Hence, it is important to understand the effect of putting together PV modules either in series or in parallel or a combination of both.

3.1. Series Circuits

An electric circuit is simply defined as the current path from one potential to another. A series circuit is described as an electric circuit in which an identical current flows in succession through all the components. In Figure 14, resistors R1 and R2 are in series with the photovoltaic (PV) module (power source).

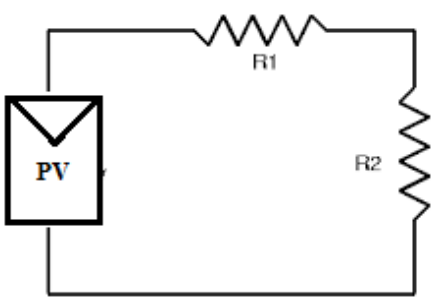

Figure 14. Electrical components connected in Series.

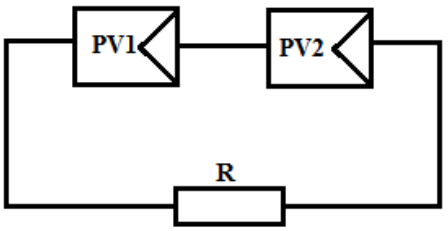

Figure 15. PV Modules n Series.

In a series circuit, current follows only one path and therefore the current will be the same in all parts of the circuit. This current will be opposed by all the individual components in the path (i.e., R1 and R2), such that the total resistance R_T is:

$$R_T = R_1 + R_2 \tag{8}$$

The total voltage V_T applied to a series circuit will be shared proportionally by all the components, V_1 and V_2.

$$V_T = V_1 + V_2 \tag{9}$$

For instance if the PV module in Figure 15 is producing 12 volts, the voltage across the two resistors is determined as follows:

a. If $R_1 = R_2$, then the voltage across R_1&R_2 will be equal at 6volts each
b. If $R_1 = 2 \times R_2$, then the voltages would be 4 volts across R_2 and 8 volts across R_1.
c. To clarify this, assume R_1 = 4 Ohms and therefore the current, I, would be 12V/(4+2) = 2Amps. So the voltage across R_1 is 2A×4Ω= 8V while for R_2, it is 2A×2Ω = 4V.

In Figure 15, the power sources, V_1 and V_2 are two PV modules (PV_1 and PV_2) connected in series with a resistor R.

In this case, the voltages of the individual PV modules will combine to obtain a total voltage V_T.

3.2. Parallel Circuits

A parallel circuit is a circuit made of many components connected across the same voltage source. Each parallel component forms an individual ‘branch’, and although each branch will have the same voltage applied, but the current in each branch may differ according to the impedance of the branch.

The total current flow, I_T, in the circuit shown in Figure 16 is equal to the sum of individual currents $I_1$and I_2 flowing in each parallel branch; nevertheless, the voltage V is the same across all branches. If we provide multiple energy sources in parallel, such as solar

modules, and assuming that they are all the same voltage, the potential difference remains constant, but the current capability is equal the sum of the individual suppliers, i.e.,

$$V_T = V_1 = V_2 \tag{10}$$

$$I_T = I_1 + I_2 \tag{11}$$

If we continue to add modules in parallel, the voltage will remain constant but the current capability of the complete array will continue to increase.

3.3. Combination of Series and Parallel Circuits

Solar modules are made up of several combinations of solar cells in series and parallel. Solar modules can also be arranged in series and parallel to obtain desired voltage and current suitable for specific applications. A combination of modules in series or parallel is known as solar array as illustrated in Figure 17.

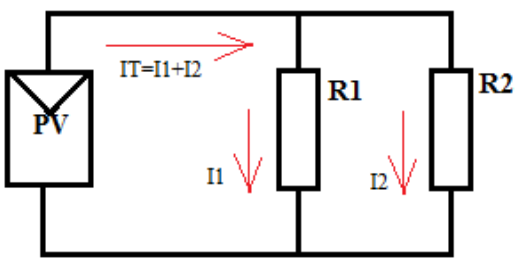

Figure 16. A parallel circuit.

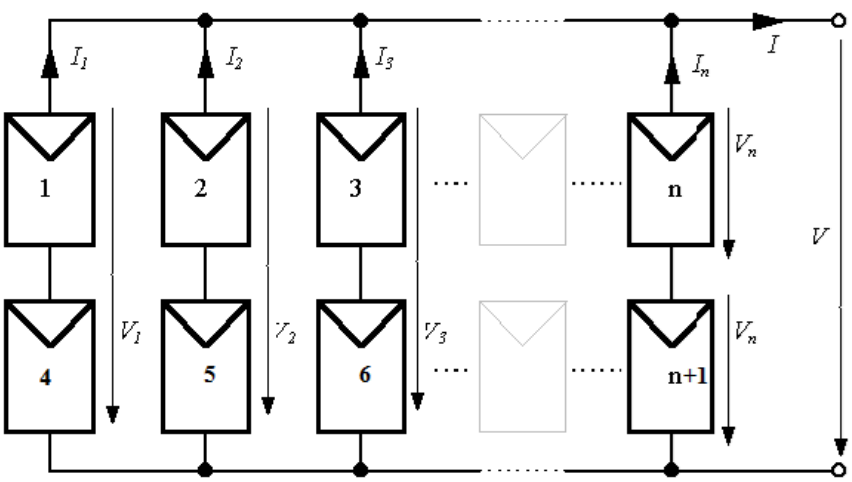

Figure 17. A solar array with PV modules in series and parallel.

3.4. Remarks I

- When solar modules are placed in series, the voltages add together whereas the current remains the same. The equivalent current of a number of modules put in series also known as string is the same as the current of the module producing the least current of the modules that are in series.
- Similarly**,** when the solar modules are placed in parallel, the array voltage stays the same and is equal to the average output voltage of the parallel modules. The current in the parallel modules' circuit is additive: the sum of the output currents of the parallel modules.

4. PHOTOVOLTAIC CELL, MODULE AND ARRAY

The PV module is the core component for a PV system. Understanding how a module is designed, manufactured and assembled provides a key insight into the design of real systems. This section provides a description of PV cell, PV module and PV array with their essential parameters as well as the STC and Nominal Operating Cell Temperature for solar modules (NOCT).

4.1. PV Cells

The characteristics of a solar cell, how they work, in addition to PV module and array are presented below.

a. Characteristics of a Solar Cell

A solar cell is mainly characterized by two curves known as current-voltage characteristic and power-voltage characteristic. The first one informs the variations of the output current with respect to the output voltage. Figure 18 illustrates the characteristics of a solar cell**.** When light is shown on the solar cell, electrons can be released through photovoltaic effect and will become mobile, implying the existence of an electric current. It is also important to observe that both the output current and voltage of the solar cell change with respect to the variations of the load.

The maximum current produced by a solar panel can be obtained when the panel or module is shorted meaning the positive and negative probes are connected together. The resulting current is denoted Short Circuit Current and is abbreviated as I_{SC}. It is however important to note that when the cell is shorted the voltage across its terminal is zero.

On the other hand, the maximum voltage is obtained when the circuit is opened meaning there is no close circuit between the positive and negative probes. The resulting voltage is called Open Circuit Voltage (Voc). It must also be noted that the resistance value of an open circuit is infinity and the current is zero since there is no close path for current to flow through.

At some point, the internal resistance of the solar cell will be equal to the resistance of the load. The maximum power will then be generated by the solar cell, and this is called the

Maximum Power Point(MPP). This maximum power is attained at the 'Knee' of the IV curve; where the current starts to decrease more rapidly (as shown in Figure 18). For each solar cell, there is an I-V curve, where Isc and Voc are illustrated to help characterize the cell.

4.2. Power Characteristic of a Solar Cell

The power characteristic is used in addition to the I-V curve to fully characterize a solar cell. The power generated by a solar cell is the product of the voltage and the current under some particular operating conditions.

$$P = V \times I \tag{12}$$

The power is zero when either the current or voltage is zero. This happens at I_{SC} (when Voltage = 0) and V_{OC} (when Current = 0). For every voltage along the I-V curve that a solar cell can produce, there can be only one corresponding current output. This means that the power generated by the PV module will also vary depending on what voltage the cell is operating.

By plotting power as a separate axis in relation to the I-V diagram below (Figure 18), the power variations between the two extremes can be clearly illustrated.

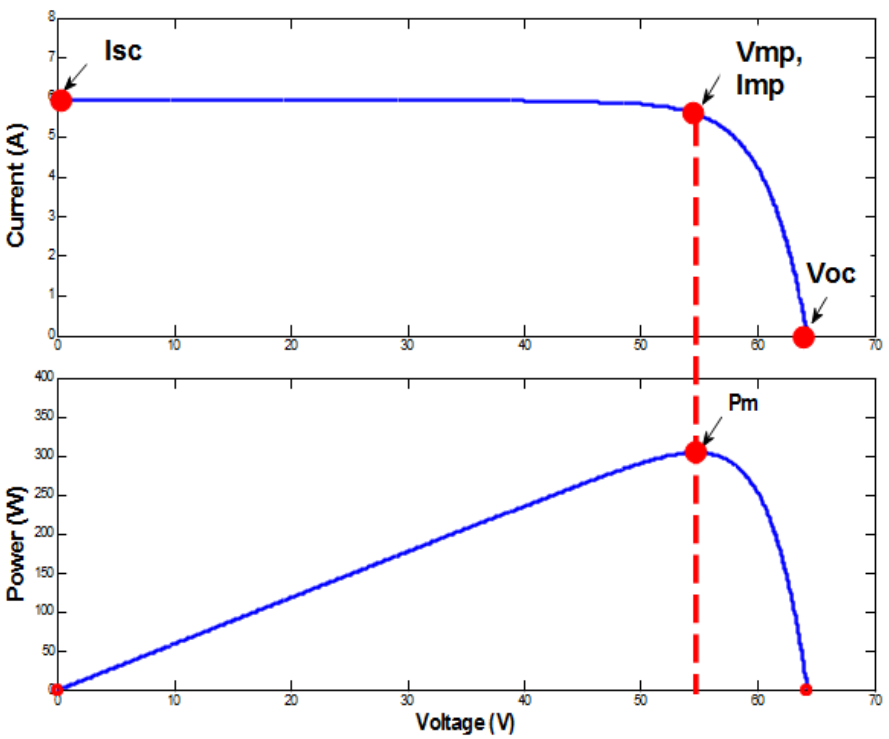

Figure 18. IV and Power curve of a solar cell.

The power generated by a solar cell will reach a maximum when the internal resistance of the cell is the same as the resistance of the load, and this is known as the maximum power point (MPP or Pmax). The current and voltage at this point are respectively referred to as I_{MP} (current at maximum power) and V_{MP} (voltage at maximum power). It is desirable to ensure that solar cells operate close to the maximum power point, so that the PV system has the highest possible output.

a. Fill Factor and Equivalent Solar Cell Circuit

The fill factor (FF) is a parameter used to indicate how 'square' the I-V curve is. It is a reflection of the amount of series resistance as compared to shunt resistance that exists in a solar cell and its circuit.

The fill factor is defined as the ratio of maximum power to the product of I_{SC} and V_{OC} and is an operating characteristic which indicates the performance of a cell (Molleo, 2012). Decreases in fill factor may indicate problems with the cell. The fill factor can be calculated as follows:

$$FF = \frac{I_{MP} \cdot V_{MP}}{I_{SC} \cdot V_{OC}} \tag{13}$$

$$FF = \frac{P_{MP}}{I_{SC} \cdot V_{OC}} \tag{14}$$

The fill factor of a solar cell is affected by parasitic resistances in the solar cell itself (such as resistance within the metallic contacts), which is known as the series resistance. A high value of series resistance implies a loss of power that is dissipated as heat, and therefore reducing the cell output power. The resistance across the solar cell junction is called the shunt resistance. Areas of the solar cell junction having low shunt resistance, may witness a leakage of current across the cell junction and therefore reducing the solar cell's output.

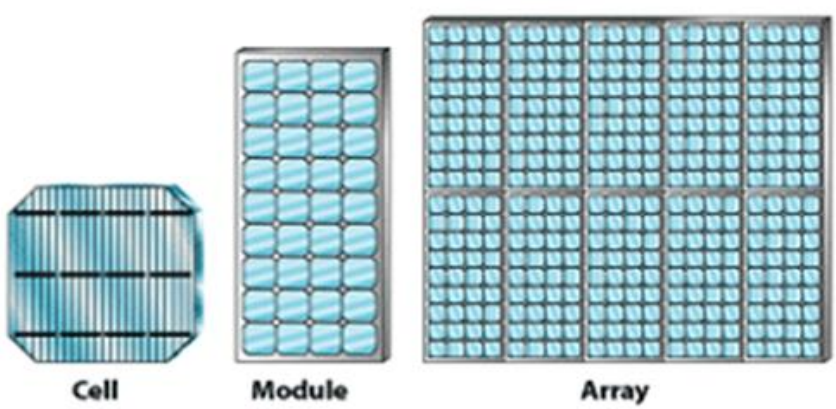

Figure 19. Module wired in series to make a string and string wired in parallel to make an array (US Department of Energy. http://mycommunitysolar.org/ucommunitysolar/images/Cell-Module-Array.png).

Typical fill factor values range between 0.6 and 0.7 and are always less than 1. For a cell that is reasonably efficient, the fill factor can be expected to be between 0.7 and 0.85. With poorer quality cells, the difference in voltage between V_{OC} and V_{MP} is greater, and hence the fill factor is reduced.

4.3. Modules and Arrays

As mentioned in the previous paragraph, a solar array or simply an array is a combination of many solar modules connected both in parallel or in series whereas a photovoltaic module itself is a combination of several photovoltaic cells put in both series and parallel. An array comprises of PV modules connected in a string (see Figure 19) and the strings are then connected in parallel, to form the array. It is important to note that some array may consist of a single string (i.e., in a typical 1kW grid-connect system).

The arrays are constructed with typical characteristics that may suit common loads; the load may be an inverter in a grid connected system, a battery or a DC appliance.

A PV cell produces about 0.5-0.6V open circuit under STC. The original solar module consisted of thirty (36) cells connected in series to form a module so that it produced sufficient voltage and current, at the expected operating temperature, to charge the battery bank.

Module manufacturers now produce higher output modules (called ‘large area’ modules) in response to the market for grid connected solar systems. The most common module voltage now is 24V DC nominal. These standard modules are used for both grid connect and battery charging applications.

4.4. STC and NOCT

STC are normally used to determine the specifications of manufacturers. This is necessary due to the fact that the performance of solar modules varies with conditions such as temperature and irradiance. It therefore corroborates that cells must be tested under the same standard conditions to determine and compare their performances. Under international standards, all modules are tested at the following standard test conditions:

- Cell Temperature 25^{o}C
- Irradiation of 1000W/m2
- Air Mass of 1.5

STC testing is useful in rating the power output of modules in order to compare different modules and modules are sold based on their power output measured at STC.

However, under normal operating temperature conditions, when the module is under full sun, especially in regions like West Africa, the temperature of the solar cell can be 25^{o}Cabove ambient temperature and therefore higher than the standard test cell temperature of 25^{o}C. For this reason it is essential to provide the nominal operating cell temperature, *NOCT*. This is the temperature of the cells within their modules under the following reference condition:

- Ambient air temperature 20ºC
- Irradiance of 800W/m2
- Wind Speed of 1m/s
- Electrically open circuit

The difference between the *NOCT* provided by the manufacturer, and the ambient temperature of 20ºC, can be used to estimate the actual cell temperature for the typical ambient temperature in the location where the module is located.

5. MODELLING OF A PHOTOVOLTAIC CELL

This section presents both an analytical and a simulation model on the operation of a PV cell, developed under Matlab, Simulink. Also the effects of temperature and irradiance on the operation of the cell have been clarified.

5.1. Analytical Modelling of Solar Cell Operation

According to (Acakpovi and Hagan, 2013), Figure 20 presents a general model of photovoltaic cell that illustrates a series a parallel resistance.

For purpose of modelling a solar module, it is assumed that a module will be made of Ns solar cells connected in series and Np solar cells connected in parallel. PV modules are made of many cells put in series to form strings and strings are equally put in parallel to achieve a desired level of voltage. By varying the number of cells in parallel and the number of cells in series, one can achieve a solar panel with preferred outputs mostly suitable for common applications. Assuming the total number of cells in series is Ns and the total number of cells in parallel is Np, the model of a module can be derived from Figure 21 as illustrated in Figure 22.

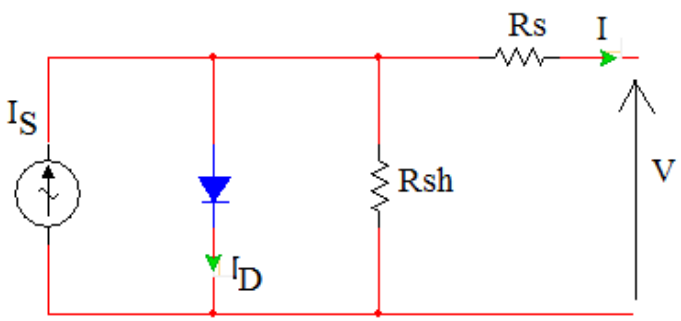

Figure 20. Model of Photovoltaic Cell (Acakpovi and Hagan, 2013).

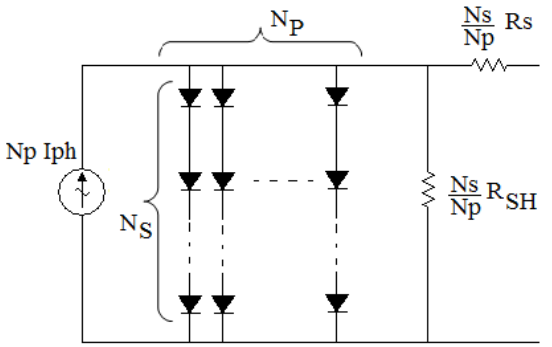

Figure 21. Model of Solar Module with N_s and N_p cells connected respectively in series and in parallel (Acakpovi and Hagan, 2013).

Consequently, the following equations, previously established by (Acakpovi and Hagan, 2013), (Tsai et al., 2008) hold:

$$I = N_P I_{PH} - N_P I_S \left[\exp\left(\frac{q}{k \cdot T_C \cdot A} \cdot \left(\frac{V}{N_S} + \frac{I R_S}{N_P} \right) \right) - 1 \right] - \frac{1}{R_{SH}} \cdot \left(\frac{N_P \cdot V}{N_S} + I R_S \right) \tag{15}$$

With:

$$I_{PH} = \left[I_{SC} + K_I \left(T_C - T_{\mathrm{Re}f} \right) \right] \cdot \lambda \tag{16}$$

$$I_S = I_{RS} \left(\frac{T_C}{T_{\mathrm{Re}f}} \right)^3 \cdot \exp\left[\frac{q \cdot E_G}{k \cdot A} \left(\frac{1}{T_{\mathrm{Re}f}} - \frac{1}{T_C} \right) \right] \tag{17}$$

$$I_{RS} = \frac{I_{SC}}{\exp\left(\frac{q \cdot V_{OC}}{N_S \cdot k \cdot A \cdot T_C} \right) - 1} \tag{18}$$

Where,

I_{PH} : photocurrent
I_S : Cell saturation current
q : Electron charge. $(1.6 \times 10^{-19}\ {}^0\mathrm{C})$
k : Boltzmann's constant $(1.38 \times 10^{-23}\ \mathrm{J/K})$
T_C : Cell operating temperature
A : Ideal factor dependent of the PV characteristic, (1.3 for poly-crystalline solar cell)
R_{SH} : Shunt resistance (100Ω)

R_S : Series resistance (0.01Ω)
I_{SC} : Cell short-circuit current at 25°C, 1kW/m^2
V_{OC} : Open-circuit voltage
K_I : Short-circuit current temperature coefficient
T_{Ref} : Cell reference temperature
λ : Solar insolation (irradiance) in kW/m^2
I_{RS} : Cell reverse saturation current
E_G : Band gap energy of semiconductor used in a cell (1.11eV)
N_P : Number of cells in parallel
N_S : Number of cells in series

In addition, Table 3 gives some intrinsic characteristics of PV cell, extracted from manufacturer data (Trinasolar, 2012) that would be used for the Simulink modelling:

Table 3. Characteristics of a PV Cell from a Manufacturer

Parameters	Specifications
Peak power (P_P)	235W
Voltage at peak power (V_{PP})	29.3 V
Current at peak power (I_{PP})	8.03A
Short-circuit current (I_{SC})	6.9A
Open-circuit voltage (V_{OC})	34 V
Temperature coefficient of open-circuit voltage	-73mV/°C
Temperature coefficient of short-circuit current (KI)	0.047mA/°C
Approximate effect of temperature on power	-0.43W/°C
Nominal operating cell temperature (NOCT)	45°C

Source: Trinasolar Specification Sheet, 2012.

5.2. Simulink Modelling of a Solar Module

A Simulink model which is derived directly from the mathematical model presented above is presented in Figure 24. Simulink provides a graphical simulation platform where mathematical formula can be implemented using appropriate boxes and signals of different natures ranging from constant, ramp, impulse and many others can be generated to mimic excitations to the model. Also the sink library of Simulink provides access to scope and other intelligent blocks that help in displaying graphs and other relevant scientific results. The final model is illustrated in Figure 24 with the name of parameters defined as constant.

5.3. Factors Affecting the Performance of Solar Cells

Two main factors affect the power characteristic of solar cells: temperature and irradiance (Guechi, 2012).

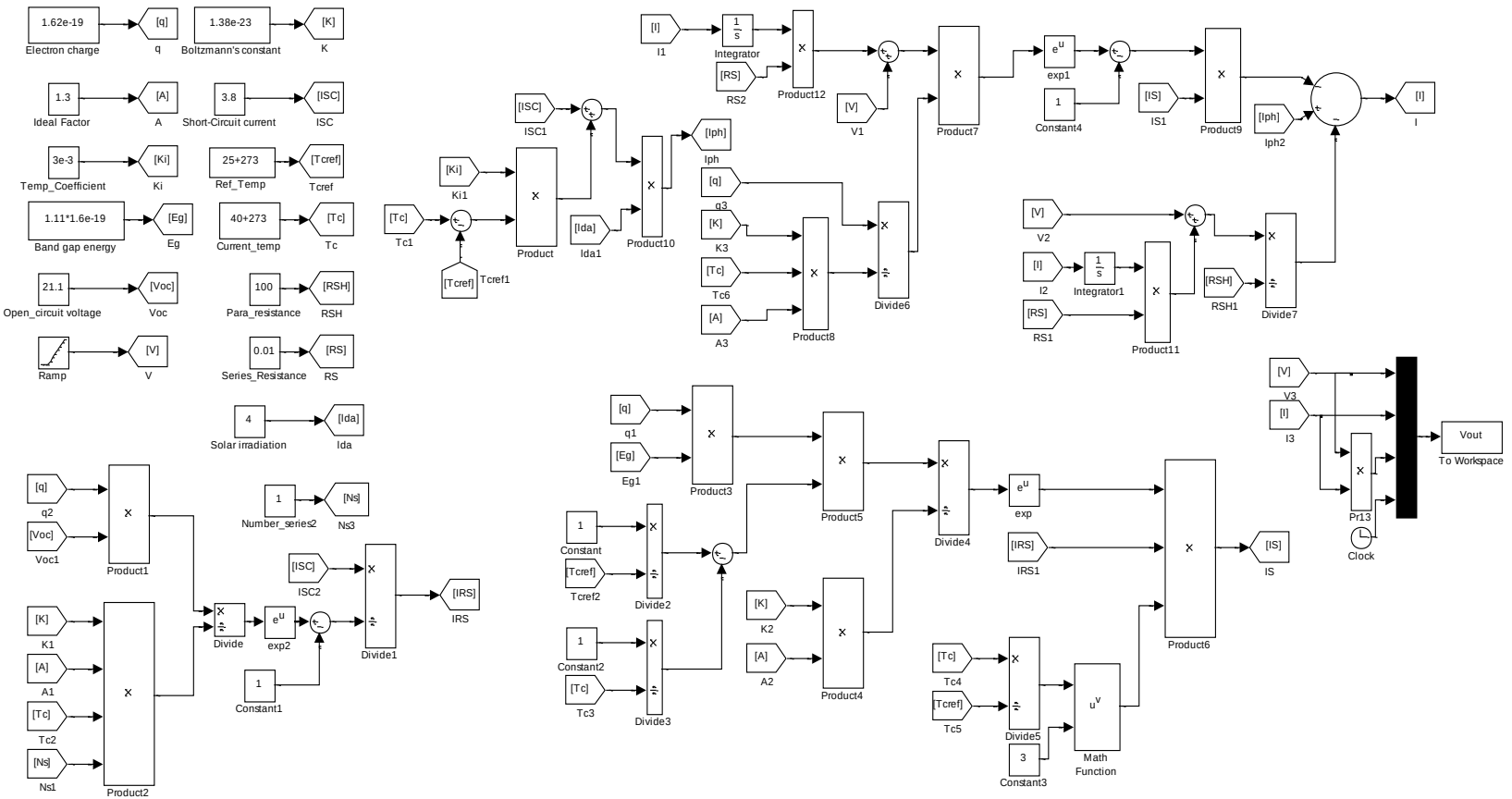

Figure 22. Model of Solar Module Developed under Matlab/Simulink (Acakpovi and Hagan, 2013).

a. Temperature Effect

Temperature has an adverse effect on cell voltage. As the solar cell temperature increases, the open circuit voltage V_{OC} decreases but the short circuit current I_{SC} increases slightly. The maximum power voltage V_{MP} of the cell also decreases and hence the power output also decreases, as shown in Figure 25 below.

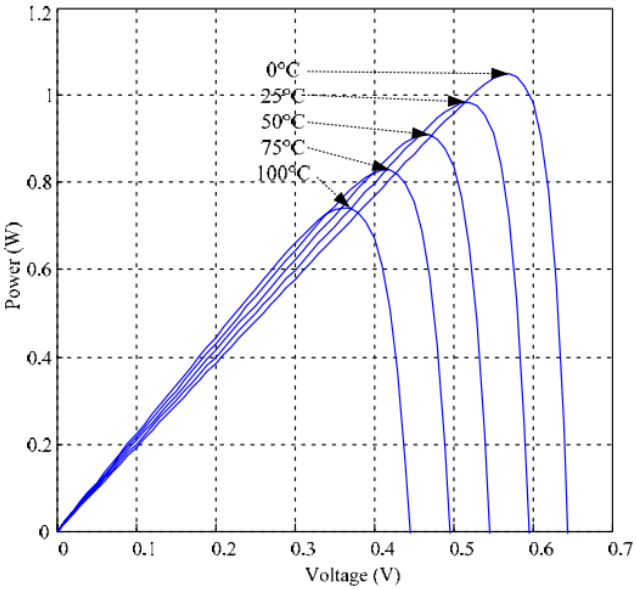

Figure 23. P-V Output characteristics with different values of temperature (Tsai, 2008).

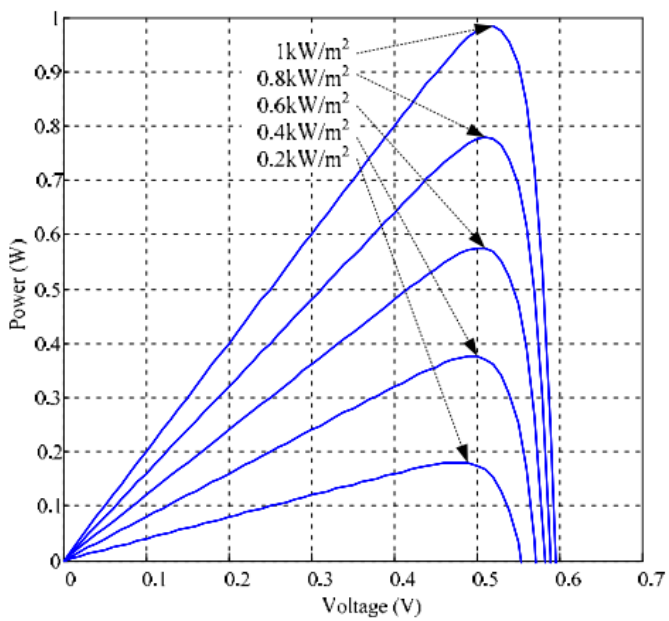

Figure 24. P-V Output characteristics with different values of irradiance (Tsai, 2008).

Figure 25. Typical Monocrystalline module.

From Figure 25 it can be derived that as temperature increases, voltage decreases with only a very slight increase in current. As the current does not vary greatly with temperature, the change in power occurs at a similar proportion to the change in voltage; that is, approximately 0.4 – 0.5% for every 1^{o}C variation in temperature.

b. Irradiance Effect

Unlike the temperature, the irradiance has a positive effect on the solar cell operating characteristics. An increase in irradiation produces an increase of the short circuit current in the same proportion. However, this increase is not much felt with voltage. The change in voltage due to irradiance is marginal. This is shown in Figure 26, although the graph assumes that the cell temperature is constant, i.e., it is unaffected by the differing irradiance.

6. TYPES OF SOLAR CELLS

There are two main types of solar cells: Crystalline Cells and Thin layer (film) Cells. Most PV modules available on market are based on Crystalline Silicon. The process of manufacturing crystalline silicon includes growing ingots of silicon, slicing the ingots into wafers to make solar cells, electrically interconnecting the cells, and encapsulating the strings of cells to form a module. Crystalline cells are further divided into two categories: monocrystalline (single) and polycrystalline (multi-crystalline). A number of solar module manufacturers according to Sonnenenergie (2008) is listed below

- Ribbon-Drawn Silicon Cells and Crystalline Silicon Thin Film Cells
- Polycrystalline EFG Silicon Cells
- Polycrystalline String –Ribbon Silicon Cells
- Monocrystalline Dendrite – Web silicon cells
- Poly crystalline APEC Cells

Figure 26. Typical Polycrystalline module.

6.1. Monocrystalline Solar Cells

According to (Sonnenenergie, 2008), the most effective and at the same time most expensive solar cell are Monocrystalline silicon (mono-Si) solar cells. Solar panels made of mono-Si cells exhibit a unique pattern of small white diamonds. Figure 27 illustrates a typical monocrystalline module.

Recently, some laboratories developed monocrystalline cells of high efficiencies, almost 24%. In the laboratory conditions, adverse factors such as reflection and grid coverage have been considerably reduced. It must however be emphasized that good production conditions obtained in laboratory cannot be afforded for mass production; in reality the efficiencies encountered on market for mass production are always lower than that of laboratories. They vary in the range of 15% to 18%.While monocrystalline cells typically have a higher efficiency than other types of cells, they are more difficult to make than other types of solar cells.

6.2. Polycrystalline or Multicrystalline Solar Cells

Crystalline silicon (c-Si) cells are the most encountered solar cells available on market. They are also known as solar grade silicon. Multiple types of these crystalline silicon cells exist according the crystallinity and crystal size in the wafer. Their operation principle derives from the principle of PN junction. A potential disadvantage of polycrystalline cells is that the boundaries among the thin crystals tend to attract electrons. These boundaries either provide a path for electrical short across the cell or act as barriers, which slow carrier motion. A polycrystalline cell is illustrated below in Figure 28.

Manufacturers of polycrystalline cells need to ensure that the crystals are large enough for photo-generated electrons to be collected by the "PN" junction and the metal contacts of the cell/module before they reach a crystal boundary. Efficiencies of 13% to 16% are normal, although research cells have reached 21%. Polycrystalline modules are very common, and are used in a wide variety of installations, including both domestic and commercial installations.

6.3. Thin Film Cells

Thin film cells are produced as a result of depositing very thin layers of photosensitive materials on other inexpensive materials like stainless steel, plastic lead or glass. The first series of thin film cells produced on market is the Amorphous Silicon (a-Si). The efficiency of the Amorphous Silicon (a-Si) cell can be increased by combining the thin amorphous with microcrystalline silicon cells. Other existing thin film technologies include cadmium telluride (CdTe) and copper, indium, gallium, diselenide (CIGS).

The major advantages of thin films solar cells are related to the fact that they relatively consume a lower rate of raw materials; the production process is highly automated and efficient; they can easily be integrated to building and produce a beautiful appearance; they keep good operation performance at high temperature; and exhibit a reduced sensitivity to overheating (Chopra et al., 1983). The main limitation of thin film is low efficiency

Thin films have gain widespread use on the market over the past five years. The drives for this technology acceptance include:

1. Growing price of silicon making the silicon solar cells more expensive.
2. Availability of silicon.
3. High volume demand for PV world-wide.
4. Potential markets waiting for PV to reach 'grid parity'- this will be achievable faster with thin film product because of the potentially lower cost of production.

Industry estimates show that thin film products could be supplying up to 30% of the PV market within a relatively short space of time. Their main market advantage is the price reduction over conventional silicon PV product. The volume market is looking at thin film purely on a price basis even though the comparative efficiency between thin film and conventional silicon is lower. According to the International Energy Agency (IEA), thin film product provided 30% of the 337,268Wp of PV product by the US solar industry. This figure is in comparison to only 12% of the US solar industry in 2004. Cadmium telluride PV (CdTe PV) is the only thin film technology that has provided better pricing against conventional silicon PV in the market place. Figure 29 provides an illustration of thin film module.

6.4. New Trends in Solar Cells Production

Research on new solar modules is continually being undertaken. In recent years a number of new technologies have been released or are in the pilot manufacturing stage. These include:

a. Dye Sensitized nanocrystalline cells- Light is absorbed in an organic dye of Titanium dioxide (TiO2)
b. Microcrystalline and micromorphous solar cells are deposited at 900-1000◦C for the first type and 200-300◦C for the second. The first is based on depositing high quality silicon films onto a substrate such that they have similar characteristics as polycrystalline structures but deposited the same way as amorphous modules hence the term micromorphous.

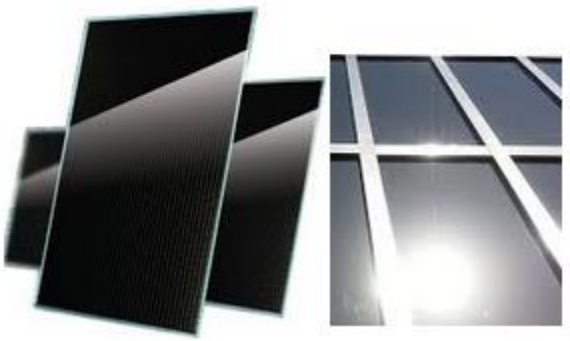

Figure 27. Typical Thin-Film module.

Table 4. Efficiency of various solar cell materials

Classification	Cell efficiency (laboratory)
Si (Crystalline)	25.0 ± 0.5
Si (Multicrystalline)	20.4 ± 0.5
Si (thin film transfer)	16.7 ± 0.3
GaAs (thin film)	27.6 ± 0.8
CdTe	16.7 ± 0.5
Si (amorphous)	10.1 ± 0.3
GaAs (Multicrystalline)	18.4 ± 0.5
Si (nanocrystalline)	10.1 ± 0.2
Thin film Chalcogenide CIGS cell	19.6 ± 0.6
Dye sensitized (submodule)	10.4 ± 0.3
Organic polymer	8.3 ± 0.3

Source: Green et al., 2011

c. Hetro-junction with intrinsic Thin Layer (HIT) – this is a hybrid solar cell which combines crystalline and thin film solar cells.
d. Sliver cells- very small slivers of silicon are connected to form modules. These modules can be made with much less silicon than traditional silicon wafer technologies.

The efficiencies of the different types of solar cells are shown in Table 4.

7. COMMERCIAL MODULES AND PROTECTION DIODES

In recent years the number of solar modules manufactured has increased from 39MWp in 1994 to cover 7.3GWp (7,300MWp) in 2009. This growth in the industry has resulted in many more manufacturers now producing solar modules. It is important that standards are established to monitor the quality of the solar modules installed.

7.1. Existing Standards

Some of the most popular international standards used for PV modules are:

- IEC612-Crystalline Silicon Terrestrial photovoltaic (PV) modules. Design qualification and type approval.
- IEC161646-crystalline Thin-Film Terrestrial photovoltaic (PV) modules. Design qualification and type approval.
- ICE61730- photovoltaic (PV) module safety qualification. Requirements for construction &Requirements and testing.

A quality manufacturer should provide at least the following information on their specification sheets:

- Rated Power (PMAX)
- Warranty
- Power Tolerance
- Maximum system voltage
- Voltage at Pmax (VMP)
- Open Circuit Voltage (Voc)
- Current at Pmax(IMP)
- Short Circuit Current (Isc)

If not provided on the standard brochure or specification sheet, a quality manufacturer should be able to provide on request the following information:

- Temperature co-efficient of PMAX
- NOCT
- Temperature co- efficient of VOC
- Temperature of co-efficient of Isc

An example of a specification sheet for a typical solar module is given in Figure 30.

Table 5. Performance under Standard Test Conditions (STC)

Maximum power	P_{max}	250w
Open circuit voltage	V_{oc}	37.8v
Maximum power point voltage	V_{mpp}	31.1
Short circuit current	I_{sc}	8.28A
Maximum power point current	I_{mpp}	8.05A
*STC:1000W/m2,25◦C, AM1.5		

Source: Specifications sheet for a 250Wp Sun module.

Table 6. Thermal Characteristics

NOCT	46◦c
TCI_{sc}	0.004%/k
TC_{voc}	- 0.30%/k
TC P_{mpp}	- 0.45%/k
Operating temperature	- 40◦cto85°C

Source: Specifications sheet for a 250Wp Sun module.

Table 7. Additional Data

Power tolerance2)	- 0Wp/+5Wp
J-Box	IP65
Connector	MC4
Module efficiency	14.91%
Fire rating (UL790)	Class C

Source: Specifications sheet for a 250Wp Sun module.

Table 8. Performance at 800 W/m^2, NOCT, AM 1.5

Maximum Power	P_{max}	183.3Wp
Open circuit voltage	V_{oc}	34.6 V
Maximum Power point voltage	V_{mpp}	28.5 V
Short circuit current	I_{sc}	6.68A
Maximum power point current	I_{mpp}	6.44A
Minor reduction in efficiency under partial load conditions at 25°C. At 200W/m^2,95% (+/-3%) of the STC efficiency (1000W/m^2) is achieved.		

Source: Specifications sheet for a 250Wp Sun module.

Table 9. Component Materials

Cells per module	60
Cell type	Mono crystalline
Cell dimensions	6.14 in x 6.14 in (156 mm x 156 mm)
Front	tempered glass (EN12150)
Frame	Clear anodized aluminium
Weight	46.7 lbs (21.2kg)

Source: Specifications sheet for a 250Wp Sun module.

Table 10. System Integration parameters

Maximum system voltage SC II		1000 V
Max. system voltage USA NEC		600 V
Maximum reverse current		16A
Number of bypass diodes		3
UL Design Loads*	Two rail system	113psf downward
		64 psf upward
UL Design Loads*	Three rail system	170psf downward
		64 psf upward
IEC Design Loads*	Two rail system	113 psf downward
		sf upward

Source: Specifications sheet for a 250Wp Sun module.

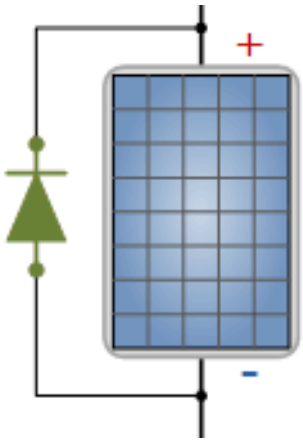

Figure 28. Illustration of a Bypass diode.

7.2. Bypass Diodes

To ensure continuity of supply from a string made of many solar cells in series, a protection measure is needed around individual cells to provide a current path should one of them be faulty or shaded. Bypass diodes are used in this capacity; they are connected in parallel on individual cells as shown in Figure 31 and provide a path for current to flow even in case the cell is damaged. Subsequently the existence of bypass diode explains the fact that a solar module will continue supplying even if one or some cells are damaged or shaded, however the power produced in this case may be lower than the normal one.

The polarity shown on the cell/module above exists for normal operation. If the cell/module is shaded or damaged, the polarity produced by series connected elements is reversed, causing the diode to be forward biased and therefore conducting any current flow.

In most commercial crystalline modules, bypass diodes are not fitted to every cell, though this would be the ideal situation. Most manufacturers provide a bypass diode across a string of 24 cells; that is three diodes in a 72 cell modules (nominal 24 volt module). Module manufacturers' specifications should indicate the number of bypass diodes fitted.

It is recommended that in an array where the modules are connected in series, each module should have at least one bypass diode fitted, if not already provided by the manufacturer.

7.3. Blocking Diodes

Blocking diodes, also known as series or isolation diodes, connect current during normal system operation and are placed in series with a module, or string of series wired modules. The main purpose is to prevent current from flowing backwards through the modules at night and to prevent current flowing into a faulty parallel string. Figure 32 illustrates a blocking diode.

The need for blocking diodes depends upon the PV technology. These were common in the past in stand-alone power systems, but are not often used in systems today.

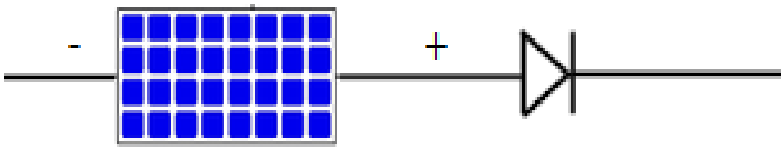

Figure 29. Blocking Diode in Series on Solar Panel.

7.4. Selecting Diodes

The major parameters that are important in diodes selection are:

- The maximum current that the diodes will allow in the forward direction (maximum continuous forward current IF).
- The maximum voltage that the diodes will tolerate in the reverse direction before failure (peak inverse voltage VR)

Note: 9A, 600V diodes are commonly used for bypass and blocking diodes, however IEC 62548 and all relevant Standards should always be consulted.

A further consideration is the voltage drop across the diodes. The voltage drop of a silicon rectifier diodes at its rated current is 0.6-0.7V i.e., the above diodes will consume 3.6W at 6A (6A × 0.6V). Schottky diodes only have a 0.2to 0.4V drop and so if the voltage drop (and power loss) is critical, then schottky diodes should be used. As most modules incorporate bypass diodes, it is uncommon for installers of grid-connected PV systems to install individual bypass diodes.

CONCLUSION

In summary, this chapter presented the basics of solar energy that are essential for its understanding and collection. The available solar radiation is presented, followed by the definition of some common terms related to solar energy such as irradiance and irradiation. Subsequently, a sunpath diagram was presented and used to determine the sun location anytime and anywhere. The importance of tilting of solar module correctly to obtain sun radiation at 90 degrees has also been elaborated together with the determination of magnetic North and true North.

Furthermore, the second section of this chapter dealt with solar electricity where the impact of connecting solar cells in series, parallel or series/parallel has been thoroughly discussed. This was also followed by the description of PV cell, module and arrays. Subsequently, both analytical and simulation models of photovoltaic solar module were respectively presented and developed under Matlab/Simulink. The models were later used to interpret the effect of irradiance and temperature on solar cells. It was shown that irradiance has a positive effect on the output of solar module while temperature has a negative effect. Additionally, existing types of solar modules available on market such as mono-crystalline, poly-crystalline and thin-film were discussed with the essential characteristics of solar to be

considered while purchasing them. Finally the importance of bypass and blocking diodes as well as their selection criteria have also been explained.

This chapter is rich in information concerning the fundamentals of solar and may be very useful in introducing a beginner to solar energy as well as providing reliable and necessary information to a designer or practitioner in Solar Energy Engineering.

REFERENCES

Acakpovi, Amevi., and Hagan, Essel. B. 2013. "Novel Photovoltaic Cell Model Using Matlab Simulink" *International Journal of Computer Application* (IJCA), 83:27-32.

American Society for Testing and Materials (ASTM) *Terrestrial Reference Spectra.* 2013.

Atchison, Clay. 2015. "Measuring the sun's position by azimuth and altitude." photograph, viewed August 2016.www.solarschoolhouse.org.

Basu, Dipak. 2001. Dictionary of Geophysics Astrophysics and Astronomy, 2001. Wanshington DC: CRC Press.

Deutsche, Sonnenenergie G. 2008. *Planning and Installing Photovoltaic Systems - A Guide for Installers*, Architects and Engineers, 3rd Edition. New York: The Earthscan Expert Handbook for Planning, Design and Installation.

Earth orbit around the sun, photograph, viewed August 2016 <http://wp.patheos.com.s3. amazonaws.com/blogs/progressivesecularhumanist/files/2014/02/earth_sun.jpg>

Earth's Energy Budget, Oklahoma Climatological Survey, photograph, viewed August 2016, <https://edro.wordpress.com/energy/earths-energy-budget/>

GAISMA, Sunpath Diagram, photograph, viewed August 2016 <http://www.gaisma.com/ en/sunpath/kuching.png>

Ganoe, R. D., Stackhouse, P. W. and DeYoung, R. J. 2014. RETScreenPlus Software Tutotrial. NASA Technical Report Servers.

Geoff, Stapleton., and Susan, Neill. (2012).Grid-Connected Solar Electric Systems. New York: *The Earthscan Expert Handbook for Planning*, Design and Installation.

Guechi, A., Chegaar, M.,andAillerie M. 2012. *Environmental Effects on the Performance of Nanocrystalline Silicon Solar Cells*, Energy Procedia.

International Renewable Energy Agency. 2012. "Prospects for the African Power Sector, Scenarios and Strategies for Africa Project." Khalidiyah, United Arab Emirates.

Iqbal, Muhammad. 1983. "*An Introduction to Solar Radiation."* Elsevier.

Kasturi, L. Chopra., and Suhit R. Das. 1983. *Thin Film Solar Cells.* New York:Springer Science.

Mahdavinejad, Mohammadjavad., and Khazforoosh, Sina. 2014. Combination of Wind Catcher and Chimney for More Energy Efficient Architectural Buildings. Sustainable Energy. doi:10.12691/rse-2-1-7.

Martin A. Green, Keith Emery, Yoshihiro Hishikawa and Wilhelm Warta 2011. "Solar cell efficiency tables (version 37)". *Progress in Photovoltaics: Research and Application Prog*. Photovolt, Wiley Online Library, DOI: 10.1002/pip.1088.

Michael, Boxwell. 2012. *Solar Electricity Handbook: A Simple, Practical Guide to Solar Energy* 2012, New York: Greenstream.

Molleo, Max., Thomas, Schmidt J., and Brian, Benicewicz C. 2012. Polybenzimidazole Fuel Cell polybenzamidazole (PBI) fuel cell Technology, Encyclopedia of Sustainability Science and Technology.

Navigation on chartwork, photograph, viewed August 2016, http://www.sailtrain.co.uk/navigation/variation.htm.

Peter Peeters. 1979. *"Can We Avoid a Third World War Around 2010?: The Political, Social, and Economic Past and Future of Humanity."* United Kingdom: Palgrave Macmillan.

Petersen, James., Sack, Dorothy., and Gabler, Robert.2015. *Fundamentals of Physical Geography* (2nd Ed.).University of British Coloumbia Okananga.

RETScreenTM International. 2013. *"A Standarized Tool for Assessing Potential Renewable Energy Projects, Natural Resources Department of Canada."* CANMET Energy Diversification Research Laboratory (CEDRL).

Schillings, Christoph., Meyer, Richard., and Trieb, Franz. 2004. "High Resolution Solar Radiation Assessment for Ghana." *Solar and Wind Energy Resource Assessment* (SWERA), GEF, UNEP, Germany.

Solar radiation on a tilted surface, photograph, viewed August 2016, <http://pvcdrom.pveducation.org/SUNLIGHT/Images/TILTARR.gif>

Specifications sheet for a 250Wp Sunmodule, accessed, August 2016, https://www.solarworld-usa.com/

Stickler, Greg. 2013. "Educational Brief - Solar Radiation and the Earth System. National Aeronautics and Space Administration." Accessed 23 July 2016.https://blogs.nasa.gov/educationexpress/2016/06/23/nasa-education-express-june-23-2016/

The International Bank for Reconstruction and Development and the World Bank. 2010. "Africa's Infrastructure A Time for Transformation." Washington, DC.

Tsai, H., Tu, S., and Su, J. 2008. Development of Generalized Photovoltaic Model Using MATLAB/SIMULINK. Proceedings on the world congress on Engineering and Computer Science. WCECS, ISBN: 978-988-98671-0-2, 6p.

US Department of Energy, photograph, viewed August 2016, http:// mycommunitysolar.org/ucommunitysolar/images/Cell-Module-Array.png.

Wikimedia Commons, photograph, viewed August 2016, <http://commons.wikimedia.org/wiki/File:Solar_spectrum_ita.svg>

Wirth, Harry. 2016. "Recent Facts about Photovoltaics in Germany, Division of Photovoltaic Modules, Systems and Reliability." Fraunhofer ISE, Germany.

World Bank. 2008. "Africa Infrastructure Country Diagnostic – Underpowered: The State of the Power Sector in Sub-Saharan Africa." UK.

In: Renewable Energy Systems
Editor: Sandip A. Kale
ISBN: 978-1-53610-423-3

Chapter 2

EMERGING SOLAR PV TECHNOLOGIES: A PARADIGM SHIFT

Sarita Baghel[1,*] and Nandini Sharma[2]
[1]Physics Department, Shivaji College, University of Delhi, Delhi, India
[2]Research Lab for Energy Systems, Netaji Subhas Institute of Technology, Delhi, India

ABSTRACT

To meet ever growing global energy requirements, solar energy is a readily available renewable energy resource possessing both scalability and technological maturity. With 43% rise in cumulative installed capacity in the world, Solar Photovoltaics (PV) emerges as the most widely used technology to harness sunlight. For decades crystalline Silicon (c-Si) based solar cells have dominated the PV market. Now with the emergence of latest PV technologies due to cutting edge research in new materials, the dominance of c-Si is being questioned. This chapter reviews the current scenario of rapidly developing technologies which can be close competitors to Si solar cell, revolution arising the current market dynamics. Materials are analyzed on the basis of their large scale applicability together with cross industry synergistic potential. Top four technologies are identified as the front-runners namely perovskites, multi-junction concentrator photovoltaics, quantum dot photovoltaics and graphene. These photovoltaics show potential to displace and disrupt the traditional PV if provided with sufficient financial and academic investments.

Keywords: material, photovoltaic, solar

1. INTRODUCTION

The world wide increase in energy demands and rapid depletion of fossil fuels has motivated a search for alternate energy sources. Inexpensive and environment friendly renewable energy sources are now being seriously considered as the potential candidates to

* Corresponding author: E-mail: nsitsarita@gmail.com.

replace conventional energy sources. Our dependence on fossil fuels has also lead to climate change as a result of global warming. Solar energy is the most promising alternative due to its easy availability. The earth receives 1.367 kW/m^2 of solar radiation out of which only 47% of solar power reaches the earth surface (Radosavljević and Đorđević 2001). Even if a small proportion of this abundant energy is harnessed, it shall be enough to fulfill the needs of mankind.

Renewable energy sources currently take care of 13% of global energy consumption (Timilsina, Kurdgelashvili, and Narbel 2012). Therefore still burning of fossil fuels contributes a largest share. Close to 20% of world electricity needs are covered by hydropower (Barta, Van Dijk, and Van Vuuren 2011). Though there is a constant increase in renewable energy capacities, for past twenty years but the growth has been slow. Majority of nations today are implementing progressive energy policies to expedite the establishment of renewable. Particularly European countries, namely Germany has incepted the concept of 'green economy' boom in renewable energy quarters like wind and solar electricity (photovoltaics). Wind sector in general surpasses photovoltaics in context to installed capacities (Figure 1). However, it is worth noticing that the photovoltaics have been growing as the efficient power generation technology at the annual rate of 43% (Jean et al. 2015).

There is a clear need to shift the burden of global energy consumption has to green energy sources in coming years with depletion of coal and oil.

1.1. Fundamentals of Photovoltaic Conversion

Photovoltaic effect is defined as the conversion of sunlight into electricity. Photovoltaic device consists of two electrodes, a cathode and an anode. Whenever a photon strikes the semiconductor material, an electron in the valence band of the semiconductor gets excited to the conduction band, leaving a hole behind. The electron hole pair hence generated are separated and transferred via external circuit producing electricity.

The generation of voltage between two electrodes enveloping a solid or liquid system upon illumination was discovered by Edmond Bequerel in 1839 and since then it is known as the photovoltaic effect (Becquerel 1839). Later in the year 1883, Charles Fritts reported first selenium and gold junction based solar cell with 1% efficiency. More than hundred years after that Pearson demonstrated 6% efficiency for a diffused silicon (Si) p-n junction solar cell (Cummerow 1954).

Presently, physics behind the working of classical crystalline and multicrystalline silicon based solar cells is well comprehended. Photo generated electron hole pairs are separated and collected by the p-n junction formed by p type and n type silicon semiconductors. Today silicon photovoltaics dominate the commercial market. However, thin film photovoltaic technology e.g., CdTe, Cu (In, Ga) Se_2 have made their way as inexpensive alternates to Si wafer based solar cells. There is renaissance of other versatile hybrid technologies making use of new organic and inorganic materials like dye sensitized solar cells, organic/polymer and perovskites based photovoltaics.

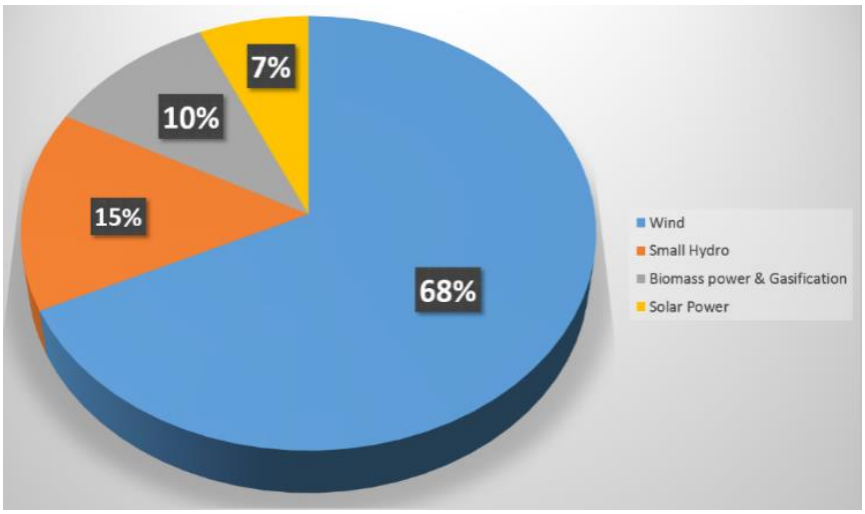

Figure 1. Renewable energy distribution chart (Verbruggen et al. 2010) (adapted simplification).

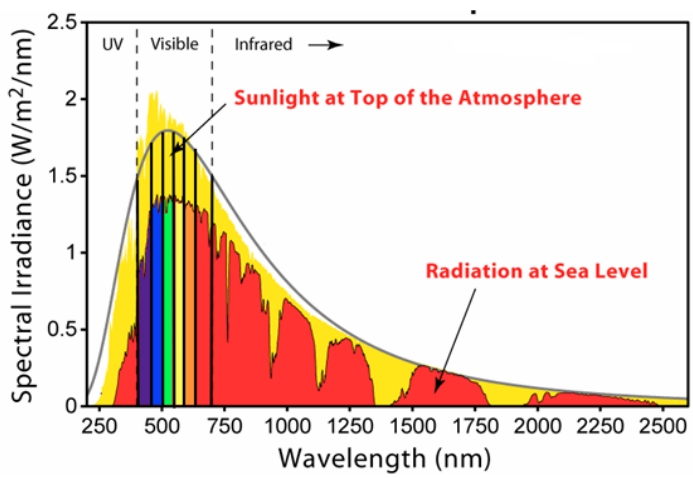

Figure 2. The solar spectrum (Gueymard 2004).

1.2. The Solar Spectrum

The solar radiation can be closely estimated as a black body irradiating at a temperature of 5800K described by the Planck' distribution law (Planck 1901). Solar radiation measured on the surface of earth (AM 1.5G) is lower than outside the earth's atmosphere (AM 0) as given by Planck's law as shown in Figure 2. This happens due to loss of intensity as sun's radiation has to pass through earth's atmosphere resulting in absorption, scattering and reflection of some fraction of the solar radiation. Oxygen (O_2), Ozone (O_3), methane (CH_4) and nitrous oxide (N_2O) are responsible for light absorption in visible and UV region, while infra-red region is captivated by water vapour (H_2O) and carbon dioxide (CO_2).

So, the intensity of spectrum thus obtained is marginally diminished by an appropriate geometric factor. The integral of the curves provides the measure of the absolute incident radiation as,

IAM0 = 1366.1 W m^{-2} and IAM1.5G = 1000.4 W m^{-2}

Absorption is directly proportional to the path travelled by the light through the atmosphere. If ***l*** is the path length of the light through the thickness ***lo*** of the atmosphere, then $l = lo/cos\alpha$, where α is the angle of incidence of solar radiation with the normal to the earth's surface. The l/lo is termed as the air mass (AM) coefficient. The α is also known as solar zenith angle. Value of zenith angle is zero when sun is directly overhead and as a consequence AM shall be equal to unity. However, as the optical path of sunlight increases through the atmosphere, air mass coefficient increases. While it reduces as land elevation increases lowering the thickness of the atmosphere. The spectrum outside the earth's atmosphere is indexed as AM 0.

In photovoltaics, the standard reference spectrum is designated as AM1.5G and defines a standard direct normal spectral irradiance and standard total with reference to global hemisphere within limit of 2π steradian field of view of the tilted plane with 38° inclination with the horizontal plane as prescribed by the American Society for Testing and Materials (ASTM) (ASTM 2013).

2. SOLAR PV BACKGROUND

2.1. The Dominance of C-Si Photovoltaics

Single or multicrystalline Si based solar cells currently dominate 85% of photovoltaic market share. They are the first generation solar cells consisting of large area single crystal p-n junction diode. Since crystalline silicon has a low absorption coefficient as a result of indirect nature of its band gap, the junction contains relatively thick (~300 μm) sheet of p-type silicon and a thinner (~1 μm) layer of n-type silicon. However, they also suffer enhanced charge recombination due to various structural defects (e.g., point defects, dislocations and grain boundaries). They, generally, require high purity silicon and high temperature for their fabrication process making them an expensive affair.

Another traditional PV technology consists of thin films of polycrystalline compounds like $CuInGaSe_2$, $CuInS_2$, $CuInSe_2$, CdTe or microcrystalline silicon (μc-Si) and amorphous silicon (a-Si), currently constituting 15% of market share. Such compounds have direct band gap which enable thin film absorber layer ≤1 μm. CIGS under optimized conditions has a band gap of 1.1 eV while band gap of CdTe is about 1.5 eV. The solar cell are prepared by (co)evaporating the absorber material in a vacuum chamber. Toxicity and scant availability of materials like Cd, In, Te is a major cause of concern for this technology. Figure 3, shows a continuous rise in annual PV production capacities of thin film and crystalline silicon based solar modules since last few years. However, their record efficiency is still lower than conventional silicon counter parts (Figure 4).

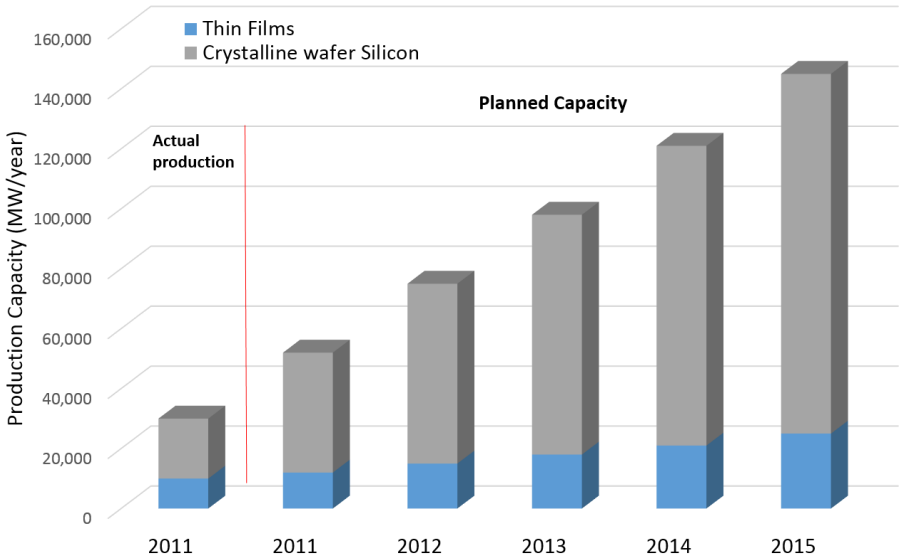

Figure 3. Annual PV production capacities of thin film and crystalline silicon based solar modules (Pandey et al. 2016) (adapted simplification).

3. Disrupting the Traditional Solar PV

3.1. Defining the Credentials for the Upcoming Technologies

In recent years, cutting edge research advancements in PV technologies have brought innovative concepts in the front line including multijunction photovoltaics with concentrators (M-CPV), Quantum dot photovoltaics, Organic photovoltaics, perovskites, and (still not fully comprehended) graphene. These latest technologies possess the required capabilities to disrupt the commercial space of c-Si PV.

Important characteristics for any potentially disruptive technology

1. Long term Cost per watt potential to outshine current c-Si module market
2. Cross industry synergistic potential, to be able to find applicability in other industries apartfrom PV industry.

Together with other relevant prerequisites, potential competitors are identified and explained in next section.

4. Defining the Contenders

The framework to define an alternative spectrum of PV competitors depends on numerous factors. Stability, module efficiency, raw material abundance, processing complexity, manufacturing cost and structural flexibility, are some of the performance characteristics that are required to determine the potential of any emerging PV technology.

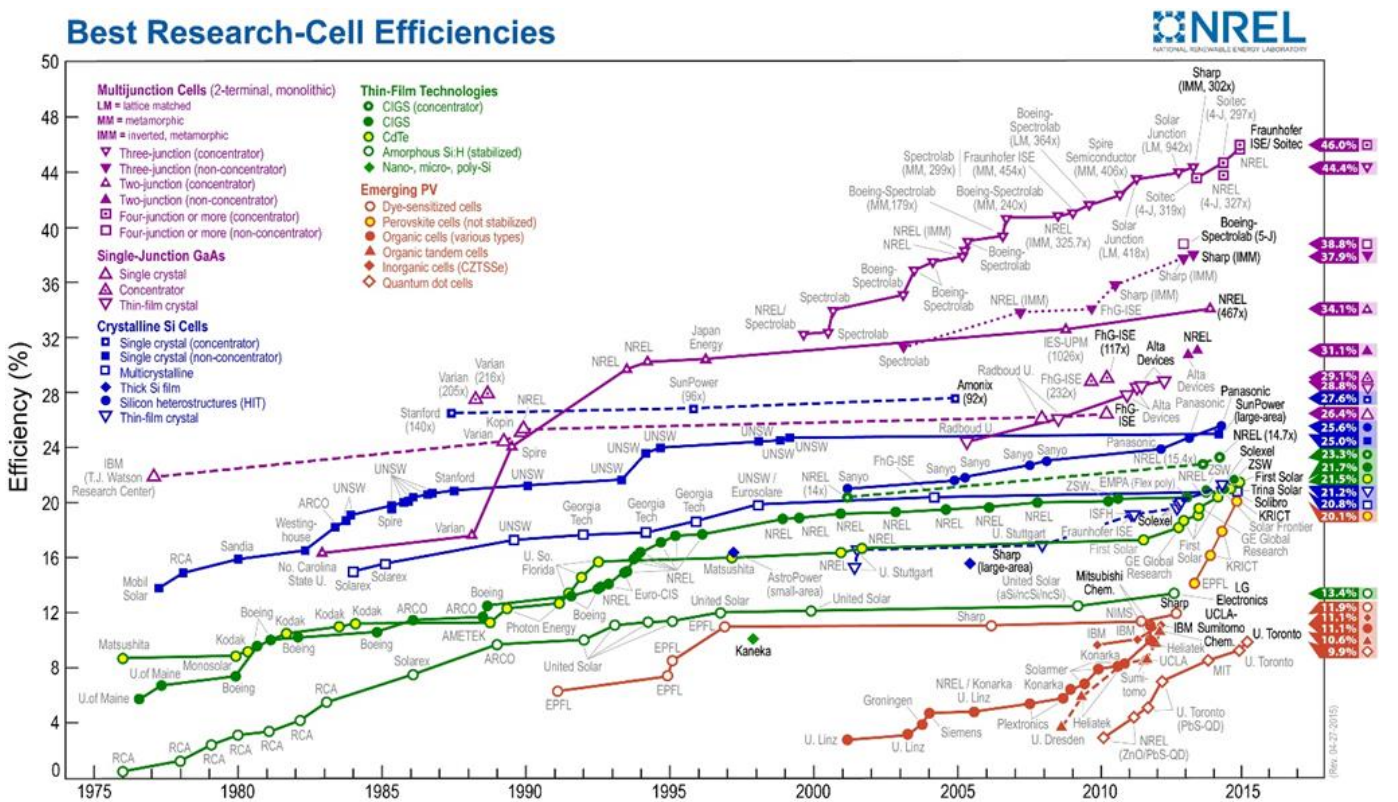

Source: NREL, Colorado, US, http://www.nrel.gov/ncpv/images/efficiency_chart.jpg.

Figure 4. Best research-cell efficiencies.

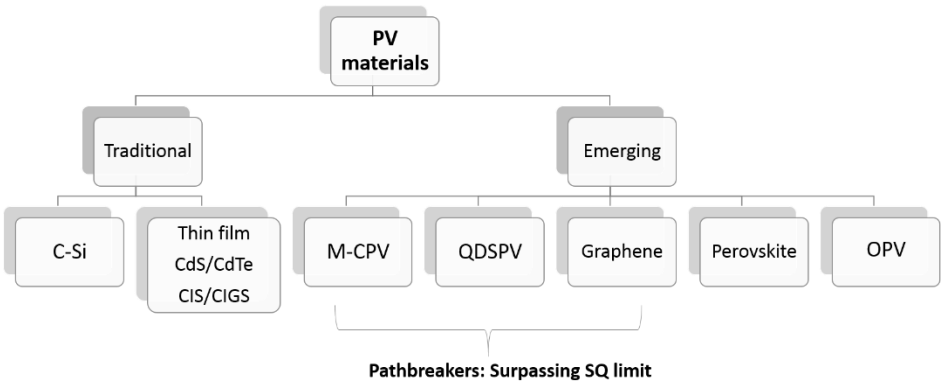

Figure 5. PV material chart.

Intense innovations in recent years, in the field of material research and device engineering have given rise to latest generation of PV technologies. Such solar cells are based on the use of nanostructured materials that can be exploited and engineered to generate desired electronic and optical attributes. With simple room temperature fabrication processes and the utilization of earth abundant elements as raw material, next generation low cost photovoltaics are anticipated to bring the change.

Based on the above described performance matrices, key emerging contenders of PV technology are listed in Figure 5. Identified technologies are Multijunction (concentrator) Photovoltaics (M-CPV), Quantum Dot Sensitized Solar Cells (QDSPV), Organic Photovoltaics (OPV), Perovskites and graphene.

4.1. Multijunction (Concentrator) Photovoltaics (M-CPV)

Deviating from the conventional PV systems, this class of photovoltaics uses parabolic troughs and tracking set up which focuses the sunlight on to the solar cells while keeping them aligned towards the direction of sun. They form the most recent and upcoming league of photovoltaics to yield a single multi-spectrum solar cell. Various absorber layers with increasing band gaps are stacked together for efficient absorption of solar spectrum. Such multi junction solar cells do not adhere to Shockley–Queisser limit.

4.1.1. Advantages

System facilitates upto 10% increase in production of electricity per 100 grams of silicon. As evident from the latest NREL data chart, M-CPV are leading the field with highest recorded efficiencies close to 40%. While conventional c-Si solar cells have not yet crossed 28% mark even in laboratory conditions. Recently, Fraunhoffer Institute of Solar Energy Systems have successfully demonstrated the 46% conversion of direct sunlight into electricity.

4.1.2. Challenges and Way Ahead

Though efficiency figures are promising, it may be erroneous to declare it as the technology of future. Concentrated sunlight ordinarily causes overheating of solar cells

resulting into degradation of photovoltaic effciency, impairing their performance. Therefore, to extract surplus thermal energy this system uses heat sinks and convectional cooling medium. However, the extacted heat energy can be harnessed leading to substantial increase in overall conversion efficiency of the combined system.

4.2. Quantum Dot Sensitized Photovoltaics (QDSPV)

Quantum Dots (QDs) have received lot of attention because of their remarkable opto-electronic properties. QDs are small scale semiconductor nanocrystals with size (2-10 nm) comparable to Bohr radius.

4.2.1. Advantages

Their absorption spectrum can be tailored by changing their band gap, which makes them potential candidates for applications as a light absorbing material for photovoltaics. Their potential to have "tunable bandgaps" provide a big edge over bulk materials such as silicon. They can absorb variable wavelengths in the solar spectra depending on their sizes.

They can be prepared via various simple methods namely plasma synthesis, colloidal synthesis and mechanical fabrication. Material Science Centre at NREL, promulgated the cutting edge technique called "multiple exciton generation (MEG)" as a milestone in quantum dot PV research. MEG process cools hot excitons by utilizing excess energy in photons, hence enhancing the quantum yield of QDSPV.

4.2.2. Challenges and Way Ahead

Research cell efficiency is low, which is however just one of the components determining its cost per watt potential. There are other significant factors such as cross industry potential apart from PV technology such as light emitting diodes, high efficiency transistors and optical communication. QDs have high absorption.

4.3. Organic Photovoltaics (OPV)

Organic photovoltaic, also known as polymer solar cells, is one of the emerging solution processed thin film solar cell technology. It has got a major push owing to recent advances in functional and nanostructured energy materials research.

4.3.1. Advantages

It has become preferred choice as an alternate material for solar cells due to simple fabrication techniques and low cost casting methods involved. Large scale fabrication for OPV modules is possible with latest "roll to roll" process.

4.3.2. Challenges and Way Ahead

Certified efficiencies for Small-molecule and polymer OPV cells are found to be around 11%, while module efficiencies are close to 8.7% (NREL), (Martin A. Green et al. 2015). Apart from low efficiency, other major concerns involve inefficient exciton transport and

poor long-term stability. However, there is a synergistic scope for cutting edge research in applied science and engineering.

4.4. Perovskites

Evolved from solid state dye sensitized solar cells, these solar cells use lead hailde based coumpounds called "perovskites," having crystal structure similar to calcium titanate.

They have rapidly emerged as the promising alternate thin film PV technology.

4.4.1. Advantages

Displaying close to 20.1% conversion efficiencies, within three years of R&D, they hold huge potential to be the front runner in PV technology (M A Green et al. 2012). The rate, at which efficiency is increasing, is faster than that of commercial c-Si. The "Nature" journal has contextualised innovative perovskite device structures to make this technology market-viable (Jeon et al. 2015). Other important advantages of this class of material are low materials cost and band gap tunability. Looking at its unprecedented rise across efficiency table, this material can bring about a radical change in PV technology.

4.4.2. Challenges and Way Ahead

Presently, stability of perovskite solar cells is a challenge, due to their high sensitivity to moisture. With unproven cell stability at room temperature and use of toxic lead, there is an urgent need to counter this issue with comprehensive understanding of degradation mechanisms.

4.5. Graphene

Graphene is made up of repeated hexagonal pattern of carbon atoms as a single layer. Solar cells need materials that are conducting and transparent enough to allow light to get through. This makes graphene, a promising solar energy material for improving the existing products.

4.5.1. Advantages

Graphene has an endless potential as a highly exotic transparent conducting material, not only in PV, but across other industries as well. Hence, there is an emerging patent battle for graphene among the corporate world.

4.5.2. Challenges and Way Out

Despite being a good conductor, Graphene is not very efficient at collecting the electrical current produced inside the solar cell. Therefore, researchers are working towards making suitable modifications in graphene for this purpose. Graphene Oxide (GO) is one of such example, which is less conductive but more transparent having better charge collector capacity which can be useful for solar panels.

Table 1. Comparative overview of emerging PV technologies

PV	Efficiencies (maximum theoretical)	Strengths	Weaknesses	Future scope of developments
M-CPV	86.0%	• High efficiencies • Mature manufacturing technology • Maximum theoretical efficiency beats SQ limit	• High cost of equipments and labor: expensive manufacturing • Degradation due to heat	• Harness surplus heat: increase overall efficiency
QDSPV	66.0%	• Low cost manufacturing • Potential efficiency beyond SQ limit • High absorption rate	• Toxicity • Degradation under heat and UV	• Enhance cross industry potential
OPV	24.0%	• Low cost manufacturing for large scale devices • Large scale printing possible: flexible substrate	• Low efficiency • Low technological maturity • Poor material stability over long term	• For roofing applications: overcome material instability
Perovskites	33%	• Simple and low cost manufacturing • High rate of efficiency improvement	• Stability issue: degradation under moisture • Toxicity	• Research and development (R&D) needed
Graphene	60.0%	• Transparent and conducting	• Poor charge collection capacity	• Modifications in graphene structure

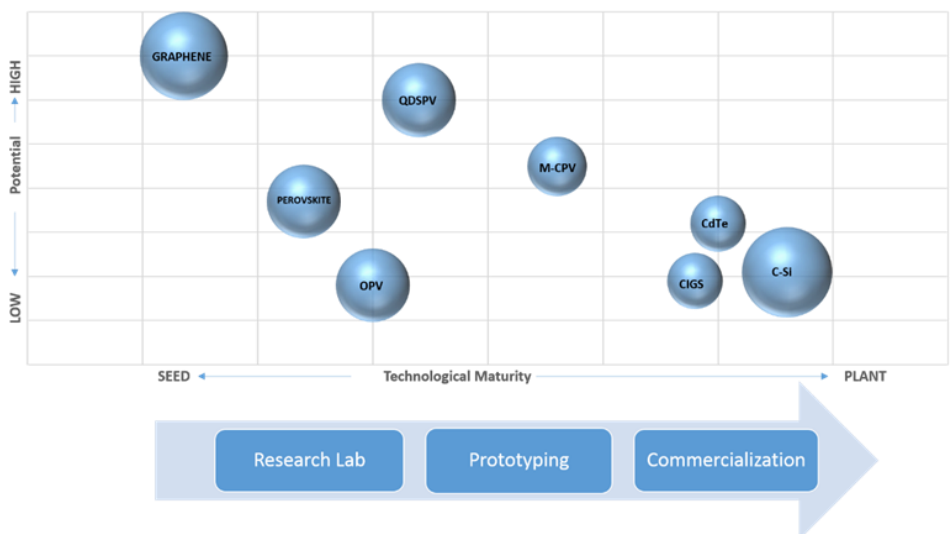

Figure 6. Potential Vs technological maturity for PV technologies.

Table 1 summarizes and provides the comparative overview for the above described PV technologies.

5. THE TOP - MOST PV TECHNOLOGIES OF TOMORROW

5.1. Identifying the Possible Pathways-Breaking the Shockley Queisser Barrier

Power conversion efficiency is known to be therefore most decisive factor for evaluating the potential of anyemrging PV technology.

While Shockley-Queisser limit, puts a theoretical restriction on the maximum efficiency that could be achieved by a solarcell (Yu, Sandhu, and Fan 2014). New generation photovoltaics have to aim towards achieving efficiency beyond this limit. Multijunction (concentrator) Photovoltaics (M-CPV), Quantum Dot Sensitized Photovoltaics (QDSPV) together with graphene, belong to this class of photovoltaics. Lowcost and simple fabrication procedures are their biggest advantages over c-Si. Record conversion efficiencies slightly over 40% have been observed for multi junction cells using concentrated sunlight. Apart from the above three, perovskites also form a potential contender.

Though they are still in early laboratory phase, but if provided with sufficient R&D attention, they would rise rapidly in PV installed capacity rankings (Figure 6). In additiion to this, these technologies also posses unique device level qualities such as transparency, flexibility and high power to weight ratio. These properties can provide new dimensions to novel solar PV applications.

Once the technologies with highest potential are identified, there follows a need to assist their navigation from laboratory conditions to market entry domain. However there are various stages that have to be traversed for a successful commercial launch.

CONCLUSION

Dominance of c-Si Photovoltaics definitely have a certain time limit. The emerging PV technologies presented in this article have all prerequisites to beat the c-Si in long term. This chapter analyses that the most promising technologies among the available emerging alternates, are M-CPVs, QDSPVs, perovskites and graphene. The technological evolution of these alternative PV technologies needs to be viewed through the prism of application based performance matrices and uncertain global economy. These conditions point towards the need to develop an integrated approach of R&D in the field of solar PV. Low cost, high power conversion efficiency, simplified manufacturing process, and reduced material consumption form the foundation for any successful PV technology.

While M-CPVs are already displaying record breaking efficiencies, the other three, can overcome many limitations of presently available photovolaics at much lower cost, provided the improvements in efficiency and stability are accomplished.

REFERENCES

ASTM. 2013. Standard Tables for Reference Solar Spectral Irradiances: Direct Normal and. *Astm 03* (Reapproved): 1–21. doi:10.1520/G0173-03R12.2.

Barta, Bo, Marco Van Dijk, and Fanie Van Vuuren. 2011. Renewable Energy: Hydropower. *Civil Engineering* 19 (5): 37–41.

Becquerel, A.E. 1839. Memoire Sur Les Effects D'electriques Produits Sous L'influence Des Rayons Solaires [Memory on the Effects D'electriques Products under the Influence of Solar Rays]. *Academie Des Sciences* Vol. 9: 561–67. doi:citeulike-article-id:2203331.

Cummerow, R. L. 1954. Photovoltaic Effect in P-N Junctions. *Physical Review* 95: 16–21. doi:10.1103/PhysRev.95.16.

Green, Martin A., Keith Emery, Yoshihiro Hishikawa, Wilhelm Warta, and Ewan D. Dunlop. 2015. Solar Cell Efficiency Tables (Version 45). Progress in Photovoltaics: *Research and Applications* 23 (1): 1–9. doi: 10.1002/pip.2573.

Green, M A, K Emery, Y Hishikawa, W Warta, and E D Dunlop. 2012. Solar Cell Efficiency Tables (Version 40). *Progress in Photovoltaics* 20 (5): 606–14. doi:Doi 10.1002/Pip.2267.

Gueymard, Christian A. 2004. The Sun's Total and Spectral Irradiance for Solar Energy Applications and Solar Radiation Models. *Solar Energy* 76 (4): 423–53. doi:10.1016/j.solener.2003.08.039.

Jean, Joel, Patrick R Brown, Robert L Jaffe, Tonio Buonassisi, and Vladimir Bulovic. 2015. Pathways for Solar Photovoltaics. *Energy Environ. Sci*. 8 (4): 1200–1219. doi:10.1039/C4EE04073B.

Jeon, Nam Joong, Jun Hong Noh, Woon Seok Yang, Young Chan Kim, Seungchan Ryu, Jangwon Seo, and Sang Il Seok. 2015. Compositional Engineering of Perovskite Materials for High-Performance Solar Cells. *Nature* 517 (7535): 476–80. doi:10.1038/nature14133.

Pandey, A.K., V.V. Tyagi, Jeyraj A/L Selvaraj, N.A. Rahim, and S.K. Tyagi. 2016. Recent Advances in Solar Photovoltaic Systems for Emerging Trends and Advanced Applications. *Renewable and Sustainable Energy Reviews* 53: 859–84. doi:10.1016/j.rser.2015.09.043.ASTM.2013. Standard Tables for Reference Solar Spectral Irradiances: Direct Normal and Astm 03 (Reapproved): 1–21. doi:10.1520/G0173-03R12.2.

Pandey, A.K., V.V. Tyagi, Jeyraj A/L Selvaraj, N.A. Rahim, and S.K. Tyagi. 2016. Recent Advances in Solar Photovoltaic Systems for Emerging Trends and Advanced Applications. *Renewable and Sustainable Energy Reviews* 53: 859–84. doi:10.1016/j.rser.2015.09.043.

Planck, Max. 1901. Über Das Gesetz Der Energieverteilung Im Normalspektrum [About the Law of energy distribution in the normal spectrum]. *Annalen Der Physik* 4 (4): 553–63. doi:10.1002/andp.19013090310.

Radosavljević, Jasmina, and Amelija Đorđević. 2001. Defining of the Intensity of Solar Radiation on Horizontal and Oblique Surfaces on Earth. *Environmental Protection* 2: 77–86.

Timilsina, Govinda R., Lado Kurdgelashvili, and Patrick A. Narbel. 2012. Solar Energy: Markets, Economics and Policies. *Renewable and Sustainable Energy Reviews* 16 (1): 449–65. doi:10.1016/j.rser.2011.08.009.

Verbruggen, Aviel, Manfred Fischedick, William Moomaw, Tony Weir, Alain Nada, Lars J. Nilsson, John Nyboer, and Jayant Sathaye. 2010. Renewable Energy Costs, Potentials, Barriers: Conceptual Issues. *Energy Policy* 38 (2): 850–61. doi:10.1016/j.enpol.2009.10.036.

Verbruggen, Aviel, Manfred Fischedick, William Moomaw, Tony Weir, Alain Nada, Lars J. Nilsson, John Nyboer, and Jayant Sathaye. 2010. Renewable Energy Costs, Potentials, Barriers: Conceptual Issues. *Energy Policy* 38 (2): 850–61. doi:10.1016/j.enpol.2009.10.036.

Yu, Zongfu, Sunil Sandhu, and Shanhui Fan. 2014. Efficiency above the Shockley-Queisser Limit by Using Nanophotonic Effects to Create Multiple Effective Bandgaps with a Single Semiconductor. *Nano Letters* 14 (1): 66–70. doi:10.1021/nl403653j.

In: Renewable Energy Systems
Editor: Sandip A. Kale
ISBN: 978-1-53610-423-3

Chapter 3

STUDY OF PERFORMANCE ANALYSIS OF MODERN MATERIALS FOR TRANSPARENT THIN FILM SOLAR CELLS

Abhishek S. Oswal[1,*], Mahasidha R. Birajdar[1], Mohammed Hussien Rady[2] and Sandip A. Kale[1]

[1]Trinity College of Engineering and Research,
Pune, Savitribai Phule Pune University, India
[2]College of Engineering, Wasit University, Iraq

ABSTRACT

The photovoltaic effect principle is the best possible option for conversion of solar energy into electricity. The solar power generation depends upon factors like material of thin film, the intensity of solar rays, angle of incidence between solar rays and cells, surface coating for the cells, etc. Among these, the material of a thin transparent film plays an important role in the conversion of solar energy into electricity. The material of transparent thin film, which gives better results, should be selected for solar power generation. This chapter presents the properties of different materials for transparent thin film solar cells. The materials are selected based on performance parameters such as transmittance, current density, voltage and efficiency and other properties like thermal stability, non-toxicity, mobility, reflection, etched texture, band gap, crystalinity. In this chapter the recent transparent thin film materials such as Ga-doped ZnO thin film, W-doped In_2O_3 thin film, ZnMgO/ITO multilayer thin film and CdTe thin film are analyzed and their performance is compared.

Keywords: glass substrates, thin film solar cells, transparent conductive films

* E-mail: abhioswal5395@gmail.com.

1. INTRODUCTION

From 1973 oil crisis, the world understands the importance of power generation and its necessity in daily life. The coal storage in the world is limited and will be fulfilled up to a limited span. To provide continuous power supply for the future many researchers are actively involved in the energy sector. They arrived at a solution to replace the conventional energy sources with renewable energy sources. The major sources of renewable energy are solar energy, wind energy, geothermal energy, tidal energy, wave energy and biomass energy. They are freely available, eco-friendly, abundant in nature, clean source of energy. The major challenge is an efficient conversion of the available renewable energy into useful energy, i.e., electricity. Among above stated energy sources the solar and wind energy sources are available abundantly and easily convertible and universally accepted. The solar photovoltaic cells directly convert the solar energy into electrical energy. Generally, the solar power generation depends upon the material of cell, the intensity of solar rays, angle of incidence between solar rays and cells, surface coating for the cells, etc.

In the application of solar window, the conversion efficiency depends upon the major parameters like material of thin film, the angle of incidence between the sun rays and cells, size of solar windows, surface coating of solar windows, altitude and latitude of solar window, etc. In these listed parameters, the transparent thin film material of solar cells is a pre-dominant factor to obtain better performance. In this chapter the study about four recent materials for thin films for solar cells is carried out and compared for various performance criteria.

1.1. Photovoltaic Effect

Photovoltaic modules (solar modules) are used to convert sunlight into electricity. Photovoltaic modules are made up of semiconductors that are especially similar to those used to create integrated circuits for electronic equipment. The most common type of semiconductor in use is made of silicon crystals. Silicon crystals are laminated into n-type and p-type layers which are stacked over each other. Light striking the silicon crystals induces the photovoltaic effect which generates electricity. The electricity produced can be used immediately or stored in a battery. For household systems an inverter is installed for converting direct current (DC) into alternating current (AC).

1.2. Power Generation Using P-N Gate and Processing Wafers

The high purity silicon crystals are used in the manufacturing of solar cells. The melt and cast method is used to process crystals into solar cells.

The cube-shaped casting is cut into ingots and sliced into very thin wafers. The valency of silicon atom is “4.” They become perfect insulators under stable conditions. By combining a small number of five-armed atoms (with a surplus electron), a negative charge will occur when sunlight (photons) strikes the surplus electron and then the electron is discharged from

the arm to move around freely. This is called the n-type (negative) semiconductor and is formed by having the silicon 'doped' with a boron film.

In contrast, combining three armed atoms that lack one electron results in a hole with a missing electron. As a result, the semiconductor will carry a positive charge. This is called a p-type (positive) semiconductor and is obtained when phosphorous is doped with silicon. Figure 1 shows the principle behind the conversion of solar energy to electricity.

The p-n junction is formed by placing p-type and n-type semiconductors next to each other. The p-type semiconductor having one less electron attracts the surplus electron from the n-type to stabilize itself. Thus the electricity is displaced and generates a flow of electrons which is known as electricity. When sunlight strikes the semiconductor, an electron jumps and is attracted toward the n-type semiconductor. This causes more electrons in the n-type semiconductors and more protons in the p-type semiconductors, thus generating a higher flow of electricity. This is known as photovoltaic effect.

1.3. Transparent Conductive Films (TCFs) for Solar Cells

Transparent conductive films (TCFs) are thin films of optically transparent and electrically conductive materials. These are important components of many electronic devices including liquid crystal displays, touch screens and photovoltaic. Indium tin oxide (ITO) is most widely used conductive material compared to other alternatives like transparent conductive oxides (TCO), metal grids, carbon nanotubes (CNT), nanowire meshes and ultra thin metal films (Li Gong, et al., 2014).

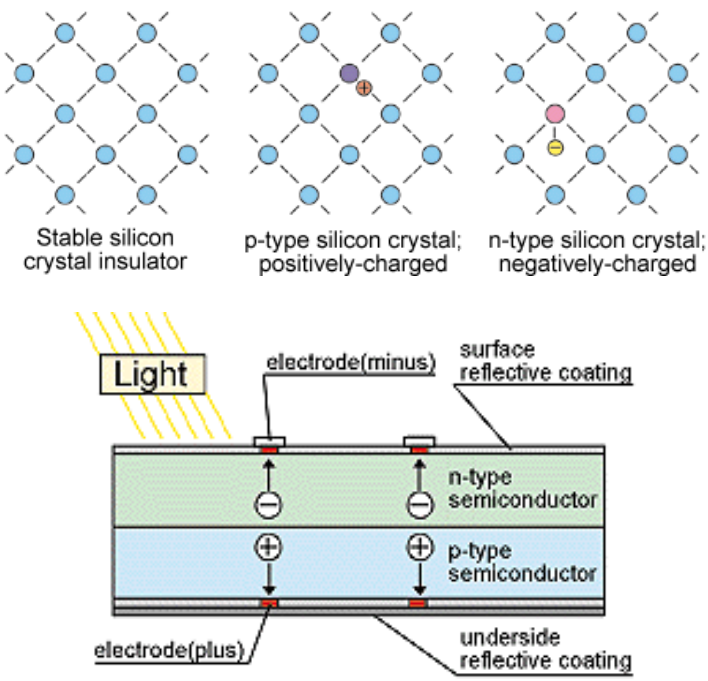

Figure 1. Principle behind conversion of solar energy into electricity.

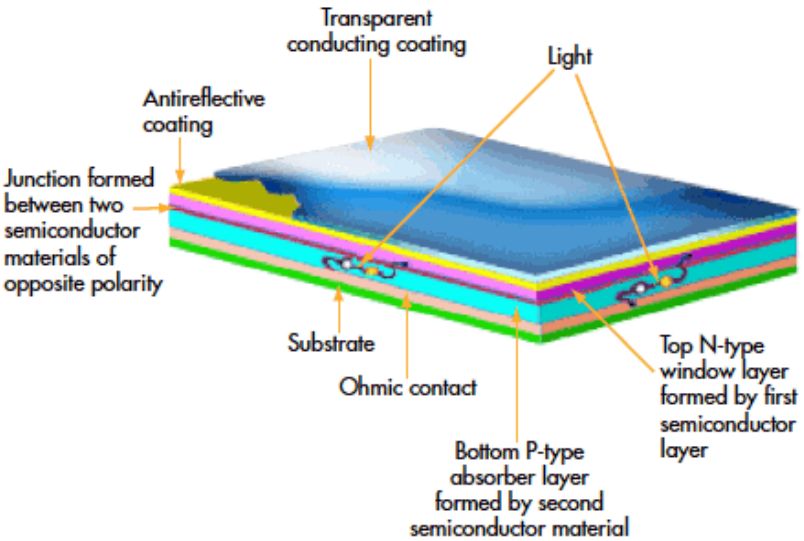

Figure 2. Transparent Conductive Films.

Transparent Conductive Films (TCFs) have been fabricated from both inorganic and organic materials for photovoltaic applications. Typically inorganic films are made up of a layer of transparent conducting oxide (TCO), mostly indium tin oxide (ITO); fluorine doped tin oxide (FTO), or doped zinc oxide. Organic films are being developed using carbon nanotube networks and graphene, which can be fabricated to be highly transparent to infrared light, along with networks of polymers such as poly(3,4-ethylenedioxythiophene) (Fanying Meng, et al., 2014).

Transparent conducting films are typically used as electrodes when a situation calls for low resistance electrical contacts without blocking light (e.g., LEDs, photovoltaic). Transparent materials are used because they possess wide band gaps whose energy value is greater than those of visible light. Photons having energies below the band gap value are not absorbed by these materials and visible light passes through. Some applications such as solar cells often require a wider range of transparency beyond visible light to make efficient use of the full solar spectrum (Dong-Won Kang, et al., 2015).

Figure 2 shows the transparent conductive films which are highly transparent, therefore when applied on windows, it will not change the brightness level inside our homes or hotels or wherever applied. The thickness of these transparent films is of the order of nano or micrometers.

For converting solar energy available from the sun to electrical energy the transparent and thin conductive thin films are deposited on glass substrates. The main application is windows which are installed in our homes, which will save a lot of energy because all the sunlight available in the day striking the window will be converted into electricity.

Windows are not only available in our homes, but also in schools, colleges, etc. can help in saving a lot of energy. It can be applied to the sky scrapers all over the world whose outer covering is made up of glass. It can be installed on the windows and front and rear glass of cars, busses, etc to charge their batteries. The concept of solar energy is also used in wristwatches. The sunlight is used to charge the battery of the watch which helps in the long run.

2. MATERIALS OF THIN FILMS FOR SOLAR WINDOWS

It is very important to study various materials and then select the best available material based on its characteristics and various properties. Properties such as transmitivity, reflectivity, energy conversion efficiency, etc are studied and factors such as cost and availability of the materials are considered. Some effective materials for transparent conductive thin films are listed below.

- Ga-doped ZnO thin film
- W-doped In2O3 thin films
- ZnMgO/ITO multilayer thin film
- CdTe thin film
- Ti-doped indium oxide thin film
- Mo-doped ZnO film
- Amorphous InZnAlO film
- Al-doped ZnO film
- Nano-wire window layers
- Transparent conducting films with silver nanowire
- Sn-doped ZnO transparent film
- Semitransparent quantum dot solar cell
- ZnMgBeO/Ag/ZnMgBeO transparent multi layer film

Cadmium Telluride (CdTe) has a direct band gap of approximately 1.5eV which matches very well with the solar spectrum and high optical absorption coefficients. Since the sixth decade of twentieth century CdTe is considered as one of the most promising thin film solar cell materials. Alloying of CdTe absorber with Se during preparation process can enhance the photocurrent collection in the long wavelength region (greater than 960nm). The multilayer structure attracts much attention because the optical properties can be enhanced and charge transfer characteristics in the surface interface regions of hetero-structure can also be improved. The composite window is made up of Cadmium Sulphide (CdS) and Cadmium Selenide (CdSe) stacked together layer by layer alternately and combined with CdS layers. One of the functions of the CdS layer is to prevent $SnO_2/CdTe_{1-y}Se_y$ interface. This improves the p-n junction and shunt resistance of the CdTe based solar cells.

Transparent Conductive Oxides (TCOs) are stable and their behaviour is excellent at high temperature (up to 500^0C). Sn-doped In_2O_3 (ITO) and fluorine doped tin oxide (FTO) are the most common transparent conductive oxides materials used for photovoltaic applications. The conductivity of ITO decreases after heat treatment which reduces the performance of dye-sensitized solar cells; therefore it is not suitable for dye sensitized solar cell applications. The transmittance in the non infrared light of the FTO thin film is limited; therefore it is not suitable for improving the photovoltaic efficiency of dye sensitized solar cells. Alternatively the ZnO doped with donar elements is a promising option for ITO and FTO because it is cheap, non toxic and has long term environmental stability.

The band gap of ZnO widens when alloyed with MgO which decreases its electrical conductivity. Until now, there is no study about practical applications to the silicon thin film solar cells by employing surface textured $Zn_{1-x}Mg_xO$.

In_2O_3W (IWO) thin films were studied for its application to Silicon Hetero Junction (SHJ) solar cells. This film serves as antireflection coating and a conductive layer on the front surface of SHJ solar cells. It gives high mobility without the requirement of any post annealing treatment.

The Ti-doped indium oxide (TIO) transparent films were prepared by polymer assisted solution (PAS) process for growing different metal oxide thin films. Here the polymer incorporated in the coating solution plays two main roles; first is it encapsulates target metal ions and second, it controls the viscosity of the solution. The first role ensures that the homogenous distribution of metal ions in the solution limits unwanted chemical reaction leading to undesired phases in the films and eliminates the formation of metal oxide in the solution that ultimately leads to the formation of dense, crack-free film. The second role makes the process more compatible with a broad range of solution coating techniques such as spin-coating, inkjet printing, dip coating and spray coating and their viscosity can be controlled by both the molecular weight of the polymer and concentration of the polymer in the solution. The TIO thin films were used as electrodes for fabrication of inverted organic solar cells.

For maximizing the surface functionality in the window layer for high efficient solar energy harvesting the Al-doped ZnO nano rods are reinforced. The Al-doped ZnO nano rods are used to get an anti-reflective, self cleanable and electrical conductive window layer for thin film solar cells. Al-doped ZnO nano rods have a rugged surface morphology with the scale roughness of the order of micro and nanometer. It also exhibits super hydrophobicity and extremely small water contact angle below 1^0.

The Mo-doped ZnO (MZO) films were prepared using pulsed direct current magnetron sputtering technique at various substrate temperatures. This optimal MZO film was suitably used as the front contact in single p-i-n type hydrogenated microcrystalline silicon germanium solar cell. In the range 400-1200 nm a lower resistivity of $7.68x10^{-4}\Omega$ cm and higher average transmittance (more the 80%) was observed when MZO film was deposited at an optimal substrate temperature of 280^0C.

The transparent thin film materials are selected based on parameters such as transmittance, current density, voltage and efficiency and other properties like thermal stability, non-toxicity, mobility, reflection, etched texture, band gap, crystalinity. Based on these parameters the materials such as Ga-doped ZnO thin film, W-doped In_2O_3 thin film, ZnMgO/ITO multilayer thin film and CdTe thin film gave better performance. The following section will give a detailed study about the transparent thin film materials and their performative superiority is concluded.

2.1. Ga-Doped ZnO (GZO) Thin Film

In Ga-doped ZnO thin film the GZO transparent conductive films were deposited on glass substrates by radio frequency magnetron sputtering. Theses GZO films were heated in air at 500^0C for 30 min in order to investigate the optical and electrical stabilities of films at a higher temperature. Figure 3 shows the surface morphology of GZO thin films deposited at different growth temperatures before and after heating.

These GZO thin films were then used as transparent conductive substrates. The dye-synthesized TiO_2 nano-particles based solar cells were fabricated on these films and the solar

to electrical energy conversion properties were investigated. The porous TiO_2 nano particle films were synthesized on GZO glass substrates by a spin coating method. The surface morphology was measured by field emission scanning electron microscopy (FESEM). Figure 4 shows the optical transmittance of GZO films in the wavelength range of 300-2800nm. In the visible region the average transmittance is above 90%.

Figure 5 shows the Current density and voltage characteristics of DSSCs fabricated on GZO. The dye-synthesized TiO_2 nano particles based solar cells were fabricated on the GZO film. The dye synthesized solar cell (DSSC) fabricated on GZO film gave a superior conversion efficiency of 4.56%. The transparent conductive glass on which the DSSCs are applied should have a low sheet resistance, a high transmittance in the ultra-violet visible infrared region and an excellent surface microstructure (Li Gong, et al., 2014).

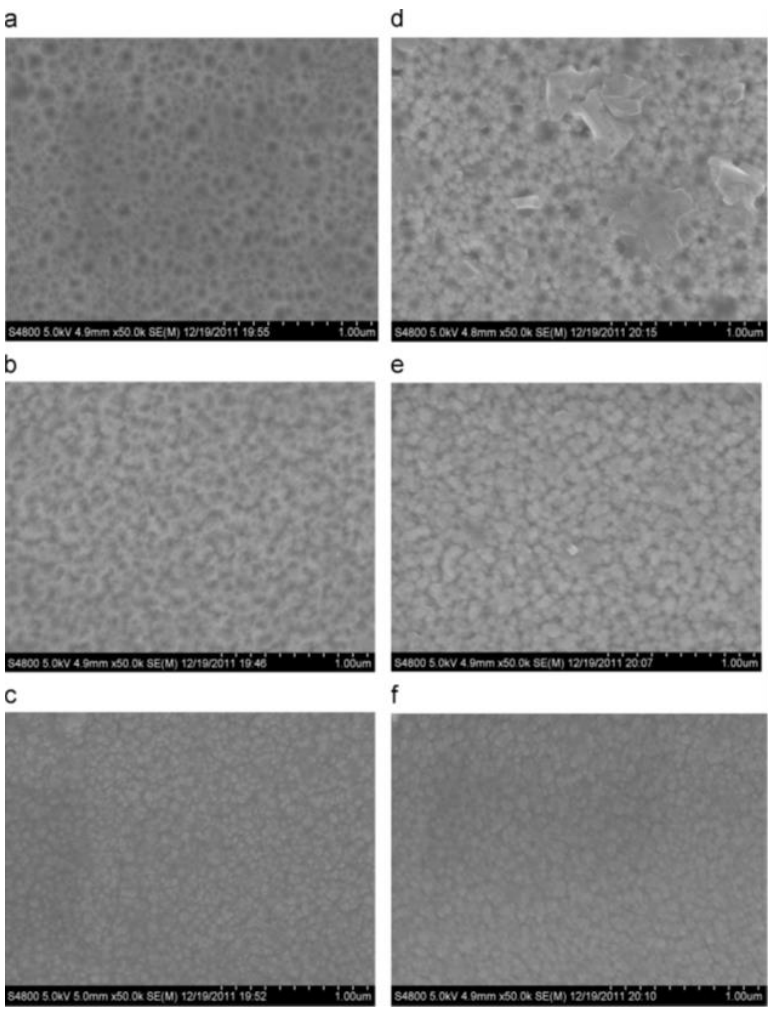

Figure 3. The surface morphology of GZO thin films deposited at different growth temperatures before and after heating (a)300^0C, (b)350^0C, (c)400^0C, (d)T300^0C, (e)T350^0C and (f)T400^0C (Li Gong, et al., 2014.

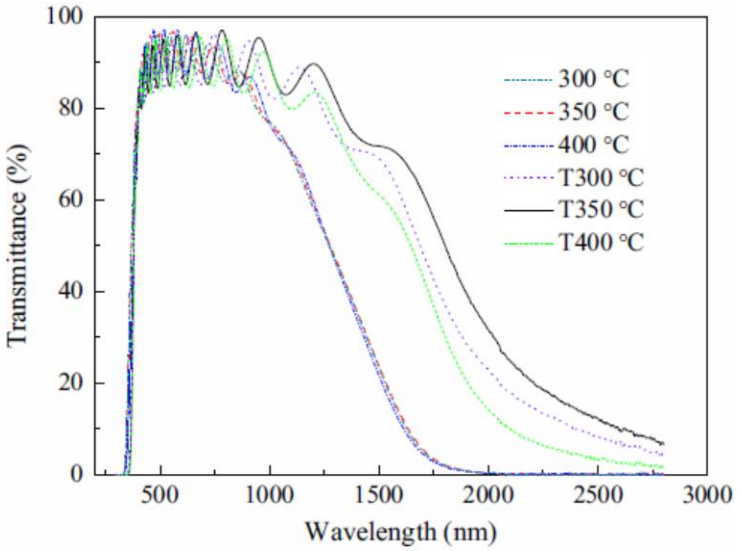

Figure 4. Optical transmittance of GZO films (Li Gong, et al., 2014).

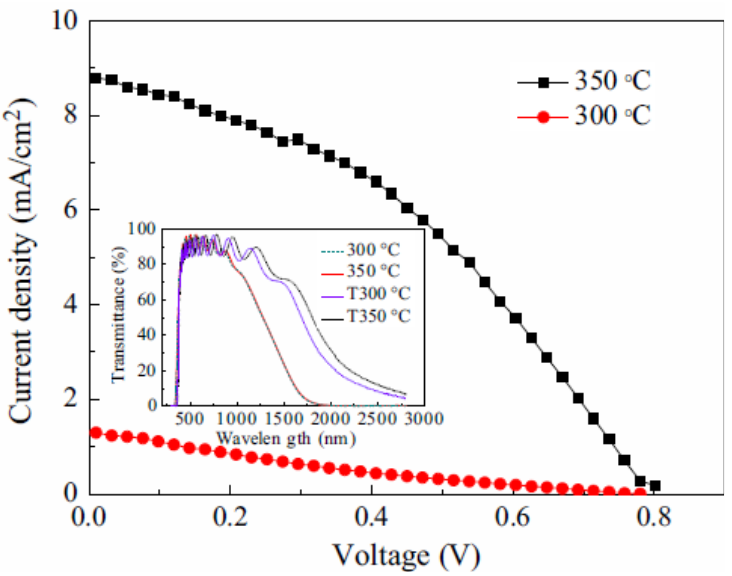

Figure 5. Current density and voltage characteristics of DSSCs fabricated on GZO (Li Gong, et al., 2014).

2.2. W-Doped In_2O_3 Thin Films

W-doped In2O3 thin films are transparent conducting films having high mobility. The mobility is a very important parameter for TCOs because conductivity increases with increase in mobility without sacrificing the transparency. The In2O3W (IWO) was studied for its application on heterojunction solar cells. Here, this film serves as an anti-reflection coating

and a conductive layer on the front surface of heterojunction solar cells. The IWO thin films were prepared on glass substrates by reactive plasma deposition techniques. The thickness of these IWO films deposited on glass substrate is 1μm. As shown in Figure 6, the transmittance increases for 70% to 95% in the near infrared region.

The IWO conductive film when applied to heterojunction solar cells gives a conversion efficiency of 20.8% under optimized experimental conditions.

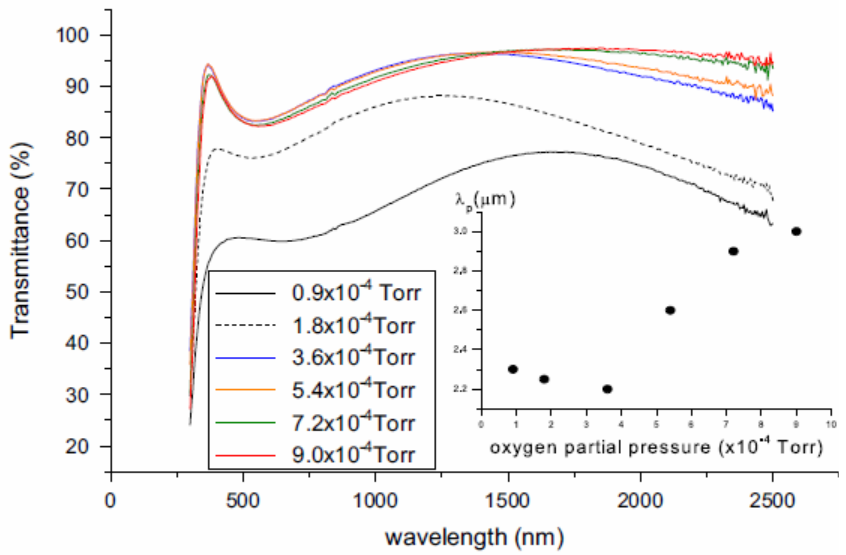

Figure 6. Optical transmittance of IWO films (Fanying Meng, et al., 2014).

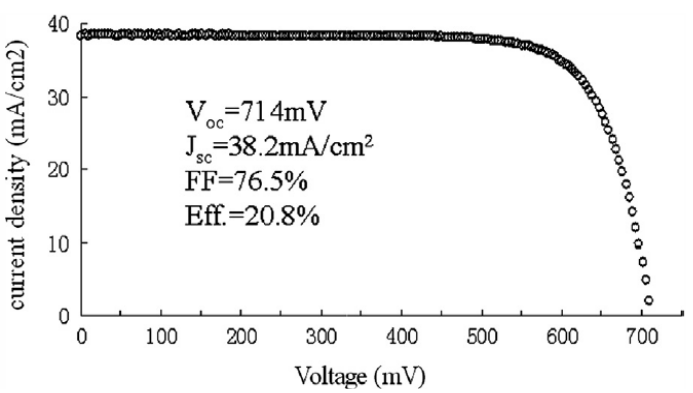

Figure 7. Current density-voltage characteristics of heterojunction solar cell utilizing an optimized IWO layer (Fanying Meng, et al., 2014).

2.3. ZnMgO/ITO Multilayer Thin Films

Multi-junction structures such as triple or quadruple junction thin film solar cells have recently been used for better spectral utilizations. ZnMgO alloy has higher transmittance and wider band gap. The texture etched $Zn_{0.65}Mg_{0.35}O$ film as a light scattering window layer is

shown in Figure 8. The thin ITO film having a thickness of 50nm was coated on $Zn_{0.65}Mg_{0.35}O$ textured layer as an electrically conducting layer. It is noted that the transmittance of ZnMgO films improved with increase in Mg concentration due to increase in the band gap of the films from the increase of the MgO portion of the film. As doping is not applied on these films the optical transmission in visible and near infrared wavelength regions is very good as shown in Figure 9.

The Zn0.65Mg0.35O/ITO substrate for microcrystalline silicon solar cells were shown to be an efficiency of 9.73% with the proper anti-reflection coating. The results indicate that the Zn0.65Mg0.35O/ITO multilayer front contact can be beneficial for reinforcing performances of silicon-based thin film solar cell devices (Dong-Won Kang, et al., 2015).

2.4. Cadmium Telluride (CdTe) Thin Film

CdS/CdSe films were prepared by pulsed laser deposition technique for CdTe solar cells. It is considered as one of the most promising thin film solar cell material. The theoretical conversion efficiency of CdTe polycrystalline thin film solar cell is 28%. Recently, multi layered structure attracts more attention because the optical properties can be enhanced and charge transfer characteristics in the surface and interface regions of hetero-structure can also be improved.

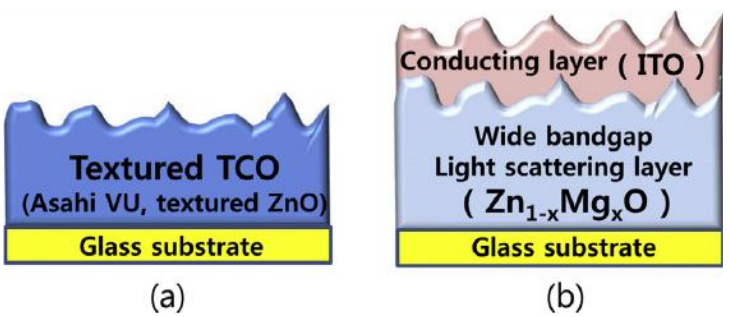

Figure 8. Structures of substrates (Dong-Won Kang, et al., 2015).

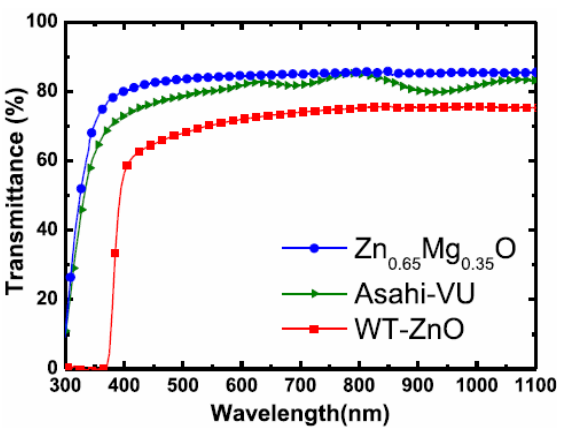

Figure 9. Transmittance of $Zn_{0.65}Mg_{0.35}O$ film (Dong-Won Kang, et al., 2015).

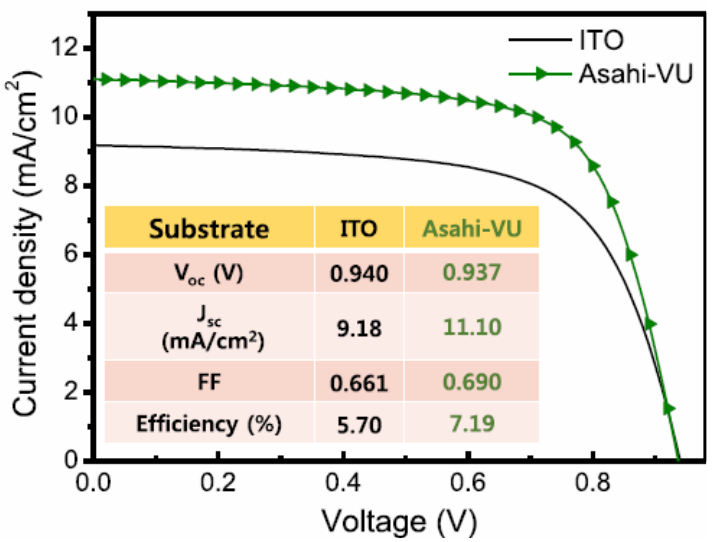

Figure 10. Current density-voltage characteristics of $Zn_{0.65}Mg_{0.35}O$ film (Dong-Won Kang, et al., 2015).

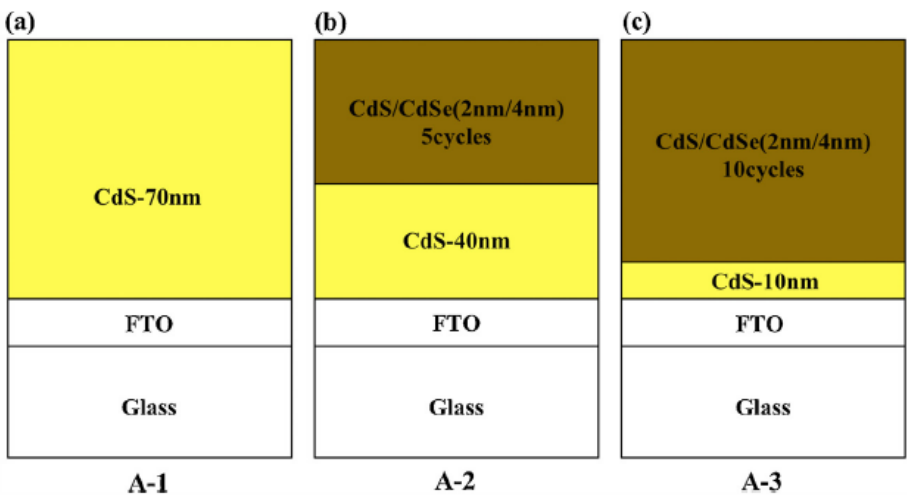

Figure 11. Schematic illustration of the three window layers (Xiaoyan Yang, et al., 2016).

Hence, a novel composite window structure for CdTe thin film solar cells was designed. In the CdS/CdSe composite layer the thickness of CdS layer is 2nm and that of CdSe layer is 4 nm as shown in Figure 11.

The Figure 12 shows the graph of transmittance vs. Wavelength of CdTe thin films for different thickness of CdS layer and Figure 12 describes the Current density-voltage characteristics of CdTe thin film solar cell. The composite window layer showed a conversion efficiency of 12.61%.

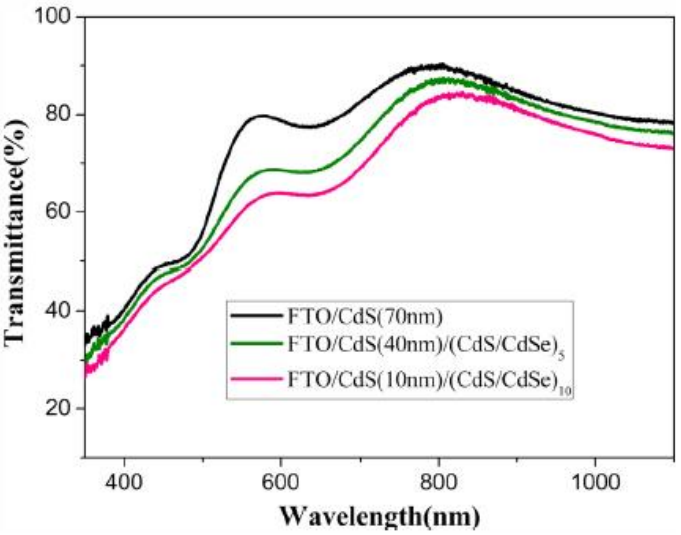

Figure 12. Transmittance of CdTe thin film solar cell (Xiaoyan Yang, et al., 2016).

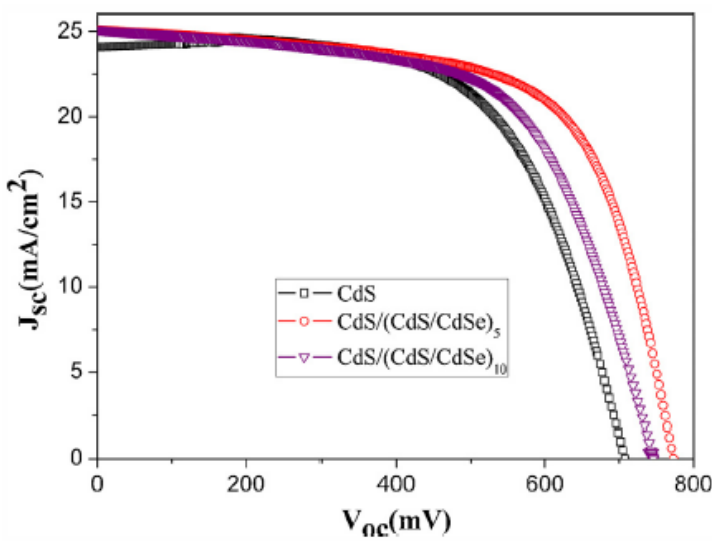

Figure 13. Current density-voltage characteristics of CdTe thin film solar cell (Xiaoyan Yang, et al., 2016).

3. Comparative Analysis of Selected Materials

The materials discussed above have been compared with respect to the properties like transmitivity, efficiency, current density and voltage. The Table 1 shows the Performance comparison of different materials like Ga-doped ZnO thin film, W-doped In_2O_3 thin film, ZnMgO/ITO multilayer thin film and CdTe thin film and from this comparison it is cleared that the efficiency of the W-doped In_2O_3 thin film material is highest amongst them i.e., 20.8%. The efficiency increases with increase in current density as indicated in the Table 1. Also based on voltage, the material with lowest voltage gives better efficiency.

Table 1. Performance comparison of different film materials for solar windows application

Material		Ga-doped ZnO thin film	W-doped In_2O_3 thin film	ZnMgO/ITO multilayer thin film	CdTe thin film
Properties		Thermally stable, non-toxic	High mobility, anti-reflection coating	Texture etched, wider band gap	Good crystallinity
Performance	1. Efficiency (%)	4.56	20.8	9.73	12.61
	2. Maximum Transmittance (%)	96	95	83	89
	3. Current density (mA/cm^2)	8.8	38.2	13.8	25.11
	4. Voltage (V)	0.8	0.714	0.962	0.772

CONCLUSION

Based on the study of various transparent thin film materials for glass substrates the following points are enlightened. The film materials, when used for solar windows will help to save a lot of conventional energy. Considered four thin films are highly transparent, conductive and have a better energy conversion efficiency compared to other existing materials. These composite layered thin transparent films are very effective because they do not require any extra space for their installation unlike the solar panels which have been installed till date. These thin films serve to be the most promising thin film solar cells and a viable structure of these window layers can have a positive impact on the solar cells. The thin film material having higher current density has higher efficiency. The transparent thin film material having lower voltage has higher efficiency. The transmittance of different film materials may vary from material to material. Based on the performance comparison it is found that W-doped In_2O_3 thin film material has highest efficiency of 20.8%.

REFERENCES

Da-Young Cho, Ki-Hyun Kim, Tae-Woong Kim, Yong-Jin Noh, Seok-In Na, Kwun-Bum Chung, Han-Ki Kim,(2015) Transparent and flexible amorphous InZnAlO films grown by roll-to-roll sputtering for acidic buffer free flexible organic solar cells, *Organic electronics* 24, 227-233.

Do Hoon Kim, Ji-Hyeon Park, Tae Il Lee, Jae-Min Myoung, (2016) Super hydrophobic Al-doped ZnO nano rods-based electrically conductive and self-cleanable anti-reflecting window layer for thin film solar cell, *Solar Energy Materials and Solar Cells* 150, 65–70.

Dong-Won Kang, Amartya Chowdhury, Porponth Sichanugrist, Yusuke Abe, Hirofumi Konishi, Yuki Tsuda, Tomohiro Shinagawa, Hidetada Tokioka, Hiroyuki Fuchigami, Makoto Konagai,(2015) Highly transparent ZnMgO/ITO multilayer for window of thin film solar cells, *Current Applied Physics* 15, 1022-1026.

Fanying Meng, Jianhua Shi, Zhengxin Liu, Yanfeng Cui, Zhongdan Lu, Zhiqiang Feng,(2014) High mobility transparent conductive W-doped In2O3 thin films prepared at

low substrate temperature and its application to solar cells, *Solar Energy Materials and Solar Cells* 122, 70–74.

Hongmei Dang, Vijay P. Singh, Sai Guduru, Jeffery T. Hastings,(2016) Embedded nano wire window layers for enhanced quantum efficiency in window-absorber type solar cells like CdS/CdTe, *Solar Energy Materials and Solar Cells* 144, 641-651.

Li Gong, YunzhenLiu, XiuquanGu, JianguoLu, JieZhang, ZhizhenYe, ZhaoyongChen, LingjunLi,(2014) Study on the thermal stability of Ga-doped ZnO thin film: A transparent conductive layer for dye-sensitized TiO2 nano particles based solar cells, *Materials Science in Semiconductor Processing* 26, 276–281.

Ngoc Minh Le, Byung-Teak Lee, (2016) ZnMgBeO/Ag/ZnMgBeO transparent multilayer films with UV energy band gap and very low resistance, *Ceramics International* 42, 5258–5262.

Sujaya Kumar Vishwanath, Won-Yong Jin, Jae-Wook Kang, Jihoon Kim,(2015) Polymer assisted solution processing of Ti-doped indium oxide transparent conducting oxide thin films for organic solar cells, *Journal of Alloys and Compounds* 631, 67-71.

W. Favre, J. Coignus, N. Nguyen, R. Lachaume, R. Cabal, D. Munoz,(2013) Influence of the Transparent conductive oxide layer deposition step on electrical properties of silicon heterojunction solar cells, *Appl. Phys. Lett.* 102, 181118-1-4.

Wei Xu, Qingsong Xu, Qijin Huang, Ruiqin Tan, Wenfeng Shen, Weijie Song,(2016) Fabrication of Flexible Transparent conductive films with silver nano wire by vaccum filtration and PET Mould transfer, *Journal of Materials Science and Technology* 32, 158-161.

Woojin Lee, Taehyun Hwang, Sangheon Lee, Seung-Yoon Lee, Joonhyeon Kang, Byungho Lee, Jinhyun Kim, Taeho Moon, Byungwoo Park,(2015) Organic-acid texturing of transparent electrodes toward broad band light trapping in thin-film solar cells, *Nano Energy* 17, 180–186.

Xiaoyan Yang, Bo Liu, Bing Li, Jingquan Zhang, Wei Li, Lili Wu, Lianghuan Feng,(2016) Preparation and characterization of pulsed laser deposited a novel CdS/CdSe composite window layer for CdTe thin film solar cell, *Applied Surface Science* 367, 480–484.

Y. Hu, B. Caia, Z. Huc, Y. Liua, S. Zhanga, H. Zenga, (2015), The impact of Mg content on the structural, electrical and optical properties of MgZnO alloys: a first principles study, *Curr. Appl. Phys*. 15, 383-388.

Yanfeng Wang, Xiaodan Zhang, Xudong Meng, Yu Cao, Fu Yang, Jingyu Nan, Qinggong Song, Qian Huang, Changchun Wei, Jianjun Zhang, Ying Zhao, (2015) Simulation, fabrication, and application of transparent conductive Mo-doped ZnO film in a solar cell, *Solar Energy Materials and Solar Cells.*

In: Renewable Energy Systems
Editor: Sandip A. Kale
ISBN: 978-1-53610-423-3

Chapter 4

PERFORMANCE EVALUATION OF A DOMESTIC PASSIVE SOLAR FOOD DRYER

Collins N. Nwaokocha[1,*], Oguntola J. Alamu[2], Olayinka Adunola[3], Solomon O. Giwa[4] and Adeyemi A. Adeala[4]

[1,4]Mechanical Engineering Department,
Olabisi Onabanjo University, Ibogun Campus, Nigeria
[2]Mechanical Engineering Department,
Osun State University, Osogbo, Nigeria
[3]Mechanical Engineering Department,
Federal University of Agriculture, Abeokuta, Nigeria
[5]Mechanical Engineering Department,
Vaal University of Technology, Vanderbijlpark, South Africa

ABSTRACT

The use of solar energy in Nigeria is very favourable. Nigeria, located between latitude 4°16"N and13°32"N, is endowed with abundant sunshine all year round, with daily sunshine hours in the southern part averaging about 8 hours during dry season and about 4hours during wet season. On this premise, a domestic passive solar food dryer was designed. The design was based on the geographical location which is Abeokuta and meteorological data were obtained for proper design specification. Locally available materials were used for the construction, chiefly comprising of wood (gmelina), polyurethane glass, mild steel metal sheet and net cloth for the trays. The result obtained from the testing showed that a temperature of 60°C (which is the designed optimum temperature) is attainable and that the highest temperature 60°C recorded was at 2.00pm. An average temperature of 52.8°C, was obtained for a typical sunshine day, which is suitable as the drying temperature for most food crops. 4kg of sweet pepper (Capsicum spp.) and 8kg of yam chips and peelings (Discorea spp.) were dried and the percentage moisture removed was 78.6% and 64% respectively.

*E-mail: collinsnwaokocha@gmail.com.

Keywords: solar energy, moisture content, peelings, solar dryer

1. INTRODUCTION

Drying of agricultural produce is a significant operation in the food processing system and food material handling system. The basic essence of drying is to reduce the moisture content of the product to a safe level that prevents deterioration over a certain period of time, regarded normally as the "safe storage period." Drying was probably the first ever food preserving method used by man, even before cooking. In technical terms, drying in its simple and direct application, is a heat and mass transfer process, involving vapourisation of water in the liquid state, mixing the vapour with the drying air and removing the vapour by naturally or mechanically carrying away the mixture, which is often vapour and moisture, that finally leads to a stable nature of the agricultural produce before further processing, storage or transport(Ekechukwu, 2010; Eze, 2010; John, et al., 2014; Sharma et al., 1987).

The application of solar energy to produce high temperature dates back to ancient times. Solar energy has been used by man since the beginning of time for heating his environ, for agricultural purposes and for personal ease. Historians believe that Archimedes, a Greek mathematician of the 2nd century BC, set fire on Roman ships by concentrating the ray of the sun on them using flat mirrors. In 1774, the French chemist Antoine Lavoisier built a solar furnace with a lens 1.2m in diameter. His furnaces reached a temperature of 3092^{o}F (1700^{o}C). Also, the same year, Joseph Priestly used lenses to concentrate rays to decompose oxide of mercury into mercury and oxygen (Alamu, et al., 2010; Dorf, 1978; Eze, 2010; Nandi, 2009; Nordin, et al., 2014).

In 1872, in the desert of North Chile, a solar distillation unit was built covering 4750sq meters of land to provide fresh water from salt water. This plant operated for 40 years producing 6,000 gallons of water per day (Dorf, 1978). Also, during the period 1870's and 1880's, the Swedish-American engineer, John Ericson, tried to develop a system to convert solar energy into mechanical energy. One of his developed device supposedly produced 1hp (746W) for each space of 9.3m^2 of collecting surface.

Modern research on the use of solar energy started around the 1930's. Research outcomes include the invention of a solar boiler by Charles G. Abbot an American physicist and the start of the Godfrey Cabot solar programmes at Harvard University and the Massachusetts Institute of Technology (The World Book Encyclopedia, 1982). Small powered steam engines were also developed between the period of 1930 to 1960. But, there was difficulty in marketing them in competition with engines running on inexpensive gasoline (Dorf, 1978). In 1954, Bell Telephone Laboratories developed a solar battery. The same year, solar energy scientists in the United States formed the Association for Applied Solar Energy to investigate ways to harness the sun's energy (Olaleye, 2008; The World Book Encyclopedia, 1982).

During the mid 1970's crises of shortages of oil and natural gas, increase in the cost of fossil fuels and the depletion of other resources stimulated efforts in the United States to deploy solar energy into a practical power source. Thus, interest was rekindled in harnessing renewable energy sources to help in bridging the gap between the increasing energy demand and dwindling energy supply. An example is the use of solar energy for heating and cooling the generation of electricity and other purposes. In 1974, the United States Congress passed

the Solar Energy Research, Development and Demonstration Act. The systems for collecting, concentrating and storing energy form the sun (The World Book Encyclopedia, 1982).

1.1. From Primitive Drying to Solar Drying

An age long means of preserving agricultural produce is by means of drying. Drying is an excellent way to preserve agricultural produce and in more recent time, solar food dryers are appropriate food preservation technology for sustainable development. Drying involves the removal of moisture from agricultural produce so as to provide a product that can be safely stored for longer period of time. Sun drying is the earliest mode of drying farm produce ever known to man and it involves simply laying the agricultural products in a space available to the sun rays using various means such as mats, roofs or drying floors (Alamu, et al., 2010; John, et al., 2014; Nordin, et al., 2014; Scalin, 1997).

The disadvantages associated with this method is enormous, since the farm produce are laid in the open sky, there is a greater risk of contamination and spoilage due to adverse climatic conditions such as rain, wind, moist, dust, loss of produce to birds, insects and rodents (pests); totally dependent on good weather and very slow drying rate with danger of mold growth thereby causing deterioration and decomposition of the produce. The process also requires a large area of land, takes time and its highly labour intensive. With cultural and industrial development, artificial mechanical drying came into practice, but this process is highly energy intensive and expensive which ultimately increases product cost. Recently, efforts to improve "sun drying" have led to "solar drying." In solar drying, solar dryers are specialized devices that handle and control the drying process and protect agricultural produce from damage by insects, pests, dust and rain. In comparison to natural "sun drying," the use of solar dryers generate higher temperatures, lower relative humidity, lower product moisture content and reduced spoilage during the drying process. In addition, it takes up less space, takes less time and relatively inexpensive compared to artificial mechanical drying method. Thus, solar drying is a better alternative solution to all the drawbacks of natural drying and artificial mechanical drying (Alamu, et al., 2010; GEDA, 2003; John, et al., 2014; Nordin, et al., 2014).

The solar dryer can be seen as one of the solutions to the world's food and energy crises. With drying, most agricultural produce can be preserved and this can be achieved more efficiently through the use of solar dryers. Solar dryers are a very useful device for:

- Agricultural crop drying.
- Food processing industries for dehydration of fruits and vegetables.
- Fish and meat drying.
- Dairy industries for production of milk powder.
- Seasoning of wood and timber.
- Textile industries for drying of textile materials, etc.

Thus, the solar dryer is one of the many ways of making use of solar energy efficiently in meeting man's demand for energy and food supply.

1.2. Capturing Solar Energy

The use of solar drying as a means of food preservation seems to be the most promising and modest approach for preservation of various agricultural products. In solar drying, solar energy (which is a rewenable energy source) is used as either the sole source of the required heat or as a supplemental source. Solar radiation can be converted either into electrical energy or thermal energy (heat). The use of solar drier is an energy efficient option in the drying processes (Pangavhane and Sawhney, 2002). Literatures abound with various methods used for drying of agricultural materials using solar drier for copra drying, for onion drying, and for pineapple drying(Jain and Jain, 2004; Mohanraj & Chandrasekar, 2008a, 2008b, 2009a; Sarsavadia, 2007). The use of forced convection solar driers seems to be an advantage compared to traditional methods and this improves the quality of the product considerably well. In such cases, thermal storage systems are employed to store the heat, which includes sensible and latent heat storage. Common sensible heat storage materials used to store the sensible heat are water, gravel bed, sand, clay, concrete, etc. (Ahmad, et al. 1996; Hawlader, et al., 2003; Mohanraj & Chandrasekar, 2009b; Midilli, 2001; Shanmugam & Natarajan, 2007; Sohda, et al. 1985).

An earlier developed solar dryer is the reflector type solar cooker. However, a reflector type solar cooker did not become popular due to its inherent defects, e.g., it required tracking towards the Sun every ten minutes, cooking could be done only in the middle of the day and only in direct sunlight, its performance was greatly affected by dust and wind, there was a danger of the cook being burned as it was necessary to stand very close to the cooker when cooking and the design was complicated. These defects were taken care of in the hot box type solar cooker. Different types of solar cookers have been tested and the solar oven has been found to be of best performance. Though the performance of the solar oven is very good but it also requires tracking towards the Sun every 30 minutes, it is too bulky and is costly. Therefore, the hot box solar cooker with a single reflector is being promoted. This chapter focused on the application of thermal collectors for conversion into heat energy or photovoltaic collectors for conversion into electrical energy. Two main collectors were used to capture solar energy and to convert it to thermal energy, these collectors are a flat plate collectors and concentrating collectors. For this chapter, flat plate collectors which are also known as non-focusing collectors will be considered (Alamuet al., 2010; Dorf, 1978; Eze, 2010; Eze & Agbo, 2011; Nahar, 2009; Olaleye, 2008).

1.3. Importance of Solar Dried Food

For centuries, people of various nations have been preserving fruits, other crops, meat and fish by drying. Drying is also beneficial for hay, tea and other income producing non-food crops. With solar drying almost available everywhere, the availability of all these farm produce can be greatly increased. It is worth noting that until around the end of the 18thcentury when canning was developed, drying was virtually the only method of food preservation. The energy input for drying is less than what is needed to freeze or can, and the storage space is minimal compared with that needed for canning jars and freezer containers. It

was further stated that the nutritional value of food is only minimally affected by drying. Also, food scientists have found that by reducing the moisture content of food to 10 to 20%,bacteria, yeast, mold and enzymes are all prevented from spoiling the food content. Microorganisms are effectively killed when the internal temperature of food reaches 145°F. Thus, the flavour and most of the nutritional value of dried food is preserved and concentrated. Dried foods may not necessarily require any special storage equipment and are easy to transport. Dehydration of vegetables and other food crop by traditional methods of open-air sun drying is not satisfactory, because the products deteriorate rapidly. Various studies showed that agricultural produce dried in a solar dryer were superior to those which are directly sun dried when evaluated in terms of taste, colour and mold counts. Solar dried foods are quality products that can be stored for extended periods, easily transported at less cost while still providing excellent nutritive value(Alamu,et al., 2010; Ayensu, 2000; Eze, 2010; Eze & Agbo, 2011; GEDA, 2003; Herringshaw, 1997; John, et al., 2014; Nandi, 2009; Nordin, et al., 2014; Olaleye, 2008; Scalin, 1997; Whitefield, 2000).The performance of a domestic passive solar dryer with improvement in heat energy storage and reduced drying time are discussed in this chapter.

2. MATERIALS AND METHODS

A domestic passive solar food dryer was designed and constructed at the College of Engineering, University of Agriculture, Abeokuta, Nigeria. The solar dryer is designed to have a solar collector (air heater) and a solar drying chamber containing racks of four cheese cloth (net) trays which is integrated together. The air is allowed to pass through the air inlet and heated up in the solar collector and then channelled through the drying chamber where it is utilized in drying (that is removing the moisture content from the food substance or the loaded agricultural produce). The design took into cognizance the geographical location which is Abeokuta and meteorological data of the location was obtained for proper design specification. Locally source materials were used for the construction, comprising of wood (gmelina), polyurethane glass, mild steel metal sheet and net cloth for the trays (Alamu, et al., 2010).

2.1. Description of the Solar Food Dryer

The most commonly design types of Solar Dryer are of cabinet type (having wooden boxes with glass cover), some types are even improved making use of cardboard boxes and transparent nylon or polythene. For the design reported in this chapter (Figure 1), consideration is given to the greenhouse effect and thermosiphon principles are the theoretical basis. There is an air vent (or inlet) to the solar collector where air enters and is heated up by the greenhouse effect, thereafter hot air rises through the drying chamber passing through the trays and around the food, removing the moisture content and exits through the air vent (or outlet) near the top of the shadowed side.

The hot air serves as the drying medium, which helps to extract and conveys the moisture from the produce (or food) to the atmosphere under free (natural) convection, thus the system

is a passive solar system and no mechanical device is required to control the intake of air into the dryer. The solar food dryer consists of two major compartment or chambers being integrated together:

- The solar collector compartment, which is also referred to as the air heater.
- The drying chamber, designed to accommodate four layers of drying trays made of netcloth (cheese cloth) on which the produces (or food) are laced for drying.

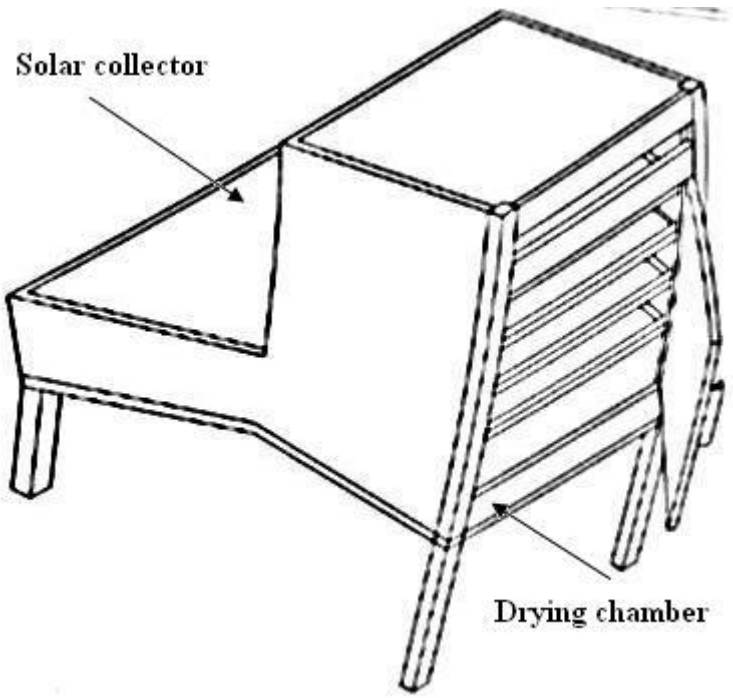

Figure 1. A schematic of the experimental setup.

2.2. Materials Used

The following materials were used for the construction of the domestic passive solardryer:

- Wood (gmelina) –this serves as the casing (housing) of the entire system; wood was selected because of its good insulating properties and its relatively cheaper than metals.
- Glass –serves as the solar collector cover and the cover for the drying chamber. It permits thesolar radiation into the system but resists the flow of heat energy out of the system.
- Mild steel sheet of 1mm thickness (dimension 80cm × 60cm) painted black with tar – to allow for absorption of solar radiation.
- Net cloth (cheese cloth) and wooden frames for constructing the trays.

- Nails and glue as fasteners and adhesives.
- Insect net at air inlet and outlet - to prevent insects from entering into the dryer.
- Hinges and handle for the dryer's door, to allow for easy movement.
- Paint (black and grey)–to allow for maximum absorption of heat energy and minimize the adverse effects of weather.

2.3. Design Consideration

1) Temperature - The minimum temperature for drying food is 30°C and the maximum temperature for drying food is 60°C, and so 45°C and above is considered average and normal for drying vegetables, fruits, roots and tuber crop chips, crop seeds and some other crops.
2) The design was made for the optimum temperature $T_0$for the solar dryer. T_0 of 60°C and the air inlet temperature or the ambient temperature T_1 = 30°C (approximately outdoor temperature).
3) Efficiency - This is defined as the ratio of the useful output of a device to the input of the device.
4) Air gap - It is suggested that for hot climate passive solar dryers, a gap of 5 cm should be created as air vent (inlet) and air passage.
5) Glass and flat plate collector – It is also suggested that the glass covering should be 4 - 5 m thick. In this work, 4mm thick transparent glass was used. It's also suggested that the metal sheet thickness should be between 0.8 – 1.0 m thickness; here a mild steel of 1.0mmthickness was used. The glass used as cover for the collector was 60 × 60cm^2.
6) Dimension – It is also recommended that a constant exchange of air and a roomy drying chamber should be attained in solar food dryer design, thus the design of the drying chamber was made as spacious as possible of average dimension of 60 × 57 × 55cm with air passage (air vent) out of the cabinet of 60 × 5cm^2. The drying chamber was roofed with glass of 60 × 60 cm tilted at the same angle with that of the solar collector (17.11°).This is to keep the temperature within the drying chamber fairly constant due to the greenhouse effect of the glass.
7) Dryer Trays - Net cloth was selected as the dryer screen or trays to aid air circulation within the drying chamber. Four trays were made of wooden edges. The tray dimension is 50 × 50cm of 2.5cm × 2.5cm wooden sticks used as frame.

In summary, the design of the dry chamber making use of wooden wall sides and a tilted glass top is to protect the food to be placed on the trays from direct sunlight since this is undesirable and tends to bleach colour, removes flavour and causes the food to dry unevenly (Alamu,et al., 2010; Sukhatme, 1996; Whitefield, 2000).

2.4. Design Calculations

1. Angle of Tilt (β) of Solar Collector/Air Heater.

It states that the angle of tilt (β) of the solar collector should be

$$\beta = 10^0 + \text{Lat}\phi \text{ (Sukhatme, 1996)} \quad (1)$$

where, Latϕ is the Latitude of the collector location.

2. Insolation on the Collector Surface Area.

$$I_c = H_T = HR \quad (2)$$

where, I_c=insolation on the collector surface
H = average daily radiation
R = average effective ratio

3. Determination of Collector Area and Dimension.

$$A_c = L \times B \quad (3)$$

4. Determination of the Base Insulator Thickness for the Collector.

The rate of heat loss from air is equal to the rate of heat conduction through the insulation. The following equation holds for the purpose of the design.

$$Fm_aC_p (T_0 - T_i) = K_a(T_a - T_b)/t_b \quad (4)$$

The side of the collector was made of wood, the loss through the side of the collector was considered negligible.

5. Determination of Heat Losses from the Solar Collector (Air Heater).

Total energy transmitted and absorbed is given by

$$I_cA_c\tau_\alpha = Q_u + Q_L + Q_s \quad (5)$$

where Q_s is the energy stored which is considered negligible therefore,

$$I_cA_c\tau_\alpha = Q_u + Q_L \quad (6)$$

Thus Q the heat energy losses

$$Q_L = I_cA_c\tau_\alpha - Q_u \quad (7)$$

Since

$$Q_u = m_aC_p (T_0 - T_i) = m_aC_p\Delta T \quad (8)$$

and

$$Q_L = U_L A_c \Delta T \quad (9)$$

then

$$U_L A_c \Delta T = I_c A_c \tau_\alpha - m_a C_p \Delta T \quad (10)$$

$$U_L = (I_c A_c \tau_\alpha - m_a C_p \Delta T)/(A_c \Delta T) \quad (11)$$

This heat loss includes the heat loss through the insulation from the sides and the coverglass.

Table 1. Summary of design calculations

S/N	Specification	Values
1	Angle of Tilt, β	$l7.11^0$
2	Insolation, I_c	982.11 W/m^2
3	Mass flow rate of air, M_a	5.76×10^{-3}kg/s
4	Collector Area, A_c	0.36 m^2
5	Base Insulator Thickness, t_b	7 cm
6	Heat Losses	100.01

2.5. Construction

The solar food dryer was constructed making use of locally available and relatively cheap materials. The entire casing is made of wood and the cover is made of glass, the major construction works is carpentry works by means of joinery. The following tools were used in measuring and marking out on the wooden planks:

- Carpenter's pencil.
- Steel tapes (push-pull rule type).
- Steel meter rule.
- Vernier caliper.
- Steel square.
- Scriber.

The following tools were also used during the construction:

- Hand-saws (Crosscut saw and Ripsaw).
- Jack plane.
- Wood chisel.
- Mallet and Hammer.
- Pinch bar and pincers.

The construction was made of simple butt joints using nails as fasteners and glue as adhesive where necessary. The construction was sequenced as follows for the wood work:

- Marking out on the planks to cut into desired shape.
- Cutting out the already marked out parts.
- Planning of cut out parts to smoothen the surfaces.
- Joining and fastening of the cut out parts with nails and glues.

The metal sheet used was mild steel of 1mm thickness. It was cut to the size of 80 ×60cm to minimize the top heat loss. It was painted black with tar for maximum absorption and radiation of heat energy. The metal sheet, together with the insulator of 7cm thickness, was placed inside the air heater (solar collector) compartment. The glass was cut into size of 60 × 60cm size and two of these were required, one for the solar collector's cover, and the other, as the drying cabinet cover. The glass used was clear glass with 4 mm thickness. The trays were made with wooden frames and net cloth to permit free flow of air within the drying cabinet (chamber). Four trays were used with average of 10cm spacing arranged vertically one on top of the other, the tray size was 56 × 52cm.The interior of the solar food dryer was painted black with tar to promote adsorption of heat energy while the exterior was painted gray to minimize the adverse effects of weather and insect attack on the wood and also for aesthetic appeal.

3. RESULTS

The open space (lawn) in front of the College of Engineering Building, University of Agriculture, Abeokuta, was selected as the site for the testing of the solar dryer. The site was selected to avoid obstruction by buildings casting shadows and also there is free movement of air (gentle breeze). The solar dryer was placed on the lawn with the collector facing South.

Several stages were involved in the testing which are:

i. Testing the solar food dryer when no food item is loaded to know the range of temperatures for which it can work and to know the maximum temperature attainable by the dryer (no load test).

A period of five days was used for this exercise. The air inlet temperature T_i allowed into the solar collector and the temperature of the drying chamber which is the air outlet temperature T_o from the solar collector (air heater) were taken with the aid of Mercury-in-glass thermometer (0 – 110^{o}C temperature range) and recorded.

ii. Test was also conducted while the solar dryer was loaded with selected food crops namely Sweet pepper *Capsium spp.* And Yam *Discorea spp.* respectively.

Table 2. Solar Dryer Temperature for Day 1

Time of the day	Air inlet temperature T_i(°C)	Air outlet temperature T_o(°C)
10.00	30	43
12.00	31	56
14.00	30	60
16.00	30	55
18.00	29	44

The average solar dryer temperature for the day T_o = 51.6°C.

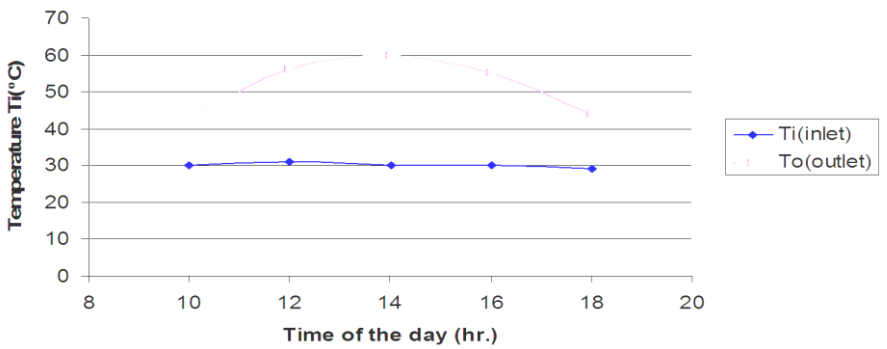

Figure 2. Graph of temperature against time for day 1.

Table 3. Solar Dryer Temperature for Day 2

Time of the day	Air inlet temperature T_i(°C)	Air outlet temperature T_o(°C)
10.00	29	44
12.00	30	55
14.00	31	60
16.00	30	58
18.00	30	47

The average solar dryer temperature for the day T_o = 52.8°C.

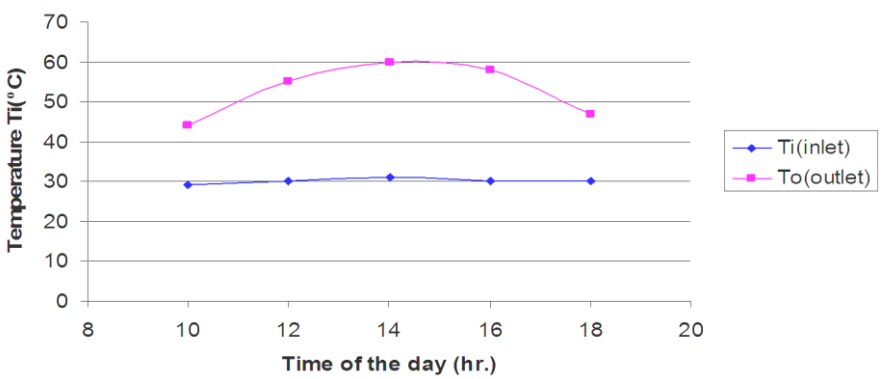

Figure 3. Graph of temperature against time for day 2.

Table 4. Solar Dryer Temperature for Day 3

Time of the day	Air inlet temperature T_i(°C)	Air outlet temperature T_o(°C)
10.00	30	45
12.00	30	56
14.00	30	60
16.00	30	57
18.00	30	46

The average solar dryer temperature for the day T_o = 52.8°C.

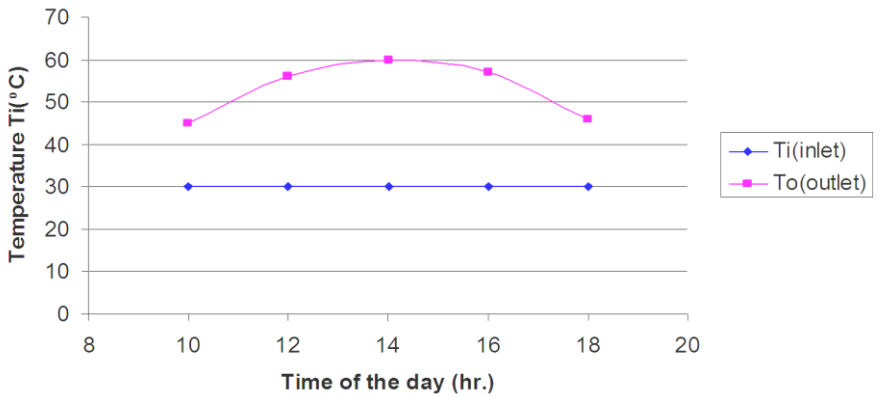

Figure 4. Graph of temperature against time for day 3.

Table 5. Solar Dryer Temperature for Day 4

Time of the day	Air inlet temperature T_i(°C)	Air outlet temperature T_o(°C)
10.00	30	44
12.00	30	57
14.00	31	60
16.00	30	58
18.00	29	47

The average solar dryer temperature for the day T_o = 53.2°C.

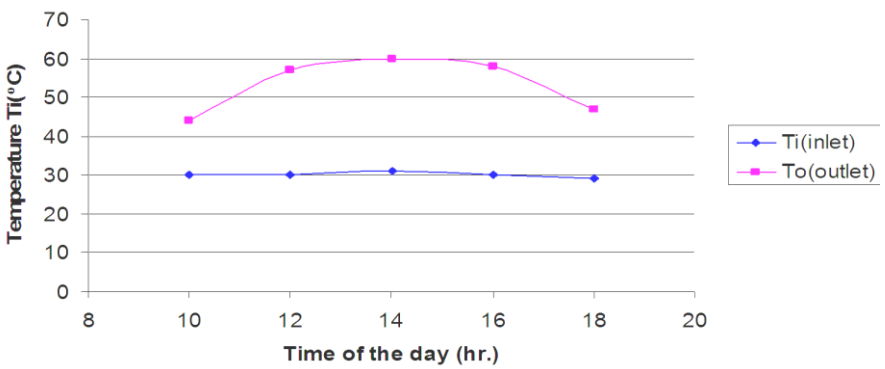

Figure 5. Graph of temperature against time for day 4.

Table 6. Solar Dryer Temperature for Day 5

Time of the day	Air inlet temperature T_i(^{o}C)	Air outlet temperature T_o(^{o}C)
10.00	29	46
12.00	30	57
14.00	31	60
16.00	30	56
18.00	30	46

The average solar dryer temperature for the day To = 53.3^{0}C.

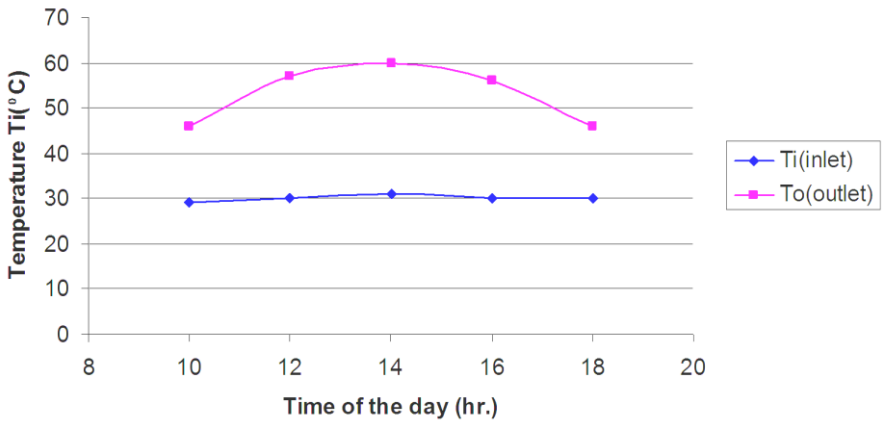

Figure 6. Graph of temperature against time for day 5.

The solar dryer was loaded with 4kg of sweet pepper and the mass of the sample was checked after drying in the solar dryer everyday until a constant mass was achieved. Then, all the removable moisture content must have been removed when the dry mass of produce was constant.

Table 7 shows the results obtained at the end of the drying days for the percentage moisture content for Sweet Pepper sample.

Table 7. Moisture Content Measurement for Sweet Pepper Sample

Day	Mass before drying (kg)	Mass after drying (kg)
1	4.00	3.22
2	3.22	2.58
3	2.58	2.30
4	2.30	2.27
5	2.27	2.24
6	2.24	2.24

In determining the moisture content, the quantity of moisture present in the material can be represented on wet basis and expressed as a percentage. The initial mass, M_i, and final mass, M_f, of the samples were recorded. The percentage moisture content was calculated by

using Equation (12). The procedure was repeated for every one hour interval till the end of drying.

$$\%\,\text{Moisturecontent} = \frac{\text{mass of water removed}}{\text{mass of dry sample}} = \frac{M_i - M_f}{M_f} \times 100 \tag{12}$$

The solar dryer was also loaded with yam chips and peelings of 8kg and of average 5 – 10mm thickness. The mass of the sample was measured and recorded everyday after solar drying.

Table 8 explains the results obtained at the end of the drying days for the percentage moisture content for Yam chips sample.

Table 8. Moisture Content Measurement for Yam chips Sample

Day	Mass before drying (kg)	Mass after drying (kg)
1	8.00	6.50
2	6.50	5.20
3	5.20	4.84
4	4.84	4.84

$$\%\,\text{MoistureContent} = \frac{M_i - M_f}{M_f} \times 100 \tag{13}$$

Note: m_i is the initial mass of produce before drying and m_f is the final mass of produce after drying.

Thus for the Sweet pepper *Capsium spp.* approximately 79% moisture content was removed by solar drying and for the Yam chips and peelings approximately 64% moisture content was removed by solar drying.

4. DISCUSSION

With the result obtained from the no load test, it can be observed that the maximum temperature of 60°C for which the solar dryer was designed for is attainable and can be noticed at the peak hour of sunshine period (solar time) which is around 1.00pm – 2.00pm.

Also an average drying temperature T_o of 52.68°C (average of the average temperature) can be obtained from the readings which are also within the range of the working temperature of the solar dryer to efficiently dry notable agricultural produce.

The test was conducted during the beginning of the dry season, this made the results favourable, and since the design was even made for the condition of average possible insolation in Abeokuta. Also, it is the period in which most agricultural produce which are known to contribute to wastage are harvested.

It can also be deduced that if the two selected crops namely sweet pepper and yam can be successfully dried, then all other agricultural produce and varieties in food crops can be dried

successfully by the solar dryer. Other agricultural produce recommended for drying in the solar dryer included:

- Leafy vegetables like bitter leaf, spinach, *Celosia spp.* etc.
- Fruit vegetables like pepper, onion, carrot, etc.
- Fruit crops like banana, plantain, apple, mango, etc.
- Roots and tuber crops like cassava, sweet potato, Irish potato.
- And seeds of cereal and legume crops.

It was also observed that drying of the yam chips and peelings was completed in 3 days using a solar dryer, whereas if it was sun dried (i.e., open sun dryer), it might have taken 4-5 days. Also, drying of the sweet pepper took 5days, which might have taken 7-8 days if it was dried in the open sun.

Thus, the solar dryer was seen to have minimized the drying time. It is also easily controlled and monitored (the trays were rotated at intervals during drying to allow for uniform drying).

It has also minimized the floor space on which the four trays would have been spread into 4 layers of trays in the drying chamber.

There is no cause of looking out for pest and wandering animals which might feed on the produce. The risk of contamination of the agricultural produce was also minimized.

CONCLUSION

In rekindling the interest in harnessing renewable energy sources to help in bridging the gap between the increasing energy demand and dwindling energy supply in the agricultural sector, the use of solar radiation can be effectively and efficiently utilized for drying of agricultural product. Proper design and procedures should be followed. This was well demonstrated in this chapter and the solar dryer exhibited sufficient ability to dry agricultural produce most especially food items to appreciable reduced moisture level and increased drying time.

Locally sourced materials were used in constructing the solar dryer so as to allow for affordability by peasant farmers. If the solar food dryer can be adopted and efficiently utilized, it will go a long way to help in reducing food wastage, food spoilage and at the same time food shortages, since it can be used extensively for majority of the agricultural food crops. This on the long run will a positive impact on the standard of living of rural dwellers and peasant farmers.

Aside this, solar energy is required for the solar dryer operation which is readily available in the tropics, and it is also a clean form of energy thereby promoting the health and welfare of the people. It also protects the environment to a large extent, since it's a green energy source. It also help save cost and time spent on open sun drying of agricultural produce since it dries food items faster. The food items are also well protected in the solar dryer than in the open sun, thus minimizing contamination by pest and insect attack.

However, the performance of existing solar food dryers can still be improved upon especially in the aspect of enhancing reduced drying time and probably storage of heat energy

in the system. Also, information on climate change and other meteorological data should be readily available to users of solar products to help in ensuring maximum efficiency and effectiveness of the system. Such information will help a local farmer to determine when to dry his agricultural produce or otherwise.

REFERENCES

Ahmad A., Saini J. S. and Varma H.K. (1996).Thermohydraulic Performance of Packed Bed Solar Air Heaters. *Energy Conversion and Management,* 37(2): 205-214.

Alamu, Oguntola J., Nwaokocha, Collins N. &Adunola Olayinka (2010).Design and Construction of A Domestic Passive Solar Food Dryer, *Leonardo Journal of Sciences,* 16: 71 – 82.

Ayensu A. (2000).Dehydration of Food Crops Using Solar Dryer with Convective Heat Flow,2000, Research of Department of Physics, University of Cape Coast, Ghana.

Dorf, R. G. (1978).“Energy, Resources and Policy.” Addison Werley Publishing Company, Massachusetts.

Ekechukwu, O. V. (1987). Experimental Studies of Integral-type Natural-Circulation Solar-energy. Tropical Crop Dryers. Ph.D Thesis, Cranfield Institute of Technology, United Kingdom.pp.23-52.

Ekechukwu V.O. (2010).Solar Drying Technology: An Overview, Paper presented at FUTO Alternative Energy Conference, Federal University of Technology Owerri. 16th 20 May 2010.

Eze J. I. (2010). Evaluation of the efficacy of a family sized solar cabinet dryer in food preservation, *American Journal of Scientific and Industrial Research,* 1(3): 610-617. doi:10.5251/ajsir.2010.1.3.610.617.

Eze J. I. &Agbo K. E. (2011). Comparative Studies of Sun and Solar Drying of Peeled and Unpeeled Ginger, *American Journal of Scientific and Industrial Research,* 2(2): 136-143. doi:10.5251/ajsir.2011.2.2.136.143.

Fisk M. J. and Anderson H. C. (1982).Introduction to Solar Technology, Addison-Wesley Publishing Company Inc., Massachusetts.

GEDA-Gujarat Energy Development Agency, 2003, www.geda.com.

Hawlader M.N.A., Uddin M. S. and Khin M.M. (2003).Microencapsulated PCM Thermal Energy Storage System. *Applied Energy,* 74 (I-2), 195-202.

Herringshaw D. (1997).All About Food Drying, The Ohio State University ExtensionFactsheet-hyg-5347-97, www.ag.ohio-state.edu/.

Jain D. and Jain R.K. (2004).Performance evaluation of an inclined multipass solar air heater with in-built thermal storage on deep-bed drying application. *Journal of Food Engineering*,65(4): 497–597.

John A. Mathews, Mei-Chih Hu &Ching-Yan Wu (2014).Concentrating Solar Power: A Renewable Energy Frontier, *Carbon Management,* 5(3): 293-308.doi: 10.1080/17583004. 2014.987492.

Midilli A. (2001). Determination of pistachio drying behavior and conditions in a solar drying system. *International Journal of Energy Research*, 25(8): 715-725.

Mohanraj M. and Chandrasekar P. (2008a).Drying of Copra in a Forced Convection Solar Drier.*Bio-Systems Engineering,* 99(4): 604-607.

Mohanraj M. and Chandrasekar P. (2008b).Comparison of drying characteristics and quality of copra obtained in a forced convection solar drier and sun drying. *Journal of Scientific and Industrial Research,* 67(5), 381-385.

Mohanraj M. and Chandrasekar P. (2009a).Performance of a solar drier with and without heat storage material for copra drying. "Special issue onRecent trends in solar energy technology*." International Journal of Global Energy Issues,* 32(2): 112-121.

Mohanraj M. and Chandrasekar P. (2009b).Performance of a Forced Convection Solar Drier Integrated with Gravels as Heat Storage Material for Chili Drying, *Journal of Engineering Science and Technology*, Vol. 4, No. 3, 305 – 314.

Nahar N. M. (2009). Design and Development of a Large Size Non-Tracking Solar Cooker, *Journal of Engineering Science and Technology,* Vol. 4, No. 3, 264 – 271.

Nandi P. (2009).Solar Thermal Energy Utilization in Food Processing Industry in India, *Pacific Journal of Science and Technology*, 10(1), p. 123-131.

Nordin Ibrahim, M. S. H. Sarker, Ab. Aziz N., Mohd Salleh, P. (2014). Drying Performance and Overall Energy Requisite Of Industrial Inclined Bed Paddy Drying In Malaysia. *Journal of Engineering Science and Technology,* Vol. 9, No. 3: 398 – 409.

Olaleye D. O. (2008).The Design and Construction of a Solar Incubator, Unpublished BSc. Thesis, submitted to Department of Mechanical Engineering, University of Agriculture, Abeokuta.

Pangavhane, D. R. and Sawhney, R.L. (2002).Review of research and development work on solar driers for grape drying. *Energy Conversion and Management,* 43(1): 45 –61.

Sarsavadia, P.N. (2007). Development of a solar-assisted dryer and evaluation of energy requirement for the drying of onion. *Renewable Energy*,32(15): 2529–2547.

Scalin D. (1997).The Design, Construction and Use of an Indirect, Through-pass, Solar FoodDryer. *Home Power Magazine,* 57: 62-72.

Sharma, S., Ray, R. A. and Sharma, V. K. (1987).Comparative Study of Solar Dryer for Crop Drying, In: Invention Intelligence Centre for Energy Studies, *Indian Institute of Technology*, New Delhi, India, pp.105-113.

Shanmugam V. and Natarajan E. (2007).Experimental study of regenerative desiccant integrated solar dryer with and without reflective mirror. *Applied Thermal Engineering,* 27(8-9), 1543-1551.

Sodha M. S., Dang A., Bansal P. K., Sharma S.B. (1985). An Analytical and Experimental Study of Open Sun Drying and a Cabinet Type Dryer. *Energy Conversion Management*,25(3): 263-271.

Sukhatme S.P. (1996).Solar-Energy-Principles of Thermal Collection and Storage, Tata McGraw Hill Publishing Company Limited.

The World Book Encyclopedia (1982). World Book-Child Craft International Inc., Chicago, USA.

Whitfield D. E. (2000).Solar Dryer Systems and the Internet: Important Resources to Improve Food Preparation, *Proceedings of the International Conference on Solar Cooking*, Kimberly, South Africa.

In: Renewable Energy Systems
Editor: Sandip A. Kale
ISBN: 978-1-53610-423-3

Chapter 5

DIFFERENT TECHNIQUES FOR PREDICTION OF WIND POWER GENERATION

Azim Heydari[1,*] and Farshid Keynia[2]
[1]Young Researchers and Elite Club, Kerman Branch,
Islamic Azad University, Kerman, Iran
[2] Energy Research Institute, Institute of Science and High Technology and Environmental Science, Graduate University of Advanced Technology, Kerman, Iran

ABSTRACT

The prediction of wind power has become so important due to the rapid advances in wind energy production. Also, wind power is believed to be a complicated signal for modeling and production. Looking at previous studies done in this field, an efficient method is needed for wind power. In this study, two new methods are used to predict wind power: 1. MGDM neural network combined with Particle Swarm Optimization algorithm (MGDM-PSO), 2. MGDM neural network combined with Genetics Algorithm (MGDM-GA). The proposed prediction method's effectiveness is the prediction of wind power output of wind farms. The obtained results indicate that the proposed methods are better than other methods used in previous researches.

Keywords: ANOVA, MGDM-GA method, MGDM-PSO method, MGDM network, neural network, wind power

1. INTRODUCTION

Wind energy is transformed into useful kinds of energy such as electrical energy or mechanical energy. Nowadays, wind power has an annual production capacity of 430 TWh, which is 2.5% of the total global electricity consumption (World Wind Energy Association). Wind energy is generated in great amounts in wind farms and is linked to the electrical

* Corresponding Author Email: azim_heydari@yahoo.com.

network. A low number of turbines are used to provide electricity in remote regions. There are some factors that affect the production power of wind turbines such as wind speed, wind direction, and meteorological parameters (i.e., temperature-pressure, pressure, density, air humidity, etc.). Therefore, it is critical for the wind-electricity industry to predict electricity generation for next minutes or hours. In the recent years, the increase in the proportion of wind plants in total electricity production of major networks has led in a consideration in load distribution economical calculations related to wind energy and its production power (Burton and Bossanyi, 2001; Watson et al., 1994). Prediction is an important issue in future decision making. Future energy life of a country depends on prediction of wind power and velocity.

In the recent years, several studies have been conducted to investigate the prediction of wind power and speed. In these researches, different methods have been employed. Salcedo-Sanz et al., 2011, investigated wind speed prediction in a Spanish wind farm using SVM. In order to enhance classic SVM performance, two combination methods EP-SVM and PSO-SVM were proposed. Their results showed satisfactory performance of both methods. Liu et al., 2010, investigated TK model performance in wind speed prediction; the results show better performance of TK as compared to ARIMA. In their survey, Shi et al., 2012, compared ARIMA, ANN, and

SVM for short-term prediction of wind speed. Results showed that performance of a combination of ARIMA-ANN and a combination of ARIMA-SVM is better than ARIMA, ANN, and SVM single models. Amjady et al., 2011a, proposed a model for prediction of short-term wind power, which performed better than previous models. Amjady et al., 2011b, presented a novel HIFM model to predict wind speed, based on the mutual effect of wind temperature and wind speed. Prediction based on actual results of Iran and Spain shows effective performance of the HIFM model. Taylor et al., 2009, changed over all wind speed density predictions into wind power density forecasts for evaluating their relative worth. The resultant point forecasts were meaningfully different from those based on traditional high resolution wind speed point forecasts from an atmospheric model and those generated by the time series models and. Khosravi et al., 2013, used two approaches for the construction of PIs for wind farm power generation. For forecasting aggregated power generation in wind farms, Feed-forward NN models are developed and used. The results gained from this study can be applied in both theoretical and practical studies of wind power generation. From a scientific standpoint, other statistical models including support vector machines or neuro-fuzzy systems can be employed to produce quality prediction intervals and uncertainty quantification. Khosravi and Nahavandi, 2013, provided an enhanced version of the nonparametric LUBE method. The results of their method introduce the proposed nonparametric method as a practically efficient method for quantification of uncertainties associated with wind power point forecasts. Wan, et al., 2014, proposed a novel HIA approach combining extreme learning machine and particle swarm optimization which is developed and successfully applied for interval forecasting of wind power without the prior knowledge of forecasting errors. A novel objective function accounting for PIs coverage probability and overall skill is constructed to obtain optimal PIs at multiple confidence levels simultaneously through one single performance-oriented optimization process to ensure both reliability and sharpness. Heydari and Keynia, 2015, provided a combination of Elman neural network and Particle Swarm Algorithm (El-PSO) to predict wind power. The results were compared to a combination of Elman neural network and genetic algorithm and also other previous methods. The results also

show excellent performance. Results of El-PSO suggested method and El-GA method were compared and evaluated by analysis of variance method (ANOVA).

In the current study, in order to predict wind power, the combination of GMDH neural network and Particle Swarm Algorithm (PSO) and Genetic Algorithm (GA) are used. Afterwards, the results were compared to other previous methods. The results also show excellent performance. This (MGDM-PSO) and (MGDM-GA) methods can be used as an intelligent remedy in many problems. The motivations of the proposed methods include:

- Adjusting the parameters of this model is very simple. The calculation speed of the proposed methods is a lot higher than other methods.
- Since there is too much dispersion of data in this problem, the proposed methods can solve this problem with minimum error.
- The amount of dispersion solutions obtained by the proposed method shown in this paper is very low and this is the indicator of the efficiency of the proposed method.

2. INTELLIGENT METHODS

2.1. Group Method Data Handing (GMDH)

GMDH neural network contains a set of neurons that link different pairs through the quadratic polynomials arise. By combining network quadratic polynomial approximation of entire neuronal function, with output $\hat{y}$, for a given set of inputs $X=(x_1,x_2,x_3,\ldots,x_n)$ with minimal errors, compared to the real output y, are described. So, for the M data consisted of n inputs and one output, actual results will be displayed as follows:

$$y_i = f(x_{i1},x_{i2},x_{i3},\ldots,x_{in}) \qquad (i=1,2,\ldots,M) \tag{1}$$

The network can forecast the output values $\hat{y}$ for each input vector X, according to equation (2):

$$\hat{y}_i = \hat{f}(x_{i1},x_{i2},x_{i3},\ldots,x_{in}) \qquad (i=1,2,3,\ldots,M) \tag{2}$$

So that the mean squared error between actual and predicted values is minimized.

The general form of the connection between input and output variables can be shaped using a polynomial function, as follows:

$$y = a_0 + \sum_{i=1}^{n} a_i x_i + \sum_{i=1}^{n}\sum_{j=1}^{n} a_{ij} x_i x_j + \sum_{i=1}^{n}\sum_{j=1}^{n}\sum_{k=1}^{n} a_{ijk} x_i x_j x_k + \ldots \tag{3}$$

Equation (3) is called the polynomial Ivakhnenko. In many cases the application of the second and bivariate polynomial is used in equation (4):

$$\hat{y} = G\left(x_i, x_j\right) = \mathrm{a}_0 + \mathrm{a}_1 x_i + \mathrm{a}_2 x_j + \mathrm{a}_3 x_i^2 + \mathrm{a}_4 x_j^2 + \mathrm{a}_5 x_i x_j \tag{4}$$

Unknown coefficients a_i of equation (4) obtained by regression techniques, the difference between the actual output y and the values calculated $\hat{y}$ for each pair of input variables x_i and x_j 'is minimized. A set of polynomials are made using equation (4). They were all using the least squares (LS) method the unknown coefficients obtained. For each function G_i (each neuron is made). Each neuron equation coefficients to minimize the error whole thing in order to adapt the optimum input on all pairs of input or outputs are achieved.

$$E = \frac{\sum_{i=1}^{M} \left(y_i - G_i\right)^2}{M} \rightarrow Min \tag{5}$$

In basic methods of algorithm GMDH, all binary compounds (neurons), the n input variables known and unknown coefficients of all the neurons are obtained using the least squares method.

So $\binom{n}{2} = \frac{n(n-1)}{2}$ neurons in the second layer are made, which can be displayed as equation number (6):

$$\left\{ \left(y_i, x_{ip}, x_{iq}\right) \middle| \left(i = 1, 2, \ldots, M\right) \& \; p, q \in \left(1, 2, \ldots, M\right) \right\} \tag{6}$$

$$A\mathrm{a} = \mathrm{Y} \tag{7}$$

Where, A a vector coefficient of quadratic equation is shown in Equation (4):

$$\mathrm{a} = \left\{ \mathrm{a}_0, \mathrm{a}_1, \ldots, \mathrm{a}_5 \right\} \tag{8}$$

$$Y = \left\{ y_1, \; y_2, y_3, \ldots, y_M \right\}^T \tag{9}$$

And a function of the input vector is easily visible:

$$A = \begin{bmatrix} 1 & x_{1p} & x_{1q} & x^2{}_{1p} & x^2{}_{1q} & x_{1p}x_{1q} \\ 1 & x_{2p} & x_{2q} & x^2{}_{2p} & x^2{}_{2q} & x_{2p}x_{2q} \\ \vdots & \vdots & \vdots & \vdots & \vdots & \vdots \\ 1 & x_{Mp} & x_{Mq} & x^2{}_{Mp} & x^2{}_{Mq} & x_{Mp}x_{Mq} \end{bmatrix} \tag{10}$$

Method of least squares multiple regression analysis, makes it possible to solve the equations (11):

$$a = \left(A^T A\right)^{-1} A^T Y \tag{11}$$

This vector equation coefficient (4) for all M series provides triplex.

GMDH neural network design theme with perceptron neural network is different. In this type of design, the purpose is to prevent the growth divergence related to the form and structure of the network and the network to one or more numerical parameters. So that by changing these parameters, the network structure will also be changed. Evolutionary methods such as genetic algorithms and particle swarm algorithm are widely used in various stages of designing neural networks because of their unique capabilities to find the optimal values and unpredictable searchable spaces, (Nariman Zadeh et al. 2002). In the present study, genetic algorithm and particle swarm algorithm are used in order to design and determine the coefficients of the neural network.

2.2. Elman Neural Network

Elman networks are kind of back-propagation multi-layer network involving a feedback from input of the hidden layer to output of the hidden layer. With the help of this feedback, the network can detect transient and time-dependent patterns. Tansing neurons are used in these networks and they have Tansing and Purelin functions in their hidden layer and output layer, respectively. In two-layer networks, with a limited number of discontinuities, this sequence is capable of estimating any function. Consequently, the network should own sufficient number of neurons in its hidden layer. The higher matching to the objective function will be higher if more neurons are used in this layer (Hagan et al., 2002). The neural network structure consists a number of layers, which has a number of neurons. Each neuron has its own input and output. The output of each neuron is determined by its input or output, its attachment to other neurons, and external inputs. Weights and biases which are the parameters of neural network can be calculated using the following equations:

$$X = \begin{bmatrix} W \\ b \end{bmatrix} \tag{12}$$

$$X^{new} = X^{old} + e.Z \tag{13}$$

$$X_{(k)} = X_{(k-1)} + Z_{(k-1)} \tag{14}$$

$$\{Z_1, Z_2, \ldots, Z_Q, -Z_1, -Z_2, \ldots, -Z_Q\} \tag{15}$$

Here, *X*, *Z*, *b*, *W*, *Q*, and *K* are non-adjustable parameters matrix, input data matrix, bias, weight, number of training steps, and number of training samples respectively, *e* is the correction coefficient (decreasing, increasing, without correction), which indicates whether the weights require correction or not. The following equation can be used for network output:

$$Net = I.W + b \tag{16}$$

Here, *Net* and *I* are the neural network's output and input respectively.

2.3. Genetic Algorithm (GA)

Genetic algorithm is a learning method based on biological evolution. John Holland introduced this algorithm in 1970 (Kusiak et al., 1986). Genetic algorithm is initiated from a set of primary random solutions – called initial population; each element of the population is a chromosome, which indicates a solution to the problem. To apply a concept of genetic evolution to an optimization problem in the real word, two points should be taken into account: 1. encoding potential solutions, 2. defining the fitness function (objective function). (Hsu et al., 2005). In the genetic algorithm, solutions are known as chromosomes and each chromosome consists of several genes. The general structure of the genetic algorithm is summarized as following stages (Mühlenbein, 1997):

Phase 1: definition of the problem solution as a genetic problem.

Phase 2: forming an initial population $P(0) = x_1^0, , x_1^0.$ $Set\ t = 0.$

Phase 3: the calculation the mean of fitness $\bar{f}(t) = \sum_i^N f(x_i)/N$. Allocating fitness value to each person $f(x_i)/\bar{f}(t)$.

Phase 4: selection operator; tournament selection operator is used for selection of parents for the next stage in the current study (crossover).

Phase 5: run the crossover operator with a defined probability for each pair.

Phase 6: application of mutation operator with a defined probability for each child.

Phase 7: forming a new population $p(t+1)$ using surviving mechanism.

Phase 8: setting $t = t + 1$ and returning to the third stage.

2.4. Particle Swarm Optimization (PSO)

PSO algorithm is a population-based algorithm, which is inspired by mass motion of natural species, such as birds, fish, etc. In this algorithm, each solution is modeled as a particle that has a value and a fitness value.

Particle Swarm Optimization algorithm (PSO) was firstly proposed by Russell Ebechart and James Kennedy, in 1995 (Kenedy and Eberhart, 1995). In PSO, vector method is used to search for the solution. This algorithm has been employed in many study fields, including optimization problems, economic problems, and neural network training (Onwunalu and Durlofsky, 2010). PSO is designed to search for the best global solutions, using a swarm of particles and is updated in each stage (Zhou et al., 2013). Each particle indicates a potential solution in the search space which specifies its velocity and location based on its best experience and location (local best) or the best experience or location of all particles (global best) (Zhang et al., 2005).

Consider an *N* dimensional problem with *i* particle and *t* generation. $X_{i,N}(t)$ and $V_{i,N}(t)$ are location and velocity of the i^{th} particle, respectively. The velocity of the i^{th} particle for the $(t+1)^{th}$ generation can be derived from the following equation (Chen et al., 2009; Lu et al., 2008).

$$V_{i,N}(t+1) = \omega(t+1)V_{i,N}(t) + c_1 r_1\left(X_{pbest,N} - X_{i,d}(t)\right) + c_2 r_2\left(X_{gbest,N} - X_{i,d}(t)\right) \quad (17)$$

$$X_{i,N}(t+1) = X_{i,N}(t) + V_{i,N}(t+1) \quad (18)$$

Here $1 \le i \le m$, $1 \le t \le k$, c_1 and c_2 have constant value ($c_1 = c_2 = 2$), r_1 and r_2 are two independent random numbers that follow uniform functions in the [-1 1] interval; ω is the inertia weight that controls the effect of the previous velocity, on the current one.

$$\omega(t) = \omega(1) - (\omega(1) - \omega(k))\, t/k \quad (19)$$

Here, $\omega(1)$ is the initial inertia weight and $\omega(k)$ is inertia weight; the evolved swarm in the final generation of k and t equals the generation maximum repetition and initial repetition of the maximum generation. PSO, as a simple and effective random search algorithm can lead to better results than gradient descent method, penalty function method, or the genetic algorithm in solving some nonlinear optimization problems (Yu et al., 2010).

3. PROPOSED METHODS (GMDH-PSO AND GMDH-GA)

This section aims to explain the proposed methods. In addition, the methods of using and combining GMDH neural network and particle swarm optimization algorithm (GMDH-PSO), GMDH neural network and genetic algorithm (GMDH-GA), will be described.

Since PSO is an optimization algorithm, it is used in this investigation optimize neural network parameters, such as weights and biases, in the training stage. Firstly, the weights and biases should be defined as an optimization problem and then be optimized by PSO and GA algorithms. In PSO, a particle with a specific vector may test different locations in different repetitions (Kennedy and Eberhart, 1997). For neural network training, Sigmund tangent transfer function is used as follows:

$$Tansig\ (\theta) = \frac{2}{(1+\exp(-2\theta))-1} \quad (20)$$

Objective function or the fitness of the proposed methods (GMDH-PSO and GMDH-GA) in this study is Minimum Mean Squared Errors (MMSE), as follows:

$$MSE = \frac{1}{m}\sum_{i=1}^{m}\left(X_{ACTi} - X_{FORi}\right)^2 \tag{21}$$

$$MMSE = Min\left(\frac{1}{m}\sum_{i=1}^{m}\left(X_{ACTi} - X_{FORi}\right)^2\right) \tag{22}$$

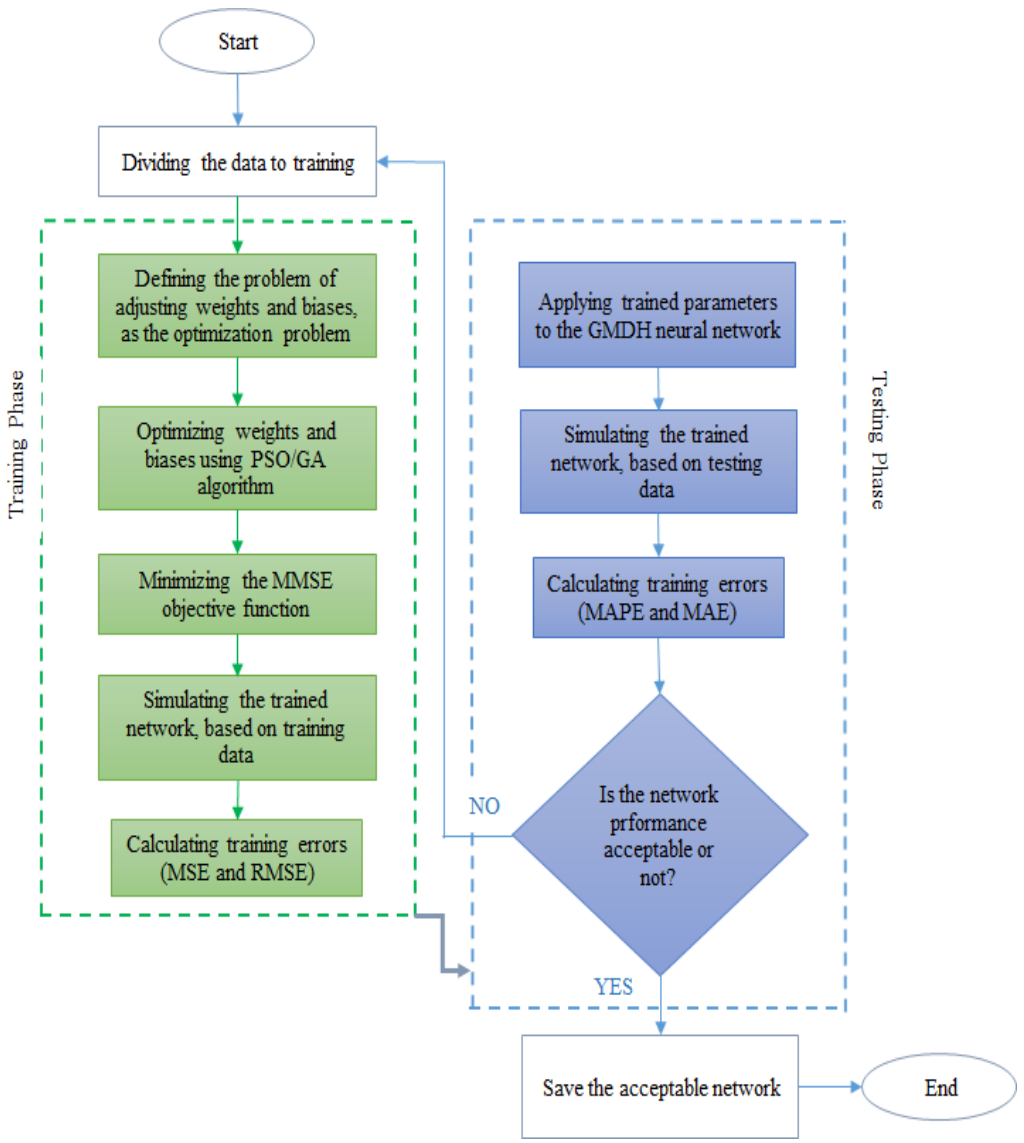

Figure 1. Flowchart of the proposed (GMDH-PSO/GA) method.

Here, X_{FOR} is the predicted value, X_{ACT} is the actual value, and m is the number of hour. We aim to minimize the MMSE value, which shows better training of the network and its better preparation to enter the testing stage. In addition, to check correctness of the training stage, Mean Squared Errors (MSE) and Root Mean Square Error (RMSE) are used; RMSE is as follows:

$$RMSE = \sqrt{\frac{1}{m}\sum_{i=1}^{m}\left(X_{ACTi} - X_{FORi}\right)^2} \tag{23}$$

In this phase, the trained network should be tested based on error criteria. If the testing error has a small value, it means that the network is trained correctly and acceptable. Otherwise, if still there are high test errors, it should be trained again. Figure 1 shows the flowchart of the proposed methods.

In this study, to test the trained network, Mean Absolute Error (MAE), Mean Absolute Percentage of Error (MAPE), and its modified version (MMAPE) have been used (Amjady et al., 2011a):

$$MAE = \frac{1}{m}\sum_{i=1}^{m}\left|X_{ACTi} - X_{FORi}\right| \tag{24}$$

$$MAPE = \frac{100}{m}\sum_{i=1}^{m}\left|\frac{X_{ACTi} - X_{FORi}}{X_{ACTi}}\right| \tag{25}$$

$$MMAPE = \frac{100}{m}\sum_{i=1}^{m}\left|\frac{X_{ACTi} - X_{FORi}}{X_{ave-ACTi}}\right| \tag{26}$$

$$X_{ave-ACTi} = \frac{1}{m}\sum_{i=1}^{m} X_{ACTi} \tag{27}$$

X_{ACT} and X_{FOR} are the actual and the predicted values respectively.

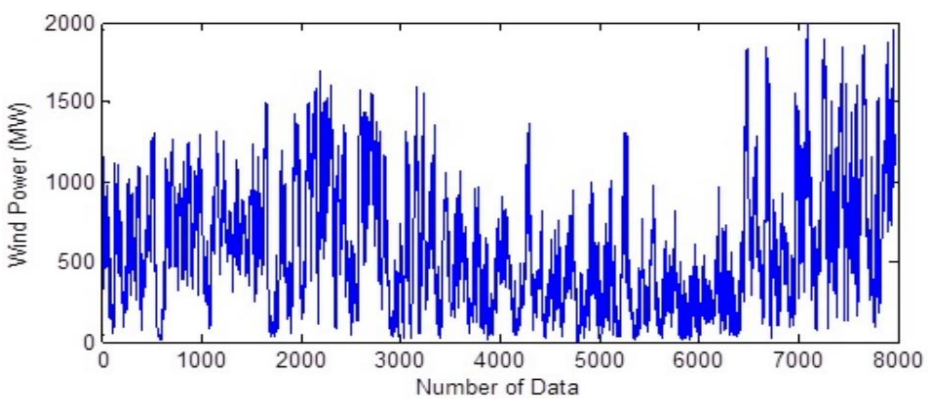

Figure 2. Actual wind power data used in this study.

In the present investigation, two combination of GMDH and PSO, GMDH and GA are employed to predict wind power. Figure 2 illustrates actual wind power data use in this paper. Using their real data obtained from (http://www.sotaventogalicia.com/tiemporeal.english/instantaneos.php; http://www.eirgrid.com/operations), the proposed methods are used for both predicting the aggregated wind power of Irish power system wind-power and forecast of Sotavento wind farm in Spain.

Having uniform distribution, data have been normalized in an interval between [-1 1], using the following normalization formula:

$$X_{norm} = \frac{(X - Min(X))}{(Max(X) - Min(X))} \times 2 - 1 \tag{28}$$

Here, Xnorm is the normalized value; X is the non-normalized value, Min (x) and Max (x) are minimum and maximum of the non-normal, in a row. In addition, 80% and 20% of the data were used in the training and testing phases of the neural network.

4. RESULTS

As it was stated in Section 1, wind power is of great importance in generation of different kinds of energy. In addition, it is important to propose a method to predict wind power with negligible error and have a better performance compared with previous methods – which has a very important place in today's decision making and studies. In this study it has been tried to compare the performance of GMDH-PSO and GMDH-GA methods with previous studies, for short-term prediction of wind power. Table 1 shows the performance of the GMDH-GA and GMDH-PSO methods in neurons and different layers. Four months, from April to July, have been selected, trained, and tested to investigate the performance of the suggested methods. Table 2 indicates the RMSE and MMAPE results of prediction of aggregated wind power of Irish power system in September and October 2010. Table 3 illustrates the performance of GMDH-PSO and GMDH-GA methods, and other methods from April to July 2010. All the stages of optimization, training, and testing of the proposed methods are done in MATLAB 2014 software.

Table 1. Different performance of the proposed methods (GMDH-PSO and GMDH-GA), in different layers and neurons

Layers	Neurons	El-GA (Heydari and Keynia, 2015)				El-PSO (Heydari and Keynia, 2015)				Proposed Method (MGDH-PSO)				Proposed Method (MGDH-GA)			
		MSE	RMSE	MAE	MAPE (%)	MSE	RMSE	MAE	MAPE (%)	MSE	RMSE	MAE	MAPE (%)	MSE	RMSE	MAE	MAPE (%)
2	28-1	0.161	0.401	0.332	2.827	0.156	0.395	0.326	1.943	0.047	0.2167948	0.189	1.145	0.101	0.317805	0.231	1.57
3	32-2-1	0.162	0.402	0.342	10.179	0.151	0.389	0.318	2.991	0.086	0.2932576	0.201	2.1	0.129	0.3591657	0.275	2.21
3	30-19-1	0.159	0.399	0.33	9.0179	0.154	0.392	0.33	5.94	0.013	0.1140175	0.219	1.87	0.089	0.2983287	0.268	3.02

Table 2. RMSE and MMAPE results obtained for prediction of Irish power system's aggregated wind power in September and October 2010

Methods	Error Criteria	Test Month (2010)		
		September	October	Average
Persistence method (Kavasseri and Seetharaman, 2009; Damousis et al., 2004)	RMSE (MW)	125.33	164.12	144.73
	MMAPE (%)	24.11	25.91	25.01
Irish EirGrid company (http://www.eirgrid.com/operations)	RMSE (MW)	118.21	160.56	139.38
	MMAPE (%)	23.93	23.71	23.82
SA (Amjady et al., 2011a)	RMSE (MW)	127.91	139.64	133.77
	MMAPE (%)	24.22	25.61	24.91
GA (Amjady et al., 2011a)	RMSE (MW)	118.41	119.71	119.06
	MMAPE (%)	21.54	22.14	21.84
PSO (Amjady et al., 2011a)	RMSE (MW)	111.84	110.48	111.16
	MMAPE (%)	19.83	19.76	19.79
DE (Amjady et al., 2011a)	RMSE (MW)	102.42	100.24	101.33
	MMAPE (%)	17.19	16.09	16.64
NDE (Amjady et al., 2011a)	RMSE (MW)	77.21	73.28	75.24
	MMAPE (%)	15.87	14.69	15.28
El-GA (Heydari and Keynia, 2015)	RMSE (MW)	64.19	65.05	64.62
	MMAPE (%)	11.02	9.19	10.105
El-PSO (Heydari and Keynia, 2015)	RMSE (MW)	25.83	21.48	23.655
	MMAPE (%)	7.82	6.23	7.025
Proposed Method (MGDH-GA)	*RMSE(MW)*	*21.09*	*21.34*	*19.18*
	MMAPE(%)	*7.19*	*6.35*	*6.56*
Proposed Method (MGDH-PSO)	*RMSE(MW)*	*18.721*	*19.21*	*15.83*
	MMAPE(%)	*6.87*	*6.12*	*6.67*

Table 3. RMSE and MMAPE results for Sotavento wind farm's wind power forecast of in April–July 2010

Methods	Error Criteria	Test Month (2010)				
		April	May	June	July	Ave-rage
Persistence method (Kavasseri and Seetharaman, 2009; Damousis et al., 2004)	RMSE (MW)	1.12	0.85	0.78	0.83	0.9
	MMAPE (%)	35.91	30.84	34.33	36.84	34.48
Multivariate ARIMA (Kavasseri and Seetharaman, 2009)	RMSE (MW)	0.84	0.74	0.7	0.69	0.74
	MMAPE (%)	28.74	27.21	28.91	29.54	28.6
RBF (Sideratos and Hatziargyriou, 2007)	RMSE (MW)	0.59	0.52	0.59	0.5	0.55
	MMAPE (%)	25.08	18.11	26.45	27.75	24.35
MLP (Costa et al., 2008)	RMSE (MW)	0.51	0.62	0.52	0.47	0.53
	MMAPE (%)	22.44	19.82	25.24	26.14	23.41
NDE (Amjady et al., 2011a)	RMSE (MW)	0.46	0.44	0.44	0.38	0.43
	MMAPE (%)	7.75	11.43	16.06	9.33	11.14
El-GA (Heydari and Keynia, 2015)	RMSE (MW)	0.4	0.4	0.4	0.4	0.4
	MMAPE (%)	12.99	7.88	8.37	8.04	9.32
El-PSO (Heydari and Keynia, 2015)	RMSE (MW)	0.38	0.38	0.37	0.39	0.38
	MMAPE (%)	5.65	6.98	4.87	6.53	6.01
Proposed Method (MGDH-GA)	*RMSE(MW)*	*0.12*	*0.09*	*0.11*	*0.2*	*0.19*
	MMAPE(%)	*4.34*	*5.34*	*5.89*	*4.39*	*6.12*
Proposed Method (MGDH-PSO)	*RMSE(MW)*	*0.08*	*0.1*	*0.076*	*0.89*	*0.101*
	MMAPE(%)	*2.34*	*4.12*	*3.09*	*3.89*	*4.55*

CONCLUSION

Wind power is a multivariate nonlinear function that has a non-uniform and unique space. The wind-power data which have been used in this paper have a relatively broad distribution; consequently, the more the data distribution, the weaker the performance of the neural network. In this survey, wind power prediction is performed using a novel and highly efficient method. GMDH neural network requires an intelligent method for parameters optimization. PSO and GA algorithms are used to optimize weights and biases. GMDH-PSO methods has a better performance as compared to previous methods and GMDH-GA method.

REFERENCES

Amjady, A., Keynia, F. and Zareipour, H., 2011a. Short-term wind power forecasting using ridgelet neural network. *Electric Power Systems Research,* Vol. 81, pp. 2099– 2107.

Amjady, N., Keynia, F. and Zareipour, H., 2011b. A new hybrid iterative method for short term wind speed forecasting," *Eur Trans Electr Power, Vol*. 21, pp. 581–595.

Burton, N.J. and Bossanyi, E., 2001. *Wind Energy Handbook.* Wiley.

Chen, J.H., Yang, L.R. and Su, M.C., 2009. Comparison of SOM-based optimization and particle swarm optimization for minimizing the construction time of a secant pile wall. *Automation in Construction,* Vol. 18, pp. 844–848.

Costa, A., Crespo, A., Navarro, J., Lizcano, G., Madsen, H. and Feitosa, E., 2008. A review on the young history of the wind power short-term prediction. *Renew. Sustain. Energy Rev*; 12 (6): 1725–1744.

Damousis, L.G., Alexiadis, M.C., Theocharis, J.B. and Dokopoulos, P.S., 2004. A fuzzy model for wind speed prediction and power generation in wind parks using spatial correlation. *IEEE Trans. Energy Convers* 2004; 19 (2): 352–361.

Fan, S., Liao, J.R., Yokoyama, R., Chen, L. and Lee, W.J., 2009. Forecasting the wind generation using a two-stage network based on meteorological information. *IEEE Trans. Energy Convers; 24* (2): 474–482.

Hagan, M.T., Demuth, H.B. and Beale, M.H., 2002. *Neural Network Design.* Colorado ISBN-13: 978 0971732100: University of Colorado.

Heydari, A. and Keynia, F., 2015. Prediction of wind power generation through combining Particle Swarm Optimization and Elman neural network (El-PSO), *International Energy Journal*, 15, 93-102.

Hsu, C.M., Chen, K.Y. and Chen, M.C., 2005. Batching orders in warehouses by minimizing travel distance with genetic algorithms. *Computers in Industry,* Vol. 56, pp. 169–178.

Ireland wind power data http://www.eirgrid.com/operations/ system performance data.

Kavasseri, R.G. and Seetharaman, K., 2009. Day-ahead wind speed forecasting using f-ARIMA models. *Renew. Energy;* 34 (5): 1388–1393.

Kenedy, J. and Eberhart, R., 1995. Particle swarm optimization. Proc. IEEE Int. Conf. Neural Networks, pp. 1942-1948.

Kennedy, J. and Eberhart, R.C., 1997. A discrete binary version of the particle swarm algorithm. In Proceedings of the world multiconference on systemics, cybernetics and informatics, *Piscataway*, NJ pp. 4104–4108.

Khosravi, A. and Nahavandi, S., 2013. Combined Nonparametric Prediction Intervals for Wind Power Generation. *IEEE Transactions on Sustainable Energy*, 849 - 856, VOL. 4, Oct.

Khosravi, A., Nahavandi, S. and Creighton, D., 2013. Prediction Intervals for Short-Term Wind Farm Power Generation Forecasts. *IEEE Transactions on Sustainable Energy*, VOL. 4, NO. 3.

Kusiak, A., Vanelli, A. and Kumar, K.R., 1986. Clustering analysis: models and algorithms. *Control and Cybernetics*, Vol. 15, pp. 139–153.

Liu, H.P., Shi, J. and Erdem, E., 2010. Prediction of wind speed time series using modified Taylor Kriging method," *Energy*, Vol. 35, pp. 4870–4879.

Lu, M., Lam, H.C. and Dai, F., 2008. Resource-constrained critical path analysis based on discrete event simulation and particle swarm optimization. *Automation in Construction*, Vol. 17, pp. 670–681.

Mühlenbein, H., 1997. Genetic Algorithms. in: E. Aarts, J.K. Lenstra (Eds.), *Local Search in Combinatorial Optimization*, Wiley, New York, pp. 137–171.

Nariman-zadeh, N.; Darvizeh, A.; Darvizeh, M.; Gharababaei, H., (2002), Modelling of Explosive Cutting Process of Plates Using GMDH-type Neural Network and Singular Value Decomposition. *Journal of Materials Processing Technology,* 128 (1-3): 80-87.

Onwunalu, E. and Durlofsky, J., 2010. Application of a particle swarm optimization algorithm for determining optimum well location and type. *Computers and Geosciences*, Vol. 14, pp: 183–198.

Salcedo-Sanz, S., Ortiz-Garcia, E.G., Pérez-Bellido, A.M., Portilla-Figueras, A. and Prieto, L., 2011. Short term wind speed prediction based on evolutionary support vector regression algorithms, *Expert System Application*, Vol. 38, pp. 4052–4057.

Shi, J., Guo, J.M. and Zheng, S.T., 2012. Evaluation of hybrid forecasting approaches for wind speed and power generation time series. *Renew Sustain Energy Rev*, Vol. 16, pp. 3471–3480.

Sideratos, G. and Hatziargyriou, N., 2007. Using radial basis neural networks to estimate wind power production," *IEEE Power Engineering Society General Meeting*, doi:10. 1109/PES. 385812.

Sotavento wind farm data http://www.sotaventogalicia.com/tiemporeal.english/instantaneos. php.

Taylor, J.W., McSharry, P.E. and Buizza, R., 2009. Wind Power Density Forecasting Using Ensemble Predictions and Time Series Models. *IEEE Transactions on Energy Conversion*, 24, 775-782.

Wan, C., Xu, Z., Pinson, P., Yang Dong, Z. and Wong, K.P., 2014. Optimal Prediction Intervals of Wind Power Generation. *IEEE Trans. Power Syst*, VOL. 29, NO. 3, May.

Watson, S.J., Landberg, L. and Halliday, J.A., 1994. Application of Wind Speed Forecasting to the Integration of Wind Energy into a Large Scale Power System," *IEE Proceeding of Generation*, Transmission and Distribution, Vol. 141, pp, 357-362.

World Wind Energy Association WWEA 2011 Date of publication: April.

Yu, C., Teo, K.L., Zhang, L.S. and Bai, Y.Q., 2010. A new exact penalty function method for continuous inequality constrained optimization problems. *Journal of Industrial and Management Optimization*, Vol. 6, pp. 895–910.

Zhang, H., Li, X., Li, H. and Huang, F., 2005. Particle swarm optimization-based schemes for resource-constrained project scheduling. *Automation in Construction,* Vol. 14, pp. 393–404.

Zhou, C., Ding, L.Y. and He, R., 2013. PSO-based Elman neural network model for predictive control of air chamber pressure in slurry shield tunneling under Yangtze River. *Automation in Construction,* Vol. 36, pp. 208–217.

In: Renewable Energy Systems
Editor: Sandip A. Kale
ISBN: 978-1-53610-423-3

Chapter 6

PERFORMANCE EVALUATION OF WIND FARM CLUSTERS –A METHODOLOGICAL APPROACH

D. G. Rajakumar[1,*], N. Nagesha[1] and M. C. Mallikarjune Gowda[2]
[1] Department of Mechanical Engineering,
Visvesvaraya Technological University, India
[2]Gamesa Wind Turbines Private Limited, India

ABSTRACT

Energy is an essential input for the financial and societal development of any nation. Both conventional and nonconventional sources of energy contribute to total requirement of the economy as a whole. As an affordable and sparkling energy source, energy derived from wind resource is one of the world's greatest upward nonconventional energy sources. A significant number of wind turbine clusters are operating at different geographical locations across the globe. However, assessing their performance is not an easy task and there is dearth of literature in this area. In view of this, a methodological approach is made in the present study to estimate the performance of a wind turbine cluster with the aid of an indicator called Cluster Performance Index (CPI) which uses a multi-criteria approach. The proposed CPI comprises four criteria viz., Technical Performance Indicator (TePI), Economic Performance Indicator (EcPI), Environmental Performance Indicator (EnPI), and Sociological Performance Indicator (SoPI). Under each criterion a total of ten parameters are identified with five qualitative and five quantitative responses. The methodology is implemented by the method collecting raw data from two wind turbine clusters situated at Chitradurga and Gadag in the southern Indian State of Karnataka. The study covered fifteen stakeholders of wind farms through recording their responses on a researcher administered questionnaire. The questionnaire comprised all the necessary questions to gather significant primary data pertaining to the wind farm cluster. Stake holders involved engineers working in wind farms, wind farm developers, Government officials from energy department and a few selected residential people near the wind farms. The results of the study revealed that Chitradurga wind farm

Address correspondence to: *rajakumardyl@gmail.com.

performed much better (CPI of 45.267) as compared to Gadag (CPI of 28.362) wind farm.

Keywords: wind turbine cluster, performance evaluation, multi-criteria approach, CPI

1. INTRODUCTION

Analyzing the performance of wind farm depends on many parameters like, geographical locations, topography, wind resource, rated capacity of Wind Turbine Generators (WTGs), technology of WTG, hub height, etc. Wind farms in different geographical locations produces energy in diffused manner. Evaluating their performance is a complex task and not much of literature is available in this area. In this context, a methodological approach is used in this study to estimate the performance of windmill clusters through an index called Cluster Performance Index (CPI) which uses Multi-Criteria approach. The proposed CPI comprises four different criteria viz., Technical Performance Indicator (TePI), Economic Performance Indicator (EcPI), Environmental Performance Indicator (EnPI), and Sociological Performance Indicator (SoPI). Each performance criterion adopts a total of ten parameters with five objective and five subjective oriented responses. Methodological frame work uses collection of empirical data from the wind turbine clusters located at Gadag in the Northern part of Karnataka, Chitradurga Southern part of Karnataka (a Southern state of India). Totally fifteen different stake holders are interviewed through a set of structured researcher administered questionnaire to collect the relevant data in each wind farm. Main stake holders involved are site engineers working in wind farms, wind farm developers, Government officials from energy department and a few selected residential people near the wind farms.

Brief descriptions of the literatures related to the subject are discussed in the following paragraph. Among them; Zahra Shirgholamia et al. (2016) analyzed the selection of wind turbines for any location and opines that it has traditionally been based on designing a turbine which matches the wind profile of a given site. A more realistic approach in overcoming the above said method would be to select the wind turbines that match the wind resource uniqueness of a specific site among the commercially obtainable ones. The assessment of wind turbines, nevertheless, is a complex process that involves different criteria with different degrees of importance such as economic, technological, and environmental ones. The object of this study is to identify the evaluation criteria that influence the wind turbine selection and then to provide an effective model based on AHP to evaluate wind turbines when developing a wind farm. Study carried out by Selena Farris et al. (2016) highlights the challenge in attractive wind turbines that generates optimal power for a sustainable period of time considering various parameters like wind resource, topography, technology involved in the type of turbines, etc. Actual issues related to the operations of wind turbines including the accuracy and consistency of Supervisory Control and Data Acquisition (SCADA) data, modelling insecurity and the economical parameters associated with monitor campaign set hurdles in order to identify the assessment of wind turbines for power generation at the portfolio level. A systematic procedure is followed that uses fuzzy logic method which is a combination of various performance indicators based on well equipped SCADA tool and its related data with pre-construction modelling is presented. This method provided an analytical base to reduce uncertainty and helped in identifying the best performing wind turbines, there

by facilitating improved power generation. Subsequent to first investigation it has highlighted turbines to spotlight on a matching set of summarize tools which involves verifications and turbine mounted lidar depth campaigns and are presented to utilize in a deeper analysis to validate presentation issues, resolve issues, and at last validating the improvements in the performance of wind turbines. Several case studies are pinched from normal power's wide-ranging practice with working resources to express the importance added in the course of this advance in analyzing the performance of wind turbines.

It is very much needed that an important step be taken in marking the lower performing wind turbines at the most primitive achievable to avoid loss of energy or breakdowns thus minimizing the operating and maintenance cost and to boost the operating performance of wind turbines. For a case when wind turbines are bigger in size and are aged, controlling enormous quantity of SCADA data (Events and maintenance logs) is a monotonous and time killing mission. An easy concerting index investigation is framed to identify the odd turbines moderately and easily. If everything is good, wind turbine produces the maximum possible power at any given point of time. At any point of time power production capability is subjected to aerodynamic, electrical, and mechanical or controller settings. It straight away reflects in the performance analysis. Projected index evaluates the wind turbine performance unpredictability and path of a turbine surrounded by the wind farm and provides an alert to take in-depth analysis in these issues. This index concentrates on the accumulation of deprivation of the patterned wind turbines and draws course of action as per the study of (Bob Smith et al. (2016).

Except for a study here and there, much of literature is available pertaining to wind farm cluster performance especially involving technical, economic, environmental and social parameters simultaneously. In this backdrop, an attempt is made in the current analysis to estimate the performance of a wind turbine cluster through an index called Cluster Performance Index (CPI) adopting a multi-criteria approach. Present study basically explains the methodological approach used in arriving at CPI for the selected wind farm clusters and choses the best performing wind farm cluster with the help of empirical data obtained through the field study.

2. CRITERIA FOR PERFORMANCE ESTIMATION

Though there are many parameters relevant in evaluating the performance of wind farms, a proper methodology comprising important factors is required to be developed to estimate the wind turbine cluster performance. This research work has adopted significant factors influencing the wind turbine cluster performance as per World Energy Council (WEC, 2012) guidelines. The indicators of performances proposed in the study are the outcome of the work carried out by the World Energy Council (WEC) committee in view of the analysis of Performance of Generating Plants (PGP). The goal is to support in comparing the qualities and lacunas of different technologies, recognize and evaluate their concluding weaknesses, and thus leading to improvement in the performances of various energy sources and finally donate to a more efficient and vigorous development of all types of Renewable Energy Technologies (RETs). WEC has recommended four performance indicators viz., Technical Performance Indicator (TePI), Economic Performance Indicator (EcPI), Environmental

Performance Indicator (EnPI), and Social Performance Indicator (SoPI) to ascertain the performance of a wind farm comprehensively.

3. DIMENSIONS FOR PERFORMANCE CRITERIA

In order to take into account various dimensions under each of the four proposed indicators, the present study has considered a total of ten parameters. Out of the ten considered parameters, five are quantitative and the other five are qualitative response oriented. The four performance indicators and the ten dimensions under each indicator are separately discussed below.

3.1. Technical Performance Indicator (TePI)

Table 1 shows all the ten parameters which are contributories to the TePI of a wind farm and the tabulation for recording the value for a particular wind-farm. The Capacity Utilization Factor (CUF) is the ratio of entire amount of energy generated during the complete working period to the total probable energy that can be generated during the same period. Specific energy production represents the amount of energy generated during the running period of turbine to that of swept area of rotor. The third factor, corresponding complete load hours, is the availability of number of annual hours of WTGs. The plant availability factor represents the total operating hours of wind plant during the nominal period to that of total length (in terms of hrs) of operation of each WTG in wind farms. Fifth factor is very important to decide type and rating of WTGs that can be installed in any wind farm as it depends on the wind velocity and Wind Power Density (WPD) of a particular region. Sixth parameter deals with the viability of installing different rating and type of WTGs, based on the topography and siting of them. The seventh parameter is connected with design aspect and its appropriateness in the cluster. Sixth and eighth parameter needs the real groundwork to be carried out in order to manufacture components of WTG as per the design criteria and standards, and it should also be tested prior to the practical implementation. Ninth and tenth parameters are very important to maintain sustained amount of power generation in the wind farm and its evacuation to the nearby grid to ensure economic feasibility. The first five parameter values are obtained from the wind farms empirically and then converted to 1-5 scale (5 most favourable and 1 least favourable score) through normalization. The subsequent five parameter values are obtained directly on a 1-5 Scale using stake-holder responses and value judgments.

3.2. Economic Performance Indicator (EcPI)

Table 2 provides all the ten parameters which are included under EcPI criterion. First parameter represents the ratio of total annual revenue generated to the total initial investment including WTG cost and up-to grid connection cost. Second parameter is the Internal Rate of Return (IRR) is the interest rate at which Net Present Worth (NPW) becomes zero. Pay Back

Period (PBP) is the minimum time for any investor to get back his investment. If PBP is low the investor comes forward to invest more in WETs. Labour productivity is measured in terms of total annual revenue generated to the total annual expenditure on Human Resources (HR). Maintenance charges cover expenses towards annual Operation and Maintenance (O&M) of WTG and accessories in order to keep-up the machine availability to the maximum extent. As the variation of wind velocity and its distribution leads to the variation of annual energy output of any wind farm, it is captured in the form of site factor. Increase in Feed In Tariffs (FITs) attracts the investors and motivates them to invest more. Favourable situation should be created in order to support the chance of repowering, if any, in the wind farm. Final parameter is an important economic aspect since the good accessibility to the cluster saves time, money, etc. Again the first five parameter values are to be gathered from the wind farm empirically and then normalized on a 1-5 scale (5 most favourable and 1 least favourable score). Similarly the last five parameters are measured on 1-5 scale directly using qualitative value judgement of stake holders in the wind farms.

Table 1. Technical Performance Indicator (TePI) for the Wind Farms

Sl. No.	Parameters
1	Capacity Utilization Factor (CUF in %)
2	Specific Energy Production (kWh/m^2)
3	Equivalent Full load Hours (h)
4	Plant Availability Factor (in %)
5	Wind resources or Wind conditions (velocity) during the generation period (in m/s)
6	Topography and Siting of Wind Turbines (WTG rating and type)
7	Development of Appropriate Design Criteria, Specification and Standards
8	Full scale testing prior to Commercial Introduction
9	Condition Monitoring System (CMS) for Turbine maintenance (O&M, identify problems/errors to rectify at the earliest, gear box, reliability, collaboration)
10	Power Evacuation (up to the grid)

Table 2. Economic Performance Indicator (EcPI) for the Wind Farms

Sl. No.	Parameters
1	Turnover Ratio
2	Internal Rate of Return (IRR, in %)
3	Pay Back Period (PBP, in years)
4	Labour productivity
5	Maintenance charges in Crores of Rupees
6	Site Factor (wind speed distribution)
7	Variation in Annual Energy Output
8	Feed in Tariffs (FIT)
9	Situations Favorable for Repowering
10	Accessibility to the Wind Cluster

3.3. Environmental Performance Indicator (EnPI)

Table 3 shows the various parameters covered under the EnPI criterion. First parameter provides the contribution made to the reduction of Green House Gas (GHG) emissions concentrating on the major pollutant CO_2, on an annual basis. The second parameter deals with other emissions like NO_x, and SO_x, along with CO_2 for the whole life cycle of WTGs installed in the wind farm. Third, fourth and sixth parameters capture the safety aspects by maintaining minimum distance away from nearby dwellings to avoid landscape, sound and shadow flickering. While the fifth parameter records the number of birds killed during the development and maintenance of wind farm. Seventh, eighth and ninth parameter indicates the importance of protecting historical heritage and environment by assessing its effects on parameters like flora and fauna, climate change, etc., before the development of any wind farm. Final parameter is relevant when the wind farm is nearby the dwellings where there is interruption for communication systems like mobile towers, antennas, etc. Yet again data pertaining to the quantitative parameters are obtained empirically and then normalized on 1-5 scale (5 most favourable and 1 least favourable score), and qualitative parameters are directly assessed on 1-5 scale using value judgements.

Table 3. Environmental Performance Indicator (EnPI) for the Wind Farms

Sl. No.	Parameters
1	Contribution to the reduction of GHG emissions (Avoided CO_2 in t/MW/y)
2	Pollutant Emissions during Life Cycle; $Q_{CO2,}$ Q_{Sox}, Q_{NOx} (t/kWh)
3	Visual Effects/Landscape Protection Distance (least space away from dwelling in meters.)
4	Noise from Wind Turbines (in dB)
5	Birds Fatalities (No. of birds killed/WTG/Year Numbers/Year)
6	Shadow Casting to nearby Residence (No. of hrs/yr when the neighboring Dwelling go through of darkness casting)
7	Archaeological and Historical Heritage
8	Hydrological Assessment
9	Assessment of Flora and Fauna/Climate Change (e.g., Danger caused to Species, Migrating Birds)
10	Interference with Telecommunication Systems

3.4. Sociological Performance Indicator (SoPI)

Table 4 gives all the ten parameters which are used in evaluating the SoPI of a wind farm. First parameter considers the number of jobs that a wind farm can generate from the manufacturing to the erection and commissioning stage and also during maintenance. Number of households electrified due to the development of wind farm, is covered in the second parameter. Third parameter is very crucial for the smooth functioning and development of wind energy farm by ensuring safety. Fourth parameter is vital for land owners and nearby villagers who have given land for setting up the wind farm. Fifth parameter deals with the

contribution made towards educational and cultural development of locality. Sixth parameter considers the degree of improvement in tourism due to the attraction of wind farm. The degree of damage caused by wind farm to nearby environment, people, etc., is covered by the seventh parameter. The last three parameters tries to figure out the positive effect of wind farm on the development of agricultural and rural industrialization, poverty alleviation, and migration/birth rates of nearby people. As in previous cases the quantitative parameters are converted to 1-5 scale and qualitative parameters are directly assessed on 1-5 scale.

Table 4. Sociological Performance Indicator (SoPI) for the Wind Farms

Sl. No.	Parameters
1	Jobs Created by the Plant (No. of direct/indirect jobs created by 1MW WTG at different stages, like manufacture, installation, O and M period)
2	Provide admittance to electrical energy (No. of households/total No. of public have now access to the electrical energy created by a 1MW plant)
3	Industrial Safety Accident Rate (SAR)
4	Monetary Benefit to the Land Owners per acre of wind farm (For leased lands, in terms of % annual revenue)
5	Contribution made to the Educational/Cultural Development of the Local Area (in terms of % annual revenue)
6	Degree of Improvement in the Tourism Development
7	Extent of Social Costs (environment damage/nuisance caused to people, etc.)
8	Positive Effect on Agricultural Production and Rural Industrialization
9	Positive Effect on Incomes and Poverty Alleviation
10	Positive Effect on Migration and Birth rates of Labour due to the Wind Farm

4. CLUSTER PERFORMANCE INDEX - AN INDICATOR OF CLUSTER EFFICIENCY

The financial performance of the wind farms mostly relies on the accessible wind power and the wind turbines' generated power, technical parameters availability, economic feasibility, etc. It is always better to verify the by and large presentation of a wind farm rather than the performance of individual WTGs. According to World Energy Council (WEC) Working Group on the Performances of Generating Plants (PGP), it is said that for the performance analysis of any wind energy farm it is necessarily important to consider various performance indicators such as TePI, EcPI, EnPI and SoPI. Power output obtained from the wind farm is measured at the point of grid connectivity and measurements taken at the normal atmospheric wind conditions. All these data are obtained by installing the wind masts in the region of the wind farms. Power curves considered for different rating WTGs and different wind direction or wind regime sectors are mostly important parameters to be considered. Power curves for directional wind farms are compared with the power output obtained from wind farms as per the assured generation guarantee or WTG manufacturer power curve. There exists a big prospect of ambiguity regarding the power production from wind farms. A minimization of economic threat involved in the wind farm may start in the phase of planning itself by performing high class wind measurements near the location of wind farms. Once the

wind farm is in operation the origin for a lower or higher than predicted energy production can be identified only by a wind farm concert authentication based on capacity measurement. Cost involved for such type of performance authentication is usually in the level of magnitudes lower than the connected reduction of the financier's risk. In addition, wind farm routine verification also pays for itself, as rapidly as a result it leads in analyzing the optimization of the wind farm's efficiency. In this context, an index called CPI has been developed.

Intention of the present study is to develop a comprehensive performance index called Cluster Performance Index (CPI) to evaluate the performance of wind farms and compare it with the performance of other wind farm clusters by considering various performance indicators. This is accomplished under a multi-criteria frame-work and using a mathematical tool called as Analytic Hierarchy Process (AHP). The main reason for using AHP is to expand a theory and providing a methodological tool for modeling the shapeless problems in various fields like economic, technical, social, and management sciences (Satty, 1980). It is a commanding tool which provides flexible weighted scoring result making method in assisting and it helps the people to set their priorities and make the suitable decision when looked together qualitative and quantitative aspects of a conclusion need to be considered (Satty, 1990). AHP engages in the assessment of makers in breaching down a statement into parts, it starts with the goal (at the top level) and meets the criteria (at the subsequent level). The declaration makers then make straightforward pairwise comparison judgments through the hierarchy to meet the levels at overall condition for the selected criteria (Nagesha 2004; and Nagesha and Balachandra, 2006). Though AHP can be used for a variety of purposes, the current work aims at adopting it for fixing relative importance of each of the four criteria in evaluating the performance of a wind farm.

Units of all identified dimensions in the above Tables (Table 1 to 4) are different from each other and the first five parameters are quantative and the next five parameters are qualitative in nature**.** Since all the ten parameters are having different units, it is difficult to add them to get the total. Hence, the quantitative values are also converted into a scale of 1-5, so as to make it compatible with the qualitative parameters which are on 1-5 scale. After ensuring that all the ten parameters are on 1-5 scale the study uses an 'additive model' to compute CPI and compare it with the other two.

5. DEVELOPMENT OF A MULTI-CRITERIA FRAME WORK FOR CLUSTER PERFORMANCE ESTIMATION

Utilizing accessible literature in order to evaluate the performance of wind farms and additional discussion with the experts working in the field of wind energy sector, a cluster performance study structure is developed. Study considers four important criteria which are relevant in evaluating the CPI of a wind farm. Proposed Multi Criteria based CPI is depicted in Figure 1. Since, the relative weight of each performance criterion is obtained using AHP methodology, the network is shown in the hierarchial structure. The AHP method computes the weights of the criteria (at the level 2) with respect to the goal (defined at level 1). In order to do this, pair-wise comparison of criteria with respect to the goal is essential. This is carried out using value judgement of stake holders in wind farms.

Different performance indicators considered in the study are, Technical Performance Indicator (TePI), Economical Performance Indicator (EcPI), Environmental Performance Indicator (EnPI) and Sociological Performance Indicator (SoPI). They are taken based on the consequences of the work carried out by the committee framed by WEC on the performance study of power generating plants. Under each performance indicators ten parameters are included, with first five parameters proposed by WEC Committee, and the next five relevant for the local wind farms. Each indicators is assessed on 1-5 scale (5 is most favourable and 1 is least favourable condition) and were included after consulting the people working in the field of wind energy (researcher/R&D institutions, and engineers/officers from wind industry).

The proposed CPI can be estimated as:

$$(CPI)_k = \sum_{i-1}^{n} W_i C_i \tag{1}$$

where, $(CPI)_k$ = CPI of wind farm cluster "k"

i = 1, 2, ----- n, Criteria used for comparison in a cluster

W_i = Weight of the respective criterion (obtained using AHP methodology)

C_i = Score of respective criterion in a cluster

The proposed CPI has two levels comprising the goal and criteria (referring to Figure 1). Level 1 is the main goal of the study which can be obtained by summating the scores of four performance indicators in a wind farm, assuming an additive model. Prior to this, the relative importance/priority of the four performance indicators (level 2) are to be evaluated with respect to the considered goal (CPI) through pair-wise comparisons using AHP.

The values presented in Table 5 represent the pair-wise assessment for the wind farms and are obtained by evaluating geometrical means of all the individual pair-wise comparisons of opinions obtained from 15 stake holders from each of the wind farms**.** Stake holders included engineers working in the field of wind industries (minimum of 5-6 engineers), wind farm developers (minimum of 3-4 persons), government officials working in the field of power and energy department (minimum of 3 persons) and a few selected persons residing near the wind farms (minimum of 2 persons) subsequently, by dividing individual matrix elements by the summation of respective elements of the column (by normalizing the elements in the column) and after that by evaluating the arithmetic mean of each row the priority is obtained. From the Table 5 it can be observed that the stake holders accord maximum significance (43%) to TePI followed by SoPI (23%). The EcPI and EnPI get the next subsequent positions. It is an established fact that technical performance is the most important aspect in deciding the cluster performance of any wind cluster and the same is reflected by the stake holders. economic aspects are rated as the third most important criteria (20%) by the stake holders while social factors stood at the second position (23%). Low weight of the environmental factor (14%) discloses that the stake holders do not give a lot of importance to environmental performance indicators, as all the wind farms in the study are in the barren hilly regions (revenue lands).

6. Comparison of Wind Farms Based on Individual Criterion

The two wind farm clusters are compared using all the four performance indicators separately in Tables 6, 7, 8 and 9 based on TePI, EcPI, EnPI, and SoPI respectively. The first five parameters are quantitative and the next five are qualitative in nature. Since all the ten parameters are having different units, it is difficult to add them to get the total. Hence, the quantitative values are also converted into a scale of 1-5, so as to make it compatible with the qualitative parameters which are on 1-5 scale. Finally, all the ten values inside the parenthesis were added and the sum was multiplied by the weight of the respective criterion to get the total score under that criterion.

Table 5. Pair-wise assessment of criteria with the goal

Criterion	TePI	EcPI	EnPI	SoPI	Priority
TePI	1	0.88	3.44	8.33	0.43
EcPI	1.13	1	0.68	0.80	0.20
EnPI	0.29	1.46	1	0.19	0.14
SoPI	0.12	1.24	5.08	1	0.23

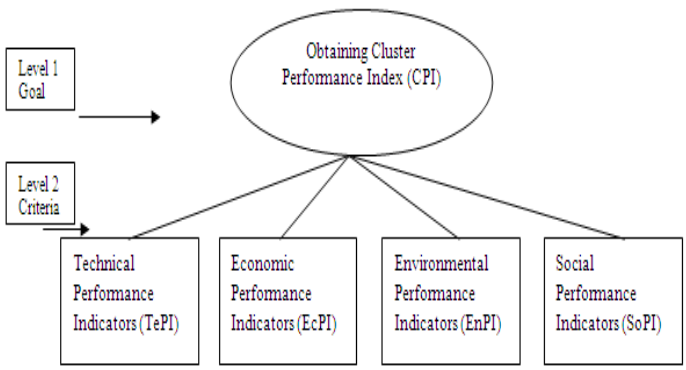

Figure 1. AHP Frame work for fixing relative weights of criteria.

Table 6. Comparison of the three wind farms based on Technical Performance Indicator (TePI)

Sl. No.	Parameters	Wind Farm Location		
		Chitradurga (CTA)	Gadag (GDG)	First Choice Wind-Farm
1	Capacity Factor (CF in %)	30.05 (5.0)#	28.73 (2.25)	CTA
2	Specific Energy Production (kWh/m^2)	65075.09 (5.0)	604465.5 (3.03)	CTA
3	Equivalent Full load Hours (h)	2655 (5.0)	2525 (2.18)	CTA
4	Plant Availability Factor (in %)	96.20 (5.0)	95.83 (2.59)	CTA
5	Wind resources or Wind conditions (velocity) during the period (in m/s)	6.64 (5.0)	6.16 (2.11)	CTA
6	Topography and Sighting of Wind Turbines (WTG rating and type)	Very High (5.0)	High (4.0)	CTA

Sl. No.	Parameters	Wind Farm Location		
		Chitradurga (CTA)	Gadag (GDG)	First Choice Wind-Farm
7	Development of Appropriate Design Criteria, Specification and Standards	Very High (5.0)	High (4.0)	CTA
8	Full scale testing prior to Commercial Introduction	High (3.0)	High (3.0)	Both are Equal
9	Condition Monitoring System (CMS) for Turbine maintenance (O&M et.,)	Extremely High (5.0)	Very High (4.0)	CTA
10	Power Evacuation (up to the grid)	Very High (4.0)	High (3.0)	CTA
Total (parentheses score x weight of TePI)		20.210	12.968	

[#]Note:- Values inside parentheses indicates the values of the parameters on a 1-5 scale.

Table 7. Comparison of the three wind farms based on Economical Performance Indicator (EcPI)

Sl. No.	Parameters	Wind Farm Location		
		Chitradurga (CTA)	Gadag (GDG)	First Choice Wind-Farm
1	Turnover Ratio	117.025 (5.0)	99.394 (3.0)	CTA
2	Internal Rate of Return (IRR, in %)	12.29 (5.0)	11.95 (1.73)	CTA
3	Pay Back Period (PBP, in years)	6.94 (5.0)	7.05 (2.17)	CTA
4	Labour Productivity	3618.27 (5.0)	3369.29(3.25)	CTA
5	Maintenance charges (Crores of Rs.)	1089.54 (0.95)	1140.28 (1.0)	CTA and GDG
6	Site Factor (wind speed distribution)	Very High (5.0)	High (4.0)	CTA
7	Variation in Annual Energy Output	Very High (5.0)	High (4.0)	CTA
8	Feed in Tariffs (FIT)	Very High (5.0)	High (4.0)	CTA
9	Situations Favorable for Repowering	Medium (4.0)	Low (2.0)	CTA
10	Accessibility to the Wind Cluster	High (5.0)	Medium (3.0)	CTA
Total (parentheses score x weight of EcPI)		8.990	5.630	

It can be observed that Chitradurga (CTA) is the preferred wind farm based on almost all criteria, individually. The same aspect is also reflected in Table 10, more conclusively by giving the overall score in terms of CPI.

Table 8. Comparison of the three wind farms based on Environmental Performance Indicator (EnPI)

Sl. No.	Parameters	Wind Farm Location		
		Chitradurga (CTA)	Gadag (GDG)	First Choice Wind-Farm
1	Contribution to the reduction of GHG emissions (Avoided CO_2 in t/MW/y)	889626 (1.77)	970997.8 (5.0)	GDG
2	Pollutant Emissions during Life Cycle; Q_{CO2}, Q_{Sox}, Q_{NOx} (t/kWh)	9363.00 (5.0)	8723.55 (3.26)	CTA
3	Visual Effects/Landscape Protection Distance (Minimum Distance Away from Dwellings in meters.)	>2073 (5.0)	>1379 (1.0)	CTA

Table 8. (Continued)

Sl. No.	Parameters	Wind Farm Location		
		Chitradurga (CTA)	Gadag (GDG)	First Choice Wind-Farm
4	Noise from Wind Turbines (in dB)	48.6 (5.0)	60 (1.0)	CTA
5	Birds Fatalities (No. of birds killed/WTG/Yr. n/yr)	02 (5.0)	06 (1.0)	CTA
6	Shadow Casting to nearby Residence (No. of hrs/yr at what time the nearby residence undergo darkness)	Very Low (5.0)	Medium (3.0)	CTA
7	Archaeological and Historical Heritage	Low (4.0)	Medium (3.0)	CTA
8	Hydrological Assessment	Very Low (5.0)	Medium (3.0)	CTA
9	Assessment of Flora and Fauna/ Climate Change (e.g., Danger caused to Species, Migrating Birds)	Very Low (5.0)	High (2.0)	CTA
10	Interference with Telecom. Systems	Very Low (5.0)	Medium (3.0)	CTA
Total (parentheses score x weight of EnPI)		6.407	3.536	

Table 9. Comparison of the three wind farms based on Sociological Performance Indicator (SoPI)

Sl. No.	Parameters	Wind Farm Location		
		Chitradurga (CTA)	Gadag (GDG)	First Choice Wind-Farm
1	Jobs Created by the Plant (No. of direct/indirect jobs created by 1MW WTG at different stages, like manufacture, installation, O and M)	58645 (5.0)	50520 (1.62)	CTA
2	Provide entrée to electrical energy (No. of household/ No. of populace having now right to use the electrical energy developed by a 1MW power plant)	200 (5.0)	100 (1.34)	CTA
3	Industrial Safety Accident Rate (SAR)	02 (5.0)	03 (2.0)	CTA
4	Monetary Benefit to the Land Owners Lakhs Rs. per acre of wind farm (For leased lands, in % annual revenue)	1.5 (1.0)	4 (5.0)	GDG
5	Contribution made to the Educational/ Cultural Development of the Local Area (in terms of % annual revenue)	2.09% (5.0)	1.78% (2.12)	CTA
6	Degree of Improvement in the Tourism Development	High (5.0)	Medium (3.0)	CTA
7	Extent of Social Costs (environment damage caused to people, etc.)	Very Low (5.0)	Medium (3.0)	CTA
8	Positive Effect on Agricultural Production and Rural Industrialization	Medium (3.0)	Low (2.0)	CTA
9	Positive Effect on Incomes and Poverty Alleviation	Medium (3.0)	Medium (3.0)	CTA and GDG
10	Positive Effect on Migration and Birth rates of Labour due to the Wind Farm	Very High (5.0)	High (4.0)	CTA
Total (parentheses score x weight of SoPI)		9.660	6.228	

Table 10. Comparison of the three wind farms based on CPI

Performance Indicators	Wind Farm Location	
	Chitradurga (CTA)	Gadag (GDG)
TePI	20.210	12.968
EcPI	8.990	5.630
EnPI	6.407	3.536
SoPI	9.660	6.228
Total	45.267	28.362

CONCLUSION

The main purpose of the present study was to provide a much needed methodology to measure the performance of the wind-farm clusters using multi-criteria approach. This helps in comparing different wind cluster performances. In this backdrop, an index called Cluster Performance Index (CPI) was proposed adopting multiple criteria. The proposed CPI comprised four criteria viz., Technical Performance Indicator (TePI), Economic Performance Indicator (EcPI), Environmental Performance Indicator (EnPI), and Sociological Performance Indicator (SoPI). Under each performance criterion a total of ten parameters were considered with five subjective and five objective oriented responses. The methodology was implemented by collecting empirical data from two wind turbine clusters located at Chitradurga, and Gadag in the southern Indian State of Karnataka. Totally fifteen different stake holders were consulted through a set of structured researcher administered questionnaire to collect the relevant data in each wind farm. The results indicated that Chitradurga wind farm was far ahead of Gadag wind farms on almost all counts. The outcome of this study establishes that wind farm clusters can be compared comprehensively using multiple criteria for performance evaluation. Further it may also help in triggering efforts for improving performance of underperforming clusters in relation to the others.

REFERENCES

Bob Smith, Vijayamohan S, and Kiran Nair, (2016), "Performance Index; A quick and efficient way to identify the odd ones," *Journal of Sustainable Energy Technologies and Assessments,* 16:1-14.

Ciprian Nemes and Florin Munteanu, (2011), "The wind energy system performance overview: capacity factor vs. technical efficiency," *International Journal of Mathemadical Models and Methods in Applied Sciences,"* 01(5):159-166.

Dimitropoulos, A. and A. Kontoleon, (2009), "Assessing the determinants of local acceptability of wind-farm investment: A choice experiment in the Greek Aegean Islands," *Energy Policy* 37:1842-1854.

Energy India 2020, published by Saket Projects Ltd. Usmanpura, Ahmedabad, October (2011).

Energy Security and Sustainable Development in Asia and the Pacific, UNESCAP, Bangkok (2010).

Fuglsang P, and Thomsen K, (2001), "Site-specific design optimization of 1.5–2.0MW wind turbines," *Journal of Solar Energy Engineering*, 123:296–303.

Google. 2015. "World Energy Scenarios Composing Energy Futures to 2050," Last modified November 15. http://www.worldenergy.orgdocumentswg3finalapj.pdf. Accessed June 25.

Ishan Purohit and Pallav Purohit, (2009), "Wind energy in India: Status and future prospects,"*journal of renewable and sustainable energy* 1(4):701-709.

M. EL-Shimy, (2010), "Optimal site matching of wind turbine generator: Case study of the Gulf of Suez region in Egypt," *Journal of Renewable Energy*, 35:1870-1878.

Mallikarjune Gowda, Head HSSE, BP-power energy limited, personal discussion held regarding the variation of wind velocity across the India in general and Karnataka in particular, 2014.

Ministry of New and Renewable Energy MNRE, 12th Plan Proposals for New and Renewable Energy, Government of India, New Delhi, (2010).

N. Nagesha, (2004), "Ranking of Barriers to energy efficiency in small scale industry clusters using Analytic Hierarchy Process: An Empirical Study of three Indian Clusters", *South Asian Journal of Management*, 12 (2): 75-94.

N. Nagesha, and P. Balachandra, (2006), "Barriers to energy efficiency in small industry clusters: Multicriteria based prioritization using the analytic hierarchy process," *International Journal of Energy*, 31: 1633-1647.

Satty T L, 1980, The analytic hierarchy process. New York: McGraw-Hill.

Satty TL. 1990, "How to make a decisio: the analytic hierarchy process," *European Journal Operation Research*, 48 (1):9-26.

Selena Farris, (2015), "A fuzzy logic approach for assessing turbine power performance," *Journal of Sustainable Energy Technologies and Assessments*, 16:1-14.

Thomsen K, Fuglsang P, and Schepers G, (2001), "Potentials for site-specific design of mw sized wind turbines," *Journal of Solar Energy Engineering*, 123:304–9.

Zahra Shirgholamia, Soudabeh Namdar Zangeneha, and Macro Bortolinib, (2016), "Decision system to support the practitioners in the wind farm design: A case study for Iran mainland," *Journal of Sustainable Energy Technologies and Assessments*, 16: 1-10.

In: Renewable Energy Systems
Editor: Sandip A. Kale
ISBN: 978-1-53610-423-3

Chapter 7

DYNAMIC ANALYSIS OF A WEAK GRID SUPPLIED FROM DIESEL AND WIND GENERATOR

A. N. Safacas[1,*] and E. C. Tsimplostephanakis[2]
[1, 2] Department of Electrical and Computer Engineering,
Electromechanical Energy Conversion Laboratory,
University of Patras, Greece

ABSTRACT

In this chapter a detailed analysis of the dynamic behavior of a weak hybrid power system supplied by a Diesel and a wind generator is presented. This dynamic energy system has been simulated by means of a developed general dynamic mathematical model based on a system of differential equations which analytically describes the electric subsystems using the Park transformation for the generators. The grid consists of a Diesel motor – synchronous generator and the necessary control systems of the frequency and the rms value of the voltage and a wind generator, including an asynchronous generator and the necessary controller for the safe and optimal operation. This dynamic model was used as basis for a general simulation program, which can be used for the study of the static and dynamic behavior of any system of the form assumed in our study. The simulation program can be employed for the determining the parameters of an under construction weak power system that lead to safe operation, satisfactory power supply (deviation of voltage and frequency under limits), and optimal exploitation of the wind potential. We used this program to investigate the dynamic behavior of the variables of a weak power system in transient phenomena. Using this model the dynamic analysis of the effects caused by the penetration of wind energy in a weak grid can be in detail investigated. Due to the developed software, some crucial transient conditions, such as the connection and the disconnection of the WECS to the weak energy grid, the wind velocity variations, three phase short circuit at the load and short circuit at the S.G.'s excitation, have been studied. Using this developed model, instead to use the Matlab software, one can check the system behavior more in details. So, we have the opportunity to study effects inside the systems components taking in account special operation conditions.

* E-mail: a.n.safacas@ece.upatras.gr.

Keywords: weak grid, Wind Energy Conversion System, control, modeling, dynamic simulation, transient analysis

1. INTRODUCTION

The countries of the European Union aim to produce 20% of its total final energy consumption from renewable sources by 2020. Renewable energy technologies – perhaps outside of hydropower – continue since the previous decade to grow at a faster rate. Of these, wind energy power electricity generation (onshore and offshore) provide the largest contribution to global renewable energy sources. The installation and maintenance cost of renewable energy applications and their financing incentives, has a very important role in energy investments. Global new investment in Renewable Power increased at 19%, during 2011 compared to the previous year (ECOMEA, 2012).

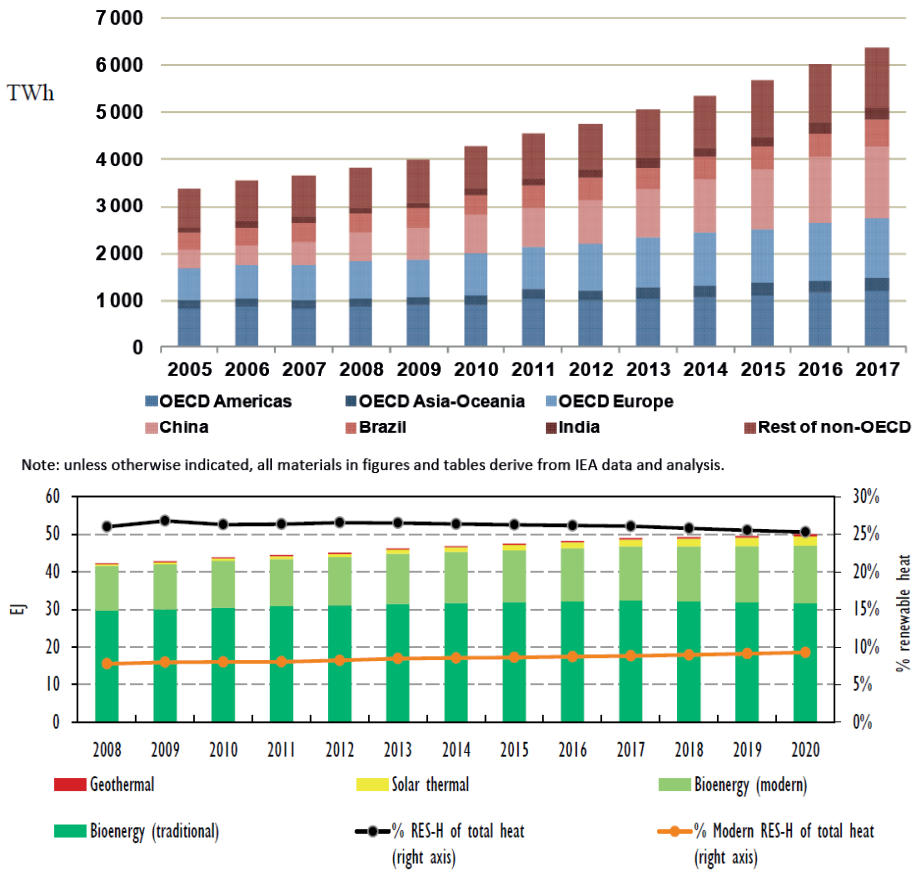

Notes: EJ = exajoules; RE-H = renewable heat. Traditional biomass is estimated here – in line with the methodology used in the International Energy Agency (IEA) *World Energy Outlook* (*WEO*) – as the use of solid biomass in the residential sector of non-member countries of the Organisation for Economic Co-Operation and Development (OECD), excluding countries in non-OECD Europe and Eurasia.

Source: Historical data derived from IEA (2015), "World energy statistics", *IEA World Energy Statistics and Balances* (database).

Figure 1. Global RES electricity production (IEA, 2015).

Table 1. World RES electricity generation in TWh (ECOMEA, 2012)

	2005	% total *Gen*	*2011*	*2012*	*2013*	*2014*	*2015*	*2016*	*2017*
Hydropower	3018	16.5%	3644	3698	3824	3962	4102	4239	4378
Bioenergy	198	1.1%	308	352	387	421	457	494	532
Wind	103	0.6%	447	527	617	705	807	927	1 065
Onshore	102	0.6%	434	509	591	672	765	868	985
Offshore	1	0.0%	12	18	26	33	43	58	80
Solar PV	4	0.0%	65	102	131	164	198	236	279
Solar CSP	1	0.0%	4	6	10	16	21	25	31
Geothermal	58	0.3%	71	73	75	78	82	87	91
Ocean	1	0%	1	1	1	1	1	1	1
Total RES-E	*3381*	*18.4%*	*4539*	*4759*	*5 46*	*5347*	*5668*	*6009*	*6377*

Notes: unless otherwise indicated, all material in figures and tables derives from IEA data and analysis. Hydropower includes pumped storage; 2011 data are estimates; the split for onshore and offshore wind is estimated for 2005 and 2011; RES-E = electricity generated from renewable energy sources.

Subsequently, production of electric power from renewable sources in Greece – only in the interconnected system - was 3.96 TWh (non including large-scale hydro-electric plants) (Monthly Bulletin of HTSO, 2012). Electricity consumption in 2011 was estimated to reach 55.7 TWh, with an installed capacity of 12.8 GW of PPC (Public Power Corporation) - operated plants and about 3 GW of auto-producers, conventional power and renewable energy sources generators.

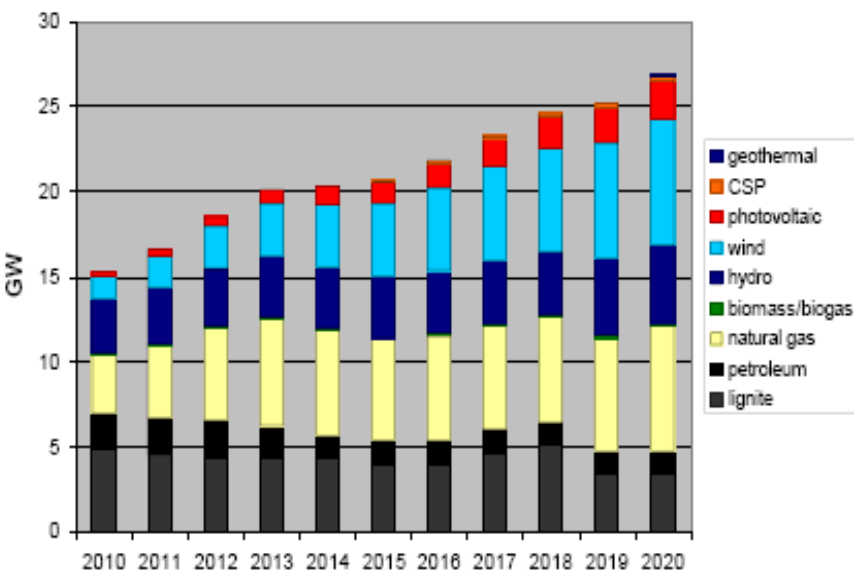

Figure 2. Estimated installed capacity of different RES technologies.

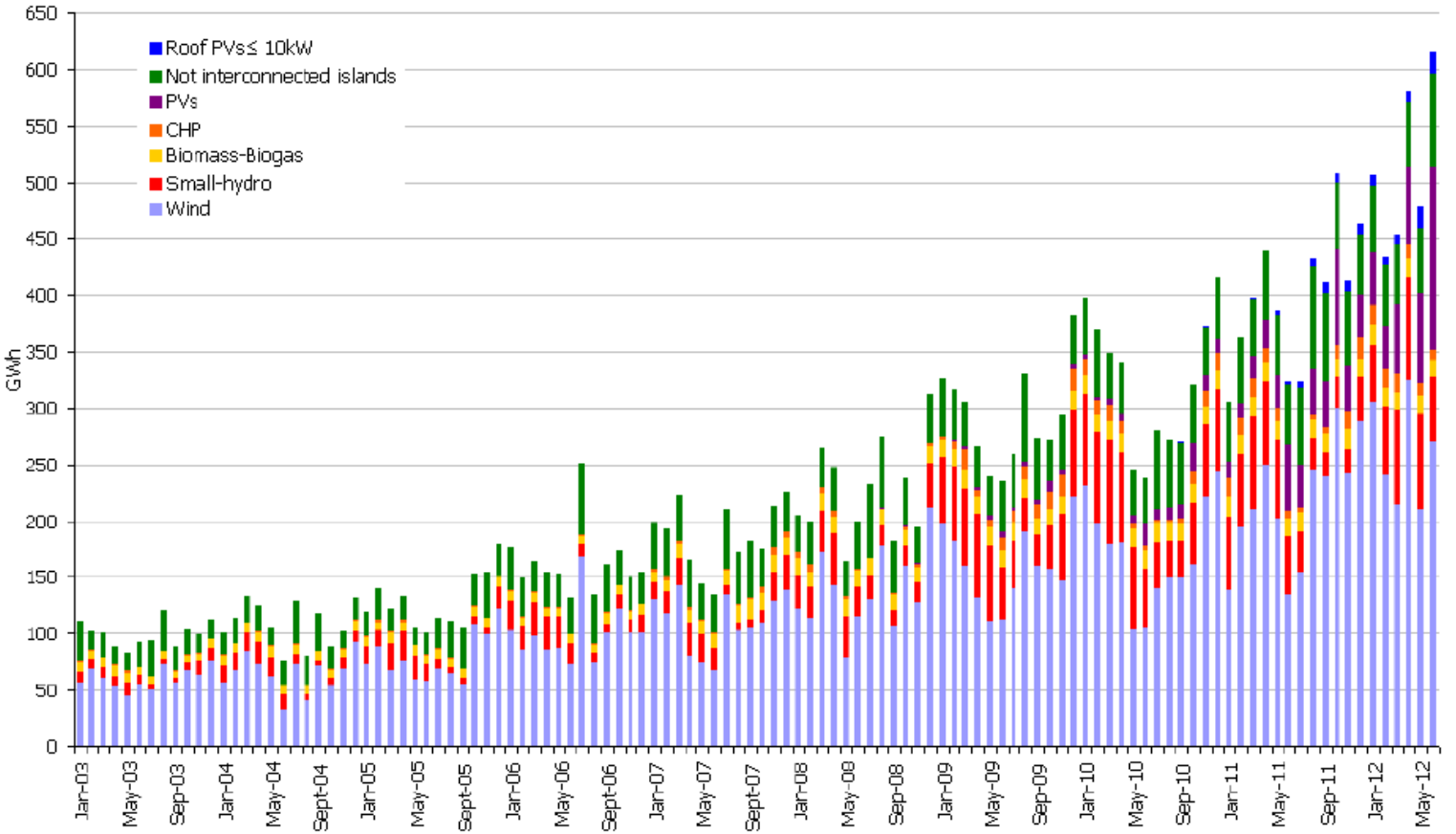

Figure 3. Total Greek electricity generation from RES and CHP and Roof PVs <10 kW (Monthly Bulletin of HTSO, 2012).

The interconnected system comprised of 12000 km of transmission lines whereas the distribution lines exceed to 230000 km (3rd and 5th National Report, 2005 and 2007). The number of customers served in Greece is some 7.55 million.

According to the above plan, the total Greek electricity generation from RES and CHP and Roof PVs <10 kW required for 2003 - 2012 in order for the target to be achieved, is presented in Figure 3.

According to the GWEC Global Wind Statistics 2014 and The World Wind Energy Association 2014 half – year report, today the power from wind reaches an account of 370 GW with a total electric energy production about 4% of the worldwide electricity production.

Because of the discontinues nature of the wind power and the fact that it is very difficult to store electric energy, systems of hybrid form have been developed. In the most common hybrid systems electrical energy is produced from both conventional sources and the wind without use of an energy storage system (Dokopoulos et al., 1996, Stavrakakis and Kariniotakis, 1995, Uhlen et al., 1994, Hatziargyriou et al., 1995, Chedid et al., 2000). In view of the power system characteristics, the use of this kind of energy systems requires appropriate control systems for the solution of instability and power quality problems.

In this research work, a hybrid system, as that shown in Figure 4, is investigated. This system consists of a conventional plant includes a Diesel – synchronous generator unit and a res unit consists of a wind motor and an asynchronous generator. There is also a short line, a transformer, an ohmic - inductive load and three control systems, one for active power – frequency control, one for control of the excitation voltage – stator voltage of the synchronous generator, and one for control of the angular velocity of the WECS. A basic feature of this system is that the supply of the required power can be satisfied only by the unit of Diesel – synchronous generator. The dynamic behavior of the weak grid is studied through the development and use of a general model for the whole system and a simulation code based on that model.

The Park equations are used for the generators and the basic aerodynamic equations are used for the wind motor. Analytical equations are also used for the description of the control systems. This computer based simulation model, offers the possibility to study any transient operation that involves the whole power system. This is important since it is well known that a qualitative and quantitative analysis of transient behavior is necessary for the power system design.

2. DEVELOPMENT OF A MATHEMATICAL MODEL

The weak grid is described using several differential equations. Twelve (12) equations describe the voltages of 12 meshes derived from the two generators, the short line, the transformer, and the load. Two (2) equations describe the torque of the generators and nine (9) equations describe the three control loops. Complete analytical models are being used for the description of the synchronous and the asynchronous generator and they are based on the Park transformation. The S.G. is described by (1), using hypermatrices, in the d-q- system.

$$\begin{bmatrix}(U_{SGT})\\(U_{SFT})\end{bmatrix}=\begin{bmatrix}(AS)_{11}(AS)_{12}\\(AS)_{21}(AS)_{22}\end{bmatrix}\begin{bmatrix}(I_{SGT})\\(I_{SFT})\end{bmatrix}+\begin{bmatrix}(BS)_{11}(BS)_{12}\\(BS)_{21}(BS)_{22}\end{bmatrix}\frac{d}{dt}\begin{bmatrix}(I_{SGT})\\(I_{SFT})\end{bmatrix} \quad (1)$$

For the part consisting of the short line–transformer–asynchronous generator, the following equations in matrix form in the a-b-c- system are used:

$$(U_{LIN}) = (DL\ R_{LIN})\ (I_{LIN}) + (DL\ L_{LIN})\frac{d}{dt}(I_{LIN}) + (U_{TRAT}) \tag{2}$$

$$(U_{TRAT}) = (R_{TR})\ (I_{LIN}) + (L_{TR})\ \frac{d}{dt}\ (I_{LIN}) + (U_{TR}) \tag{3}$$

$$(U_{TR}) = T_R\ (U_{AGS}) \tag{4}$$

$$(U_{AGS}) = (R_{SA})\ (I_{AGS}) + \frac{d}{dt}\ ((L_{SSA})\ (I_{AGS})) + \frac{d}{dt}((L_{SRA})\ (I_{AGR}) \tag{5}$$

$$(U_{AGR}) = (R_{RA})\ (I_{AGR}) + \frac{d}{dt}\ ((L_{RSA})\ (I_{LIN})) + \frac{d}{dt}\ ((L_{RRA})\ (I_{AGR})) \tag{6}$$

The parameter elements of the asynchronous machine are reduced to the primary winding of the transformer through the following relation:

$$(R_i\ ,\ L_i) = (R_i\ ,\ L_i)\ \ TR^2 \tag{7}$$

TR is the voltage ratio.

As the asynchronous generator is a squirrel-cage machine, the voltage matrix (U_{AGR}) becomes zero.

Equations (3) – (6) can be transformed to the d-q- system under consideration that the d-q- system is steadily connected with the stator. This leads to (8):

$$\begin{bmatrix}(U_{LINT})\\(0)\end{bmatrix} = \begin{bmatrix}(AA)_{11}(AA)_{12}\\(AA)_{21}(AA)_{22}\end{bmatrix}\begin{bmatrix}(I_{LINT})\\(I_{AGRT})\end{bmatrix} + \begin{bmatrix}(BA)_{11}(BA)_{12}\\(BA)_{21}(BA)_{22}\end{bmatrix} d/dt \begin{bmatrix}(I_{LINT})\\(I_{AGRT})\end{bmatrix} \tag{8}$$

The load in the a-b-c- system is described through the following equations in the form of matrices:

$$(I_{LOAD}) = -(I_{SGS}) - (I_{LIN}),\ (U_{LOAD}) = (U_{SGS}) = (U_{LIN}) \tag{9}$$

These equations must be transformed to the d-q- system.

Equation (10) in form of hypermatrices in the d-q- system, describes in compact form the weak system, composed of the generators, the line, the transformer, and the load.

$$(C)\ d(AGN)/dt = (A)\ (AGN) + (B)\ (GN) \tag{10}$$

where (A), (B), (C) are the matrices of the parameters of the power system, (GN) is the matrix of the input voltages and (AGN) is the matrix of the system variables. In this system the currents of the line (and the currents of the A.G. stator), the currents of the A.G. rotor, the currents of the stator and the rotor of the S.G. are included. In total, there are twelve unknown currents in the whole system. In the previous equations (1) - (9), the current and the voltage matrices are of dimension (1x3). All the other matrices are of dimension (3 × 3).

The proper operation of the investigated energy system requires that the frequency and the rms value of the grid voltage remain constant in any case or that variables have small deviations. The angular velocity of the A.G 's rotor is required to be between the synchronous and the brake down rotating values in generating operation. A control of the A.G.'s rotating velocity in that range is necessary because under any wind velocity the maximum power must be extracted. This of course assumes the existence of appropriate automatic control systems: one for controlling the frequency of the Diesel–S.G., shown in Figure 5, by adjusting the S.G.'s angular velocity, ω1. As it is well known the variations of this frequency must be smaller than ±1%. The frequency control takes place by changing the mechanical power on the S.G.'s axis, and this is done by changing the intake of fuel in the Diesel machine (IEEE Comitee Report, 1973 and 1981). The following equations, which describe the control of the rotating velocity ω1, can be obtained:

The torque equation of the synchronous generator:

$$(J_S / p_S)\, d(\omega_1)/dt = (p_S/ \omega_1)\, (P_{mo} - \Delta P_M) - M_{EL} \tag{11}$$

$$M_{EL} = p_S\, (I_{SGq}\, I_{SGd}\, (L_{dd} - L_{qq}) + (L_{fd}\, I_{SF} + L_{Dd}\, I_{SD})\, I_{SGq} - L_{Qq}\, I_{SQ}\, I_{SGd}) \tag{12}$$

In equation (11), P_{mo} is the initial value of the Diesel engine's output power, which is equal to the nominal value. J_S is the total inertia of the Diesel engine and the synchronous machine.

The equations of the P-I-D controller:

$$\Delta P_P = (\omega_{1o} - \omega_1) / (2\, \pi\, f_{1o}\, R) \tag{13}$$

$$d(\Delta P_I)/dt = K_I\, (\omega_{1o} - \omega_1) \tag{13a}$$

$$\Delta P_D = - K_D\, d(\omega_{1o} - \omega_1)/dt \tag{13b}$$

$$\Delta P = \Delta P_P + \Delta P_I + \Delta P_D \tag{13c}$$

The equations of the mechanical output power of the Diesel engine:

$$d(\Delta P_1)/dt = T_C^{-1}\, (\Delta P - \Delta P_1) \tag{14}$$

$$d(\Delta P_M)/dt = T_S^{-1}\, (\Delta P_1 - \Delta P_M) \tag{14b}$$

where R, K_I, $K_D < 0$.

In the previous equations T_C is the delay of the frequency control and the measurement system, T_S is the Diesel engine delay and R is the Diesel permanent speed droop. The unit for R is kW^{-1}. This proportional controller leads the system to a stable condition. The integral and differential controller are necessary for the die out and the minimization of the variables oscillations, respectively.

The control equations of the three-phase voltage of the synchronous generator, achieved through the control loop for the voltage excitation, are the following (IEEE Comitee Report, 1968),

$$d(U_5)/dt = (K_R/T_R)\,(U_{SGS}/U_{ref}) - (1/T_R)\,U_5 \quad (15)$$

$$d(U_2)/dt = -(K_A/T_A)U_4-(K_A/T_A)U_5 -(U_2/T_A)+(K_A/T_A) \quad (15a)$$

$$d(U_{fd})/dt = -(1/T_E)\,U_2 - (K_E/T_E)\,U_{fd} \quad (15b)$$

$$d(U_4)/dt = -(K_F/(T_F\,T_E))U_2 - ((K_F\,K_E)/(T_F\,T_E))\,U_{fd} - (1/T_E)\,U_4 \quad (15c)$$

The S.G.'s stator voltage (U_{SGS}) is continuously measured and compared with the reference value (Uref). The voltage error is summarized with the voltage signal U_4 at the output of the excitation stabilizer. The excitation stabilizer is necessary to stabilize the behavior of the controller via the differentiation of the excitation voltage. This controller has a delay. The sum of the signals will be amplified and then can supply the excitation winding of the S.G.

The control system for the W.T. – A.G., acts in to ensure the safe operation of the WECS and the optimal exploitation of the wind potential. In Figure 7 we can see the block diagram of the optimum control strategy for the tip speed ratio (λ). This control system includes the pitch angle controller and the velocity converter controller.

It is composed of the following sections (De La Salle et al., 1990, Leith, 1997):

a) Controlling the inclination of the WECS landscape axes and of the blades, when the wind value is higher than the nominal value ($u_{wind}>u_{WN}$).

b) Controlling the ratio of the converter velocity so as for any given wind speed, an appropriate rotating velocity of the rotor of the asynchronous generator is established. The appropriate rotating velocity is that for which the WECS operation is between the synchronous and the break down rotating velocity. This value corresponds to the best torque factor (c_{Mopt}) and consequently to the optimum power factor (c_{Popt}) or the optimum tip speed ratio (λ_{opt}). For a wind motor stands following relations (Freris, 1990, Heier, 1996 and Molly, 1990),

$$\lambda = \Omega_{WM}\,R/u_W = \omega_R\,R\,/\,(K_A\,p_A\,u_W) = \Omega_R\,R/(K_A\,u_W) \quad (16)$$

In our case, $\omega_R = \Omega_R$, because the A.M. has a pole pair.

From the aerodynamic equation of the W.T. we obtain:

$$M_{MWM} = Q\,c_M(\lambda),\ Q = 0.5\,\rho\,\pi\,R^3\,u_W^2, \quad (17)$$

where ρ is the wind's density.

For the mechanical torque, we have:

$$M_{MA} = M_{MWM} / K_{A\ new} \tag{18}$$

For the wind generator of three blades the characteristic curves $c_{M(\lambda)}$ and $c_{P(\lambda)}$ that have been chosen are presented in Fig. 8. An analytical description of these curves is suggested in this study. Specifically, the equations (19) and (19a) have been developed for a very good approximation of these diagrams. The coefficients of the suggested polynomials have been defined in such a way that the optimum value of c_M used in (17) gives the nominal torque of the wind motor.

$$0 \le \lambda \le \lambda_M: c_M(\lambda) = 0.04+0.03\lambda-0.04\lambda^2+0.005\lambda^3-0.001\lambda^4 \tag{19}$$

$$\lambda_M \le \lambda \le 9: c_M(\lambda) = 0.184 - 0.007\ \lambda - 0.0015\ \lambda^2 \tag{19a}$$

In the diagrams (Figure 8) we can see that there are values of λ that yield c_{Mmax} and c_{Pmax}. c_{Pmax} is also the optimum value c_{Popt}. For the subcase a) the equations describing the control action we mentioned are:

$$\text{if } u_{WIND} > u_{WN} \text{ then } u_W = u_{WIND} \cos\alpha, \tag{20}$$

where, $\cos\alpha = 1-x$,

$$T_{AN}\ dx/dt = K_{AN}\ (u_{WIND} - u_{WN}) - (K_{AN}\ u_{WIND} + 1)\ x \tag{21}$$

If x= 0, then cosα=1. The blades are in a normal position of operation, when they are at 90° from the flag position.

For the control subcase b) the change of the velocity converter ratio is described by the following relations:

$$T_{AS}\ d\beta/dt = K_{AS}\ (\lambda - \lambda_{opt}) \tag{22}$$

$$K_{A\ new} = K_{A\ old} / (1- \beta) \tag{23}$$

$$(J_A/p_A)\ d(\omega_R)/dt = (Q\ c_M(\lambda)/K_{Anew}) + M_{ELA} \tag{24}$$

$$\text{where, } M_{ELA} = p_A\ L_{HA}\ (I_{AGRd}\ I_{AGSq} - I_{AGRq}\ I_{AGSd}) \tag{25}$$

J_A is the total inertia of the WECS included the inertia of the three rotating parts, the wind motor, the velocity converter and the A.G. It is well known that the inertia of the W.T. (J_{WT}) is much bigger compared to the A.G.'s inertia (J_{AG}) and to the velocity converter's inertia (Dokopoulos et al., 1996, Stavrakakis and Kariniotakis, 1995, Abdin and Xu, 2000, De Battista et al., 2000). Equations (16) – (25) are illustrated in the block diagram (Figure 7).

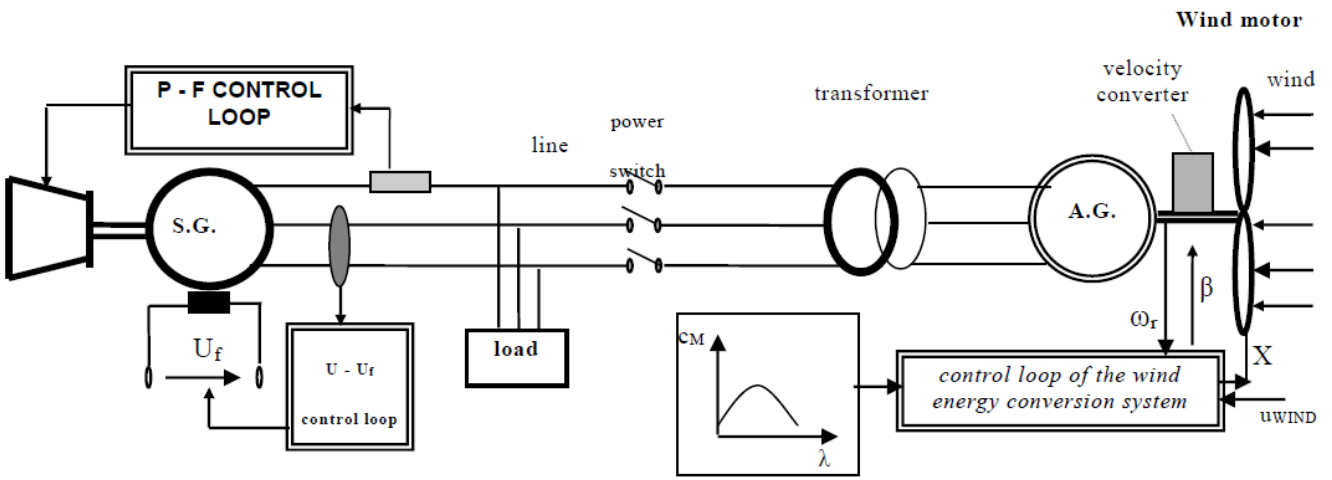

Figure 4. Basic structure of the hybrid weak energy system.

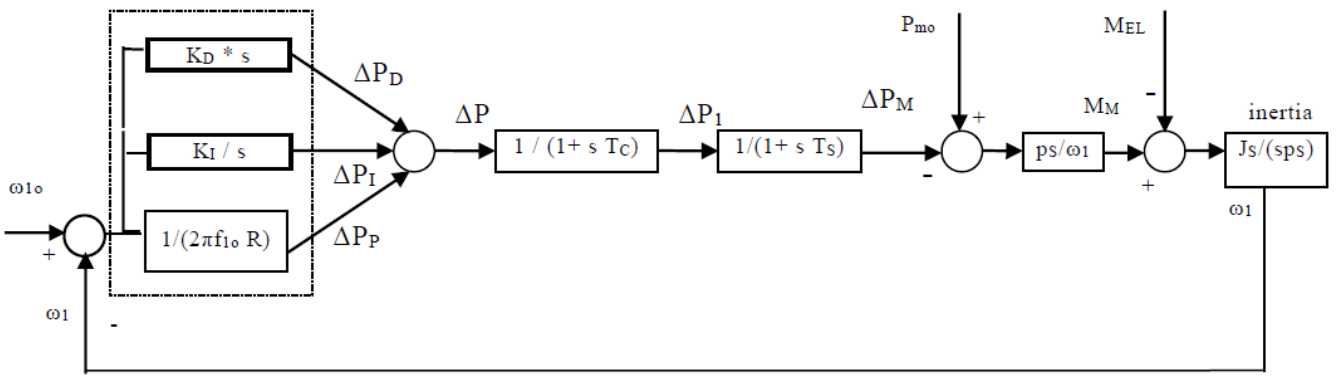

Figure 5. Block diagram of the frequency control system.

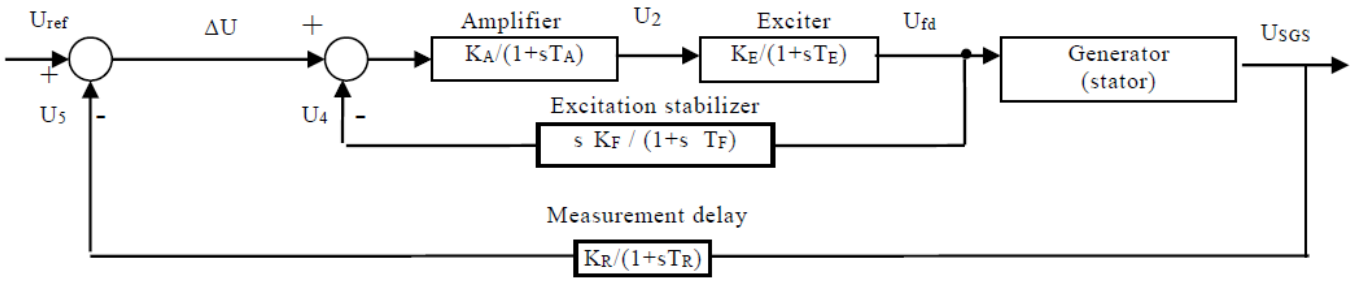

Figure 6. Block diagram of the voltage control system.

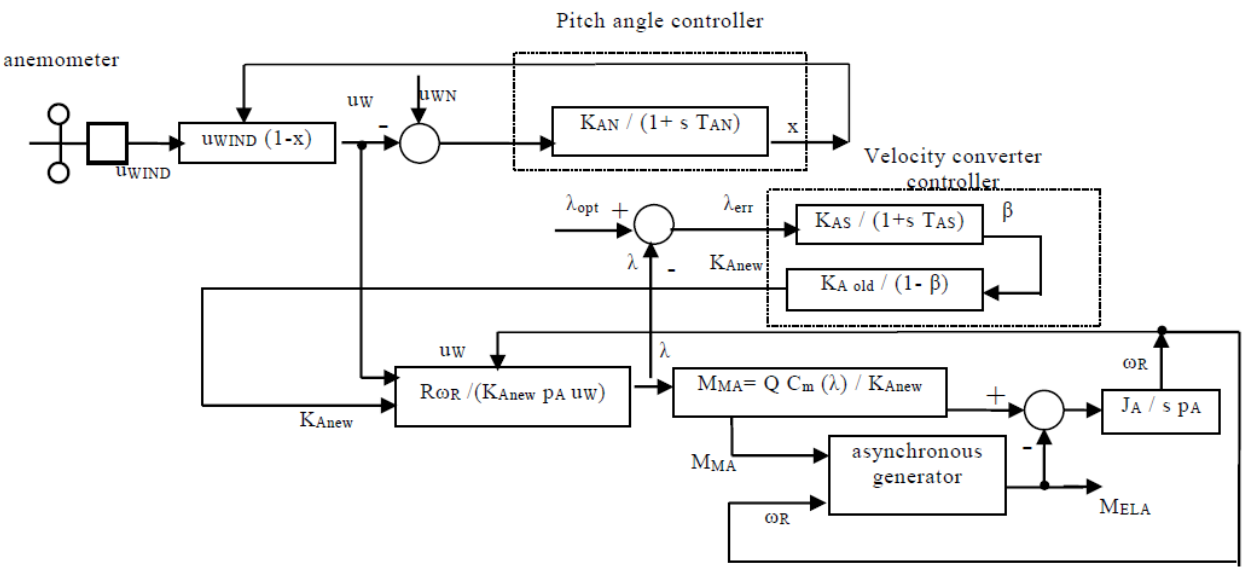

Figure 7. Block diagram of the WECS rotating velocity control system.

From the above equations it is established that when λ becomes equal to λ_{opt}, $d\beta/dt = 0$. This means that the ratio of the converter does not change. When λ becomes higher than λ_{opt}, $d\beta/dt > 0$, and as a result $K_{A\ new}$ is increasing. Therefore, the M_{MA} mechanical torque decreases, and so, the ω_R angular velocity decreases as well. Thus, λ tends to be reduced, reaching gradually λ_{opt}, at which point we have the best exploitation of the wind potential.

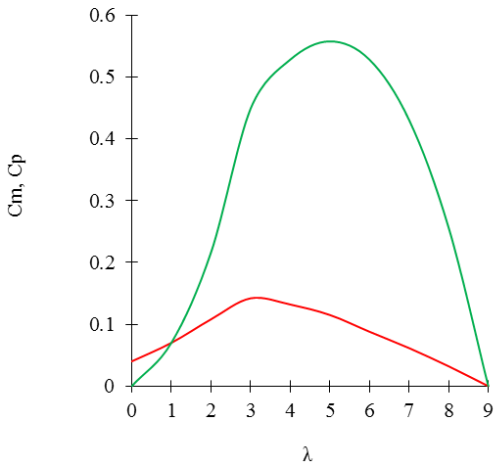

Figure 8. C_M - λ, C_P - λ curve.

In order to complete the mathematical model of the studied system, we must take the wind fluctuations into consideration. For this purpose we have formulate the equation (26) to describe the characteristic variations of the wind velocity when the height of the hub is H= 10m. The parameters of these equations are changed according to each case examined:

$$u_{WIND10} = u_{wa} + ((25 + t)/12.5) + u_{wa1} \sin (u_{wc}/(t+0.1)) + u_{wb} \sin^2 (u_{wc}\, t) + u_{wd} \sin^3 (u_{we}\, t) \quad (26)$$

Through the known equation (27) we can calculate the wind velocity at any height (Freris, L. 1990) of hub.

$$u_{WIND} = u_{WIND10}\, (H/10)^{0.14} \quad (27)$$

Because the measurement of the wind speed cannot be precise, the previous control of the wind generator does not achieve the best control, but it does manage to bring the system close enough optimal operation. In total, the model of the system under investigation consists of 23 differential equations, some of which are not linear.

3. Computational Aspects

The mathematical model that was formulated in the preceding section can be used to study the behavior of the weak grid under investigation in detail. The model can be expressed in the form of hypermatrices as follows:

$$(K)\ d(AGNT)/dt = (\Lambda)\ (AGNT) + (M)\ (GNT) \quad (28)$$

where (K), (Λ), (M) are the hypermatrices for the parameters of the power system, (GN) is the hypermatrix of the entering voltage and (AGNT) is the hypermatrix of the system's variables. Analytically, these hypermatrices are presented in appendix.

Table 2. Initial values of the variables before the WECS connection

I_{lind}	0	I_{SGd}	67.55A	ω_1	314.16rad/s	U_{fd}	1.0 pu
I_{linq}	0	I_{SGq}	-180.043A	ΔP_I	0	U_4	0.0
I_{lino}	0	I_{SGo}	0	ΔP	0	ω_R	314.16rad/s
I_{AGRd}	0	I_{SF}	1229.51A	ΔP_M	0	B	0
I_{AGRq}	0	I_{SD}	0	U_5	1.0 pu	X	0
I_{AGRo}	0	I_{SQ}	0	U_2	0.05pu		

The initial values for the variables of the whole electric system that are required for the solution of the differential equations of the system, eq. (28), are specified as follows:

We consider that the unit Diesel – S.G. initially operates in nominal steady state, that the supplied load is nominal, and that the WECS has not been connected as yet. In this way, the initial values of the variables that are related to this unit in the d-q- system are determined. We also assume that the wind speed is such that the rotating velocity of the A.M. has the synchronous value. At that time, the connection of the WECS stator with the transformer (Figure 4) takes place. A computer program, with low computational cost, written in Turbo Pascal was used to solve equations (28). The parameters used in the computations and the non zero elements of the matrices are given in appendix. A 4th order Runge–Cutta method with h = 0.001 was used to solve the equations.

4. DYNAMICAL BEHAVIOUR OF THE SYSTEM AT THE WECS CONNECTION AND DISCONNECTION

With the developed dynamic model, we can investigate every dynamic phenomenon with great accuracy, calculating the waveform of the currents, the voltages, the rotating velocities, the torque, the mechanical power, etc. Some characteristic results of the dynamic simulation in the case of the connection and the disconnection of two different WECS will be presented here. In the first WECS, the nominal power comes up to 33% of the nominal power of the Diesel-S.G. and in the second up to about 7%. In both WECS the wind velocity is assumed to be 12 m/s and remain constant. The dynamic behavior is evaluated from the waveforms of its electromagnetic and mechanical variables. The figures present the waveforms of the most characteristic variables.

In Figures 9, 10, 11, 12 and 13, we present the waveforms of the S.G. rotating velocity $\omega_1(t)$ (frequency), the S.G. voltage $U_{SGS}(t)$, the excitation current $I_{SF}(t)$, the damping current $I_{SDQ}(t)$, the S.G. electromagnetic torque $M_{EL}(t)$ and the rotating velocity $\omega_R(t)$ of the A.G., the current of the line $I_{LIN}(t)$ (stator current) and the electromagnetic torque $M_{ELA}(t)$ of the A.G.

Figure 9 depicts the waveforms of the system' s variables for connection of two WECS with nominal power of 1 MW and 200 kW, respectively. The study of these waveforms results in the following:

1) In both cases under study, the behavior of the system is qualitatively similar. We must point out the fact that during the first few periods after the connection of the WECS with the grid, a reduction of the S.G.'s angular velocity and an increase of the excitation current take place. These are due to the fact that at the beginning of the connection the asynchronous machine works as a motor because of the lack of the necessary magnetizing current, as it begins to increase slowly and so the E.M.F. of A.M. is smaller than the grid voltage.
2) The recovery time for the system to get a new steady state after connection of the WECS with nominal output power of 1 MW is about 30% longer in comparison to the WECS of 200 kW.
3) The magnitude of the oscillations of the system's variables are generally small in the case of a 200 kW WECS connection with the grid.
4) Other observations are presented in Table 3:

Table 3. Comparison of WECS connection with different nominal power

WECS CONNECTION	*0,2 MW WECS*	*1 MW WECS*	*RATIO (POWER 1:5)*
$\Delta\omega_R$	2%	9.5%	1 : 4.8
$\Delta\omega_1$ (*)	1.27%	6.3%	1 : 5
ΔI_{SF}	2.5%	14.6%	1 : 5.8
I_{SDQ}	120 A	380 A	1 : 3.2
ΔU_{SGS} (*)	9.2%	60%	1 : 6.5

*Deviation from nominal value.

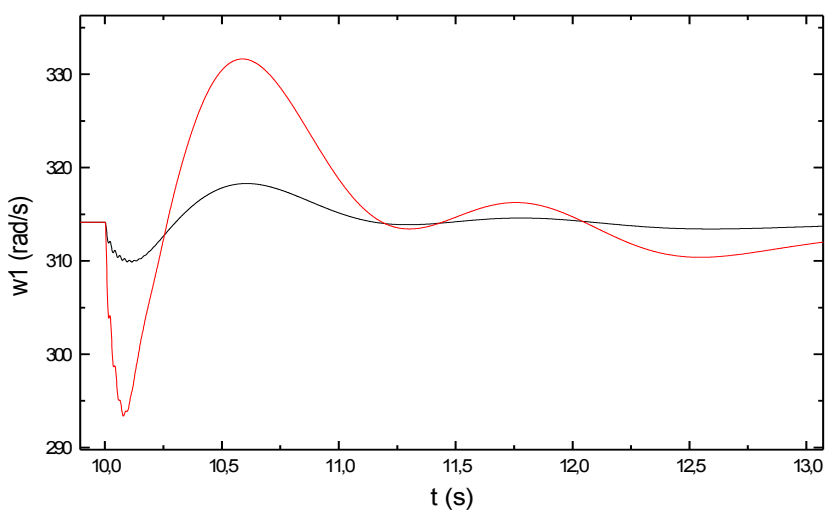

a

Figure 9. (Continued)

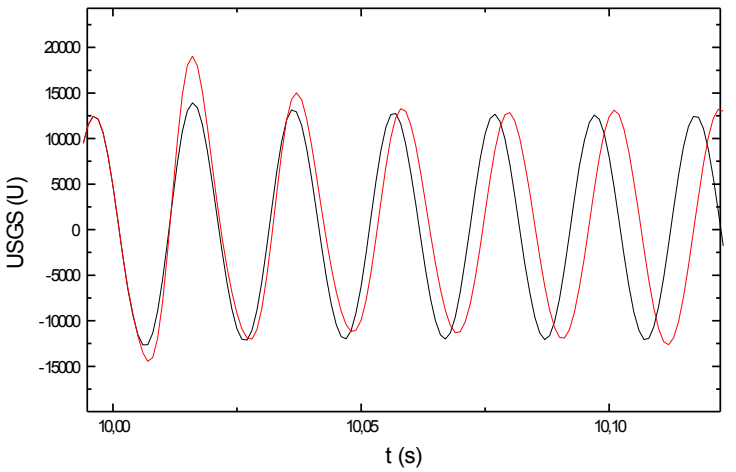

b

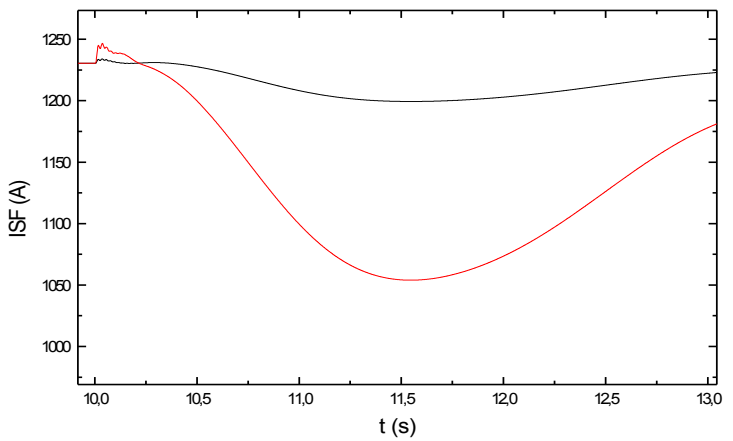

c

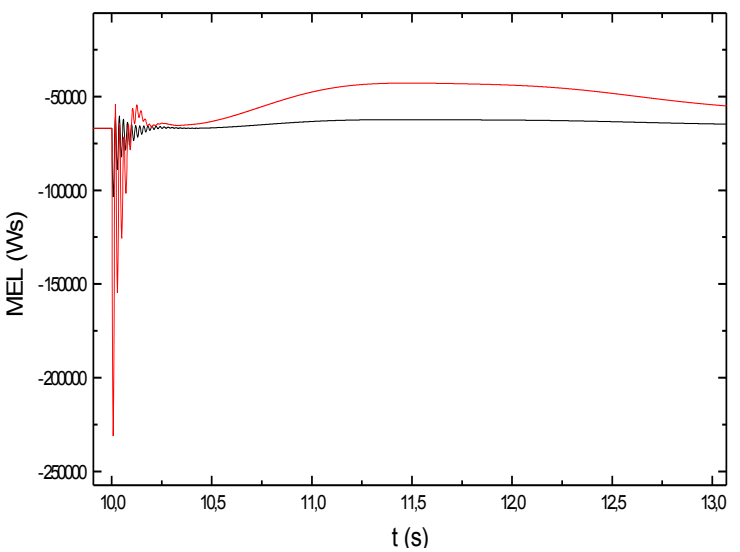

d

Figure 9. (Continued)

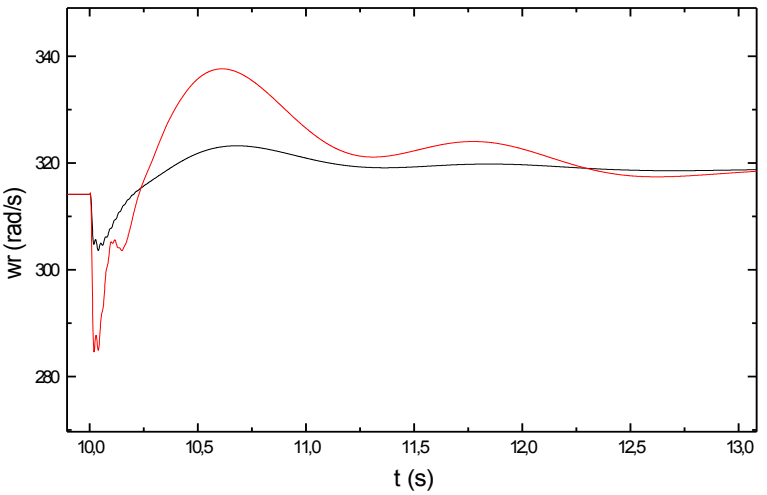

e

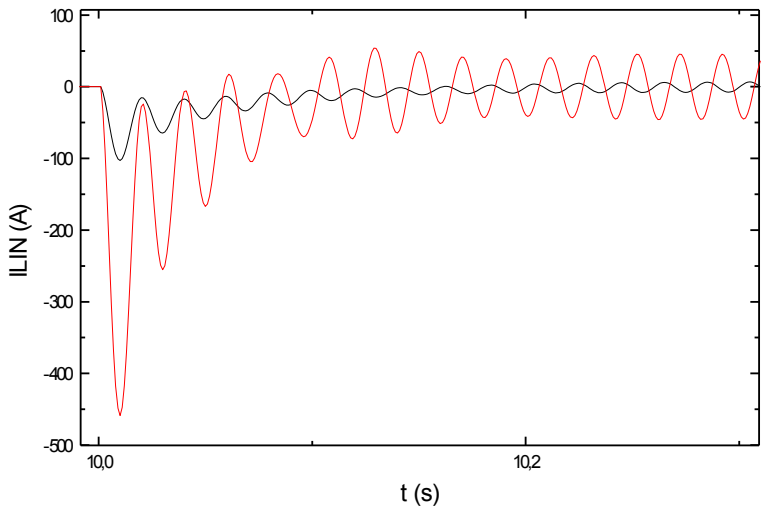

f

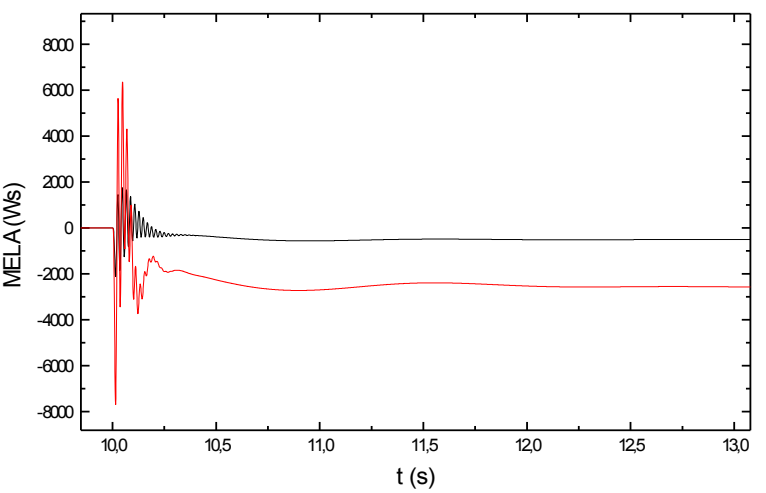

g

Figure 9. (Continued)

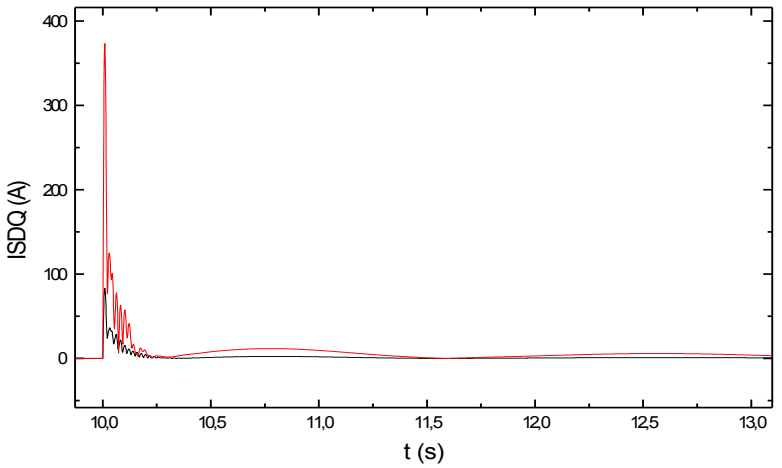

h

Figure 9. Electromechanical variables following the 1 MW WECS and the 200 kW WECS connection. (--- (red line): 1MW WECS, —(black line): 200 kW WECS).

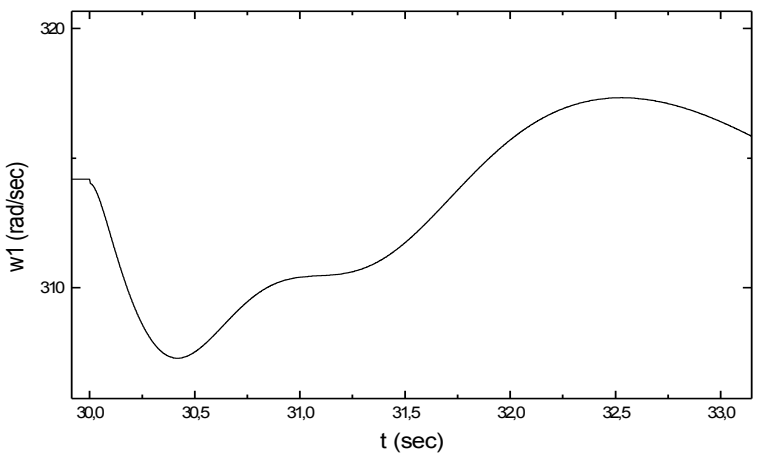

a

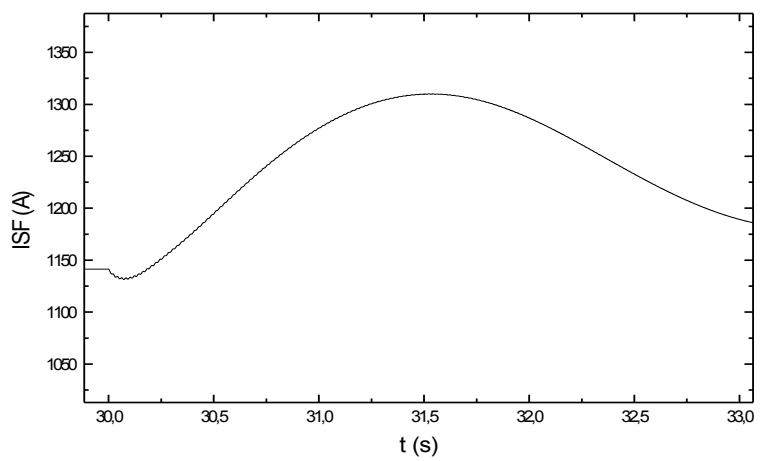

b

Figure 10. (Continued)

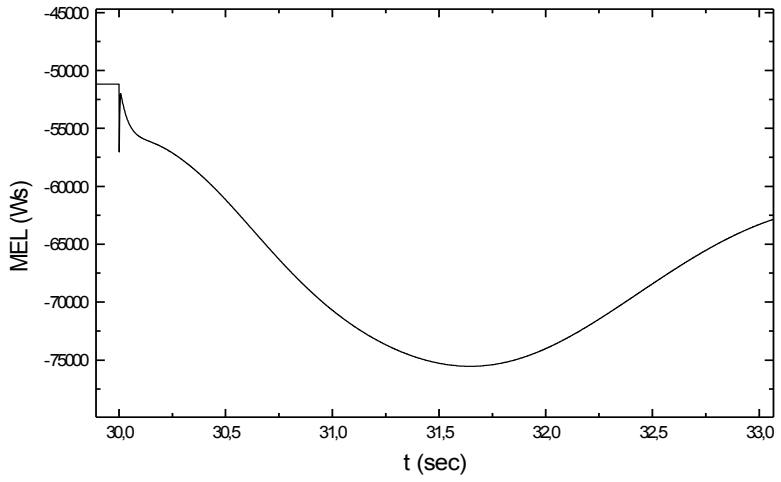

c

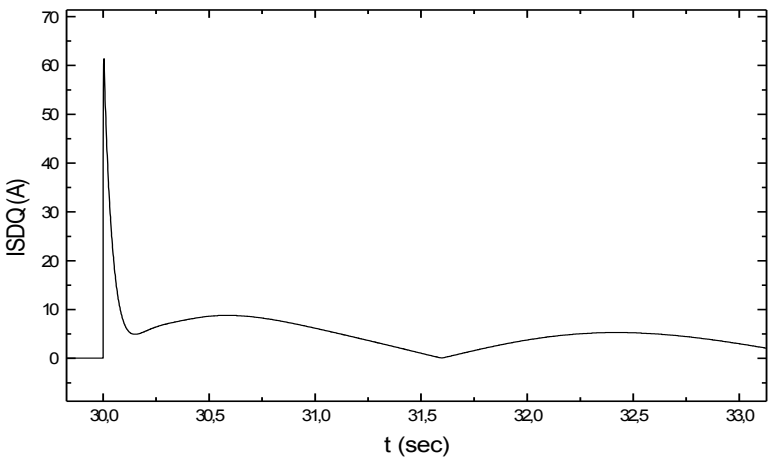

d

Figure 10. Electromechanical variables following the 1 MW WECS disconnection.

The waveforms of the system's variables being during disconnection of the 1 MW WECS from the grid are depicted in Figure 10.

The comparison of the waveforms of Figure 9 and 10 results in the following:

1) The time needed for the system to get to the new steady state is about the same. This is not surprising since there is no change in the inertia of the electro-mechanical subsystems and in the time constants of the controllers of both the generators remain the same.
2) It must be pointed out that the magnitudes of the oscillations of the system's variables are smaller during the disconnection process.

The angular velocity of the S.G. changes by about 50% during the disconnection of the WECS in comparison with the connection of the same WECS, although the corresponding changes in the excitation current and the electromagnetic torque of the S.G. are about 30%.

Other observations for deviations of critical parameters according waveforms of Figures 9 and 10, are approximately presented in Table 4:

Table 4. Comparison of parameter deviation by WECS connection and disconnection

1MW WECS	*WECS connection*	*WECS disconnection*
Δω1 max Periods if Δω1> 1%	6.3% 150	2.7% 90
ΔUSGS max Periods if ΔU>10%	60% 35	17.5% 20
I_{SDQ}	370 A	60 A
MEL init/ MELst.st.	4.1	1.5

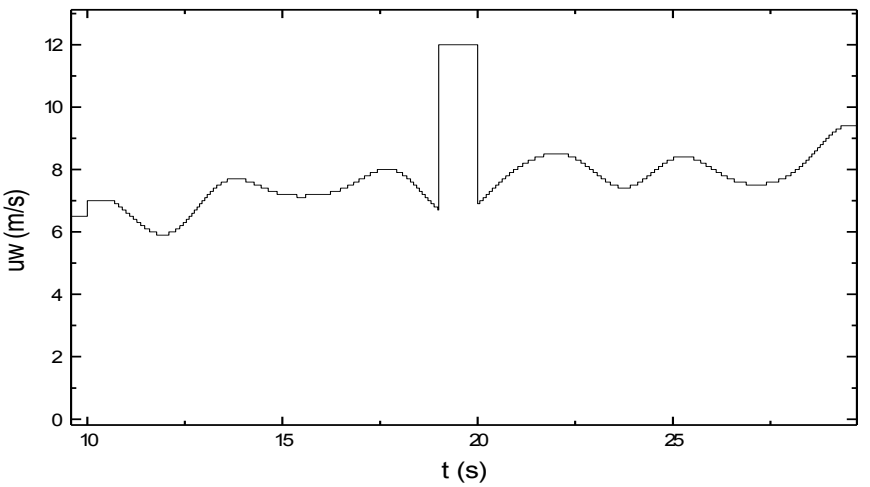

a

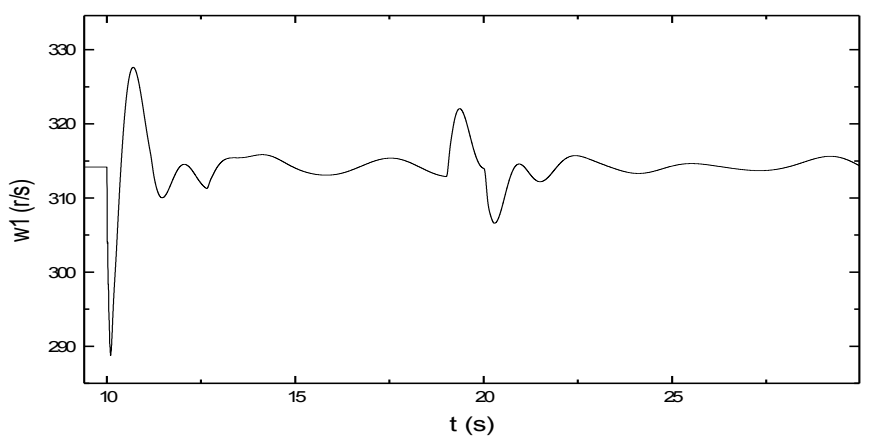

b

Figure 11. (Continued)

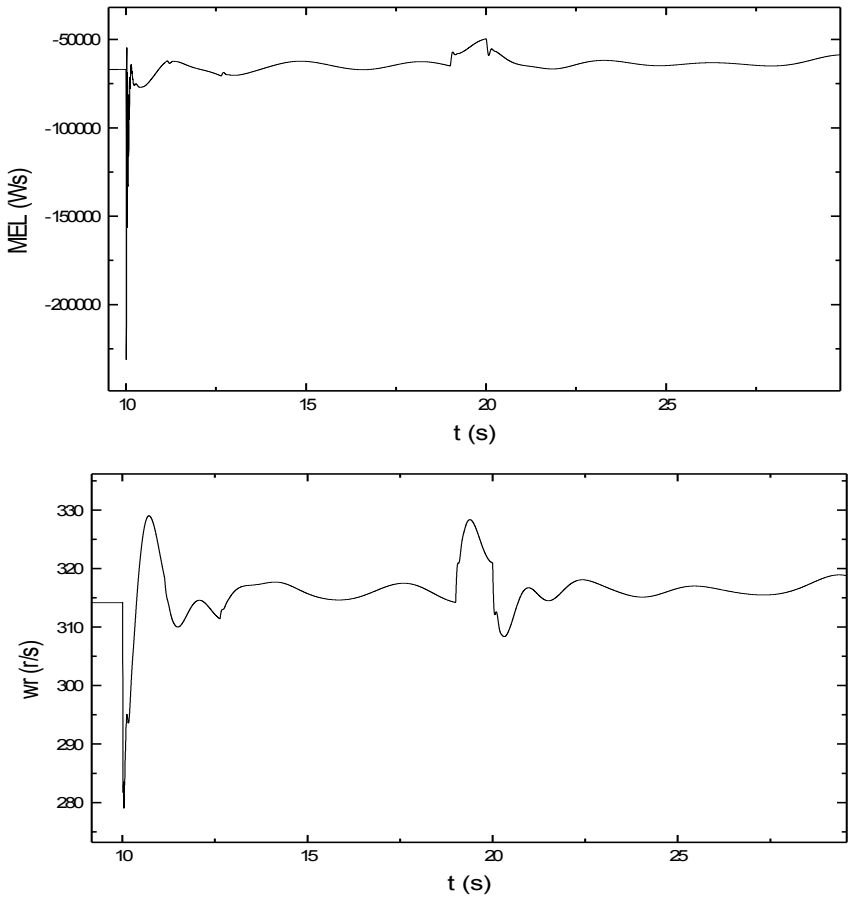

Figure 11. Electromechanical variables following the 1 MW WECS connection with wind velocity variations.

5. DYNAMIC BEHAVIOR OF THE SYSTEM BY WIND FLUCTUATIONS

The investigation of the system's variables disturbances that occur from the random wind fluctuations is necessary to obtain a reliable information about the system's behavior. For such case we can see some characteristic simulation results in Figure 8. It's supposed that the value of the wind velocity during the connection of 1 MW WECS is 7.0 m/s and after some small disturbances apears a rapidly deviation from 7.0 m/s to 12.0 m/s and then it comes back to the previous condition. Via the equations (26) and (27) and for H=10m, if the parameters are u_{wa}= 3.4, u_{wa1}= 0.08, u_{wb}= 1.2, u_{wc}= 0.8, u_{wd}= 0.5 and u_{we}= 0.9, we obtain a typical wind velocity such in Figure 11a.

The comparison of the waveforms of Figures 9 and 11 results in the following:

1) The amplitude of the oscillations during the WECS connection depends at most on the nominal value of the WECS power (and of the parameters of the W.T. and the A.G.).

2) It depends not from the generated power of the WECS (and the value from the wind velocity).
3) The amplitude and the attenuation time of the variables oscillations by the wind velocity fluctuations are smaller compared to those in the case of the WECS connection, in the three-phase short-circuit at the load and in the short-circuit at the S.G.'s excitation. Moreover they are smaller in the disconnection of the WECS.

6. DYNAMIC BEHAVIOR OF THE SYSTEM AT A THREE-PHASE SHORT-CIRCUIT

For a weak grid, the behavior during three-phase short-circuit at the load is of great interest since it is highly probable such a situation to be encountered in practice, and when it does, the consequences can be very important. When a three-phase short-circuit occurs, the voltage has the same value at the points, where the symmetrical three-phase load is connected, that is Ut= Ud= Uq= 0. It is assumed that the duration of the error is 0,5 s. Figures 9 and 12 depict the waveforms of the system variables for the case of 1 MW WECS connection to the grid and for the case of a three-phase short-circuit, respectively. A careful study of the results of these figures leads to the following:

The peak value of ω_1 during the connection of the 1MW WECS is smaller than in the three phase short-circuit. These oscillations are intense during the three-phase short-circuits. The magnitude of the fluctuation of the electro-magnetic torque of the S.G. is much bigger in the three phase short-circuit and it presents more intense characteristics in the event of the three-phase short-circuit with regard to the qualitative form of the waveforms. The damping current of the S.G. gets about 15 times bigger peak value in the case of the short-circuit and gets a value about 37 times bigger peak value compared to the nominal value of the S.G.'s nominal stator current. The angular velocity of the A.G. has the same behaviour as the angular velocity of the S.G.

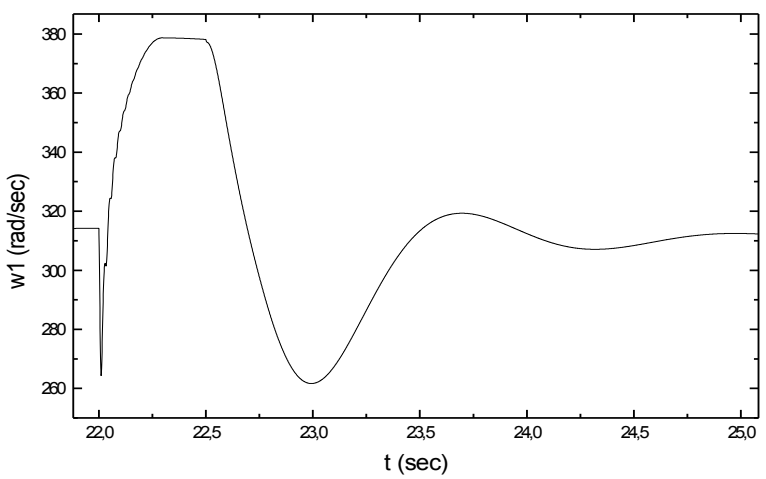

a

Figure 12. (Continued)

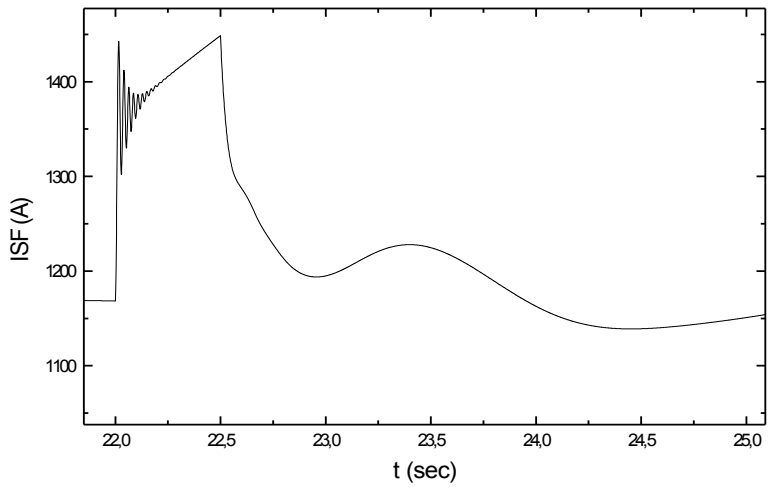

b

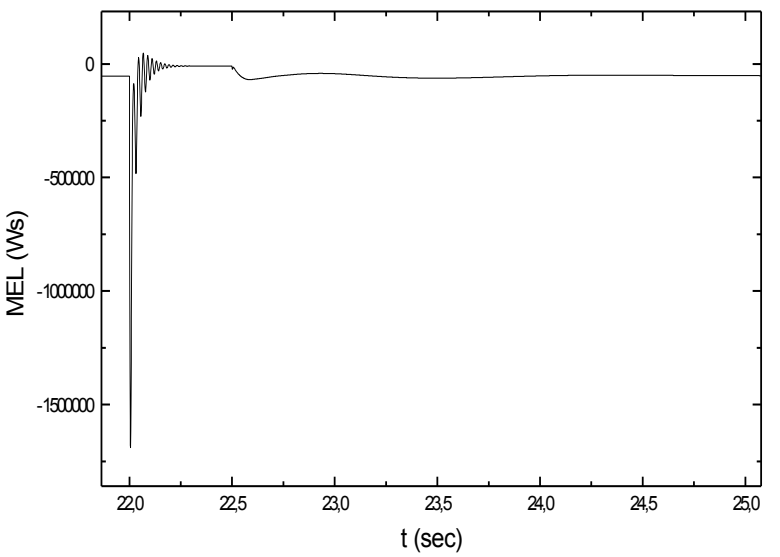

c

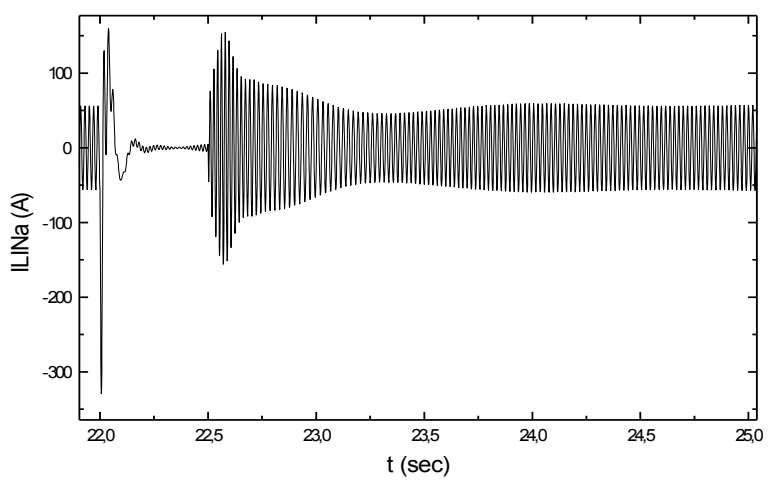

d

Figure 12. (Continued)

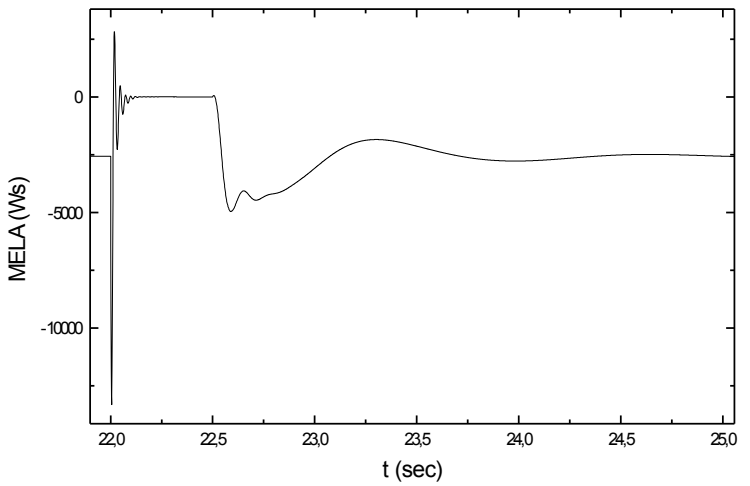

e

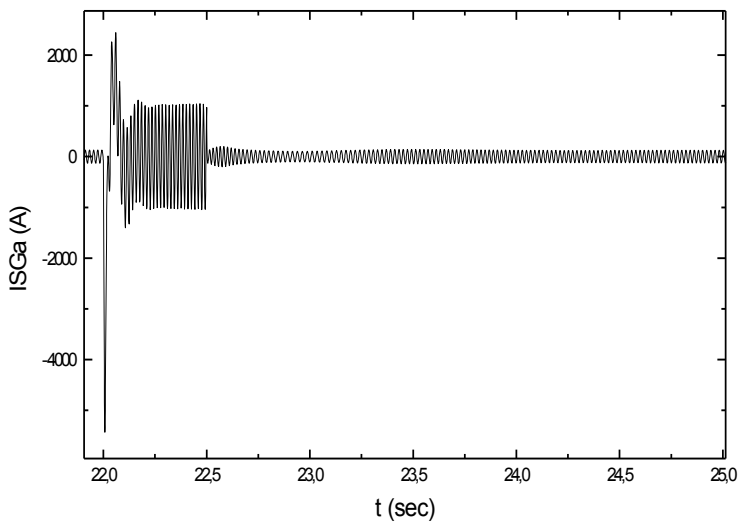

f

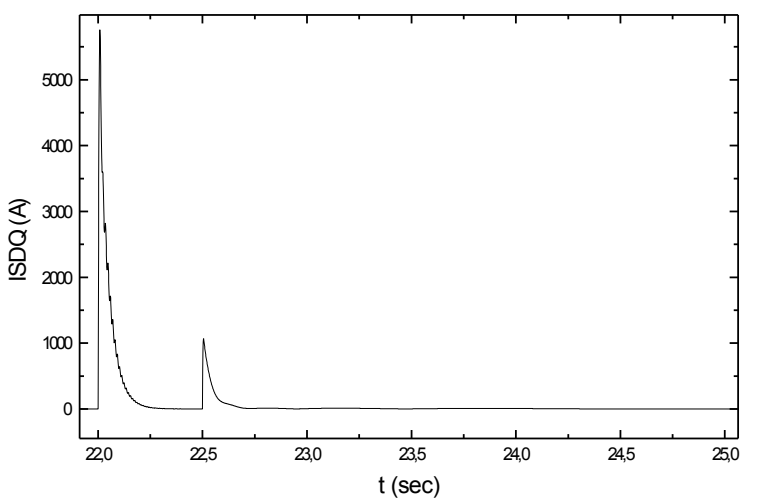

g

Figure 12. Electromechanical variables following the three phase short -circuit.

The initial value of the short circuit current (crucial current) is about 37 times bigger compared to the nominal value and the steady state short circuit current is about 6,5 times bigger, respectively.The line currents fluctuate in a more intense way under short-circuit and the magnitude of the oscillations is bigger. The A.G.'s electromagnetic torque appears to have much more intense fluctuations in both magnitude and duration in the case of short-circuit than in the connection of a WECS with nominal power of 30% that of the Diesel unit. From the above results, it is obvious that the dynamic behaviour of the system variables has more pronounced characteristics during the three-phase short-circuit than in the disconnection of a 1 MW WECS.

For an electrical system a two – phase short circuit is the most frequently short – circuit. This case has been studied analytically. In Table 5 the ratio of the electromechanical variable following a symmetrical fault (three – phase short circuit) and a non – symmetrical fault (two – phase short- circuit), are presented (the ratio of the maximum value of both cases):

Table 5. Comparison of 2–phase and 3-phase short-circuit.

	2 – phase short-circuit	3 – phase short-circuit
Max. value of the line current	1	0.65
Max. value of the S.G.'s stator current	1	0.73
S.G.'s stator current through the short - circuit	1	0.5
I_{SDQ} max	1	0.9

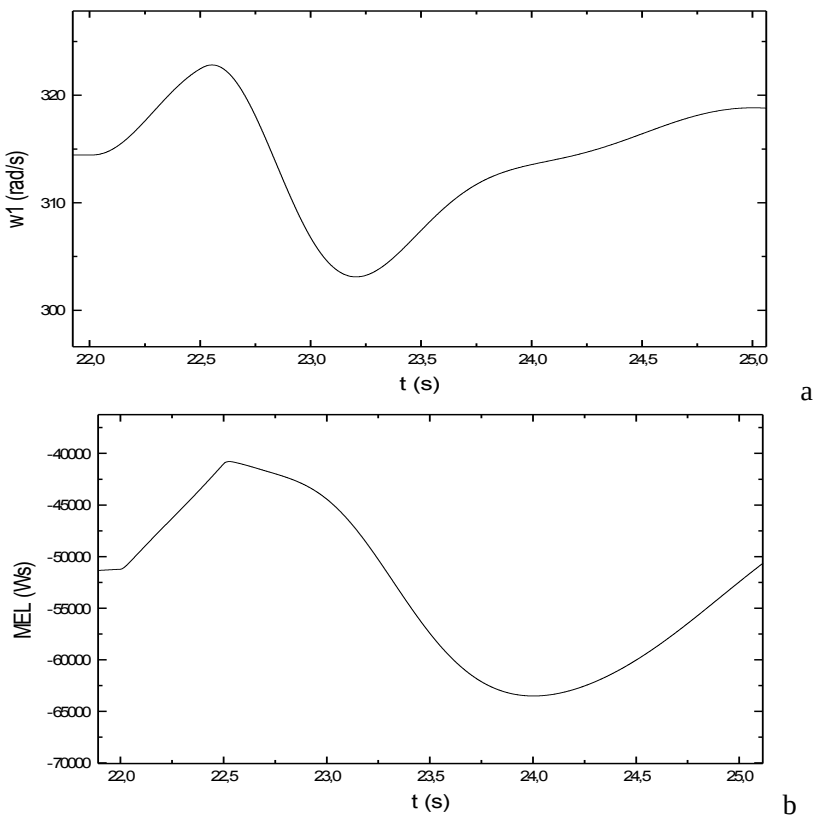

Figure 13. (Continued)

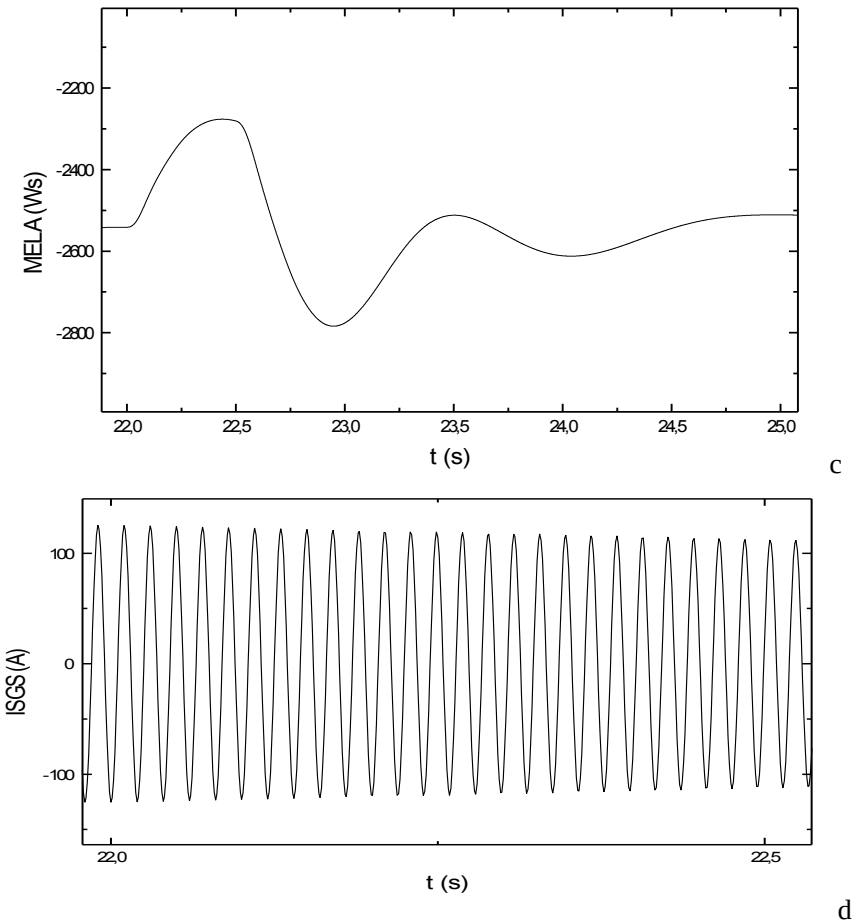

Figure 13. System's variables following short – circuit in the S.G.'s excitation.

7. DYNAMIC BEHAVIOR OF THE SYSTEM AT SHORT-CIRCUIT IN THE S.G.' S EXCITATION

Generally, the investigation of the dynamic behavior of a weak grid during faults at the Diesel-S.G. unit is necessary, as it can cause disturbances in the voltage and the frequency. The short-circuit in the S.G.'s excitation is a typical fault of this kind. This case has been studied and some characteristic simulation results for 1 MW WECS are presented in Figure 10. We can see that the maximum value of the S.G's rotating velocity is only 3.2% higher than its nominal value. After 5 seconds the frequency's deviation die out. Moreover the maximum value of the S.G's electromagnetic torque is 21% bigger compared to the nominal value, but for the A.G. it is only 10% bigger, respectively. The maximum damping current gets a very small value compared to the case of the three-phase short-circuit. We can remark that the deviation of the system's variables in this short-circuit case is negligible.

In general, via an analytical study of the transient phenomena in all the above cases and in other transient cases as the open circuit at the S.G.'s excitation and the non symmetrical

short circuits at the load, etc. We come up to the following classification taking into account the oscillations of the grid's frequency and voltage:

- Open circuit at the S.G.'s excitation
- Short interruption of the Diesel machine's operation
- One – phase short circuit
- Two – phase short circuit
- WECS connection if the nominal WECS power is bigger than 20% of the Diesel – S.G. unit nominal power,
- Three phase short-circuit,
- short circuit at the synchronous generator's excitation, wind velocity fluctuations and
- WECS disconnection.

CONCLUSION

The dynamic behavior of a weak hybrid power system, in which the production of electric energy is based on both fossil fuels and wind power, was considered in this study. A general dynamic mathematical model that can be used to study the behavior of such a system in detail was formulated. We found out that during the WECS connection, for a very small time period, the A.M. operates as a motor because of lack of the required magnetization current during this time period as it begins to increase slowly and so the E.M.F. of A.M. is smaller than the grid voltage. In all cases during the transient phenomena the amplitude of the variables oscillations depend at most on the nominal value of the WECS power, but not on the value of the wind velocity. In general, if the nominal WECS power is bigger than an amount of about 20% of the Diesel – S.G. unit nominal power, then the frequency deviation is reduced following the classification, WECS connection, three phase short-circuit, short circuit at the synchronous generator's excitation, wind velocity fluctuations and WECS disconnection. For smaller WECS the maximum frequency deviation appears at the 3 phase short-circuit.

NOMENCLATURE

(I_{AGR})	:	Rotor current matrix (a-b-c- axis) of the A.G.
(I_{AGRT})	:	Rotor current matrix (d-q- axis) of the A.G.
(I_{AGS})	:	Stator current matrix (a-b-c- axis) of the A.G.
(I_{LIN})	:	Line current matrix (a-b-c- axis)
(I_{LINT})	:	Line current matrix (d-q- axis)
(I_{SFT})	:	Rotor current matrix (d-q- axis) of the S.G.
(I_{SGT})	:	Stator current matrix (d-q- axis) of the S.G.
(U_{AGR})	:	Rotor voltage matrix (a-b-c- axis) of the A.G.
(U_{AGS})	:	Stator voltage matrix (a-b-c- axis) of the A.G.
(U_{LIN})	:	Line voltage matrix (a-b-c- axis)
(U_{LINT})	:	Line voltage matrix (d-q- axis)
(U_{LOAD})	:	Load voltage matrix (a-b-c- axis)

(U_{SFT})	:	Excitation voltages matrix (d-q- axis) of the S.G.
(U_{SGS})	:	Stator voltage matrix (a-b-c- axis) of the S.G.
(U_{SGT})	:	Stator voltage matrix (d-q- axis) of the S.G.
(U_{TRA})	:	Secondary voltage matrix of the transformer (d-q- axis)
(U_{TRAT})	:	Primary voltage matrix of the transformer (d-q- axis)
(I_{LOAD})	:	Load current matrix (a-b-c- axis)
C_M	:	Torque coefficient
$cos\varphi_{NA}$	:	Nominal power factor of A.G. (= 0.9)
$cos\varphi_{NS}$	:	Nominal power factor of S.G. (= 0.9)
C_P	:	Power coefficient
d	:	$d_o+ \omega_1 t$ space angle
DL	:	Length of the short line
H	:	Height of the hub
J_A	:	Inertia of wind turbine and A.G. (= 10 Ws^{-3})
Js	:	Inertia of diesel engine and S.G. (= 1000 Ws^{-3})
J_{WT}, J_{AG}	:	Inertia of wind turbine and A.G., respectively.
K_A	:	Ratio of the velocity converter (= 127.24)
M_{EL}	:	Electromagnetic torque of the S.G.
M_{ELA}	:	Electromagnetic torque of the A.G
M_{MA}	:	Mechanical torque on the axis of the A.G.
M_{MWM}	:	Mechanical torque on the axis of the wind motor
n_{NAG}	:	Nominal rotation speed of A.G. (= 3096 rpm)
n_{NSG}	:	Nominal rotation speed of the S.G. (= 428.5 rpm)
p_A	:	Pair pole number of A.G. (= 1)
P_{mo}	:	Initial value of mechanical power of S.G. (= 3000 kVA)
P_N	:	Nominal power of S.G. (= 3000 kVA)
P_{NA}	:	Nominal power of A.G. (= 1000 kVA)
p_S	:	Pore pair number of pole of the S.G. (= 7)
R	:	Wind turbine blade radius (= 23.708 m)
U_d, U_q	:	Voltage coordinates ($U_t=U_d+jU_q$)
U_{fd}	:	Excitation voltage (p.u.)
U_{FN}	:	Nominal excitation voltage (= 75V)
U_N	:	Nominal voltage of S.G. (= 15.75 kV = U_{ref})
U_{NA}	:	Nominal voltage of A.G. (= 6 kV)
U_{ref}	:	AVR reference voltage (p.u.)
U_t	:	S.G. terminal voltage (p.u) (=U_{dq})
u_W	:	Wind velocity after the control (m/s)
u_{wa}, u_{wa1}, u_{wb}, u_{wc}, u_{wd}, u_{we}	:	Constant of the wind velocity's equation
u_{WIND}	:	Wind velocity
u_{WN}	:	Nominal wind velocity (= 12m/s)
α	:	Inclination of the WECS landscape axes and of the blades
β	:	Changing of the ratio of the velocity converter
ΔP_M	:	Deviation of the mechanical power of the S.G
λ	:	Tip speed ratio
λ_M	:	Maximum value of λ (= 3)
λ_{OPT}	:	Pptimum value of λ (= 5)
ρ	:	Atmospheric density (= 1.2 kg m^{-3})
ω_1	:	Angular velocity of S.G. (= w1)

ω_{1o} : Synchronous angular velocity (= 314.16 rad/s), f_{1o} = 50 Hz
ω_R : Angular velocity of A.G. (= wr)
Ω_{WM} : Angular velocity of the wind motor

APPENDIX

Parameters of synchronous generator:

R_{FF} = 0.061 Ω, R_{SS}= 0.08 Ω, L_{qq}= 0.028 Ωs, L_{dd}= 0.048 Ωs, L_{Qq}= 0.022 Ωs, L_{fd}= 0.042 Ωs, L_{Dd} = 0.042 Ωs, R_D= 0.95 Ω, R_Q= 0.96 Ω, L_{FF}= 0.256 Ωs, L_{DD}= 0.044 Ωs, L_{fD}= 0.042 Ωs, L_{Df} = 0.042 Ωs, L_{QQ}= 0.025 Ωs,

$x_d = \omega_1 L_{dd}$, $x_q = \omega_1 L_{qq}$, $x_{Fd} = \omega_1 L_{fd}$

Parameters of asynchronous generator:

R_{sA}= 0.20Ω, R_{RA}= 0.776 Ω, L_{SA}= 0.2 Ωs, L_{RA}= 0.195 Ωs,

L_{S0A}= 0.0 Ωs, L_{R0A}= 0.05 Ωs, L_{HA} = 0.19 Ωs, L_{SSA}, L_{SRA}, L_{RSA}, L_{RRA}: inductivities of asynchronous generator (a-b-c- axis)

Parameters of the ohmic - inductive load, line and transformer:

R_{LOAD}= 80.974 Ω, L_{LOAD} = 0.1248 Ωs, (R_{LOAD}i, L_{LOAD}i, i= 1,2,3 respectively), R_{LIN} = 0.2381 Ω/km, L_{LIN} = 0.00107 Ωs/km, DL = D_{LIN} = 5 km, R_{TR}= 1.41 Ω, L_{TR} = 0.0428 Ωs, TR= 2.55

Parameters of the S.G. voltage and frequency controller:

T_C= 0.015 s, T_S= 0.8 s, time constant of control mechanism and Diesel engine - S.G., R= $-2\ 10^{-8}$ 1/kW, Diesel permanent speed droop

K_I =$-1.5\ 10^5$, K_D= -1.0, gains of integral and differential controller

K_A= 50, K_E= -0.05, K_F= 0.08, K_R= 1.0: gain of amplifier, excitation and stabilizing loop, and measurement system

T_A= 0.05 s, T_E= 0.5 s, T_F= 0.35 s, T_R= 0.06 s: time constant of amplifier, excitation, stabilizing loop and delay of the measurement.

K_{AN}= 0.1, T_{AN}= 0.1 s, K_{AS}= 0.1, T_{AS}= 0.1 s, time constant and delay of control mechanism of the wind motor.

Aij= hypermatrix (R_{TR}, R_{LIN}, R_{SA}, L_{HA}, L_{RA}, R_{RA}, L_{SA}, R_{SS}, L_{qq}, L_{dd}, L_{Qq}, L_{fd}, D_L, L_{dd}, R_{LOAD}i, R_{FF}, R_D, R_Q,d,ω_1, ω_R)

Cij= hypermatrix (ω_1, ω_R, L_{dd}, L_{qq}, L_{GS0}, L_{fd}, L_{Dd}, L_{Qq}, L_{ff}, L_{fD}, L_{DD}, L_{QQ}, L_{TR}, L_{LIN}, L_{LOAD}i, L_{SA}, L_{HA}, L_{RA}, L_{R0A}, D_L)

The non zero elements of the (K), (Λ), (M) matrices are:

$K_{1,1} = -L_{LOAD1}$ cosd, $K_{1,2} = -L_{LOAD1}$ sind, $K_{1,7} = -L_{LOAD1}-L_{dd}$,
$K_{1,10} = -L_{fd}$, $K_{1,11} = -L_{Dd}$, $K_{2,1} = -L_{LOAD2}$ sind, $K_{2,2} = -L_{LOAD2}$ cosd,
$K_{2,8} = -L_{LOAD2} - L_{qq}$, $K_{2,11} = -L_{Qq}$, $K_{3,3} = -L_{LOAD3}$, $K_{3,9} = -L_{LOAD3} - L_{GSO}$,
$K_{4,1} = (L_{LIN}\,DL + L_{TR} + L_{SA})$ cosd, $K_{4,2} = (L_{LIN}\,DL + L_{TR} + L_{SA})$ sind,

$K_{4,4} = L_{HA}$ cosd, $K_{4,5} = L_{HA}$ sind, $K_{4,7}= -L_{dd,}$ $K_{4,10} = -L_{fd,}$ $K_{4,11} = -L_{Dd,}$
$K_{5,1}= (L_{LIN}$ DL+L_{TR}+$L_{SA})$ (-sind), $K_{5,2} = (L_{LIN}$ DL + L_{TR} + $L_{SA})$ cosd,
$K_{5,4} = -L_{HA}$ sind, $K_{5,5} = L_{HA}$ cosd, $K_{5,8} = -L_{qq,}$ $K_{5,12} = -L_{Qq,}$
$K_{6,3} = L_{LIN}$ DL + L_{TR} + $L_{SOA,}$ $K_{6,9} = -L_{GSO,}$ $K_{7,1} = L_{HA,}$ $K_{7,4} = L_{RA,}$
$K_{8,2} =L_{HA,}$ $K_{8,5} =L_{RA,}$ $K_{9,6} = L_{ROA,}$ $K_{10,7} = L_{fd,}$ $K_{10,10} = L_{FF,}$ $K_{10,11} = L_{Fd,}$
$K_{11,7} = L_{Dd,}$ $K_{11,10} = L_{DF,}$ $K_{11,11}= L_{DD,}$ $K_{12,8}= L_{Qq,}$ $K_{12,9} = L_{QQ,}$ $K_{13,13}=J_S/p_S,$
$K_{14,14}=1.0,$ $K_{15,13}= K_D/T_{C,}$ $K_{15,15}=1.0,$ $K_{16,16}=1.0,$ $K_{17,17}=1.0,$
$K_{18,18}=1.0,$$K_{19,19}=1.0,$ $K_{20,20}=1.0,$ $K_{21,21}=J_A/p_{A,}$ $K_{22,22}=T_{AS,}$$K_{23,23}$ =$T_{AN,}$
$\Lambda_{1,1} = R_{LOAD1}$ cosd, $\Lambda_{1,2} = R_{LOAD1}$ sind,$\Lambda_{1,7} = R_{LOAD1}$-Rss,
$\Lambda_{1,8} = (L_{LOAD1} - L_{qq})$ $\omega_{1,}$ $\Lambda_{1,12} = - \omega_1 L_{Qq,}$ $\Lambda_{2,1} = -R_{LOAD2}$ sind,
$\Lambda_{2,2} = R_{LOAD2}$ cosd, $\Lambda_{2,7} = (L_{LOAD1} - L_{qq})$ $\omega_{1,}$ $\Lambda_{2,8} = R_{LOAD2} - R_{ss,}$
$\Lambda_{2,10} = \omega_1 L_{fd,}$ $\Lambda_{2,11} = \omega_1 L_{Dd,}$ $\Lambda_{3,3} = -R_{LOAD3,}$ $\Lambda_{3,9} = R_{LOAD3} - R_{ss,}$
$\Lambda_{4,1}= (R_{LIN}$ DL+R_{TR}+$R_{SA})$ (-cosd), $\Lambda_{4,2}=(R_{LIN}$ DL+R_{TR}+$R_{SA})$ (-sind),
$\Lambda_{4,7}=R_{ss,}$$\Lambda_{4,8}=-L_{qq}$ ω_1,$\Lambda_{4,12}=-\omega_1 L_{Qq,}$ $\Lambda_{5,1}=(R_{LIN}$ DL+R_{TR}+$R_{SA})$ sind,
$\Lambda_{5,2} = (R_{LIN}$ DL + R_{TR} + $R_{SA})$ (-cosd), $\Lambda_{5,7} = L_{dd}$ $\omega_{1,}$ $\Lambda_{5,10} = \omega_1 L_{fd,}$
$\Lambda_{5,11} = \omega_1 L_{Dd,}$ $\Lambda_{6,3} = R_{LIN}$ DL+R_{TR}+$R_{SA,}$ $\Lambda_{6,9} = R_{ss,}$ $\Lambda_{7,2} = -\omega_R L_{HA,}$
$\Lambda_{7,4} = -R_{RA,}$ $\Lambda_{7,5} = -\omega_R L_{RA,}$ $\Lambda_{8,1} = \omega_R L_{HA,}$ $\Lambda_{8,4}= \omega_R L_{RA,}$ $\Lambda_{8,5} = -R_{RA}$
$\Lambda_{9,6} =-R_{RA,}$ $\Lambda_{10,10}= -R_{FF,}$ $\Lambda_{10,19}= (\omega_{10} U_{fn}/\omega_1),$ $\Lambda_{11,11} = -R_{D,}$ $\Lambda_{12,12}= -R_Q$
$\Lambda_{13,7} = p_s ((L_{dd} - L_{qq})$ I_{SGq} - L_{qq} $I_{SQ})$, $\Lambda_{13,8} = p_s (L_{dd}$ I_{SD} + L_{fd} $I_{SF})$
$\Lambda_{13,13} = -p_s / \omega_{1,}$ $\Lambda_{14,13} = -K_{p,}$ $\Lambda_{15,12} = -(0.5 \pi f_o R T_C),$ $\Lambda_{15,14} = 1 / T_C$
$\Lambda_{15,15} = -1 / T_{C,}$ $\Lambda_{16,16} = 1 / T_{s,}$ $\Lambda_{16,17} = -1 / T_{s,}$ $\Lambda_{17,18} = -1 / T_R$
$\Lambda_{18,18} = - K_A / T_{A,}$ $\Lambda_{18,19} = -1 / T_{A,}$ $\Lambda_{18,20} = - K_A / T_{A,}$ $\Lambda_{19,18} = 1 / T_E$
$\Lambda_{19,19} = - K_E / T_{E,}$ $\Lambda_{20,18} = - K_F / (T_F T_E),$ $\Lambda_{20,19} = - K_E K_F / (T_F T_E)$
$\Lambda_{20,20} = -1 / T_{F,}$ $\Lambda_{21,1} = p_A L_{HA}$ $I_{AGRd,}$ $\Lambda_{21,2} = p_A L_{HA}$ I_{AGRq}
$\Lambda_{22,21} = K_{AS} R (1-\beta) / (K_{Anew} p_A u_{WIND}),$ $\Lambda_{22,23} = - (K_{AN} u_{WIND}) + 1.0)$
$M_{13,13} = p_s P_{mo} / \omega_{1,}$ $M_{14,14}= k_p \omega_{1o,}$ $M_{15,15} = \omega_{1o} / (6.28 f_{1O} R T_c)$
$M_{17,17}= U_t k_R / (U_{ref} T_R),$ $M_{18,17} = K_A / T_{A,}$ $M_{21,21} = M_{MA,}$
$M_{22,22} = -K_{AS} \lambda_{opt,}$ $M_{23,23} = K_{AN} (u_{WIND} - u_{wN})$

REFERENCES

3rd and 5th National Report - Regarding the penetration level of renewable energy sources up to the year 2010 (article 3 of directive 2001/77/ec), Hellenic republic ministry of development directorate general for energy renewable energy sources and energy saving directorate, 2005 and 2007.

Abdin, E. S. and Xu, W. 2000. Control design and dynamic performance analysis of a wind turbine - induction generator unit, I.*E.E.E Transactions on Energy Conversion*, Vol. 15, No. 1, 91-96.

Arabian – Hoseynabadi, H Tavner, PJ Oraee, H. 2010. Reliability comparison of direct - drive and geared – drive wind drive concepts, *Wind Energy*, 13: 62 -73.

Boyle. 1997. *Renewable energy*, Oxford, Open University.

Chedid, R. Karaki, S. and El-Chamali, C. 2000. Adaptive fuzzy control for Wind - Diesel Weak power systems, *I.E.E.E Transactions on Energy Conversion*, Vol. 15, No. 1, pp. 71-78.

Dahlgren, M. Flank, H. Leizon, M. Owman, F. and Walfridsson, L., 2000. Windformer: Wind power goes large scale, Cigre, Paris.

De Battista, H. Mantz, R. J. and Cristiansen, C. F. 2000. Dynamical sliding mode power control of wind driven induction generators, *I.E.E.E Transactions on Energy Conversion*, Vol. 15, No. 4, 451-457.

De La Salle, A. Reardon, D. Leithead, W. E. and Grimble, M. J. 1990. Review of wind turbine control, *INT. J. CONTROL*, Vol. 52, No. 6, pp. 1295-1310.

Dokopoulos, P. S. 1996. Saramourtsis, A. C. and Bakirtzis, A. G. Prediction and evaluation of the performance of wind - diesel energy systems, *I.E.E.E Transactions on Energy Conversion*, Volume 11, No. 2, 385-93.

Freris, L. 1990. *Wind energy conversion systems*, Prentice - Hall.

Giaourakis, D. G. Safacas, A. and Tsotoulidis, S. 2012. Dynamic Behavior of a Wind Energy Conversion System including Doubly – Fed Induction Generator in Fault Conditions, *International Journal of Renewable Energy Research* (IJREP), Vol. 2, No. 2, 227-35.

Giaourakis, D. G. Safacas, A. and Tsotoulidis, S. 2014. Simulation of a Double – Fed Induction Generator Wind Energy Conversion System under helthy and faulty conditions, Advanced Materials Research, (ISSN: 1022 – 6680), Vol. *Material Research and Applications*, 1771–76.

Giaourakis, Dimitrios G. Safacas, Athanasios N. 2016. Quantitative and qualitative behavior analysis of a DFIG wind energy conversion system by a wind gust and converter faults, *Wind Energy*, Volume 19, Issue 3, 527–47, DOI 10 1002/wc 1849.

GWEC Global Wind Statistics 2014 [online] available:http://gwec.net/wp-content/uploads/2015/02/gwec_Globalwindstats_2014_final_10.2.2015.pdf.

Hatziargyriou, N. D. Papathanassiou, S. A. and Papadopoulos, M. P. 1995 Decision trees for fast security assessment of autonomous power systems with a large penetration from renewables, *I.E.E.E Transactions on Energy Conversion*, Volume 10, No. 2, 315-25.

Heier. 1996. *Windkraftanlagen im Netzbetrieb*, Teubner, Stuttgart.

IEA, 2015.

IEEE COMITEE REPORT. 1968. Computer representation of Excitation Systems, *I.E.E.E. Transactions on Power Apparatus and Systems*, Vol. pas - 87, No. 6, pp. 1460-65.

IEEE COMITEE REPORT. 1973. Dynamic models for steam and hydro turbines in power system studies, *I.E.E.E. Transactions on Power Apparatus and Systems*, Vol. pas - 92, No. 6, 1904-1915.

IEEE COMITEE REPORT. 1981. Excitation System models for power system stability studies, *I.E.E.E Transactions on Power Apparatus and Systems*, Vol. PAS - 100, No. 2, 494-509.

Leith, A. J. 1997. *Implementation of wind turbine controllers*, Int. J. Control, Vol. 66.

Medium Term Renewable Energy Market Report 2012, Executive Summary, ECOMEA, 2012.

Mohammed, H. Nwankpa, C. 2000. Stochastic analysis and simulation of Grid-connected wind energy conversion system, I*.E.E.E Transactions on Energy Conversion*, Vol. 15, No. 1, pp. 85-90.

Molly, Jens - Petter. 1990. *Wind Energie* (Theorie - Anwendung - Messung), Verlag C. F. Muller, Karlshrue.

Monthly Bulletin of HTSO, RES AND HCP, JUN. 2012, Hellenic Transmission System Operator S.A.

National Renewable Energy Action Plan in the scope of Directive 2009/28/EC, Ministry of Environment Energy and Climate Change, 2011.

PPC, www.dei.gr.

Rahimi, M and Parniani, M 2010. Transient performance improvement of wind turbines with doubly fed induction generators using nonlinear control strategy, *IEEE Transactions on Energy Conversion*, 514-25.

RENES, *Application of Renewable Energy Sources*, Athens, 11-12/12/1998.

Ribrant, j and Bertling, LM 2007. Survey of failures in wind power systems with focus on Swedish wind power plants during 1997 – 2005, *IEEE Transactions on Energy Conversion*, 22: 167–73.

Slootweg, JG de Haan, SWH Polinder, H and Kling, WL 2003. General model for representing variable speed wind turbines in power system dynamic simulations, *IEEE Transactions on Power Systems*; 18: 144-51.

Stavrakakis, G. S. and Kariniotakis, G. N. 1995. A general simulation algorithm for the accurate assessment of isolated Diesel - Wind Turbines system interaction, *I.E.E.E. Transactions on Energy Conversion*, Vol. 10, No. 3, part I and II, 577-90.

The world directory of Renewable Energy. *Supplies and Services*, 1995, 1997JAMES and JAMES.

The World Wind Energy Association 2014 Half – year report [online] available: http://wwindea.org/webimages/WWEA_half_year_report_2014.pdf.

Tsimplostefanakis, V. C. and Safacas, A. N. 1996. Investigation of the dynamic behaviour of a weak grid during connecting a wind turbine generator via simulation, *ELECTRIMAC's* '96, 5th International Conference, Saint-Nazaire, France, September 17-19.

Tsimplostefanakis, V. C. and Safacas, A. N. 1998. Dynamic behavior of an Energy Weak Grid consisting of Diesel Motor - Synchronous Generator Unit and Wind Asynchronous Generator, OPTIM 98, Brasov, Romania, 1998.

Uhlen, K. Foss, B. A. and Gjosaeter, O. B. 1994. Robust control and analysis of a Wind - Diesel Hybrid power plant, *I.E.E.E Transactions on Energy Conversion*, Volume 9, No. 4, 701-08.

In: Renewable Energy Systems
Editor: Sandip A. Kale
ISBN: 978-1-53610-423-3

Chapter 8

STRUCTURAL ANALYSIS OF MULTISTOREY VERTICAL AXIS WIND TURBINE USING FINITE ELEMENT METHOD

Abhijeet M. Malge[1,*] and Prashant M. Pawar[2]
[1]Department of Mechanical Engineering,
MIT Academy of Engineering, Pune, India
[2]Department of Civil Engineering,
SVERI's College of Engineering,
Pandharpur, India

ABSTRACT

Multi storey Vertical Axis Wind Turbine of 100 W capacity for standalone domestic applications has been designed and developed for better self-starting at low wind speed and coefficient of power. The correct estimation of stress, strain and deformation values induced in the wind turbine components are necessary for ensuring satisfactory performance against extreme wind load. In this chapter structural aspects of the turbine has been analyzed. The turbine has been subjected to Finite Element Analysis (FEA) studies for assessment of turbine at high wind speed. The influence of dynamic velocity fluctuations of wind loads for these structures is determined using Gust Factor Method. The thickness of the turbine components was varied and stress, strain and deformation are estimated.

It has been found that the turbine having thickness of 2mm is the optimum thickness having stress strain values within acceptable range considering weight to power ratio. This work further provides insight on Eigen values, Eigen vectors at different tip speed ratios.

Keywords: VAWT, Static load, dynamic load, Eigen values, Eigen vectors

* E-mail: abhi.malge@gmail.com.

NOTATIONS

$I_{z,1}$ Terrain category factor;
$I_{z,1}$ Moment of inertia(m^4)
E Modulus of Elasticity(N/m^2);
G Gust factor;
F_a Aerodynamic force (N);
F_c Centrifugal force(N);
F_t Total force(N)
β Damping coeffcient;
N_{op} Operational Rotation(rpm);
V Max tip speed (m/s);

1. INTRODUCTION

The world is facing crises due to depletion of fossil fuels. There is a strong urge to find alternative resources of energy. Wind is one of the potent sources of energy amongst various renewable energy sources. Horizontal Axis Wind Turbines (HAWT) are suitable for generation of electric energy at large level. Due to its high installation cost and maintenance, HAWT are not suitable for domestic applications. Abilty of vertical axis wind turbines to harness power at low height makes its maintenance quite easy, low cost and most suitable for domestic applications. The analysis of Vertical Axis Wind Turbine (VAWT) is broadly categorized into two parts viz: aerodynamics and structural performance. Enhancement of the aerodynamic performance of a Darrieus wind turbine is achieved by tilting the rotation axis by (10° and 20°) with respect to the free-stream wind speed (Bedon et al. 2015). 10% of performance gain was achieved by adoption of stator vanes around a multi- stage vertical-axis wind turbine (Burlando et al. 2015). Chong et al. 2013) developed a novel power-augmentation guide-vane (PAGV), surrounds a Sistan wind turbine to improve the wind rotor performance by increasing the on-coming wind speed and guiding it to an optimum flow angle before it interacts with the rotor blades. Greenblatt and Lautman (2015) deployed inboard and outboard plasma actuations were on the blade to counter the positive and negative angle of attack that produces dynamic stall. Elkhoury et al. (2015) studied experimentally and numerically the effects of wind speed, turbulence intensity, airfoil shape, and strut mechanism with and without variable pitch on the performance of the turbine are carefully assessed.

By examining aerodynamic characteristics and the separated flow occurring in the vicinity of the blade Tiju et al. (2015) developed an optimum shape of the Darrieus-type wind turbine. A comprehensive assessment of all the configurations of Darrius turbines is articulated. (Goude and Agren 2014) numericaly studied the performance of turbine in free flow and in channel. (Cox and Echtermeyer 2012) commented on time taken for convergence of the solution and the performance of the turbine. Lavassas et al. used Finite Element Analysis (FEA) approach for the wind turbine blade made of hybrid composite material yielding low weight and high strength. Design and analysis for gravity, seismic and wind loadings of tubular tower of 44075 m high made of steel S355J2G3 is done by using two

different finite element models. Blade design was analyzed at extreme wind conditions where maximum values of deflection and bending stresses were determined at peak values of aerodynamic and centrifugal forces. (Saqib 2013) optimized the existing design toattain the structural strength i.e., reduction in deflections and bending stresses.

This chapter presents structural analysis of multi-storey VAWT developed for improving self-starting behavior along with power coefficient. Analytical assessment of turbine parts viz: blade, flap and plate have been done using beam theory. Finite Element Analysis has been done in ANSYS software. Numerical performances of three-storey turbine are compared with analytical results. The performance parameters considered are stress, deflection, Eigen frequency and Eigen vectors.

2. MULTISTOREY VERTICAL AXIS WIND TURBINE

The turbine model developed has three storeys as shown in Figure 1 shows storey details of turbine with locations and sizes of three flaps and two blades.

Figure 2 CAD model of three storey vertical axis wind turbine and Figure 3 shows working model of three storey vertical axis wind turbine. NACA 68-613 cambered aerofoils is selected for analysis as cambered aerofoil have the benefit of selfstarting, which is preferable as compared to symmetrical aerofoil.

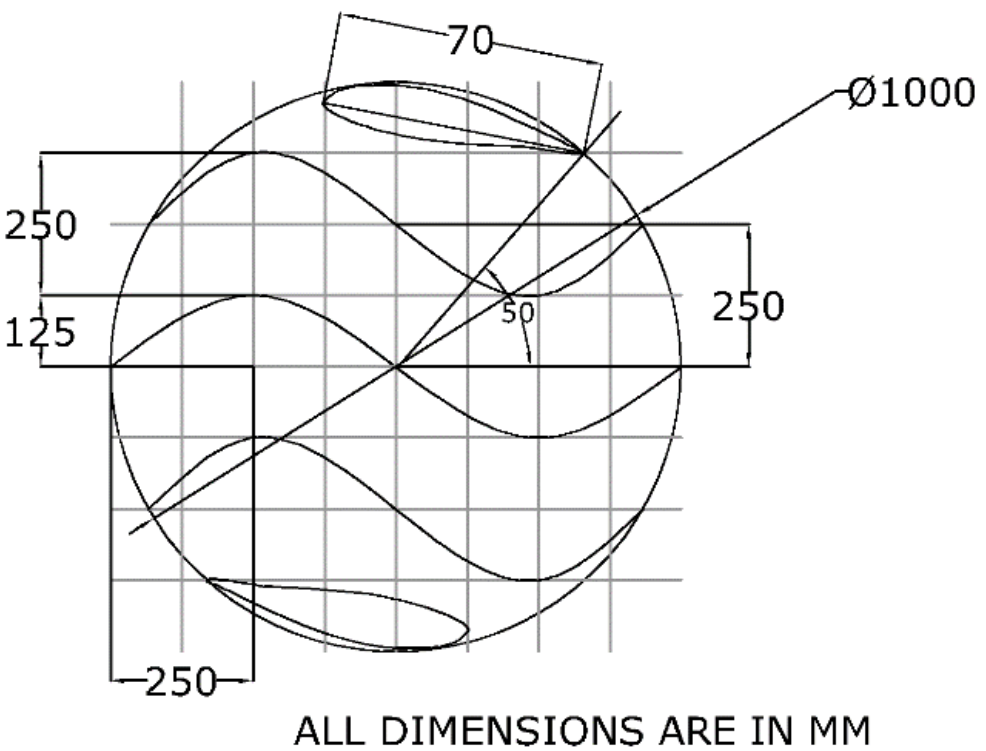

Figure 1. Details of turbine.

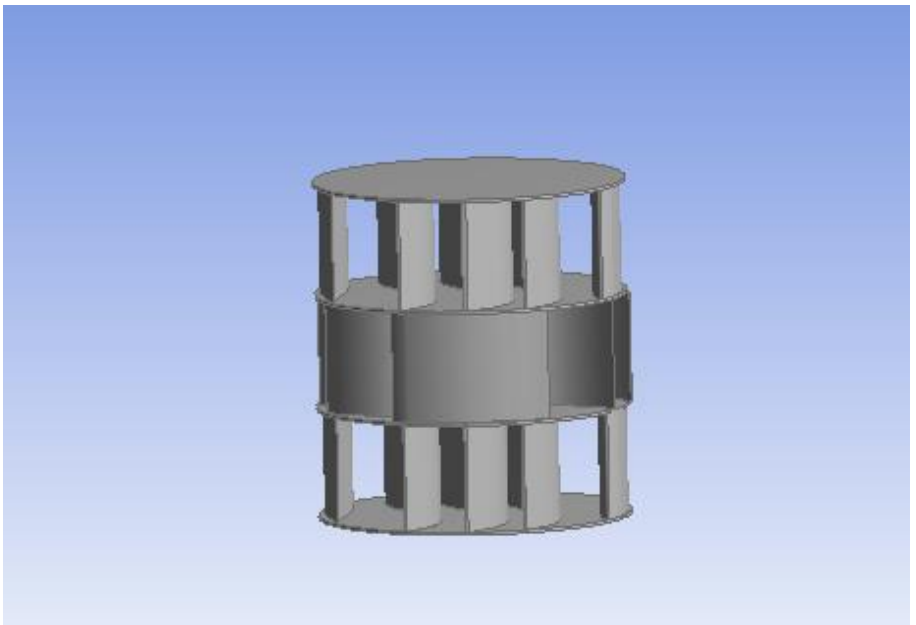

Figure 2. CAD figure of three-storey Vertical Axis Wind Turbine.

Figure 3. Model of threestorey Vertical Axis Wind Turbine.

Two blades of the storey are arranged with opposite leading and trailing edge so that the effect of drag forces at 90° and 180° assist the motion of the wind turbine. Lift force acting on the rotor blades tangentially to the plane of the rotation is producing torque. Flaps used are made up from rectangular plate 'S' shape so as to have combination of concave and convex shape. Concave shape of the flap gives the major driving force as it has more drag coefficient than convex shape, which further augments the speed of the turbine rotor. Three flaps per storey are used, in which the central flap has bigger radius of curvature as compared to flaps on either side of it. At any position of the turbine at least two flaps viz: central flap and either of the side flaps are exposed to wind so that maximum wind force can be applied on the turbine. For two storey turbine, two one-storey turbines are attached orthogonal to each other whereas for three storey turbine, three one-storey turbines are attached with first and third storey orthogonal to second storey. The height of each storey of turbine is 0.3 m and total height storey turbine is 0.9 m.The shaft diameter is 0.02 m.

3. ANALYTICAL MODELLING

3.1. Aerodynamic Force

3.1.1. Gust Factor

A positive or negative departure of wind speed from its mean value lasting for not more than 2 minutes with the peak occurring over a specified interval of time. Selection of terrain categories shall be made with due regard to the effect of obstructions which constitute the ground surface roughness. The terrain category used in the design of a structure may vary depending on the direction of wind under consideration. Wherever sufficient meteorological information is available about the wind direction, the orientation of any building or structure may be suitably planned.

Category 1: Exposed open terrain with a few or no obstructions and in which the average height of any object surrounding the structure is less than 1.5 m.

Category 2:Open terrain with well-scattered obstructions having height generally between 1.5 and 10 m.

Category 3 Terrain with numerous closely spaced obstructions having the size of building-structures up to 10 m in height with or without a few isolated tall structures.

Category 4 Terrain with numerous large high closely spaced obstructions. Behera and Mittal (2012).

Terrain category: 1

$$I_{z,1} = 0.3507 - 0.0535 \log_{10}\left(\frac{Z}{Z_{0.1}}\right) \tag{1}$$

Terrain category: 3

$$I_{z,3} = I_{z,1} + \frac{3}{7}\left(I_{z,4} - I_{z,1}\right) \tag{2}$$

Terrain category: 4

$$I_{z,4} = 0.466 - 0.135 \log_{10}\left(\frac{z}{Z_{0,4}}\right) \tag{3}$$

B_s = background factor indicating the measure of slowly varying component of fluctuating wind load caused by the lower frequency wind speed variations.

$$B_s = \frac{1}{\left[1 + \frac{\sqrt{0.26(h-s)^2 + 0.46 b_{sh}^2}}{L_h}\right]} \tag{4}$$

where, b_{sh}= average breadth of the structure between heights s and h

L_h= measure of effective turbulence length scale at the height, h in m

$$L_h = 85\left(\frac{h}{10}\right)^{0.25} \tag{5}$$

φ = factor to account for the second order turbulence intensity

$$\Phi = \frac{g_v I_h \sqrt{B_s}}{2} \tag{6}$$

H_s= height factor for resonance response

$$H_s = 1 + \left(\frac{s}{h}\right)^2 \tag{7}$$

s = Levels at which action effects are calculated.

S = a size reduction factor given by

$$S = \frac{1}{\left[1 + \frac{3.5 n_a h}{V_h}\right]\left[1 + \frac{4 n_a b_{oh}}{V_h}\right]} \tag{8}$$

where b_{0h}= Average breadth of the structure between 0 and h

E = Spectrum of turbulence in the approaching wind stream

$$E = \frac{\prod N}{\left(1 + 70.8 N^2\right)^{\frac{5}{6}}} \tag{9}$$

N = Effective reduced frequency

$$N = \frac{n_a L_h}{\bar{V}_h} \tag{10}$$

$\bar{V}_h$ = design mean value wind speed at height, h in m/s basic wind speed map of India, as applicable at 10 m height above mean ground level for different zones of the country. Basic wind speed is based on peak gust speed averaged over a short time interval of about 3 seconds.

n_a= First mode along wind frequency of the structure in Hz

g_R= Peak factor for resonant response

$$g_R = P\left[2\ln\left(3600 n_a\right)\right] \tag{11}$$

g_v= a peak factor for upwind velocity fluctuation, 3.0 for category 1 and 2 terrains and 4.0 for category 3 and 4 terrains

$$G = 1 + r\sqrt{\left[g_v^{\,2} B_s (1+\phi)^2 + \frac{H_s g_r^{\,2} SE}{\beta} \right]} \tag{12}$$

g = peak factor defined as the ratio of the expected peak value to the root mean value of a fluctuating load, and

r = roughness factor which is dependent on the size of the structure in relation to the ground roughness.

Effective Frontal Area (A_e): The projected area of the structure normal to the direction of the wind.

Force Coefficient(C_f) - A non-dimensional coefficient such that the total wind force on a body is the product of the force coefficient, the dynamic pressure due to the incident design wind speed and the reference area over which the force is required. Figure 4 shows force coefficient plot.

$\bar{p}_z$= design pressure at height z due to hourly mean wind obtained as $0.65\bar{V}_h$

$$F_a = C_f A_e \bar{p}_z G \tag{13}$$

3.2. Centrifugal Force

The turbine is subjected to high centrifugal force which depends on the aspect ratio. The values of centrifugal force is calculated for all values of thickness of turbine parts at maximum tip speed of 32.5 m/s.

$$F_c = \frac{mV^2}{r} \tag{14}$$

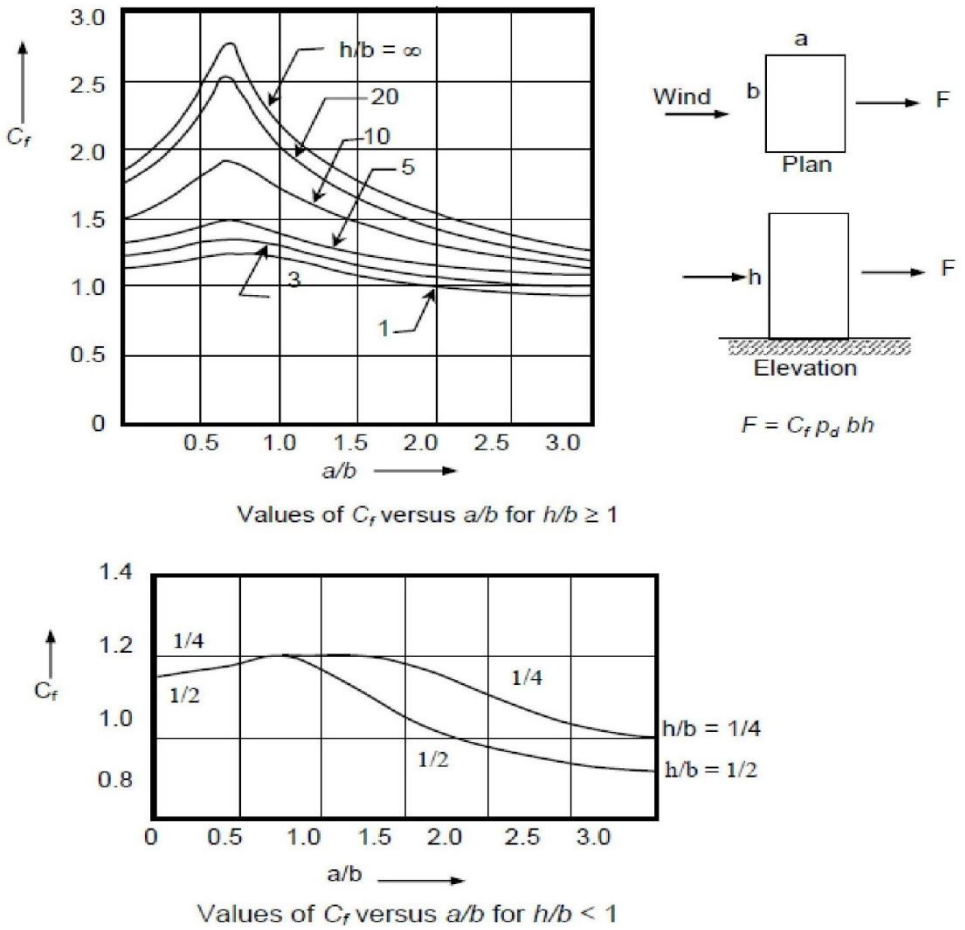

Figure 4. Chart for determination of force coefficient.

The total force acting on the turbine parts is sum of aerodynamic force and centrifugal force.

$$F_t = F_a + F_c \tag{15}$$

3.3. Evaluation of Stress and Deflection

The maximum stress and deflection of turbine parts viz: blade,flap and plate is calculated by considering fixed at both ends for wall thickness 1,1.5,2,2.5 and 3mm. Beam equation is used for calculation of maximum stress. Maximum deflection for beam fixed at both ends is

$$\frac{F_t l^2}{384 E I_x x}$$

4. NUMERICAL ANALYSIS

The Finite Element Analysis is done in ANSYS. Structural mechanics module is used with Solid mechanics as physics. The study used for the analysis is stationary, Eigen frequency and Eigen values. Linear elastic is selected as material mode. The load applied is boundary load which takes into account the uniformly distributed load. The parts of the turbine are fixed at both ends. Free tetrahedral element is used for meshing the turbine components. The mesh size control has been done and convergence has been achieved.

A three storey vertical axis wind turbine has been designed and developed with a view to increase the performance parameters such as power coefficient and self-starting speed. The turbine assembly consists of blades, flaps and plates. Each storey consists set of two blades and three flaps. The upper and lower surface of the blades and the flaps are welded to circular plates. The parts of the wind turbine are subjected to aerodynamic force and centrifugal force. To design a turbine structure which is capable of sustaining wind gust to ensure safe operation, each part of the wind turbine having a wall thickness range 1-3 mm is analyzed individually for the maximum load condition numerically and analytically. Further the turbine assembly is analyzed numerically only.

4.1. Stress Estimation

Figure 5 shows the stress estimated numerically and analytically for blade having thickness range from 1-3 mm. The stress value decreases by 37% from thickness 1 to 1.5 mm. Further it approximately decreases by a step about 15-18% from 1.5 mm to3 mm. Figure6 shows that the maximum stress is seen at the fixed ends. Figure 7 shows the stress plot for flaps.

The stress value approximately reduced by 30% from thickness range of 1-2.5mm. The reduction in stress is 10% from 2.5-3 mm thickness. Figure 8 shows that the maximum stress is induced at the upper and lower corners of the flaps. Figure 9 shows stress plot of plate. The magnitude of stress induced in plate reduces approximately 40% from 1-1.5 mm thickness. Further it reduces in step of approximately 15% between the thicknessesranges of 1.5-3mm.

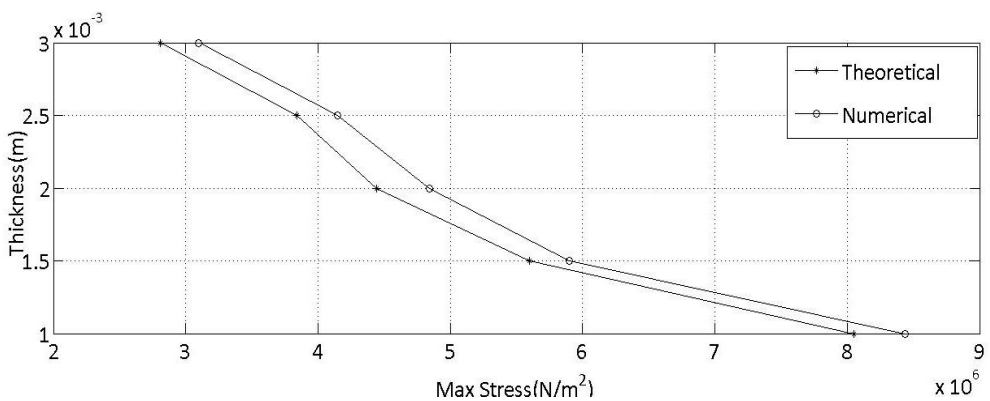

Figure 5. Maximum Stress magnitude plot for blade.

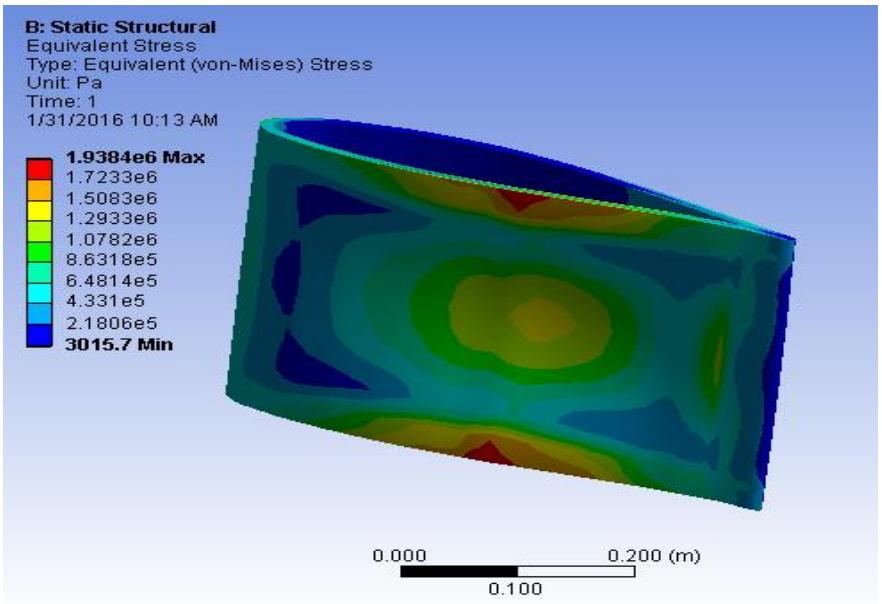

Figure 6. Stress distribution plot for blades.

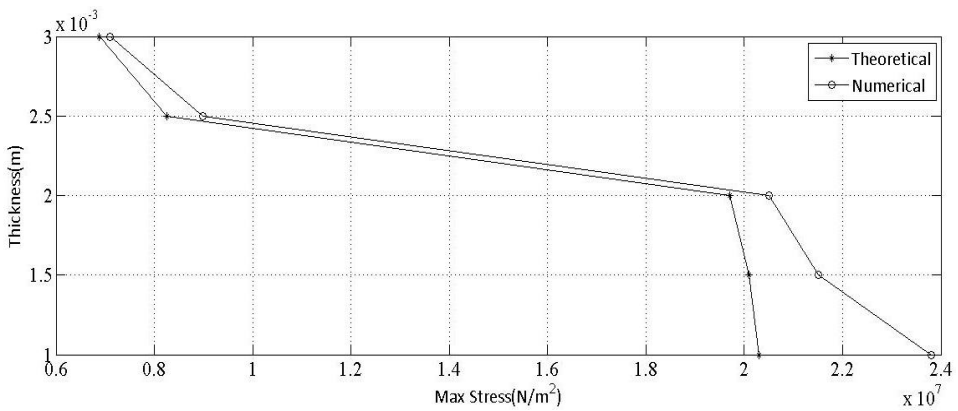

Figure 7. Maximum Stress magnitude plot for flap.

Figure 10 shows that the maximum value of stress induced is on the periphery of the plate. The maximum stress induced is 3×10^6 N/m^2. The increase in thickness of the plate increases mass and stiffness of the turbine parts. This increases the strength makes it less susceptible to failure.

4.2. Deflection Analysis

Figure 11 shows the maximum deflection estimated numerically and analytically for blade having thickness range from 1-3 mm. The deflection value decreases by 40% from thickness 1 to 1.5 mm. Further it approximately decreases by a step about 20% from 1.5 mm to3 mm.

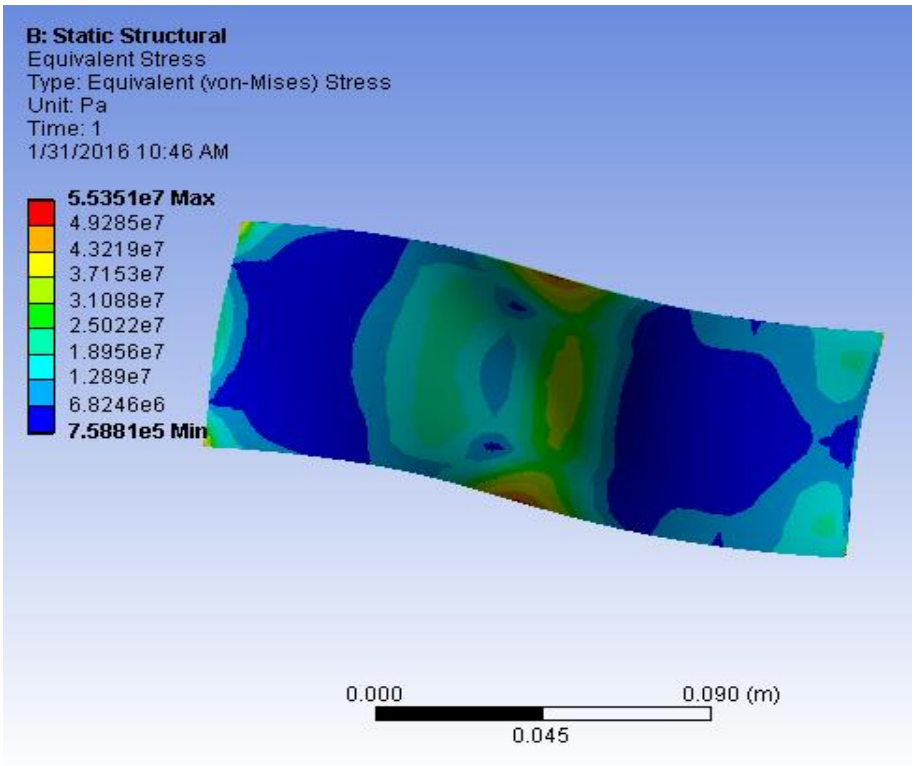

Figure 8. Stress distribution plot for flap.

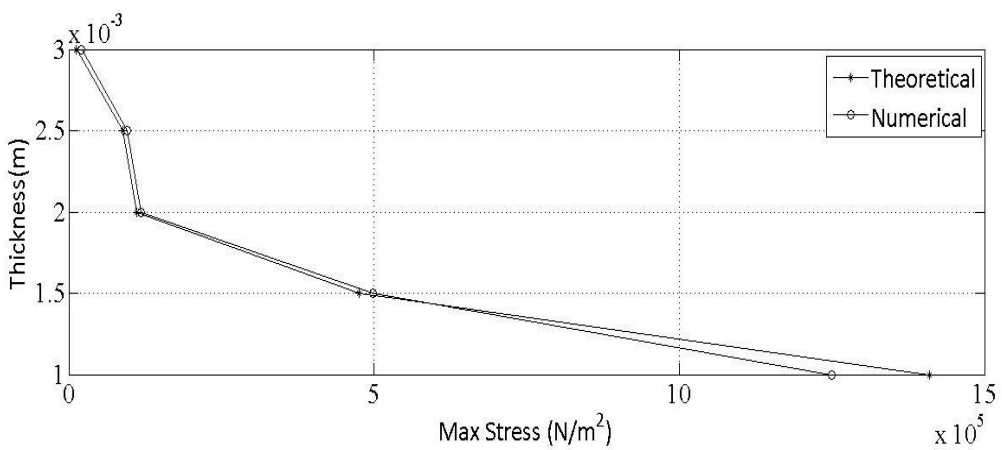

Figure 9. Maximum stress plot for plate.

m the analysis maximum deflection is seen at the centre of the blade height surface. Figure 12 shows the maximum deflection plot for flaps. The deflection value approximately reduced by 20% from thickness range of 1-2mm. The reduction in deflection is 30% from 2-3 mm thickness. Simulation shows that the maximum deflection is seen at the middle portion of the flaps. The magnitude of deflection in plate reduces approximately 40% from 1-1.5 mm thickness.

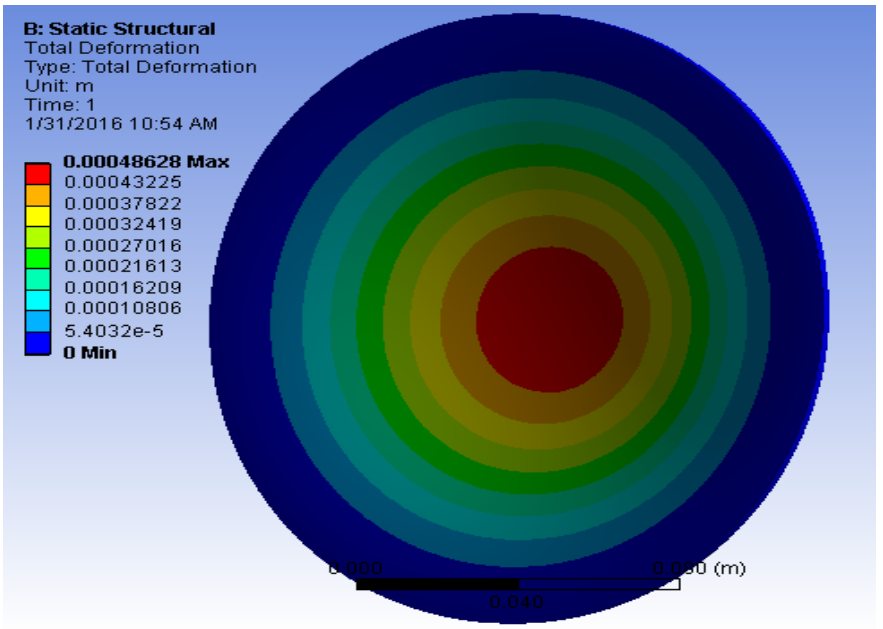

Figure 10. Stress distribution plot for plate.

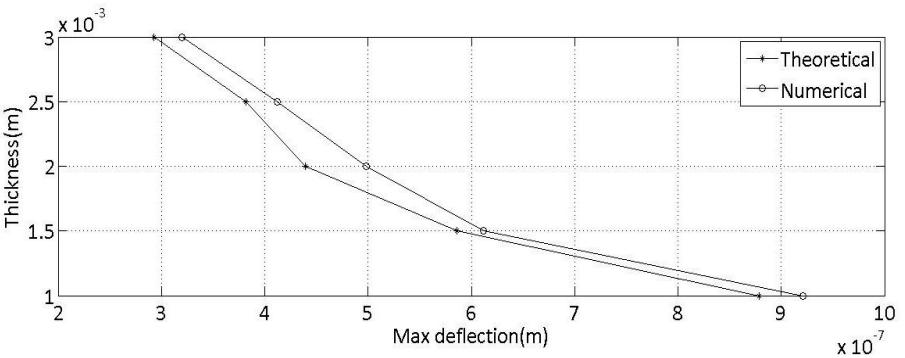

Figure 11. Maximum Deflection plot for blades.

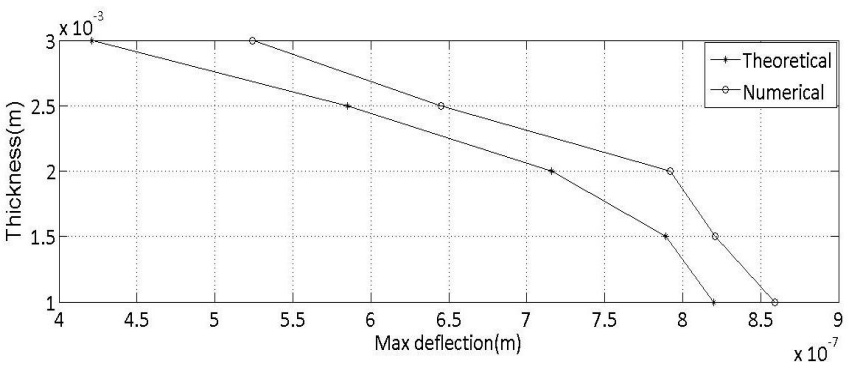

Figure 12. Maximum Deflection plot for flap.

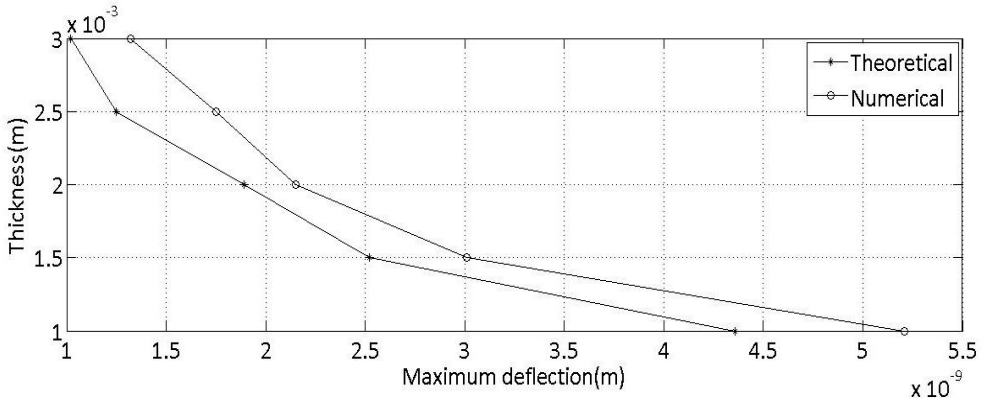

Figure 13. Maximum deflection plot for plate.

Further it reduces in step of approximately 20% between the thickness ranges of1.5-3mm. Figure 13 shows that the maximum value of deflection of the plate.

4.3. Eigen Frequency and Mode Shapes

For safe operation of Vertical Axis Wind Turbine structure, the natural frequency of the turbine parts must be well above the forcing frequency. The desired six number of Eigen frequency values are found numerically. Where forcing frequency is calculated by,

$$\omega_f = \frac{2\Pi N_o p}{60} rad/sec \tag{16}$$

The maximum tip speed velocity(r ω) is 32.5m/s. The angular velocity of turbine estimated is 62.5 rad/sec.

Fig 14-16 shows the Eigen frequency values corresponding to turbine parts. The fundamental frequency of each part of turbine is comfortably high as compared to the value of forcing frequency which is calculated as 8 Hz.

From the analysis of stress and deflection it is observed that the stress and deflection magnitude increases from thickness 1-1.5mm considerably as compared to other incremental steps of thickness.

The total mass of the turbine for 1.5 mm thickness is 88 kg, for 2 mm thickness is 118 kg and for 3 mm thickness total mass is 177.8 kg. As the thickness increases the stress and deflection reduces due to increases in mass and stiffness. As the weight of the turbine increases the other performance parameter i.e., self starting speed gets affected.

Thus optimum thickness of the turbine parts needs to be assessed from aerodynamic and structural performance. 1-1.5 mm sheet thickness cannot be used for turbine due to problems faced in metal joining process. Using 3 mm thickness sheet the mass increases by 70 kg. This will affect the self starting speed of the turbine.

Thus the turbine assembly has been manufactured using 2 mm thickness sheet. This thickness will impart sufficient strength to bear the wind gust and also other performance parameters are satiated.

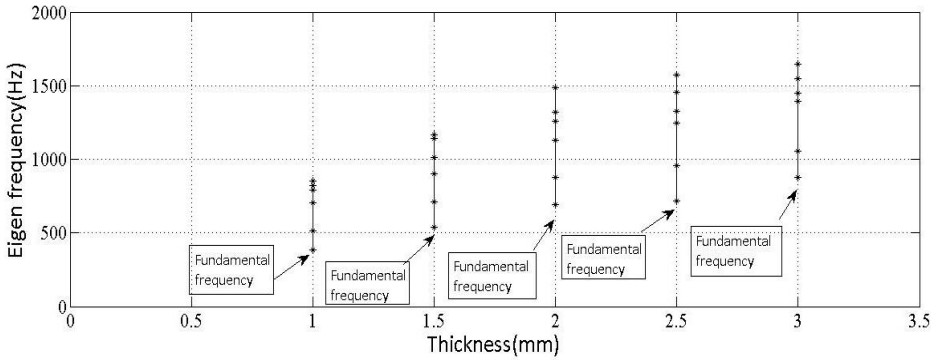

Figure 14. Eigen frequency plot of blade.

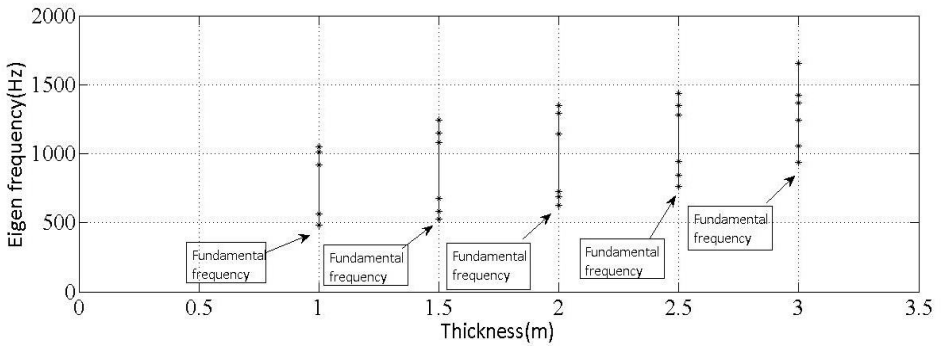

Figure 15. Eigen frequency plot of flap.

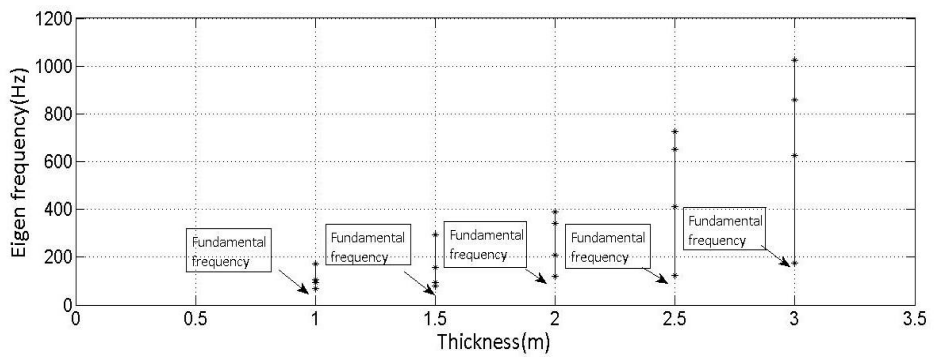

Figure 16. Eigen frequency plot of Plate.

CONCLUSION

A Multi storey Vertical Axis Wind Turbine designed and developed to enhance its performance in terms of coefficient of power and self-starting speed. Structural analysis of the

turbine parts and the turbine assembly has been carried out using ANSYS software. The physics used for analysis is solid mechanics. The structural analysis is done for three parts of turbine viz: blade, flap and plate for sheet thickness range of 1, 1.5, 2, 2.5 and 3 mm. Stress, deflection and Eigen frequency are analyzed numerically and theoretically for different sheet thickness of turbine parts. The numerical and theoretical results are in good agreement. From the analysis it is seen that the stress magnitude is high for sheet thickness of 1 mm. The stress magnitude reduces as the thickness increases. The deflection is also seen maximum in 1 mm thickness sheet as compared to that of other sheet thickness used to turbine parts. As the thickness increases the mass and stiffness of the turbine parts increases.

Eigen frequency is recorded for all the thickness of the sheet used for turbine parts. The forcing frequency calculated is considerably less that the fundamental mode frequency. The optimum sheet thickness of 2 mm is used for the turbine assembly to impart structural strength to the turbine against wind gust, which will also satisfy performance parameter of self-starting speed.

REFERENCES

Bedon, G. De Betta, S. Benini, E. A. 2015. Computational assessment of the aerodynamic performance of a tilted Darrieus wind turbine. *J. Wind Eng. Ind. Aerodyn.*, 145:263-269.

Behera, S. Mittal, A. K. 2012. A Comparative Study of Wind Forces on Tall Building and Towers as per IS 875-Part-III (1987) and Draft Code (2011) Using Gust Factor Method l. VI.National Conference on Wind Engineering. 14-15.

Burlando, M. Ricci, A. Freda, A. Repetto, M. P. 2012, Modeling passive variable pitch cross ow hydrokinetic turbines to maximize performance and smooth operation. *Renewable Energy*, 45:41-50.

Chong, W. T. Pan, K. C. Poh, S. C. Fazlizan, A. Oon, C. S. Badarudin, A. Nik-Ghazali, N.2013. Performance investigation of a power augmented vertical axis wind turbine for urban high-rise application. *Renewable Energy*, 51: 388-397.

Coxa, K. Echtermeyer, A. 2012 Structural design and analysis of a 10MW wind turbine blade. *Energy Procedia*, 24: 194 201.

Goude, A. Agren, O. 2014. Simulations of a vertical axis turbine in a channel. *Renewable Energy*, 63: 477-485.

Greenblatt D., Lautman R. Inboard/outboard plasma actuation on a vertical-axis wind turbine, *Renewable Energy*, 2015; 83: 1147-1156.

Lavassas, I. Nikolaidis, G. Zervas, P. Efthimiou, E. Doudoumis, I. N. and Baniotopoulos, C. C. 2003. Analysis and design of the prototype of a steel 1-MW wind turbine tower. *Engineering Structures*, 25:1097-1106.

Lee, Y. T. Lim, H. C. 2015 Numerical study of the aerodynamic performance of a 500 W Darrieus-type vertical axis wind turbine. *Renewable Energy*, 83: 407-415.

Lkhoury, M. Kiwata, E. T. Aoun, E. 2015. Experimental and numerical investigation of a three-dimensional vertical-axis wind turbine with variable-pitch. *J. Wind Eng. Ind. Aerodn.*, 139: 111-123.

Numericaland experimental methods to investigate the behavior of vertical-axis wind turbines with stators, *J. Wind Eng. Ind. Aerodynamics*, 2015; 144: 125-133.

Saqib Hameed M., Kamran Afaq S. 2013. Design and analysis of a straight bladed vertical axis wind turbine blade using analytical and numerical techniques. *Ocean Engineering*, 57:248-255.

Shi, L. Riziotis, V. A. Voutsinas, S. G. Wang J. 2014. A consistent vortex model for the aerodynamic analysis of vertical axis wind turbines. *J. Wind Eng. Ind. Aerody*., 135: 57-69.

Siddiqui, M. S. Durrani, N. Akhtar, I. 2015. Quantification of the effects of geometric approximations on the performance of a vertical axis wind turbine. *Renewable Energy*, 74: 661-670.

Tjiu, W. Marnoto, T. Mat, S. Ruslan, M. H. Kamaruzzaman, S. 2015.Darrieus vertical axis wind turbine for power generation I: Assessment of Darrieus VAWT configurations. *Renewable Energy*, 75: 50-67.

In: Renewable Energy Systems
Editor: Sandip A. Kale
ISBN: 978-1-53610-423-3

Chapter 9

PHYSICAL PROPERTIES OF BIODIESEL: DENSITY AND VISCOSITY

Narayan Gaonkar[1] and R. G. Vaidya[2,*]
[1]Department of Physics, University College of Science,
Tumkur University, Tumkur, India
[2]Department of Studies and Research in Physics and C.E.I.E.,
Tumkur University, Tumkur, India

ABSTRACT

This century has witnessed the beginning of a new era in the discovery ofrenewable and eco-friendly energy resources. Among the biofuels, biodiesel is one of the renewable energy resources found to have a potential to replace conventional petroleum fuels. This chapter briefly reviews the characteristic physical properties – density and viscosity –of biodiesels. The models and equations which describe the variation of density and viscosity of biodiesel as a function of temperature and blend percent are reviewed. The models and equations are used to predict the density and viscosity of biodiesel and are compared with available experimental data. An effort is made to present elaborate analysis of the predictive capability of new models using statistical tools. The variation of density and viscosity of biodiesel blends as a simultaneous function of temperature and blend volume percent is also discussed.

Keywords: renewable energy, biofuel, biodiesel, density and viscosity of biodiesel.

1. INTRODUCTION

Energy and environment have become one of the most critical current issues. The decrease in the conventional fossil fuel resources has led to the energy crisis and the increasing environmental problems. The alternate for energy resources has become real

*E-mail: ratnakarvaidya@gmail.com.

challenge at present. Biofuels with enticing features of renewable nature found to be potential alternate candidate. Biodiesel is one of the biofuels, with comparable chemical and physical properties compared to petroleum diesel. The study of physical properties of biodiesel has contributed much of our knowledge concerning employability of biodiesel as a fuel in engine.

1.1. Biodiesel and Physical Properties

Biofuels are one of the naturally available energy resources occur in the form of three phases of matter - solid, liquid and gaseous phases. Among the biofuels, biodiesel is the most important natural energy resource gaining the focus. Biodiesel is produced from transesterification reaction of vegetable oils and animal fats. Biodiesel mainly contains long chain fatty acid methyl esters (FAME) and fatty acid ethyl ester (FAEE). The use of biodiesel in the engine has many advantages over petroleum diesel. Biodiesel shows the lower toxic exhaust emissions, lower Sulphur content, better ignition quality, greater safety and cleaner burning nature. The use of biodiesel takes a part in carbon dioxide cycle. These advantageous features along with the renewable nature and biodegradability have made the biodiesel as a promising candidate for future fuel.

Biodiesel is similar to the petroleum diesel in chemical characteristics. But its physical properties are slightly differing from conventional petroleum diesel. The physical properties – density, viscosity, flash point and heating value are higher in magnitude compared to the conventional petroleum diesel. These properties prohibit direct use of biodiesel in the engine. However, this difficulty can be resolved by employing biodiesel blending process. The complete miscible nature of biodiesel in petroleum diesel allows blending in any proportion. This strategy is often adapted to make biodiesel as alternate fuel. Presently, 20% blend of biodiesel can be used in diesel engine without or minor modifications (Anandet al. 2010).

The physical properties of fuel influence the engine performance. They impact on the combustion process and exhaust emission. The design and optimization of combustion, transportation and heating units are mainly dependent on the physical properties of the fuel such as density, kinematic viscosity and surface tension. The knowledge of physical properties of the biodiesel is essential in maintaining the quality of fuel for the replacement of petroleum diesel.

Density is one of the most important physical properties of the biodiesel which affects the fuel quality. Density is defined as mass per unit volume of the matter. The density of biodiesel is higher than that of petroleum diesel. Higher density affects the injection of fuel in the engine and slightly higher mass of the fuel gets injected during the fuel spray because, the conventional engine injects the fuel on volumetric basis. This leads to incomplete combustion and solidification of fuel at low temperatures in turn increases the exhaust emissions. The other physical properties, viscosity, surface tension are interrelated to density of the fuel.

Kinematic viscosity of the fuel is another important physical property which has influence on the performance of the engine. Viscosity is the resistance offered by the fluid to flow. It is the measure of internal fluid friction which tends to oppose any dynamic change in the fluid motion. Viscosity originates from the intermolecular attraction between the molecules of the fluid. The kinematic viscosity of biodiesel is little higher compared to diesel. The higher viscosity affects the spray characteristics of the fuel. During fuel injection it

causes poor atomization and formation of larger droplets. The higher viscosity causes deposition of carbon on fuel filters and pump valves. The viscosity of biodiesel can also be modified by blending technique.

2. VISCOSITY AND DENSITY: MODELS AND EQUATIONS

The physical properties of biodiesel the density and viscosity are observed to vary not only with temperature but also with blend volume percent. The knowledge of variation of physical properties is at most important because, they directly impact on engine performance. In literature, there exist few models and equations to predict the variation of density and viscosity of biodiesels. The survey revealed that there is no generalized equation to represent the relation between the density and viscosity in terms of temperature. Most of the models compare the density and viscosity with temperature by using correlation parameters determined by regression technique from number of experimental data. Different biodiesels have different composition of fatty acid chains; they merely show different correlation parameters. The models predicting the density and kinematic viscosity by using other than regression analysis is rarely reported in literature. In this section, we outline existing models and equations to predict density and viscosity of biodiesel and its blends. In section 3, we analyze applicability of new models proposed to predict behavior of density and kinematic viscosity of biodiesel.

a) Density: The density of blend of biodiesel varies with blend percent, temperature and composition of the blend. Several models can be found in literature reporting the variation of density with temperature, percentage of components and chemical composition. Few models and equations existing in literature often employed to describe the variation of density of biodiesel are listed in Table 1. Among them, Kay's mixing rule (Kay 1936) is simple approach to estimate the density of blend which can be expressed in terms of mass fractions or mole fractions or volume fractions. The first order linear regression in temperature presented by Tat and Gerpen (2000) is used by Alptekin and Canakci (2008) and Tate et al. (2006) to predict the variation of density of biodiesel with least error. Rackett equation (1970) is the model to predict the density which requires the critical constants of the components of blend and is complex. Even though several models and equations are suggested, among them some demand for actual composition of biodiesel for estimation of density. Most of the models correlated the density of biodiesel with temperature and they use parameters adjusted to number of experimental data by regression.

b) Kinematic viscosity: The kinematic viscosity of blend also shows variation with temperature, blend percent and chemical composition. There exist a few models describing the variation of viscosity of blend with temperature and blend percent. Among the existing models and equations conveniently employed to predict the variation behavior of kinematic viscosity of biodiesel are summarized in Table 2. The models and equations correlating the kinematic viscosity require some critical properties and they use parameter fitted to the experimental data by regression. However, the method of predicting viscosity of biodiesel blend by using the viscosity of its blend components is rarely reported. In addition, the reliable model provides the opportunity to synthesize the right composition of biodiesel blend as per acceptable standards and formulation of adequate blend of biodiesels with cost

effective method and accomplish with desired quality standards. Moreover, the study of density and viscosity variation benefits for understanding the basic physics behind the nature of intermolecular interaction between the molecules of the biodiesel blends.

3. NEW MODELS FOR PREDICTION OF DENSITY AND VISCOSITY

3.1. A New Simple Model for Density

A new simple model to predict density of binary and ternary blends of biodiesel as simultaneous function of temperature and blend volume percent is presented in this section (Gaonkar and Vaidya 2016). They follow Kay's mixing rule (Kay 1936) with volume fractions to calculate the density of blend at the any two different temperatures with two different volume percent of biodiesel. The Kay's mixing rule for binary and ternary blends are respectively given by,

$$\rho = v_1\rho_1 + v_2\rho_2 \tag{1}$$

Table 1. Models and equations for prediction of density of biodiesel and its blends

Physical property	Model/ Equation	Parameters	Reference
Density of biodiesel blends	$\rho = \sum_i x_i \rho_i$	x_i – fraction of blend component ρ_i – Density of component	Kay's Mixing rule (Kay 1936)
Density	$\rho = a + bt$	a and b – correlation constants t - temperature	Tat and Gerpen (2000)
Density	$\rho = \frac{M}{\frac{RT_C}{P_C} Z_C^{\left(1+\frac{T}{T_C}\right)^{2/7}}}$	M – Molecular weight P_c, T_c and Z_c – critical constants	Rackett equation (1970)
Density	$\rho = \frac{M}{\sum_{i=1}^{n} n_i v_i}$	M – Molecular weight n_i- number of groups v_i – group volume	GCVOL method (Spencer and Danner 1972)
Density	$\rho = \frac{M}{\frac{RT_C}{P_C} Z_{RA}^{(1-T_r)^n}}$	M – Molecular weight P_c and T_c – critical constants Z_{RA} – Rackett parameter T_r – Reduced temperature n – exponent parameter	Anandet al. (2010)
Density of blends	$\rho = \alpha.V + \beta.T + \delta$	α, β and δ - adjustable parameters V – volume percentage of blend T – Temperature	Ramirez-Verduzcoet al. (2011)
Density of blends	$\rho = v_1\rho_{1,293.15} + + v_2\rho_{2,293.15} + a + bT$	$\rho_{1,293.15}$ and $\rho_{2,293.15}$ – density of blend components at 293.15K v_1 and v_2 – volume fractions a and b – correlation constants T –temperature	Moradiet al. (2013)
Density of binary and ternary blends	$\rho = a + bT + c\varphi$ $\rho = a + bT + c\varphi_1 + d\varphi_2$	a, b, c and d – correlation constants T- Temperature Φ_1 and Φ_2 – volume fractions of components	Baroutianet al. (2012)

Table 2. Models and equations for prediction of kinematic viscosity of biodiesel and its blends

Physical property	Model/ Equation	Parameters	Reference
Kinematic viscosity of blends	$\ln \mu = \sum_{i=1}^{n} v_i \ln \mu_i$	v_i– volume fraction of blend components μ_i– Kinematic viscosity of components	Grunberg-Nissan equation (1949)
Kinematic viscosity	$\ln \mu = A + \frac{B}{T} + \frac{C}{T^2}$	*A*, *B* and *C* – correlation parameters *T* – Temperature	Tat and Gerpen (1999)
Kinematic viscosity	$\ln \eta = A + \frac{B}{T} + CV_B$	*A*, *B* and *C* – correlation constants *T* – temperature V_B – volume fraction of blend component	Joshi and Pegg (2006)
Kinematic viscosity	$\ln \eta = \ln \gamma + \varphi V + \frac{\omega}{T} + \frac{\lambda V}{T}$ $\ln \eta = \ln \gamma + \varphi V + \omega T + \lambda VT$ $\ln \eta = \ln \gamma + \varphi V + \frac{\omega}{T} + \frac{\lambda V}{T^2}$ $\ln \eta = \ln \gamma + \frac{\omega}{T} + \frac{\lambda V}{T}$ $\ln \eta = \ln \gamma + \frac{\omega}{T} + \frac{\lambda V}{T^2}$	γ, φ, ω and λ – adjustable parameters *T* – temperature *V* – volume percentage of biodiesel blend (%)	Ramirez-Verduzco et al. (2011)
Kinematic viscosity of binary and ternary blends	$\eta = a + bT + c\varphi$ $\eta = a + bT + c\varphi_1 + d\varphi_2$	*a*, *b*, *c* and *d* – correlation constants *T*- Temperature $\Phi_1$and Φ_2– volume fractions of components	Baroutian et al. (2012)
Kinematic viscosity of blends	$\upsilon = \upsilon_{1,313.15}^{\ v_1} \upsilon_{2,313.15}^{\ v_2} \exp\left(c + \frac{d}{T} + \frac{e}{T^2}\right)$ $\upsilon = \left(v_1 \upsilon_{1,313.15}^{\ 1/3} v_2 \upsilon_{2,313.15}^{\ 1/3}\right)^3 \exp\left(f + \frac{g}{T} + \frac{h}{T^2}\right)$ $\upsilon = \left(v_1 \upsilon_{1,313.15}^{\ 1/3} v_2 \upsilon_{2,313.15}^{\ 1/3}\right)^3 \exp\left(f + \frac{g}{T} + \frac{h}{T^2}\right)$ $\upsilon = \upsilon_{1,313.15}^{\ v_1} \upsilon_{2,313.15}^{\ v_2} \exp\left(i + \frac{j}{T+k}\right)$ $\upsilon = \left(v_1 \upsilon_{1,313.15}^{\ 1/3} v_2 \upsilon_{2,313.15}^{\ 1/3}\right)^3 \exp\left(l + \frac{m}{T+n}\right)$	$\upsilon_{1,313.15}$ and $\upsilon_{2,313.15}$ – kinematic viscosity of components at 313.15K v_1 and v_2 - volume fractions *c* to *n* – correlation constants *T* –temperature	Moradi et al. (2013)
Kinematic viscosity of binary and ternary blends	$\ln \eta = A + \frac{B}{T} + Cw_1$ $\ln \eta = A + \frac{B}{T} + Cw_1 + Dw_2$	*A*, *B*, *C* and *D* – correlation constants $w_1$and w_2– mass fractions of blend components *T* – temperature	Nogueira et al. (2012)

$$\rho = v_1\rho_1 + v_2\rho_2 + v_3\rho_3 \tag{2}$$

where, v_1, v_2 and $v_3$are volume fractions of components *1*, *2* and *3* with densities ρ_1, $\rho_2$and ρ_3 in their pure form, respectively.

Equating the density values found using Kay's mixing rule in the form of empirical equations given by Ramirez-Verduzcoet al.(2011) and Baroutianet al. (2012) for binary and ternary blends, respectively have obtained.

$$\rho_{xy} = a + bT_x + cV_y \tag{3}$$

$$\rho_{xyz} = a + bT_x + cV_y + dV_z \tag{4}$$

where, ρ_{xy} is the density of binary blend at temperature T_x and volume percent V_y respectively and ρ_{xyz} is density of ternary blend at temperature T_x, volume percent of components V_y and V_z, respectively. By solving these equations, two set of values for *a, b* and *c* for binary blends and four set of values for *a, b, c* and *d* for ternary blends can be obtained. The average values of these parameters may be adopted for calculation of density values of binary and ternary blends of biodiesel at various temperatures and volume percent of components.

3.2. A New Simple Model for Kinematic Viscosity

A new simple model to predict density of binary and ternary blends of biodiesel as simultaneous function of temperature and blend volume percent is presented in this section. The model follows the Grunberg-Nissan equation for calculation of viscosity of blends. The logarithmic mixture laws of viscosity by Grunberg-Nissan (1949) for binary and ternary biodiesel blends are respectively given as,

$$\ln\mu = v_1 \ln\mu_1 + v_2 \ln\mu_2 \tag{5}$$

$$\ln\mu = v_1 \ln\mu_1 + v_2 \ln\mu_2 + v_3 \ln\mu_3 \tag{6}$$

Where, v_1, v_2, $v_3$and μ_1, μ_2, $\mu_3$are volume fractions, and kinematic viscosities of components 1, 2 and 3 in their pure form, respectively. These equations are applicable at constant temperature. In order to study the dependence of viscosity on temperature, regression method is conventionally used. The logarithmic viscosity of binary and ternary blends of biodiesel as a function of reciprocal of temperature and volume percent (Nogueiraet al.2012) are respectively given by,

$$\ln\mu = A + \frac{B}{T} + CV \tag{7}$$

$$\ln\mu = A + \frac{B}{T} + CV_1 + DV_2 \tag{8}$$

here, T is absolute temperature, V, $V_1$and V_2 are volume percent of blend components, A, B, C and D are correlation parameters.

Using equations (7) and (8), the viscosity of blend at two different temperatures and two arbitrary volume fractions can be calculated by taking the viscosity of pure components. The results are represented in the form of equations as below.

$$\ln \mu_{xy} = A + \frac{B}{T_x} + CV_y \tag{9}$$

$$\ln \mu_{xyz} = A + \frac{B}{T_x} + CV_y + DV_z \tag{10}$$

Where, μ_{xy} is viscosity of binary blend at temperature, T_x and volume percent V_y, μ_{xyz} is viscosity of ternary blend at temperature T_x, volume percent of components V_y and V_z, respectively. By solving these equations two sets of values for correlation parameters can be obtained. The averaged values of parameters are used to estimate the viscosity at different temperatures and blend volume percent. The dynamic viscosity can be calculated from kinematic viscosity, using the expression,

Dynamic viscosity = density × kinematic viscosity ($\mu = \rho$ x η) (11)

4. PREDICTIVE CAPABILITY OF MODEL

Always, Standard Estimate of Error (*SEE*) and Absolute Average Deviation (*AAD*) serve as good promising tools for validating the model. Lower values of *SEE* and *AAD* indicate good agreement between predicted and experimental values. The detailed error analysis also validates the predictive capability of the model. The expressions for *SEE, AAD* and percent error are respectively, given by,

$$SEE = \sqrt{\frac{\sum_{i=1}^{n} (X_i - Y_i)^2}{n - p}} \tag{12}$$

$$AAD(\%) = \frac{100}{n} \sum_{i=1}^{n} \frac{|X_i - Y_i|}{X_i} \tag{13}$$

$$Error(\%) = \frac{|X_i - Y_i|}{X_i} \times 100 \tag{14}$$

where, $X_i$andY_i are experimental and predicted values, n is number of data points used in the study and p is the number of parameters in the equation.

5. APPLICATIONS OF MODELS

The newly developed models are useful to predict the density and kinematic viscosity of binary and ternary biodiesel blends with temperature and volume percent of blend components as simultaneous variables. The model provides the density and kinematic viscosity values at different temperature and different volume percent. It avoids the conventional regression method and consequently does not require number of experimental data points for determination of correlation parameters. The models demand only density and kinematic viscosity values of the blend components in their pure form at any two different temperatures. There is no need to prepare all the mixtures.

The correlation parameters calculated using the model represents the rate of variation of density and kinematic viscosity of biodiesel blends with temperature and volume percent of blend component. They depend on the nature of molecules of biodiesel and intermolecular interaction between them. The correlation parameters *b*, *c* and *d* calculated using the model represent the rate of variation of density of biodiesel blend with change in temperature, volume percent of blends component 1 and 2, respectively. The correlation parameters *B, C* and *D* indicate the rate of variation of kinematic viscosity of biodiesel blends with respect to change in temperature and volume percent of blend component 1 and 2, respectively. The higher value of corresponding correlation parameter signifies higher rate of change of physical property of biodiesel blend. This analysis helps to synthesize the optimized biodiesel blends to meet the desired standards. In the next sections, we analyze the behavior of density and viscosity of biodiesel and its blends.

5.1. Density of Biodiesel and Its Blends

The new developed model is employed to predict the density values of biodiesel blends and predictive capability is analyzed. The experimental density results from the literature presented in Tables 3 and 4 are used for the determination of correlation parameters corresponding to different binary and ternary blend systems biodiesel in the temperature range [273.15K, 373.15K]. Table 5 and 6 depict the correlation parameters for biodiesel blends and can be used for estimation of density at different temperatures and different volume percent of blend constituents. The calculated density values are compared with respective experimental data to check the validity of the model. Figures 1-4 represent the graphical comparison of density of different biodiesel blends as a simultaneous function of temperature and volume percent of blend. Dots indicate the experimental density data and mesh represents the predicted density values of biodiesel blends.

The detailed study revealed that, all the biodiesel blends show same behavior of variation of density with change in temperature and volume percent of blend components. The density of biodiesel blend systems increases with increase in volume percent of biodiesel where biodiesel has greater density than other components. The decrease in density with increase in temperature may be attributed to the gain in thermal energy of the molecules of the blend. The force of attraction between the molecules increase with density of the fluid and influenced by temperature. Because of increase in thermal agitation of molecules, the molecular weight per unit volume of blend decreases. Therefore, the density of biodiesel

blend decreases with increase in temperature. Overall observation showed that the density values of biodiesel blends fit to surface plane with temperature and volume percent of components as two parameters.

Table 3. Experimental density data from literature used for calculations (binary blends)

Biodiesel blend	Temperature (K)	Component 1 Density (g/cm^3)	Component 2 Density (g/cm^3)
Mixture of Peanut and sunflower oil biodiesel (1) + Ultra-Low Sulphur Diesel (2) (Ramírez-Verduzcoet al.2011)	293.15	0.8869	0.8344
	373.15	0.8288	0.7779
Soybean biodiesel (1) + Diesel (2) (Moradiet al.2013)	293.15	0.8825	0.8265
	353.15	0.838	0.7865
Canola oil biodiesel (1) + Diesel (2) (Moradiet al.2013)	293.15	0.8805	0.8265
	353.15	0.8365	0.7865
Sunflower oil biodiesel (1) + Diesel (2) (Moradiet al.2013)	293.15	0.8830	0.8265
	353.15	0.8390	0.7865
Waste oil biodiesel (1) + Diesel (2) (Moradiet al.2013)	293.15	0.8765	0.8265
	353.15	0.8310	0.7865
Edible tallow oil biodiesel (1) + Diesel (2) (Moradiet al.2013)	293.15	0.8700	0.8265
	353.15	0.8265	0.7865
Coconut oil biodiesel (1) + Colza oil biodiesel (2) (Feitosaet al.2010)	293.15	0.8709	0.8846
	373.15	0.8793	0.8268
Coconut oil biodiesel (1) + Soybean biodiesel (2) (Feitosaet al.2010)	293.15	0.8853	0.8709
	373.15	0.8272	0.8093
Cotton seed biodiesel (1) + Babassu biodiesel (2) (Nogueiraet al. 2010)	293.15	0.8816	0.8762
	373.15	0.8234	0.8146
Soybean biodiesel (1) + Babassu biodiesel (2) (Nogueiraet al. 2010)	293.15	0.8858	0.8762
	373.15	0.8280	0.8146
Soybean biodiesel (1) + Diesel (2) (Nogueiraet al. 2012)	293.15	0.8855	0.8270
	373.15	0.8278	0.7708
Sunflower oil biodiesel (1) + Diesel (2) (Parenteet al.2011)	293.15	0.8830	0.8270
	373.15	0.8247	0.7708
Fish oil biodiesel (1) + Diesel (2) (Parenteet al.2011)	293.15	0.8776	0.8270
	373.15	0.8191	0.7708
Jatropha Carcus biodiesel (1) + Diesel (2) (Satish kumaret al.2011)	288.15	0.884141	0.8244
	308.15	0.869588	0.8105
Jatropha FAME[a] (1) + Jatropha FAEE[b] (2) (Baroutianet al.2012)	293.15	0.87673	0.8741
	358.15	0.82837	0.8257
Palm FAME[a] (1) + Palm FAEE[b] (2) (Baroutianet al.2012)	293.15	0.87264	0.8700
	358.15	0.82519	0.8225
Soybean biodiesel (1) + Diesel (2) (Mesquitaet al.2011)	293.15	0.8853	0.8468
	373.15	0.8272	0.7904
Soybean oil (1) + Diesel (2) (Nogueiraet al. 2012)	293.15	0.9207	0.8270
	373.15	0.8671	0.7708
Soybean oil (1) + Soybean biodiesel (2) (Nogueiraet al. 2012)	293.15	0.9207	0.8855
	373.15	0.8671	0.8278
Waste frying oil biodiesel (1) + Diesel (2) (Santos et al.2011)	283.15	0.89389	0.8541
	323.15	0.86518	0.8266
Linseed Biodiesel (1) + Diesel (2) (Nogueiraet al. 2015)	293.15	0.8833	0.8330
	333.15	0.8542	0.8047
Linseed oil (1) + Linseed Biodiesel (2) (Nogueiraet al. 2015)	293.15	0.9195	0.8833
	333.15	0.8925	0.8542
Linseed oil (1) + Diesel (2) (Nogueiraet al. 2015)	293.15	0.9195	0.8330
	333.15	0.8925	0.8047
Corn Biodiesel (1) + Diesel (2) (Nogueiraet al. 2015)	293.15	0.8818	0.8330
	333.15	0.8529	0.8047
Corn oil (1) + Corn Biodiesel (2) (Nogueiraet al. 2015)	293.15	0.9186	0.8818
	373.15	0.8651	0.8237
Corn oil (1) + Diesel (2) (Nogueiraet al. 2015)	293.15	0.9186	0.8330
	333.15	0.8920	0.8047

[a]Fatty acid methyl ester, [b]Fatty acid ethyl ester.

Table 4. Experimental density data from literature used for calculations (ternary blends)

Biodiesel blend	Temperature (K)	Component 1 Density (g/cm^3)	Component 2 Density (g/cm^3)	Component 3 Density (g/cm^3)
Jatropha FAME[a](1)+Jatropha FAEE[b] (2)+Diesel(3) (Baroutianet al.2012)	293.15	0.8767	0.8741	0.8209
	358.15	0.8284	0.8257	0.7748
Palm FAME[a] (1) + Palm FAEE[b] (2) + Diesel (3) (Baroutianet al.2012)	293.15	0.8727	0.8700	0.8209
	358.15	0.8252	0.8225	0.7748
Soybean biodiesel (1) + Soybean oil (2) + Diesel (3) (Nogueiraet al. 2012)	293.15	0.8855	0.9207	0.8270
	373.15	0.8278	0.8671	0.7708

[a]Fatty acid methyl ester, [b]Fatty acid ethyl ester.

Table 5 and 6 show the *SEE* and *AAD* (%) values obtained for different biodiesel binary and ternary blends respectively. The maximum and minimum errors observed between predicted and experimental density values among the deliberated data points are also included. *SEE* values are observed lying between 0.0003 and 0.0012 and *AAD* between 0.03 and 0.11% for biodiesel blends. The model predicts behavior of physical properties of binary and ternary biodiesel blends with low *SEE* and *AAD* (%) as presented in Table 6.

The comparison between the *AAD* values obtained in this study and presented by researchers revealed that, the model has comparatively better predictive capability. The model proposed by Moradiet al. (2013) has showed maximum *AAD* of 0.15% for different biodiesel blends. The empirical relation presented by Ramirez-Verduzco (2013) predicted the density of coconut + colza biodiesel, cotton seed + babassu biodiesel and soybean + babassu biodiesel blends with maximum *AAD* of 0.71%. The model in this study, predicted the density of the density of the same with maximum *AAD* of 0.08%. Nogueiraet al. (2012) presented the experimental data for density of binary and ternary blends and fitted to empirical formula of Baroutianet al. (2012), showed maximum *AAD* of 0.13%. The proposed model displayed the maximum of *AAD* of 0.06% for the same. The study carried by Phankosoletet al. (2014) publicized the prediction of density of blends using different models and showed maximum *AAD* of 0.14%. Overall study showed that the model has given the maximum *AAD* of 0.11%.The analysis of correlation parameters provides the information about the behavior of physical properties of biodiesel blends. From Table 5, the value of *b* is comparatively low for soybean oil, corn oil and linseed oil blend with diesel. The variation of density for oil and diesel mixture show less sensitivity towards temperature. Also, density of ternary blend of soybean biodiesel, soybean oil with diesel is less sensitive to temperature among the three ternary blends considered. The pure biodiesel blends (Coconut oil biodiesel + Colza oil biodiesel, Coconut oil biodiesel + Soybean biodiesel, Cotton seed biodiesel + Babassu biodiesel, Soybean biodiesel +variation with temperature reflect that the biodiesel is more sensitive to temperature compared to conventional diesel. The density of blends increases (decreases) with increase of volume percent of biodiesel where, biodiesel has higher (lower) density than other blend components. It is found that, the fluid with lower density have lower kinematic viscosity.

Table 5. Correlation parameters *a, b* and *c* calculated using the model, *SEE*, *AAD* (%) and percent errors (%) between experimental and estimated density values for different biodiesel binary blend systems

Biodiesel Blend	*a*	*b*	*c*	*NDP*[a]	*SEE*[b]	*AAD*[c] (%)	Max. Error (%)	Min. Error (%)
Mixture of Peanut and sunflower oil biodiesel(1)+ Ultra-Low Sulphur Diesel (2)	1.0448	-7.16E-4	5.17E-4	72	0.0003	0.03	0.07	0.008
Soybean biodiesel (1) + Diesel (2)	1.033	-7.04E-4	5.38E-4	24	0.0008	0.07	0.19	0.004
Canola oil biodiesel (1) + Diesel (2)	1.033	-7.00E-4	5.20E-4	24	0.0009	0.08	0.21	0.000
Sunflower oil biodiesel (1) + Diesel (2)	1.032	-7.00E-4	5.45E-4	24	0.0006	0.06	0.15	0.000
Waste oil biodiesel (1) + Diesel (2)	1.036	-7.13E-4	4.73E-4	24	0.0012	0.11	0.28	0.003
Edible tallow oil biodiesel (1) + Diesel (2)	1.032	-6.96E-4	4.18E-4	24	0.0008	0.07	0.19	0.002
Coconut oil biodiesel (1) + Colza oil biodiesel (2)	1.104	-7.46E-4	1.56E-4	45	0.0008	0.08	0.20	0.001
Coconut oil biodiesel (1) + Soybean biodiesel (2)	1.090	-7.48E-4	1.62E-4	35	0.0008	0.06	0.28	0.001
Cotton seed biodiesel (1) + Babassu biodiesel (2)	1.095	-7.49E-4	0.71E-4	35	0.0006	0.05	0.18	0.002
Soybean biodiesel (1) + Babassu biodiesel (2)	1.095	-7.46E-4	1.15E-4	35	0.0005	0.05	0.19	0.001
Soybean biodiesel (1) + Diesel (2)	1.0358	-7.11E-4	5.78E-4	45	0.0010	0.11	0.21	0.008
Sunflower oil biodiesel (1) + Diesel (2)	1.0370	-7.16E-4	5.49E-4	45	0.0019	0.10	0.67	0.000
Fish oil biodiesel (1) + Diesel (2)	1.0374	-7.17E-4	4.95E-4	45	0.0022	0.15	0.65	0.001
Jatropha Carcus biodiesel (1) + Diesel (2)	1.029	-7.12E-4	5.94E-4	90	0.0004	0.04	0.09	0.001
Jatropha FAME (1) + Jatropha FAEE (2)	1.095	-7.45E-4	-0.26E-4	42	0.0004	0.03	0.08	0.006
Palm FAME (1) + Palm FAEE (2)	1.087	-7.31E-4	-0.27E-4	42	0.0004	0.03	0.08	0.002
Soybean biodiesel (1) + Diesel (2)	1.057	-7.16E-4	3.77E-4	45	0.0005	0.04	0.25	0.000
Soybean oil (1) + Diesel (2)	1.028	-6.86E-4	9.50E-4	45	0.0003	0.03	0.09	0.001
Waste frying oil biodiesel (1) + Diesel (2)	1.053	-7.03E-4	3.91E-4	55	0.0007	0.07	0.19	0.006
Linseed Biodiesel (1) + Diesel (2)	1.043	-7.18E-4	4.99E-4	45	0.0004	0.03	0.14	0.000
Linseed oil (1) + Linseed Biodiesel (2)	1.089	-7.01E-4	3.73E-4	45	0.0008	0.08	0.18	0.005
Linseed oil (1) + Diesel (2)	1.036	-6.91E-4	8.72E-4	45	0.0008	0.08	0.18	0.002
Corn Biodiesel (1) + Diesel (2)	1.043	-7.15E-4	4.85E-4	45	0.0006	0.05	0.17	0.001
Corn oil (1) + Corn Biodiesel (2)	1.086	-6.98E-4	3.91E-4	45	0.0007	0.06	0.18	0.000
Corn oil (1) + Diesel (2)	1.034	-6.86E-4	8.65E-4	45	0.0006	0.06	0.15	0.003

[a]Number of data points, [b]Standard estimate of error, [c]Absolute average deviation.

Table 6. Correlation parameters *a, b*, *c* and *d* calculated using the model, *SEE*, *AAD* (%) and percent errors (%) between experimental and estimated density values for different biodiesel ternary blend systems

Biodiesel Blend	*a*	*b*	*c*	*d*	*NDP*[a]	*SEE*[b]	*AAD*[c] (%)	Max. Error (%)	Min. Error (%)
Jatropha FAME (1) + Jatropha FAEE (2) + Diesel (3)	1.031	-7.14E-4	5.47E-4	5.20E-4	56	0.0011	0.07	0.19	0.001
Palm FAME (1) + Palm FAEE (2) + Diesel (3)	1.030	-7.13E-4	5.10E-4	4.84E-4	56	0.0011	0.07	0.18	0.001
Soybean biodiesel (1) + Soybean oil (2) + Diesel (3)	1.032	-7.02E-4	9.50E-4	5.78E-4	25	0.0006	0.06	0.11	0.009

[a]Number of Data Points, [b]Standard Estimate of Error, [c]Absolute Average Deviation.

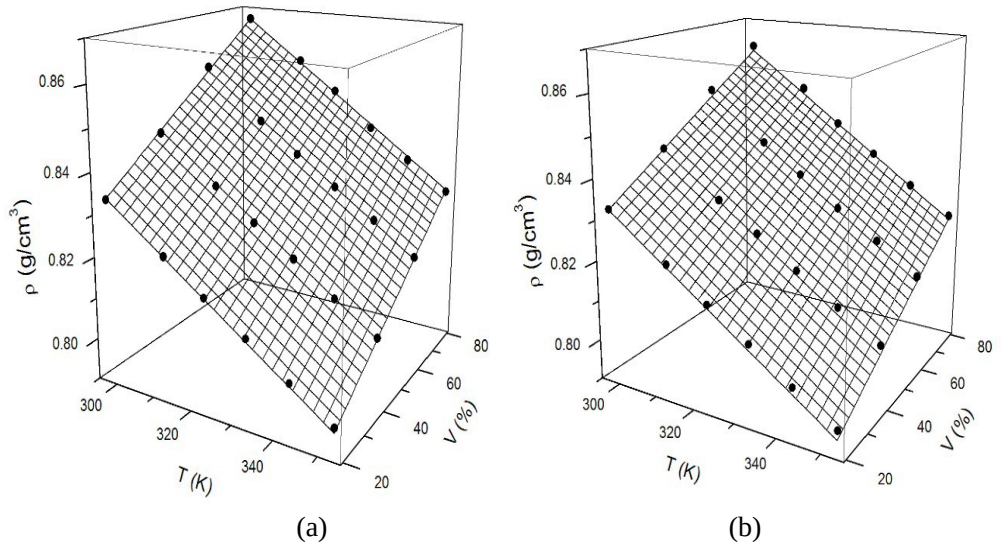

Figure 1. Graphic comparison between predicted and experimental data. (a) Sunflower oil biodiesel (1) + Diesel (2), (b) Waste oil biodiesel (1) + Diesel (2).

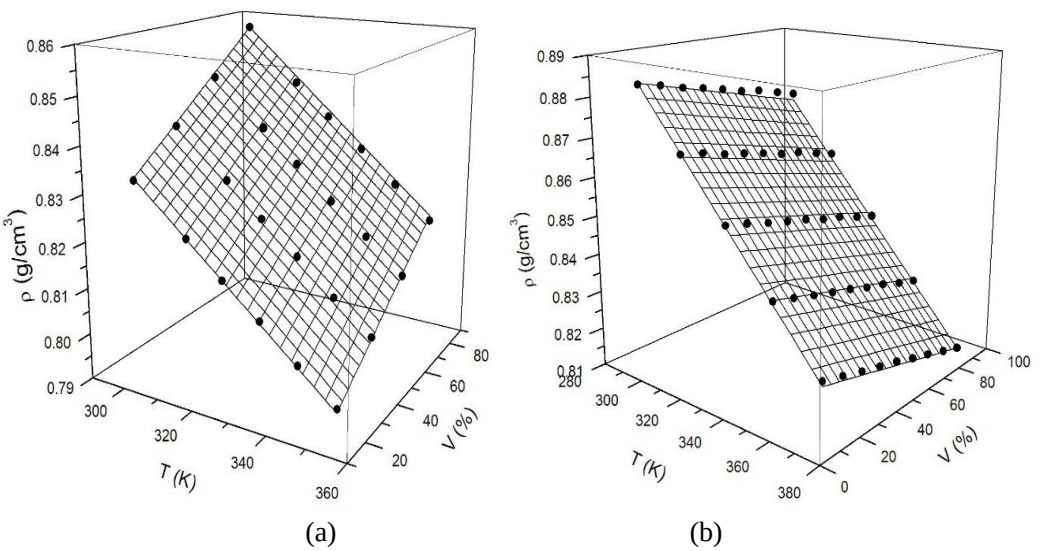

Figure 2. Graphic comparison of predicted density values and experimental data. (a) Edible tallow oil biodiesel (1) + Diesel (2), (b) Coconut oil biodiesel (1) +Colza oil biodiesel (2).

5.2. Kinematic Viscosity of Biodiesels and Its Blends

The study of variation of kinematic viscosity of biodiesel blends as a simultaneous function of temperature and blend percent using the proposed model reveals important results. The experimental data of viscosity at two different temperatures are tacked out from literature are used for calculation of correlation parameters.

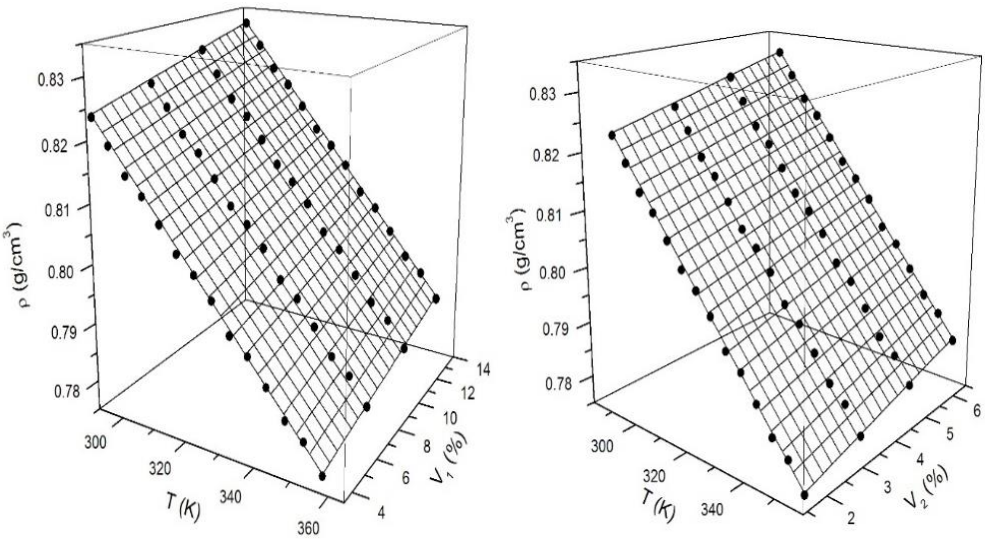

(a) (b)

Figure 3. Graphic comparison of predicted and experimental density data of ternary blend. (a) and (b) Jatropha FAME (1) + Jatropha FAEE (2) + Diesel (3).

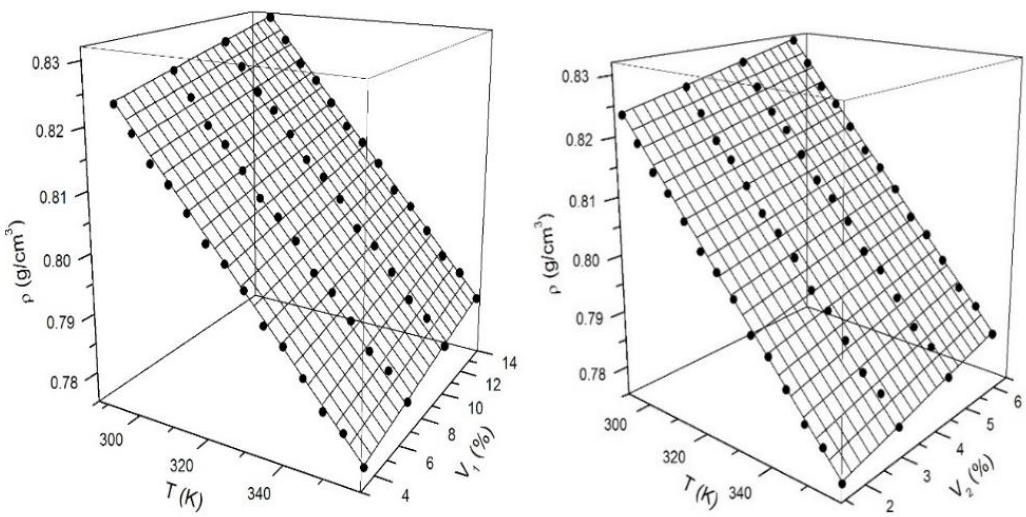

(a) (b)

Figure 4. Graphic comparison of predicted and experimental density data of ternary blend. (a) and (b) Palm FAME (1) + Palm FAEE (2) + Diesel (3).

Table 7 shows the set of viscosity data of soybean, canola, sunflower, and waste oil biodiesels at different temperatures. Table 8 shows the correlation parameters determined for the estimation of viscosity of biodiesel blends using proposed method. Figure 5 shows the variation of kinematic viscosity of blends as a simultaneous function of temperature and blend volume percent. The dots represent the experimental data and meshes represent the predicted viscosity values. All four biodiesel blends revealed same variation behavior with change in temperature and volume percent of blend. Exponential decrease in viscosity is

observed with increase in temperature. The increase in temperature leads to decrease in the cohesive attraction and increase in kinetic energy of molecules and hence the viscosity of blend decreases. Momentum transfer dominates over cohesive force of attraction among the molecules and hence kinematic viscosity decreases. The addition of biodiesel increases the kinematic viscosity of blend because of higher miscibility due to intermolecular attraction between the molecules of the blend. The increase in biodiesel percent in the blend show increase in viscosity. This is because of the fact that viscosity of biodiesel is greater than petroleum diesel.

At T = 313.15 K, the blending of biodiesel with petroleum diesel between 20%- 80% show the 26-36.6% decrease in viscosity. The waste oil biodiesel blend shows 36.6% decrease in viscosity at T = 313.15 K. The 55% decrease in viscosity of waste oil biodiesel blend (80%) is observed for the variation of temperature from 313.15 K to 363.15 K and is higher compared to others. Because of higher viscosity, the cohesive force of attraction between molecules of the fluid dominates over molecular momentum transfer during the flow of fluids. This generates the greater opposition for flow between layers of the fluid.

Table 7. Experimental kinematic viscosity data tacked out from literature for the calculation of correlation parameters

Biodiesel blend	Temperature (K)	Viscosity (mm^2/s)
Soybean oil biodiesel (Moradiet al.2013)	313.15	4.404
	363.15	2.124
Canola oil biodiesel (Moradiet al.2013)	313.15	4.791
	363.15	2.189
Sunflower oil biodiesel (Moradiet al.2013)	313.15	4.439
	363.15	2.016
Waste oil biodiesel (Moradiet al.2013)	313.15	4.768
	363.15	2.121
Petroleum diesel (Moradiet al.2013)	313.15	2.932
	363.15	1.407

Table 8. Correlation parameters *A, B* and *C*, *NDP, SEE, AAD* values and percent error (%) between experimental data and predicted values of kinematic viscosity of binary biodiesel blends

Biodiesel Blend	*A*	*B*	*C*	*NDP*[a]	*SEE*[b]	*AAD*[c](%)	Max. error (%)	Min. error (%)
Soybean oil biodiesel + Petroleum diesel	-4.23	1664.22	4.093E-3	24	0.117	4.232	6.86	0.73
Canola oil biodiesel + Petroleum diesel	-4.43	1725.72	4.665E-3	24	0.075	2.633	4.33	0.53
Sunflower oil biodiesel + Petroleum diesel	-4.45	1732.57	3.872E-3	24	0.101	3.579	7.54	0.54
Waste oil biodiesel + Petroleum diesel	-4.52	1756.14	4.483E-3	24	0.061	1.982	3.71	0.14

[a]Number of Data Points, [b]Standard Estimate of Error, [c]Absolute Average Deviation.

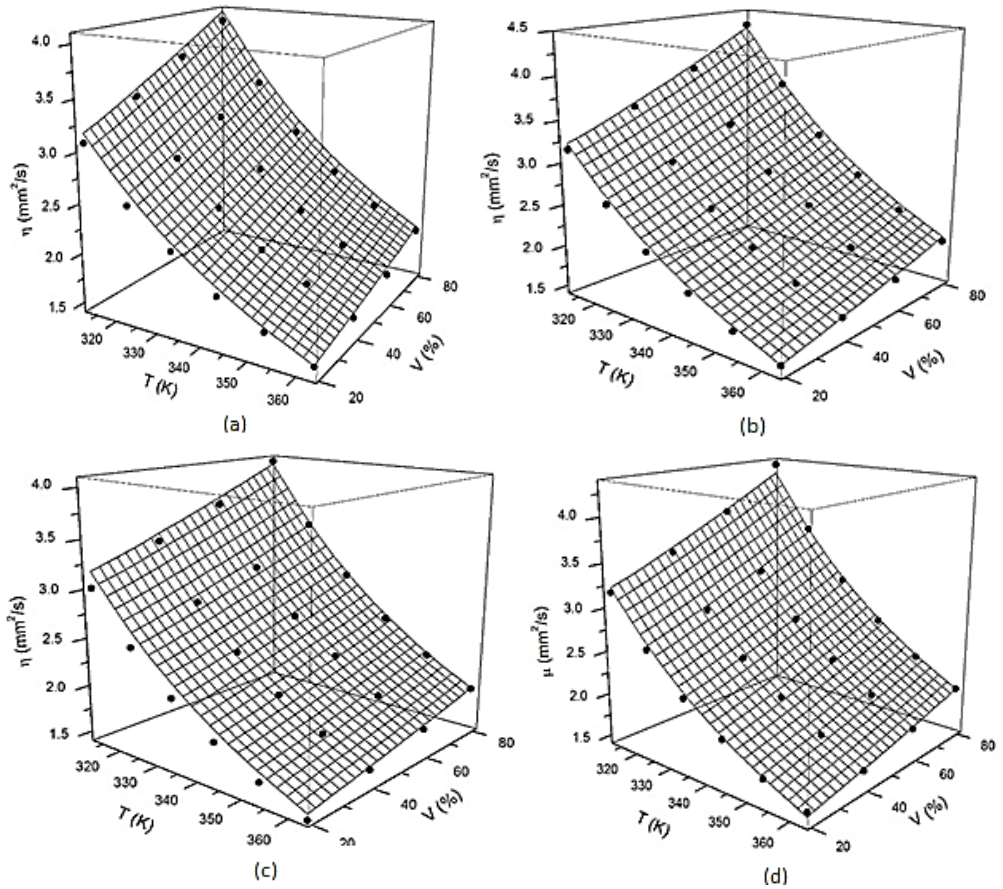

Figure 5. Variation of kinematic viscosity as a simultaneous function of temperature and blend volume percent. (a) Soybean oil biodiesel + Petroleum diesel, (b) Canola oil biodiesel + Petroleum diesel, (c) Sunflower oil biodiesel + Petroleum diesel, (d) Waste oil biodiesel + Petroleum diesel.

The correlation parameters determined for four different blend systems represent the rate of variation of viscosity with change in temperature and volume percent of blend. The correlation parameters B and C are higher for waste oil biodiesel blend signify the higher rate of change of viscosity with respect to the temperature and volume percent, respectively. This analysis helps to synthesize the optimized biodiesel blends to meet the desired standards.

Summary

In conclusion, we have reviewed the physical properties- density and viscosity of biodiesel and its blends. The role and relative importance of the characteristic physical properties of biodiesel and its blends are analyzed for employability. The present status of predictive capability of existing models and equations is discussed. The analysis of models revealed that there is no single model or equation to predict density and viscosity of biodiesel and its blends. Our review finds, there is a need of unified model to estimate the physical properties of biodiesel blends as a simultaneous function of temperature and blend percent. This paves a way to optimize the physical properties of biodiesels more accurately.

ACKNOWLEDGMENTS

This work is supported by University Grants Commission, New Delhi, India under Minor Research Project.

REFERENCES

Ambrose, D. 1979, "Correlation and Estimation of Vapour-Liquid Critical Properties. I. Critical Pressure and Volume of Organic Compounds", *National Physical Laboratory, Teddington. NPL Rep. Chem.,* 98.

Ertan Alptekin, Mustafa Canakci, 2008, "Detrmination of the Density and the Viscosities of Biodiesel-diesel Fuel Blends", *Renewable Energy* 33**:**2623-30.

Feitosa, F. X., Rodrigues, M. L., Veloso, C. B., Cavalcante, C. L., Albuquerque, M. C. G. de Sant´Ana, H. B. 2010, "Viscosities and densities of binary mixtures of coconut + colza and coconut + soybean biodiesel at various temperatures", *J. Chem. Eng. Data,* 55:3909-14.

Francisca M. R. Mesquita, Filipe X. Feitosa, Rilvia S. Santiago, Hosiberto B. de Sant'Ana, 2011, "Density, Excess Volumes, and Partial Volumes of Binary Mixtures of Soybean Biodiesel + Diesel and Soybean Biodiesel + n-Hexadecane at Different Temperatures and Atmospheric Pressure", *J. Chem. Eng. Data,* 56:153–57.

G.R. Moradi, B. Karami, M. Mohadesi, 2013, "Densities and kinematic viscosities in biodiesel-diesel blends at various temperatures", *J. Chem. Eng. Data,* 58:99-105.

Grunberg L., Nissan A.H., 1949, Mixture law of viscosity, *Nature,* 164:799-800.

Helle S. Elbro, Aage Fredenslund, Peter Rasmussen, 1991, "Group Contribution Method for the Prediction of Liquid Densities as a Function of Temperature for Solvents, Oligomers, and Polymers", *Ind. Eng. Chem. Res.,* 30 (12):2576-82.

Joback, K. G. 1984, "A unified approach to physical property estimation using multivariable statistical techniques". Ph.D. thesis, Massachusetts Institute of Technology, Cambridge, MA.

Joshi R.M., Pegg M.J., 2006, "Flow properties of biodiesel fuel blends at low temperatures", *Fuel,* 86:143-51.

K. Anand, Avishek Ranjan, and Pramod S. Mehta, 2010, "Predicting the Density of Straight and Processed Vegetable Oils from Fatty Acid Composition", *Energy and Fuels,* 24:3262-66.

Knapp, H. Doring, R. Oellrich, L. Plocker, U. Prausnitz, J. M. 1982, "Vapor-Liquid Equilibria for Mixtures of Low Boiling Substances" Chemistry *Data Series; DECHEMA: Frankfurt am Main,* Vol. VI.

L.F. Ramírez-Verduzco, B.E. García-flores, J.E. Rodríguez- Rodríguez, A.R. Jaramillo-Jacob, 2011, "Prediction of the density and viscosity in biodiesel blends at various temperatures", *Fuel,*90:1751-61.

M.E. Tat, J.H. Van Gerpen, 2000, "The specific gravity of biodiesel and its blends with diesel fuel", *JAOCS*77(2):115-19.

Maria Jorge Pratas, Samuel Freitas, Mariana B. Oliveira, Sı´lvia C. Monteiro, Alvaro S. Lima, Joa˜o A. P. Coutinho, 2010, "Densities and Viscosities of Fatty Acid Methyl and Ethyl Esters", *J. Chem. Eng. Data,*55:3983-3990.

Maria Jorge Pratas, Samuel V. D. Freitas, Mariana B. Oliveira, Sílvia C. Monteiro, Alvaro S. Lima, Jo~ao A. P. Coutinho, 2011, "Biodiesel Density: Experimental Measurements and Prediction Models", *Energy and Fuels,*25:2333-40.

Narayan Gaonkar, Vaidya R.G., 2016, "A simple model to predict the biodiesel blend density as simultaneous function of blend percent and temperature", *Environmental Science and Pollusion Research,*23(10):9260-64.

Nogueira C.A.Jr., Carmo F.R., Santiago D.F., Nogueira V.M., Fernandes F.A.N., Aguiar R.S.S., Sant'Ana. H.B., 2012, "Viscosities and densities of ternary blends of diesel + soybean biodiesel + soybean oil", *J. Chem. Eng. Data*, 57:3233-41.

Nogueira C.A. Jr., Nogueira V.M., Santiago D.F., Machado F.A., Fernandes F.A.N, Aguiar R.S.S., Sant'Ana H.B., 2015, "Density and viscosity of binary systems containing (linseed or corn) oil, (linseed or corn) biodiesel and diesel", *J. Chem. Eng. Data*, 60:3120-31.

Nogueira, Jr. C. A., Feitosa, F. X., Fernandes, F. A. N., Santiago, R. S. and de Sant´Ana, H. B., 2010, "Densities and viscosities of binary mixtures of babassu biodiesel + cotton seed or soybean biodiesel at different temperatures", *J. Chem. Eng. Data*, 55:5305-10.

R.C. Parente, C.A. Nogueira, F.R. Carmo, L.P. Lima, F.A.N. Fernandes, R.S. Santiago, R.S. Aguiar, H.B. de Sant'Ana, 2011, "Excess volumes and deviations of viscosities of binary blends of sunflower biodiesel + diesel and fish oil biodiesel + diesel at various temperatures", *J. Chem. Eng. Data*, 56:3061-67.

R.E. Tate, K.C. Watts, C.A.W. Allen, K.I. Wilkie, 2006, "The viscosities of three biodiesel fuels attemperatures up to 300 ^{0}C", *Fuel* 85:1010-15.

Rackett H. G. 1970, "Equation of State for Saturated Liquids". *J. Chem. Eng. Data* 15:514-17.

Rafael O. Santos, Ivo G. Compri, Andreia A. Morandim-Giannetti, Ricardo B. Torres, 2011, "Optimization of the Transesterification Reaction in Biodiesel Production and Determination of Density and Viscosity of Biodiesel/Diesel Blends at Several Temperatures", *J. Chem. Eng. Data,* 56:2030–38.

Ramírez-Verduzco L.F., 2013, "Density and viscosity of biodiesel as a function of temperature: Empirical models," *Renewable and sustainable Energy Reviews*, 19:652-55.

SaeidBaroutian, KavehShahbaz, Farouq S. Mjalli, Mohd A. Hashim, Inas M. AlNashef,2012, "Densities and Viscosities of Binary Blends of Methyl Esters + Ethyl Esters and Ternary Blends of Methyl Esters + Ethyl Esters + Diesel Fuel from T = (293.15 to 358.15) K", *J. Chem. Eng. Data.*,57:1387-1395.

Satish Kumar, Yadav J. S., Sharma V. K., Wonsub Lim, Jae Hyun Cho, Junghwan Kim, Il Moon, 2011, "Physicochemical Properties of Jatropha Curcas Biodiesel þ Diesel Fuel No. 2 Binary Mixture at T = (288.15 to 308.15) K and Atmospheric Pressure", *J. Chem. Eng. Data*, 56:497–501.

Spencer, C. F. Danner, R. P. 1972, "Improved equation for prediction of saturated liquid density". *J. Chem. Eng. Data* 17:236–41.

Suriya Phankosol, Kaokanya Sudaprasert, Supathra Lilitchan, Kornkanok Aryusuk, Kanit Krisnangkura, 2014, "Estimation of Density of Biodiesel", *Energy and Fuels*, 28:4633-41.

Tat M.E. and Van Gerpen J.H. 1999, "The kinematic viscosity of biodiesel and its blends with diesel fuel", *Journal of American Oil Chemical Society,* 76:1511-13.

W. Kay, 1936, "Density of hydrocarbon gases and vapors at high temperature and pressure",*Ind.Eng. Chem*.28:1014.

In: Renewable Energy Systems
Editor: Sandip A. Kale
ISBN: 978-1-53610-423-3

Chapter 10

INVESTIGATION ON A LOW HEAT REJECTION ENGINE USING NEEM KERNEL OIL AND ITS METHYL ESTER AS FUEL

Basavaraj M. Shrigiri[1,*], Omprakash D. Hebbal[2] and K. Hema Chandra Reddy[3]

[1]JNT University Anantapur, Andra Pradesh, India
[2]PDA College of Engineering, Kalburgi, Karnataka, India
[3]JNTUA College of Engineering, Anantapur, Andra Pradesh, India

ABSTRACT

The concept of the low heat rejection (LHR) is to suppress the heat rejection to the coolant and recovering this heat energy into useful work. In this study, cylinder head, exhaust and inlet valves of a CI engine are coated with metal matrix composite materials by plasma spray technique. The neem kernel oil is selected as fuel, which has high viscosity, low volatility. Neem kernel oil (NKO) is converted into neem kernel oil methyl ester (NKOME) by transesterification process. Initial investigations are conducted on a single cylinder, water cooled, direct injection, four stroke CI engine without coating using diesel as fuel. Further experiments are conducted on the CI engine for NKO and NKOME with coatings on cylinder head, valves and the results are compared with uncoated engine using diesel as fuel. Reduced brake thermal efficiency and increased brake specific fuel consumption, as well as increased NOx emission along with slight increase in CO, HC and smoke emissions are observed for NKO and NKOME used in coated engine compared with uncoated engine using diesel as fuel. It is observed from the combustion analysis that the cylinder pressure for NKOME in coated engine is near to diesel fuel in normal engine (without coating).

Keywords: Neem kernel oil, Neem kernel oil methyl ester, coated engine, uncoated engine, Emission

*E-mail:bshrigiri@gmail.com.

1. INTRODUCTION

Energy is considered as an important factor for the economic growth, social benefit and industrial development of the country. Since their exploration, the fossil fuels continued as the major source of energy. The decrease in fossil fuels, emissions produced by them and sharp increase in fuel prices make biomass energy sources more attractive. Many of the developed countries have introduced new encouraging policies to bio fuels produced from non-edible vegetable oils in transportation sector. The vegetable oils which are rich in oxygen can be used as alternative fuels for the operation of diesel engine (Senthil Kumar et al. 2001). There are different types of biodiesels available such as sunflower, soyabean, cotton seed, linseed, mahua, jatropha, pongamia etc (Tomasevi AV, et al. 2003). Biodiesel is a fuel that is manufactured from vegetable oils with the help of catalysts, and may be directly used in diesel vehicles with little or no modification (Hanbey Hazar, 2009). When biodiesel is used, HC, CO and PM ratios in exhaust emissions are lower, while sometimes very small NO_x increases occur (Tsolakis A, et al. 2004). Several methods exist for making vegetable oils usable in engines. The most significant is the transesterification method. In this method, vegetable oil is added to a mono hydroxyl alcohol (ethanol, methanol) in the presence of catalyst and the vegetable oil is broken into diesel fuel and glycerine; than that is reacted with triglyceride to form alcohol ester and glycerol (Yamane K, et al. 2001).

The viscosity of vegetable oils is many times higher than that of diesel fuel. The high viscosity is due to the large molecular mass and chemical structure of vegetable oils which in turn leads to problems in pumping, combustion and atomization in the injector systems of a diesel engine. Due to the high viscosity, in long term operation, vegetable oils normally introduce the development of gumming, the formation of injector deposits, ring sticking, as well as incompatibility with conventional lubricating oils (Ryan TW, et al. 1984), (Korus RA, et al. 1985), (Rewolinski C, et al. 1985), (Ziejewski M, et al. 1983), (Pryde EH., 1983). In normal diesel engine, about one third of the total energy is rejected to the cooling water. The basic concept of the low heat rejection engine is to reduce this heat loss to the cooling water and converting the energy in the form of useful work (Stone R, 1989). Various important advantages of the LHR concept are reduced hydrocarbons, fuel economy, carbon monoxide emissions and smoke, reduced noise due to a lower rate of pressure rise and higher energy in the exhaust gases (Gataowski JA., 1990), (Schwarz E et al. 1983), (Bryzik W, et al. 1983), (Dhinnagar SJ, et al. 1992). Within the LHR engine concept, the combustion chamber of a diesel engine is insulated by using high temperature resistant materials on engine components, such as cylinder head, valves, cylinder liners and exhaust ports. By eliminating the need for a conventional cooling system and reducing lost energy, the overall performance of this engine system will drastically improves. This could potentially result in 50% volume and 30% weight reductions in the entire propulsion system (Alkidas AC., 1989). A large number of studies on the performance, structure and durability of the LHR engine have been carried out (Wade.W.R, et al. 1984), (Jaichandra.S, et al. 2003), (Ekrem Buyukkaya, et al. 2006), (Kamo. R, et al. 1999), (Sun.X, et al. 1993). The results of the investigations have been contradictory. Most of them have concluded that insulation reduces heat transfer, improves thermal efficiency and increases energy availability in the exhaust. However, some of the experimental studies have indicated almost no improvement in thermal efficiency and claim that exhaust emissions deteriorate when compared with conventional diesel engines.

In the present work, the tests are conducted with NKO, NKOME and diesel in coated cylinder engine and uncoated engine and then performance, emission and combustion characteristics are compared. LHR engine fueled with neem kernel oil methyl ester, neem kernel oil and normal diesel engine fueled with diesel fuel are referred to by NKOME, NKO and DF, respectively, throughout the chapter.

2. EXPERIMENTAL TEST RIG, INSTRUMENTATION AND PROGRAMME

The engine used in this study is 5.2 kW, computerized Kirloskar make, single cylinder, four stroke, vertical, water cooled, direct injection diesel engine. The important engine specifications are given in Table 1. An eddy current dynamometer is used to load the test engine. Exhaust emission from the engine is measured with help of AVL DiTEST 1000 (Five gas analyzer) and smoke emission is measured with the help of AVL DiSMOKE 480 (Smoke meter).

Table 1. Specification of the test engine

Manufacturer	Kirloskar Oil Engines Ltd., India
Model	TV-SR II, naturally aspirated
Engine	Single cylinder, direct injection diesel engine
Bore/stroke/compression Ratio	87.5 mm/110 mm/ 17.5:1
Rated power	5.2 kW
Speed	1500 rpm, constant
Injection pressure/advance	200 bar/23 degree before TDC
Dynamometer	Eddy current
Type of starting	Manually
Air flow measurement	Air box with ’U’ tube
Exhaust gas temperature	RTD thermocouple
Fuel flow measurement	Burette with digital stopwatch
Governor	Mechanical governing (Centrifugal type)
Sensor response	Piezo electric
Time sampling	4 micro seconds
Resolution crank	1 degree crank angle
Angle sensor	360° encoder with resolution of 1 degree

Table 2. Properties of the test fuels

Properties	Diesel	NKO	NKOME
Calorific value(kJ/kg)	42600	40219	41543
Density (kg/m^3)	0.840	0.930	0.896
Flash point (^{o}C)	51	245	160
Fire point(^{o}C)	57	262	175
Carbon residue (%)	00	1.28	0.399

100% ZrO_2	0.1 mm
50% ZrO_2 + 50% Al_2O_3	0.1 mm
25% ZrO_2 + 75% Al_2O_3	0.1 mm
Bond Coat (Ni-Cr)	0.15mm

Figure 1. Composition of thermal barrier coating.

Crude neem kernel oil is selected for the preparation of biodiesel. 3.5 grams of sodium hydroxide (NaOH) and 200 ml of methyl alcohol (CH_3OH) are used for esterification of 1 liter of neem kernel oil. The catalyst is dissolved in the alcohol then the alcohol-catalyst mixture is poured into the neem kernel oil which is heated and mixed thoroughly. The temperature of the neem kernel oil, alcohol and catalyst mixture is maintained at 60^{o}C for an hour. When the transesterification is finished the mixture is taken into a separating funnel to settle. After the settlement of the biodiesel and the glycerine, the glycerine is drained. The biodiesel is washed thoroughly with pure water to remove alcohol and catalyst residue. After washing, the biodiesel is heated to a temperature of 110^{o}C in order to remove the traces of water in the form of vapours. The properties of the diesel, neem kernel oil and its methyl ester are determined with the help of standard procedures. As can be seen from Table 2, the calorific value of NKOME is lower than that of diesel and other properties are higher than the diesel.

The tests are conducted for variable brake power of 0%, 10% 25%, 50%, 75% and 100% at rated speed. First, diesel fuel is used as fuel in the normal engine. After completion of the test on normal engine, the cylinder head, inlet and exhaust valves are coated with metal matrix composite materials. The metal matrix thermal barrier coating is made of 25% ZrO_2 + 75% Al_2O_3 of 0.1 mm thick, 50% ZrO_2 + 50% Al_2O_3 of 0.1 mm thick and 100% ZrO_2 of 0.1 mm thick by using plasma coating method over the base of Ni-Cr bond coat of 0.150 mm thickness. Figure 1 shows the Composition of thermal barrier coating with dimensions.

Now the engine is converted to a LHR condition (coated). The same test procedure is repeated for LHR engine using NKO and NKOME as fuel and results obtained are compared with that of normal diesel engine fueled with diesel. The data is averaged from 100 consecutive cycles and recorded.

3. Results and Discussions

The main objective of this work is to investigate the performance, emission and combustion characteristics of cylinder head, inlet and exhaust valves coated engine fueled

with NKO and NKOME and uncoated engine fueled with diesel fuel. The results obtained from coated engine are compared with that of uncoated engine.

3.1. Performance Analysis

Important engine performance parameters, such as brake thermal efficiency and brake specific fuel consumption for NKO, NKOME in coated engine are calculated, analyzed and compared with diesel fuel in uncoated engine.

Figure 2 represents the variation of brake thermal efficiency with brake power for NKO, NKOME in coated engine and diesel fuel in uncoated engine. There is a steady increase in brake thermal efficiency as the load increases. At 75% load, the maximum brake thermal efficiency for NKO and NKOME in coated engine is 28.44% and 29.91% respectively against 31.09% of diesel fuel in uncoated engine, which are lower by 8.52% and 3.79% compared to diesel fuel in uncoated engine. The reason for this may be due to higher viscosity and density of these fuels. Reduced combustion efficiency due to poor fuel vaporization and atomization may also lead to lower brake thermal efficiency for NKO and NKOME. From the results it is seen that the brake thermal efficiency of NKOME with coated engine is near to that of diesel fuel in coated engine.

From Figure 3 shows variation of brake specific fuel consumption (BSFC) with brake power for NKO, NKOME in coated engine and diesel fuel in uncoated engine. The BSFC decreases as load increases. The BSFC of NKO and NKOME in coated engine is higher compared to diesel fuel in uncoated engine for the entire load range. The reason may be differences in heating values and density difference between NKO, NKOME and diesel fuel. At rated load, the BSFC of NKO, NKOME in coated engine and diesel fuel in uncoated engine is 0.33, 0.3 and 0.28 kg/kW-h respectively, which are higher by 17.85% and 7.14% respectively compared to diesel fuel in uncoated engine.

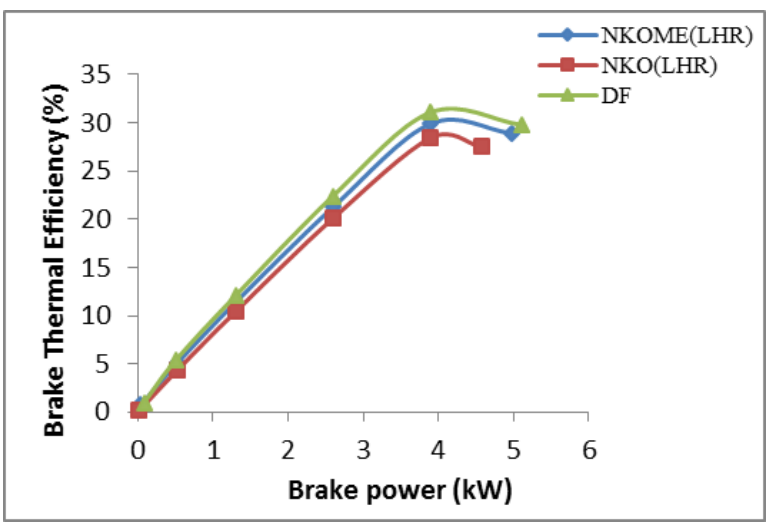

Figure 2. Variation of brake thermal efficiency with brake power.

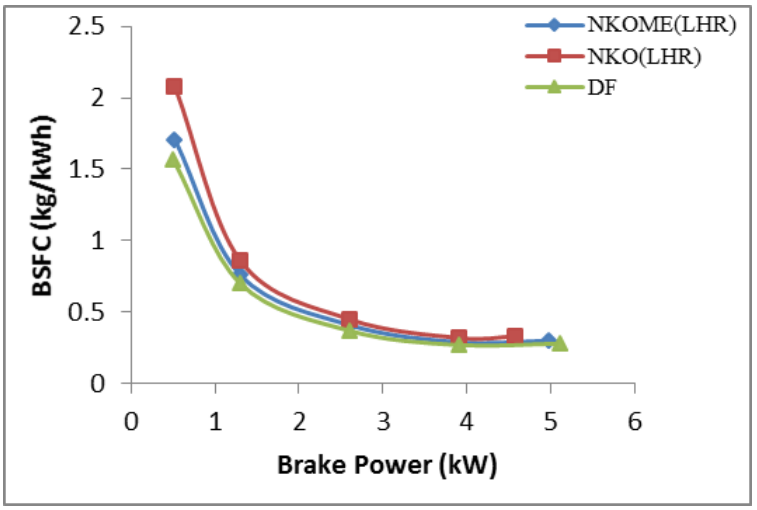

Figure 3. Variation of BSFC with brake power.

3.2. Emission Analysis

Figure 4 shows the variation of exhaust gas temperature (EGT) with brake power for NKO, NKOME in coated engine and diesel fuel in uncoated engine. The EGT is higher in coated engine compared with uncoated engine. Coating of cylinder head and valves reduces the heat loss to the cooling water, hence leads to increase in EGT. At full load, the EGT for NKO and NKOME in coated engine is 529.1^{o}C and 508.25^{o}C respectively, against 449.76^{o}C of diesel fuel in uncoated engine, which are 17.64% and 13% greater than that of diesel fuel in uncoated engine.

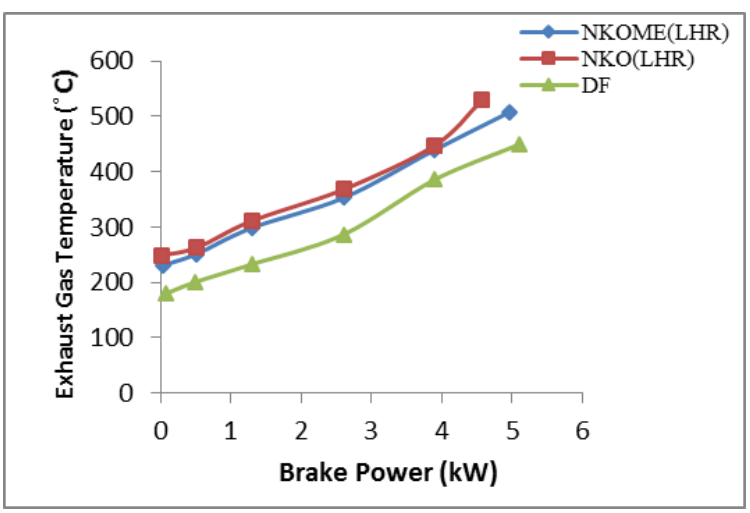

Figure 4. Variation of EGT with brake power.

Figure 5 shows the variation of carbon monoxide (CO) with brake power for NKO, NKOME in coated engine and diesel fuel in uncoated engine. The CO emission for NKO and NKOME in coated engine is higher than diesel fuel in uncoated engine. This is due to higher viscosity of these fuels. From the graph, it is clear that up to 50% of the load, the CO emissions for NKOME in coated engine are close to diesel fuel in uncoated engine. At peak load, the CO emissions for NKO and NKOME in coated engine are 0.63% and 0.42% respectively compared to 0.26% of diesel fuel in uncoated engine.

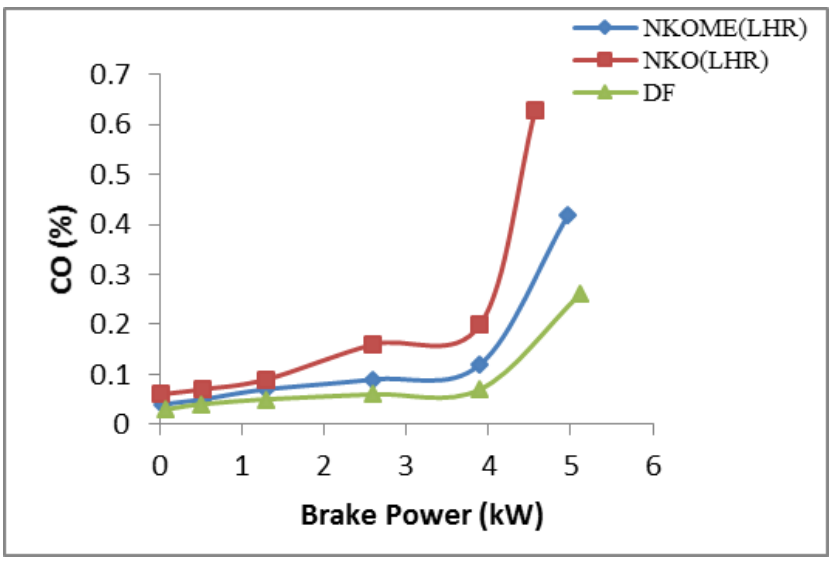

Figure 5. Variation of CO with brake power.

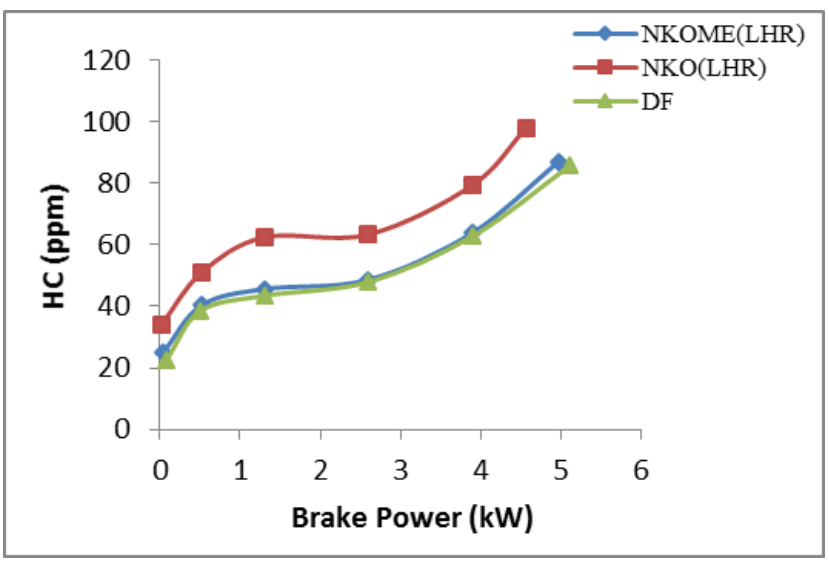

Figure 6. Variation of Hydrocarbon with brake power.

Figure 6 shows the variation of unburnt hydrocarbons (UHC) with brake power for NKO, NKOME in coated engine and diesel fuel in uncoated engine. The main reason for the production of hydrocarbons is the incomplete combustion. UHC emissions for NKO and NKOME in coated engine are higher than diesel fuel in uncoated engine for entire load range. The effects of higher viscosity and density on fuel spray quality could be expected to generate higher hydrocarbon emissions with NKO and NKOME. At full load, the UHC emissions for coated engine with NKO and NKOME are 98.01 ppm and 86.99 ppm respectively, against 85.65% of diesel fuel in uncoated engine, which are higher by 14.43% and 1.56% compared to diesel fuel in uncoated engine. From the graph, it is also observed that, the UHC emissions with NKOME in coated engine is very close to diesel fuel in uncoated engine.

Figure 7 shows the variation of oxides of nitrogen (NO_x) with brake power for NKO, NKOME in coated engine and diesel fuel in uncoated engine. The oxides of nitrogen are produced due to the oxidation of atmospheric nitrogen. The chemical reactions, which yield to the formation of NO_x, are governed by availability of oxygen and higher temperature. The NO_x emissions for NKO and NKOME in coated engine are higher than diesel fuel in uncoated engine. The reason for this could be associated with oxygen content present in NKO and NKOME, as the oxygen present in the fuels may provide supplementary oxygen for the formation of NO_x. However, up to 25% of the load, the oxides of nitrogen for NKOME in coated engine is near to that of diesel fuel in uncoated engine. At rated load, the NO_x levels for NKO and NKOME in coated engine are 723.10 ppm and 663.13 ppm respectively against 622.15 ppm of diesel fuel in uncoated engine, which are higher by 16.22% and 6.58% respectively compared to diesel fuel in uncoated engine.

Figure 8 shows the variation of smoke opacity with brake power for NKO, NKOME in coated engine and diesel fuel in uncoated engine. The smoke emissions in coated engine for NKO and NKOME are higher compared to DF in uncoated engine. This is due to higher viscosity and poor atomization. At full load, the smoke emissions for NKO and NKOME in coated engine are 98.35% and 94.99% respectively compared to 90.9% of diesel fuel in uncoated engine, which are higher by 8.19% and 4.49% against DF in uncoated engine.

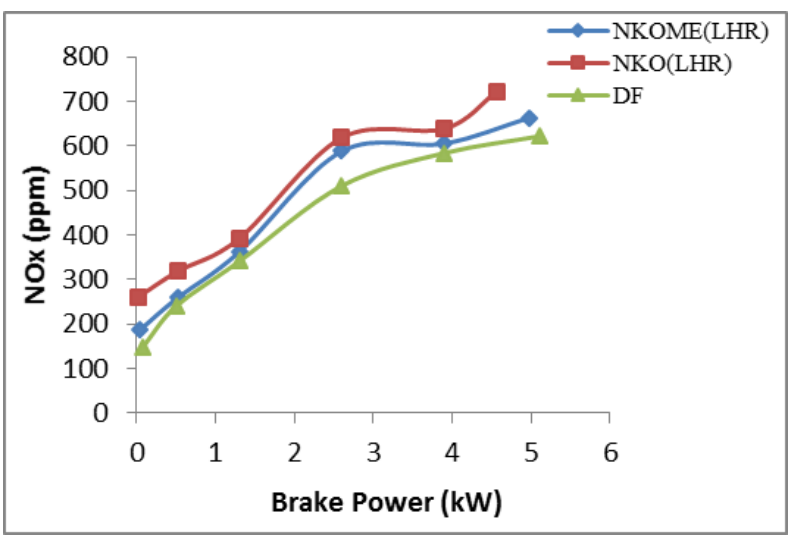

Figure 7. Variation of NOx with brake power.

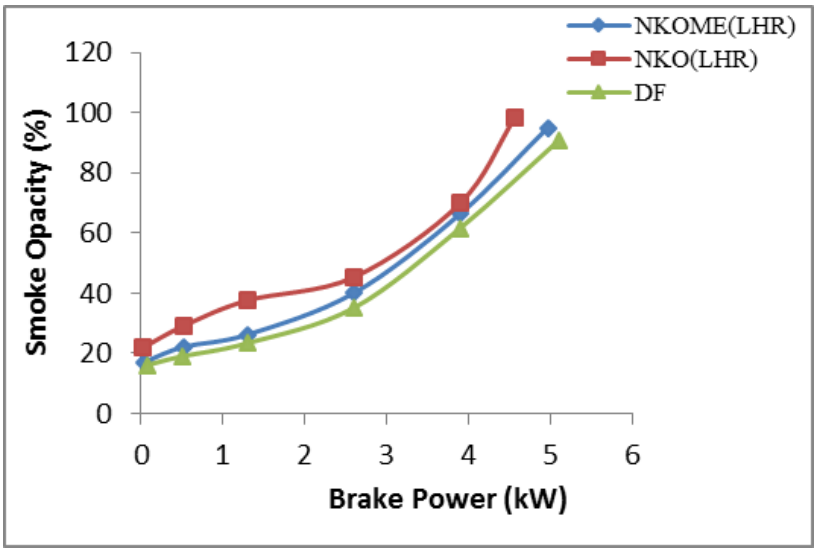

Figure 8. Variation of smoke opacity with brake power.

3.3. Combustion Analysis

For combustion analysis, the data are taken by averaging 100 cycles at 75% load.

Figure 9 shows the variation of cylinder pressure with crank angle for NKO, NKOME in coated engine and DF in uncoated engine. The cylinder pressure for NKO and NKOME in coated engine is lower than DF in uncoated engine. This is due to the higher viscosity and lower calorific values of these fuels. At 75% load, the cylinder pressure for NKO and NKOME in coated engine is 60.86 bar and 57.8 bar respectively against 61.42 bar of DF in uncoated engine. From the results, it is observed that, the cylinder pressure for NKOME with coated engine is very close to DF in uncoated engine.

Figure 10 shows variation of net heat release rate (NHRR) with crank angle for NKOME, NKO in coated engine and DF on uncoated engine at 75% load. The NHRR for NKO and NKOME in coated engine is lower compared to DF in uncoated engine. The reason for this could be lower calorific values of these fuels. The premixed combustion phase with NKO and NKOME in coated engine is shorter compared to diesel fuel in uncoated engine, this has resulted in lower heat release rate. This is the reason for lower brake thermal efficiency with NKO and NKOME in coated engine. At 75% load, the NHRR values for NKO and NKOME in coated engine are 26.99 J/^{o}CA and 28.16 J/^{o}CA respectively against 33.31 J/^{o}CA of diesel fuel in uncoated engine, which are lower by 18.97% and 15.46% compared to diesel fuel in uncoated engine.

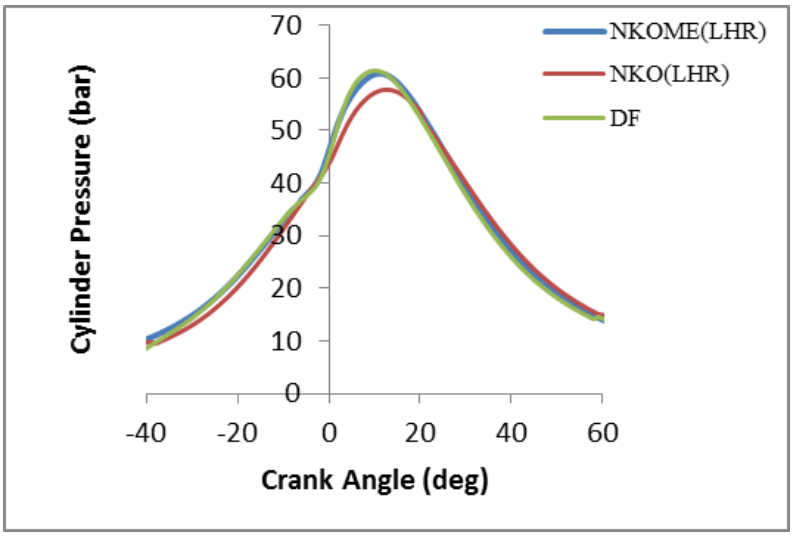

Figure 9. Variation of cylinder pressure with crank angle.

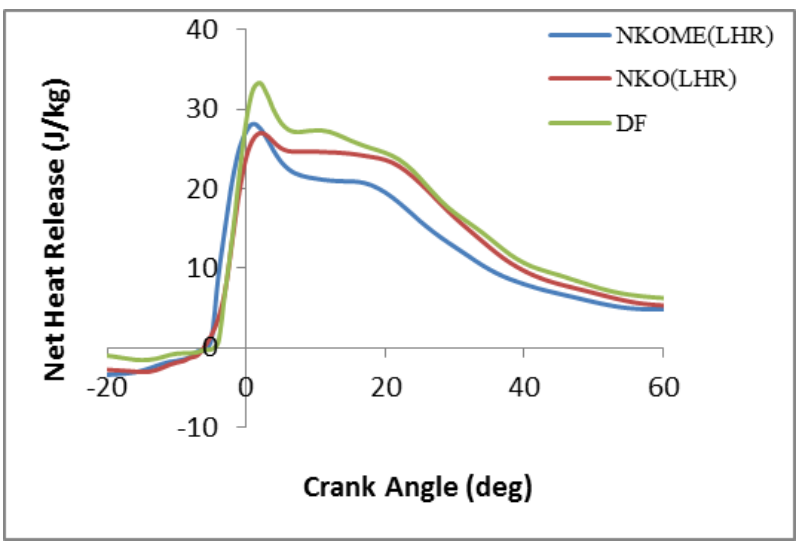

Figure 10. Variation of heat release rate with crank angle.

Figure 11 shows variation of rate of pressure rise with crank angle for NKOME, NKO in coated engine and DF on uncoated engine at 75% load. The rate of pressure rise is generally used as a measure of combustion generated noise. The rate of pressure rise for NKO and NKOME in coated engine is lower compared to diesel fuel in uncoated engine. The reason could be the higher viscosity and lower volatility of these fuels. The maximum rate of pressure rise for NKO and NKOME in coated engine is 2.4 bar/^{o}CA and 2.78 bar/^{o}CA respectively, against 3.04 bar/^{o}CA of diesel fuel in uncoated engine, which are lower by 21.05% and 8.55% compared to diesel fuel in uncoated engine.

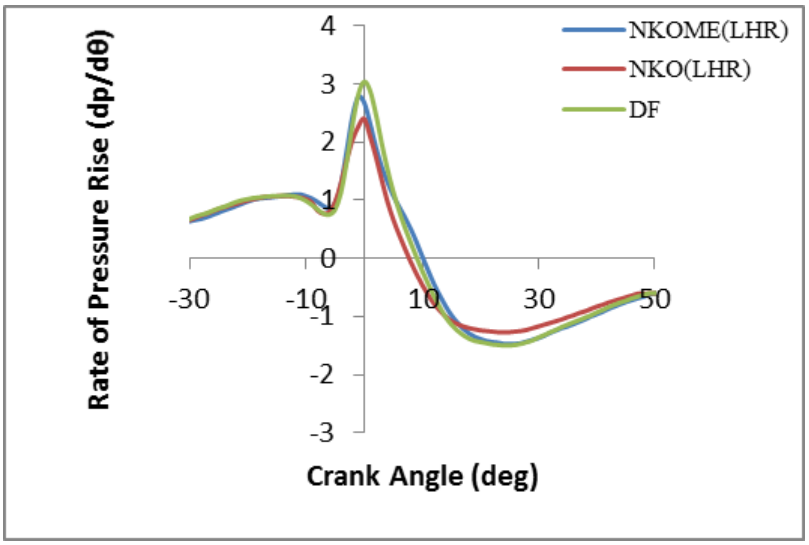

Figure 11. Variation of Rate of pressure rise with crank angle.

CONCLUSION

In the present work, experimental investigations have been conducted on coated and uncoated CI engines using NKO, NKOME and DF. The coated engine using NKO and NKOME are analyzed and compared with that of DF in uncoated engine. The conclusions are summarized as follows.

- Compared with NKO operation, NKOME resulted in better performance in coated engine. However, compared with diesel fuel in uncoated engine, the performance of the coated engine with NKOME is observed to be lower. The brake thermal efficiency values of NKO, NKOME in coated engine are lower than DF in uncoated engine by 8.52% and 3.79%.
- At full load, the BSFC values of NKO and NKOME in coated engine are higher compared to DF in uncoated engine by 17.85% and 7.14%.
- The EGT for NKO and NKOME in coated engine are higher compared to that of diesel fuel in uncoated engine by 13% and 17.14%.
- The unburnt hydrocarbon emission for NKOME in coated engine is 1.56% higher than diesel fuel in uncoated engine, whereas HC emission for NKO is 14.43% higher than DF.
- The CO emissions for NKO and NKOME in coated engine are higher than that of diesel fuel in uncoated engine at all the loads and this could be due viscosity effects of these fuels.
- The oxides of nitrogen emission for NKO and NKOME in coated engine are higher by 16.22% and 6.58% compared to diesel fuel in uncoated engine.

- Smoke emissions at full load with NKO and NKOME in coated engine are 98.35% and 94.99% respectively, whereas the smoke level in 90.9% for diesel fuel in uncoated engine.
- The cylinder pressure for NKOME in coated engine is very close to that of diesel fuel in uncoated engine and for NKO, it is 5.89% less than that of DF in uncoated engine.
- Lower heat release rates are observed with NKO and NKOME in coated engine during premixed combustion compared to diesel fuel in uncoated engine.
- The rate of pressure rise for NKO and NKOME in coated engine and diesel fuel in uncoated engine are 2.4 bar/^{o}CA and 2.78 bar/^{o}CA respectively, against 3.04 bar/^{o}CA of DF in uncoated engine, which are lower by 21.05% and 8.55% compared to diesel fuel.

On the whole, it is observed that, the coated engine operation with NKOME and NKO resulted in reduced brake thermal efficiency and increase BSFC compared with DF in uncoated engine. NO_x emissions are higher due to higher temperatures. The overall performance of the coated engine is relatively better with NKOME compared with NKO but lower compared with DF in uncoated engine.

The above comparative study clearly reveals the possibility of using the biodiesel in LHR direct injection diesel engine. The combustion, performance and emission characteristics show the suitability of using neem kernel oil methyl ester in coated CI engine.

ACKNOWLEDGMENTS

The authors thank the faculty and staff of I.C Engine laboratory, Mechanical engineering department, PDA College of Engineering, Kalaburagi, Karnataka, India for help in conducting experiment.

REFERENCES

Alkidas AC., (1989), Performance and Emissions Achievements with an Uncooled Heavy-Duty Single- Cylinder Diesel Engine, SAE Technical Paper. No. 890144.

Bryzik W, Kamo R., (1983), TACOM/Cummins adiabatic engine program, SAE paper No. 830314.

Dhinnagar SJ, Nagalinga B, Gopalakrishnan, K V., (1992), Spark assisted Diesel operation in a low compression ratio low heat rejection engine, SAE paper No. 920245.

Ekrem Buyukkaya, Tahsin Engin and Muhammet Cerit., (2006), Effects of thermal barrier coating on gas emissions and Performance of a LHR engine with different injection timings and valve adjustments, *Energy Conversion and Management*, vol. 47, pp. 1298-1310.

Gataowski JA., (1990), Evaluation of a selectively-cooled single cylinder 0.5-1 Diesel engine, SAE paper No. 900693.

Hanbey Hazar, (2009), Effects of biodiesel on low heat loss diesel engine, *Renewable Energy*, vol. 34, pp. 1533-1537.

Jaichandra.S and Tamil Porai.P, (2003), Low Heat Rejection Engines – An Overview, SAE paper No. 2003 – 01 – 0405.

Kamo. R, Kamo.L.S, Bryzik.W, Schwarz.E.E and Mavinhally.N.S., (1999), Injection characteristics that improve performance of ceramic-coated diesel engines. SAE paper 1999-01-0972.

Korus RA, Jaiduk J, Peterson CL., (1985), A rapid engine test to measure injector fouling in diesel engines using vegetable oil fuels, *Journal of American Oil Chemists' Society vol.* 62, no. 11, pp.1563–64.

Pryde EH., (1983), Vegetable oil as diesel fuels: overview. Papers from the symposium on vegetable oils as diesel fuels, presented at the 73rd AOCS annual meeting, Toronto, Canada. *Journal of American Oil Chemists'* Society vol. 60, no.8, pp.1557.

Rewolinski C, Shaffer DL., (1985), Sunflower oil diesel fuel: lubrication system contamination, *Journal of the American Oil Chemists'* Society vol. 61, no. 7, pp.1120–4.

Ryan TW, Dodge LG, Callahan TJ., (1984), The effects of vegetable oil properties on injection and combustion in two different diesel engines, *Journal of American Oil Chemists'* Society vol.61, no. 10, pp.1610–9.

Schwarz E, Reid M, Bryzik W, Danielson E., (1993), Combustion and performance Characteristics of a low heat rejection engine, SAE Technical Paper No. 930988.

Senthil Kumar, M Ramesh, Nagalingam B, (2001), Experimental Investigations on jatropha oil – Methanol dual fuel in CI engine. SAE 200–0–10153, pp.1-7.

Stone R, (1989), Motor vehicle fuel economy, Middlesex (England) Macmillan Education Ltd.

Sun.X, Wang.W.G, Lyons.D.W and Gao.X, (1993), Experimental analysis and performance improvement of single cylinder direct injection turbocharged low heat rejection engine. SAE paper 930989.

Tomasevi AV, Marinkovic S S, (2003), Methanolysis of used frying oil, *Fuel Processing Technolog*y, vol. 81. no 1. pp.1-6.

Tsolakis A, Megarities A., (2004), Exhaust gas assisted reforming of rapeseed methyl ester for reduced exhaust emission of CI engines, *Biomass Energy*, vol. 27, pp. 493-505.

Wade.W.R, Harstad.P.H, Ounsted.E.J, Trinkler.F.H and Garwin.I.J., (1984), Fuel Economy *Opportunities with an Uncooled DI Diesel Engine*, C432, /Mech E/ SAE pp. 11 – 24.

Yamane K, Ueta A, Shima Y., (2001), Influence of physical and chemical properties of biodiesel fuels on injection, combustion and exhaust emission characteristics in a direct injection compression ignition engine, *International Journal of Engine Research*, vol. 2, no. 4, pp. 249-261.

Ziejewski M, Kaufman KR., (1983), Laboratory endurance test of a sunflower oil blend in a diesel engine, *Journal of American Oil Chemists' Society*, vol. 60, no. 8, pp.1567–73.

In: Renewable Energy Systems
Editor: Sandip A. Kale
ISBN: 978-1-53610-423-3

Chapter 11

RENEWABLE ENERGY CONVERSION AND WASTE HEAT RECOVERY USING ORGANIC RANKINE CYCLES

Alberto Benato[1,2,*], Anna Stoppato[2] and Alberto Mirandola[2]

[1]Giorgio Levi Cases Interdepartmental Centre for Energy Economics and Technology, University of Padova, Padova, Italy
[2]Department of Industrial Engineering, University of Padova, Padova, Italy

ABSTRACT

The world energy balance could be remarkably improved by increasing the use of renewable sources and recovering waste heat released by several industrial processes. In this scenario, an important contribution can be offered by the use of Organic Rankine Cycles (ORCs), particularly when dealing with medium and low temperature heat sources. For this reason, in the present chapter a literature survey analyzes the research and technical activities performed by many scientists and researchers throughout the world in this field with the aim of evaluating the present state of the art and the future developments. Many different technologies have been presented, depending on the kind and nature of the energy source, its availability within the various contexts and its characteristics (temperature level, etc.). The ORCs coupled with solar energy collectors, geothermal sources, ocean thermal energy, biomass exploitation plants through firing, gasification or anaerobic digestion, heat recovery systems, etc., have been presented and discussed. As a result of this survey, it is possible to conclude that ORCs are worth to be used whenever a medium and low temperature heat source is available and can be recovered to get mechanical (electrical) energy and/or thermal energy for suitable applications.

Keywords: Organic Rankine Cycle, waste heat recovery, renewable energy sources

*E-mail: alberto.benato@unipd.it.

1. INTRODUCTION

The increasing concern about energy resources availability and pollution problems, have forced the international administrations to adopt stringent environmental protection measures and energy efficiency policies. The first international agreement was the Kyoto Protocol but, since the 1990s, the European Commission released Directives devoted to the energy sector liberalization, the environmental protection, the operators' competition and the renewable sources' progressive deployment. One of the most important packages was released in March 2007, and is called European "20-20-20" Climate and Energy package. It defines targets of primary energy consumption and Greenhouse Gases (GHG) reduction (European Parliament and Council of the European Union, 2009). The three ambitious targets for 2020 set in the Directive are: a 20% reduction in EU greenhouse gas emissions from 1990 levels, an increase of EU energy consumption produced from renewable resources by 20% and a 20% improvement in the EU's energy efficiency. Obviously, as outlined by Helm (Helm, 2014), in order to fulfill these targets, it is fundamental to introduce the following modifications in the current energy systems:

- Reduce buildings and industries energy consumption.
- Generate heat and power through renewable sources.
- Shift from fossil fuels to electricity in the transportation sector.
- Reinforce grids capacity and interconnections.
- Develop energy storage technologies.
- Exploit waste heat.
- Spread cogeneration technologies.

To this purpose, government incentives for wind, solar, biomass, electric vehicles, waste heat recovery units and systems energy efficiency have been established.

Although remarkable contribution to the electricity production is expected to be provided by wind and solar power, the efficient conversion of medium and low temperature heat into electricity is also going to play a key role in the future energy scenario. On account of this, several technologies have been developed to convert low and medium temperature heat sources into electricity, each one with its advantages, drawbacks and scale of application.

The steam Rankine cycle (SRC) is probably the most widespread cycle, while Organic Rankine Cycles (ORC) and Air Bottoming Cycles (ABC) are mature alternatives that can easily compete with SRC in medium and small scale plants. Maloney and Robertson cycle, Kalina cycle, Uehara cycle, trilateral flash cycle (TFC) and supercritical CO_2 cycle are really promising technologies and can become competitive alternatives in the next future.

The *Steam Rankine Cycle* is the most common waste heat recovery method. It is a mature technology, commonly used in large and medium scale power plants, where high efficiency can be achieved and effective abatement of polluting emissions have been set up. In fact, water/steam cycles can reach very high pressure and temperature: in the big size steam power plants, fed by fossil fuels, the pressure at the turbine inlet can approach or go beyond the critical value and the temperature can reach 500°-600°C, so bringing high efficiency. The main SRC's drawback is its complexity that makes it both bulky and heavy due to the need of

an evaporator and a condenser. These disadvantages are related to the use of water as working fluid.

When dealing with medium and low temperature sources, the technical problems encountered with water can be overcome by selecting appropriate fluids, i.e., organic fluids such as refrigerants or hydrocarbons. In this case the cycle is called *Organic Rankine Cycle* and presently is the most valid alternative to the conventional SRC for the conversion of medium and low temperature heat into electricity.

Organic Rankine Cycles have been investigated since the 1880s but they have never been popular until today's growing interest on converting medium and low grade energy sources.

The organic and the steam Rankine cycle are similar and fundamentally made up by the same devices. However, the ORC unit design is a complicated task because the heat source (HS) type and its temperature, which can vary from high to low temperatures (e.g., 80°< T< 500°C) significantly influences the working fluid (WF) choice which in turn determines the configuration, the performance and the economy of the plant (Tchanche et al., 2010).

The *Air Bottoming Cycle* (ABC) turbo generator is another valuable alternative to the conventional SRC due to its low weight and high compactness.

The simplest ABC configuration was patented by Farrell (Farrell, 1988), and is composed by an air compressor, a heat exchanger and an air turbine. This cycle uses the same principle as the well-known Brayton cycle but the combustion chamber is replaced by a gas to gas heat exchanger where air is heated up by e.g., the exhaust gases of a biomass boiler or a gas turbine. The ABC is considered a viable method to exploit medium and low temperature heat sources because it employs a non-toxic and non-flammable working fluid. Additionally, being ABC an open cycle, it does not require a condenser; a fact that assures high compactness and low weight.

In literature extensive investigations can be found about a large variety of ABC configurations (Ghazikhani et al., 2011) or steady-state and dynamic behavior (Benato et al., 2014) of ABC units. Also the selection of the heat exchanger's type is the object of numerous researches. In fact, the heat exchanger configuration and its dimensions are parameters that influence its ability to transfer heat, the efficiency and the performance of the whole system.

As said, SRC, ORC and ABC are well known technologies but, in literature, other power cycles have been presented for the exploitation of low-temperature heat sources.

In 1953, Maloney and Robertson were the first to propose a modified Rankine cycle (called *Maloney and Robertson cycle*) which employs a binary mixture of water and ammonia as working fluid and includes a flash tank (Maloney and Robertson, 1953). The first investigations did not show satisfactory results; therefore, the cycle was abandoned. However, in the 1980s, improved configurations were proposed and studied. But as previously, the comparison between the Maloney and Robertson cycle and the Rankine one demonstrated no advantages. Therefore, again, the investigations were stopped and the cycle abandoned.

In the same period, the early 1980s, Alexander Kalina developed a new family of thermodynamic cycles in which an ammonia-water mixture is used as working fluid. In 1982, the so called "*Kalina Cycle*" was patented (Kalina, 1982). As remarked by Zhang et al., 2012, the Kalina cycle constitutes the most important upgrade in thermal power plant design since the advent of the Rankine cycle. This cycle improves the efficiency of thermal power plants by 15% to 50% depending on the particular application.

In literature, several layouts of the Kalina cycle can be found but it is basically a "modified" Rankine cycle. In practice, to transform a Rankine cycle into a Kalina one it is

only necessary to design a system able to exploit the virtues of the ammonia-water mixture. For a detailed review of the Kalina cycle working principle, configurations and applications see e.g., (Zhang et al., 2012).

An improved version of the Kalina cycle is the *Uehara cycle* (Uehara et al., 1994). This cycle includes a separator, a diffuser, an after condenser, two turbines, two regenerators and two mixing units. The system is very complex in comparison to other cycles but for ocean thermal energy conversion it showed a thermal efficiency 10% and 30% higher than Kalina and Rankine cycle respectively. More details about the cycle are available, for example, on (Uehara et al., 1999).

Trilateral flash cycle (TFC) and *Supercritical CO_2* cycle are other innovative methods proposed and under development to recover waste heat from medium and low temperature heat sources.

Trilateral flash cycle is a power recovery system from single-phase low-grade heat sources. The TFC system can produce outputs of up to 80% more than simple Ranking cycle systems in the recovery of power from hot liquid streams in the temperature range from 100°C to 200°C. The estimated cost per unit net power output is approximately equal to that of Rankine cycle systems and the preferred working fluids are light hydrocarbons. For more details about this cycle see i.e., (Smith, 1993; Smith and Da Silva, 1994).

Yang et al., 2013 proposed two types of supercritical CO_2 Rankine cycles with and without internal heat exchanger to recover medium and low temperature industrial heat. Kim et al., 2012, analyzed transcritical/supercritical CO_2 cycles using both low- and high-temperature heat sources, while Yamaguchi et al., 2006, analyzed a solar energy powered Rankine cycle using supercritical CO_2 for combined production of electricity and thermal energy. A design optimization of supercritical CO_2 power cycle using genetic algorithm and artificial neural network is performed by Wang et al., 2010.

Kalina Cycle, Trilateral flash cycle and Supercritical CO_2 cycle are really innovative and promising cycles but, at the moment, they are not commercially available and only prototypes are under development. On the contrary, Steam Rankine cycle, Organic Rankine cycle and Air Bottoming Cycle are established and commercially available technologies.

Until now, the spread of medium and low temperature waste heat recovery units (WHRUs) has been limited by the high initial investment cost which in turn results in poor economic revenue and high payback times (Quoilin et al., 2011b).

However, despite the relatively high investment costs, ORCs are more suitable than conventional steam cycles and air bottoming cycles to decrease the buildings and industries energy intensity, mainly by recovering waste heat, supplying heat and power, or converting renewable heat sources into electricity.

For these reasons ORCs are studied and used to recover heat from sun's radiation, ocean warm layers, geothermal systems, biomass and industrial processes.

In this chapter, an overview of the different ORC applications related to the exploitation of renewable energy sources is presented. Firstly, an analysis of the Organic Rankine Cycle technology is provided in order to underline its advantages and drawbacks. After that, the state of the art of ORCs recovering the heat of renewable energy sources or wasted by other processes is presented. Finally, some conclusion remarks are given.

2. THE ORC TECHNOLOGY

The steam Rankine cycle and the Organic Rankine Cycle are conceptually similar because they are both based on the vaporization of a high pressure liquid which is then expanded to a lower pressure thus releasing mechanical power (Quoilin et al., 2013). The expanded fluid is then condensed and pumped back to the evaporator. Therefore, the SRC and the ORC main components are similar too: a boiler, a pump, an expander (or a turbine) and a condenser. However, in the SRC the working fluid is water while ORCs use organic compounds characterized by a lower boiling temperature than water.

In fact, water guarantees numerous advantages in many cases (Tchanche et al., 2011):

- Good thermal and chemical stability: there is no risk of thermo chemical decomposition of the fluid.
- Low viscosity: the required pumping work is really small.
- Good energy carrier: the latent and specific heat are high.
- No toxicity.
- No inflammability.
- Zero Ozone Depletion Potential (ODP).
- Zero Global Warming Potential (GWP).
- Abundant availability and cheapness.

but also drawbacks (Wali, 1980):

- Water is a "wet" fluid which means that the saturated vapor curve has a negative slope.
- High evaporating pressure.
- Need of superheating: the fluid superheating is needed to prevent condensation during the expansion process; phenomenon that causes erosion in turbine blades.
- Complex and expensive expander devices.

For these reasons, using water as working medium is mainly suitable in large power plants fed by fossil fuels where water/steam offers higher pressure ratios and better heat transfer properties than other fluids.

As said, the ORC unit is fundamentally made up by the same devices as a conventional steam power module but for medium and low temperature heat sources it is characterized by simple structure, high reliability and easy maintenance.

Obviously, the heat source type and temperature considerably influences the working fluid choice which in turn determines the plant configuration, performance and economy. To this purpose, an in-depth review of the possible working fluid candidates and plant configurations is presented before analyzing the different heat sources suitable for ORC applications.

2.1. Fluid Selection

The fluid selection is a complicated task for two reasons (Bao and Zhao, 2013):

- The heat source type and the working conditions vary widely: from low-temperature to high-temperature heat sources (e.g., 80°< T < 500°C).
- Hundreds of substances can be employed as working fluids: alcohols, aldehydes, amines, chlorofluorocarbons (CFC), hydrocarbons (HC), hydro-chlorofluorocarbons (HCFC), hydro-fluorocarbons (HFC), hydrofluoroethers (HFE), ethers, per-fluorocarbons (PFC), siloxanes, zeotropic and azeotropic mixtures and inorganic fluids.

However, the working fluids can be categorized according to the saturation vapor curve. The curves' type is one of the crucial characteristics. It affects the fluid applicability, the cycle efficiency, and the arrangement of power equipment (Hung, 2001).

There are three types of vapor saturation curves in the Temperature-entropy (T-s) diagram:

- "Dry" fluid with positive saturated vapor curve (i.e., cyclohexane).
- "Wet" fluid with negative saturated vapor curve (e.g., water).
- "Isentropic" fluid with a nearly vertical slope (i.e., R141b).

The dome of a dry, a wet and an isentropic fluid is depicted in Figure 1.

With isentropic and dry fluids, the superheating is not needed given that the fluid remains saturated or superheated at the turbine outlet section, respectively. The persistent saturation or superheating throughout the expansion process avoids the concerns of impingement of liquid droplets on the expander blades. Consequently, the superheating apparatus is not needed. Therefore, the working fluids with dry or isentropic saturation curves are more adequate for ORC systems than wet fluids. A drawback of this aspect is that the expanded vapor leaves the turbine still superheated, and this heat needs to be dissipated in the condenser. In this manner, the plant efficiency is reduced.

To mitigate this aspect a recuperator is usually inserted to increase the cycle efficiency; as a consequence, the initial investment and the plant complexity are increased.

In general, the method adopted for the selection of a generic working fluid in ORC applications is the so called "screening method." It is the most implemented method and consists in building a steady-state simulation model of the ORC cycle and running it with different working fluids.

In literature, numerous studies present optimization tools able to select the most appropriate working medium for given objective functions and different heat sources. Several examples are presented in (Quoilin et al., 2011a; Quoilin, 2011b; Tchanche et al., 2014; Branchini et al., 2013; Cavazzini and Dal Toso, 2015; Pezzuolo et al., 2016). The candidate fluids can be both a pure fluid and a mixture.

Several researchers proposed pure fluids as working medium (for a clear overview see (Bao and Zhao, 2013)) but the adoption of these fluids has a drawback: the evaporation and condensation processes occur isothermally. Therefore, the heat source and the sink

temperature profiles cannot be approached closely by the organic fluid ones in the evaporator and condenser units, leading to large irreversibility especially with medium and low temperature heat sources (Chys et al., 2012).

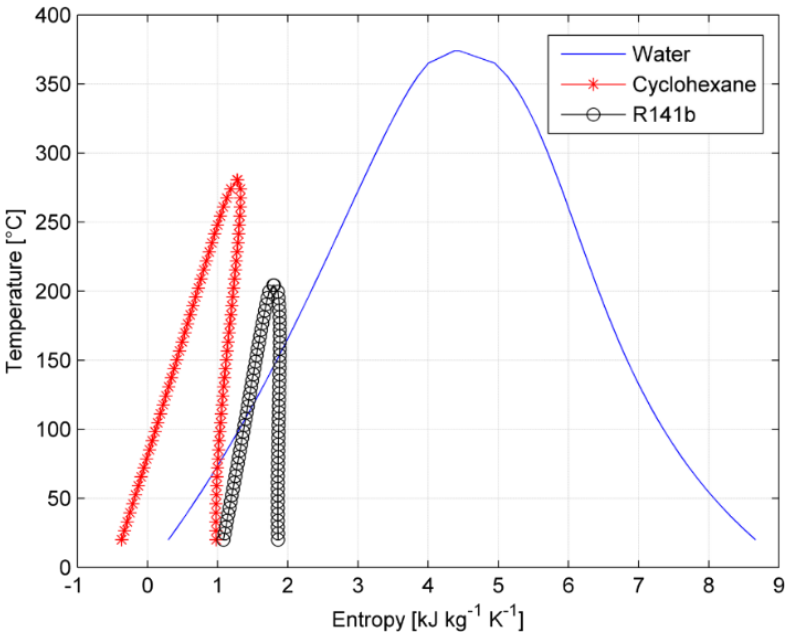

Figure 1. T-S diagram of a wet (Water), an isentropic (R141b) and a dry (Cyclohexane) fluid.

To partially solve this problem, other researchers proposed the use of mixtures with properly chosen components. Note that azeotropic mixtures have isothermal phase transitions (similar to pure fluids) while the zeotropic ones are characterized by non-isothermal phase transitions at constant pressure. Therefore, the zeotropic mixtures are able to follow the profile of the heat source due to their variable evaporation/condensation temperature profile.

Usually, the method developed by Venkatarathnam and Timmerhaus, 2008, is adopted to select the mixture components.

As discussed in (Chys et al., 2012), the method was developed for cryogenic refrigerants but it is also applicable to other fluids. A brief description of the method is given below.

The first requirement is that the first mixture component is volatile at 1-1.5 bar. In this manner, low temperatures can be obtained after the expansion process without the need to reach vacuum pressures. The second requirement is that the boiling point of the second component exceeds both the desired average condensation temperature and the boiling point of the first component. As underlined in (Chys et al., 2012), by adding a component with higher boiling point, more heat can be absorbed per unit of fluid mass. Hence, the ORC medium mass flow rate can be lower.

Despite their usefulness, in literature only few works addressing the selection and the use of mixtures as working fluid have been published. For a clear review see, for example (Chys et al., 2012; Bao and Zhao, 2014).

Even though in the scientific literature a broad range of working fluids is analysed, only few are actually employed in commercial ORC plants (Quoilin, 2011a): R134a, R245fa, N-pentane, Solkatherm, OMTS and Toluene.

In conclusion, the candidate working fluid for ORC applications must have not only suitable thermophysical properties but also safety requirements and acceptable costs. This means that there is not a working fluid suitable for any ORC system but the characteristics that can be expected from a good candidate can be summarised as:

- Vapor saturation curve with zero o positive slope → isentropic or dry fluids → the limitation of the vapor quality at the end of the expansion process disappears and there is no need to superheat the vapor before the turbine inlet section.
- High latent heat of vaporization → small equipment.
- High molecular weight → organic fluids are characterized by higher molecular weight than water. This fact increases the fluid mass flow rate for the same sizes of the expander and gives better turbine efficiencies and less turbine losses.
- Appropriate critical temperature → from 100°C to 200°C.
- Appropriate boiling temperature → from 0°C to 100°C.
- Good heat transfer properties → low viscosity and high thermal conductivity.
- High thermal and chemical stability.
- Acceptable materials compatibility → non-corrosive fluids.
- High thermodynamic performance.
- Low environmental impact → low ODP and GWP.
- Acceptable safety characteristics →non-flammable and non-toxic fluids.
- Good availability and low cost.

2.2. Plant Architecture

Different heat sources require different working fluids but also different plant configurations. To this purpose, several researchers have developed different plant layouts. In the list below, the most analyzed configurations have been reported and, subsequently, described.

- Basic Scheme.
- Recuperative configuration.
- Two-stage plant.
- Regenerative and recuperative architecture.
- Dual pressure levels.
- Dual fluid scheme.

The ORC basic scheme and the recuperative configuration are shown in Figure 2 and 3 while the two-stage ORC architecture and the regenerative and recuperative cycle are depicted in Figure 4 and 5. Finally, the dual pressure levels scheme and the dual fluid architecture are depicted in Figure 6 and 7.

In the *ORC basic scheme* (Figure 2) the heat source fluid flows into the Main Heat Exchanger (MHE), where it transfers the heat to the ORC working fluid. The MHE is used to preheat, evaporate and, if needed, superheat the working medium. In order to design a compact and not heavy ORC plant, the MHE is a once-through boiler or a reboiler. The high pressure WF vapor evolves in the expander device (EXP) and then enters the condenser (COND) as dry or slightly wet vapor. At the condenser outlet section, the WF is in liquid state and low pressure. The feed pump (FP) increases the fluid pressure and the cycle loop starts again.

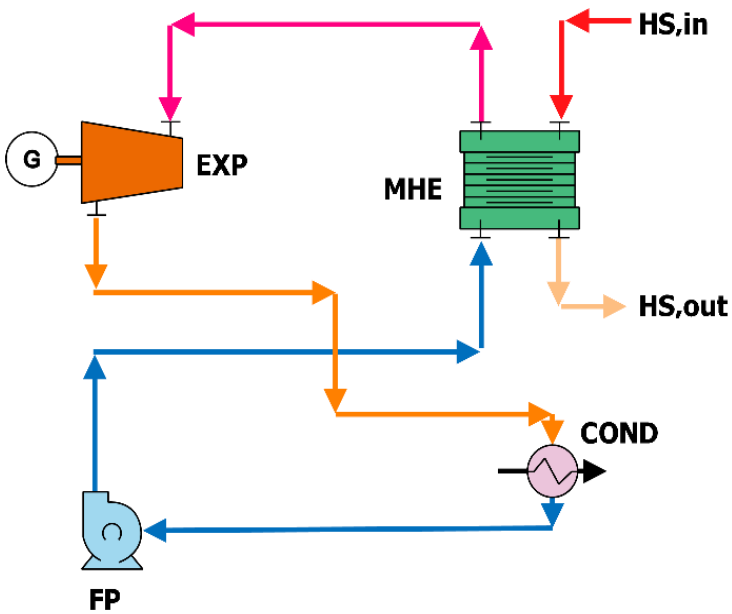

Figure 2. ORC basic scheme.

A heat exchanger called recuperator (REC) (Figure 3) can be used if the WF exits the EXP in the form of dry superheated vapor (*recuperative configuration*) in order to increase the cycle thermal efficiency and, thus, a higher output power. The REC is installed as liquid preheater between the pump drain and the expander (EXP) outlet section.

In the *two-stage ORC plant* (Meinel et al., 2014), depicted in Figure 4, the working fluid is preheated, evaporated and, if advisable, superheated in the MHE by the heat source. The high pressure WF vapor enters the first turbine stage (EXP1), where it is expanded to an intermediate pressure level. The main WF stream proceeds to the second turbine stage (EXP2), where a further expansion to the condensing pressure takes place. The WF leaves the condenser (COND), is pressurized in the low pressure feed pump (FP1) and is sent to the saturator (SAT). In SAT, the vapor extracted from EXP1 is used to saturate the liquid coming from FP1. A second feed pump (FP2) is used to increase the fluid pressure that enters the MHE. Then, the cycle loop starts again.

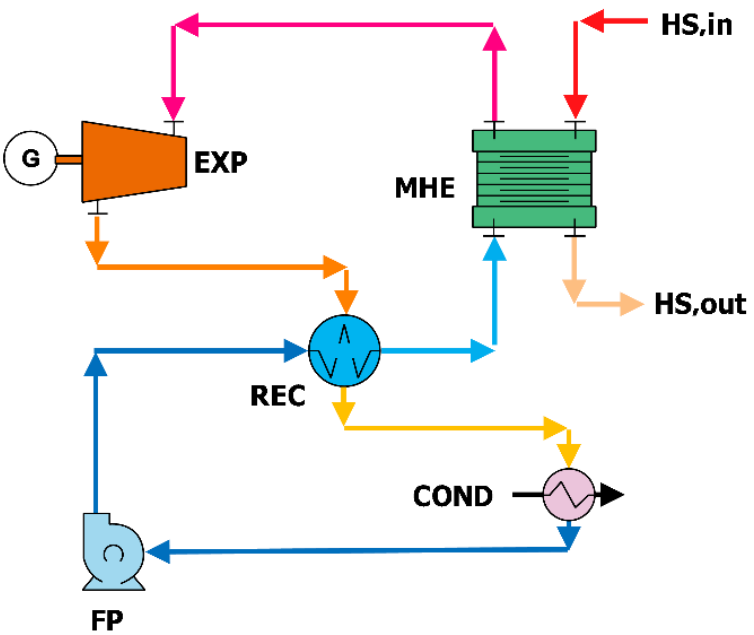

Figure 3. ORC recuperative scheme.

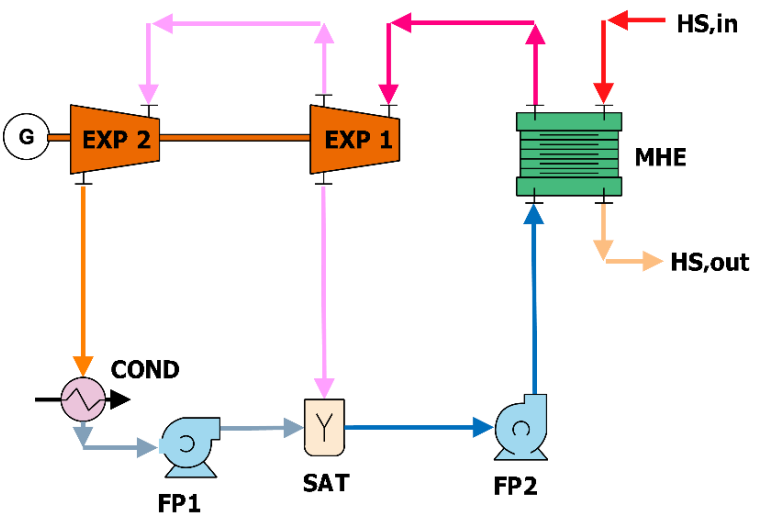

Figure 4. Two-stage ORC layout.

The *regenerative and recuperative architecture* (Branchini et al., 2013), depicted in Figure 5, is similar to the two-stage plant because a turbine extraction is used to preheat the organic medium before the MHE but includes a recuperator (REC) to transfer the heat recovered from the turbine outlet to the fluid entering the MHE.

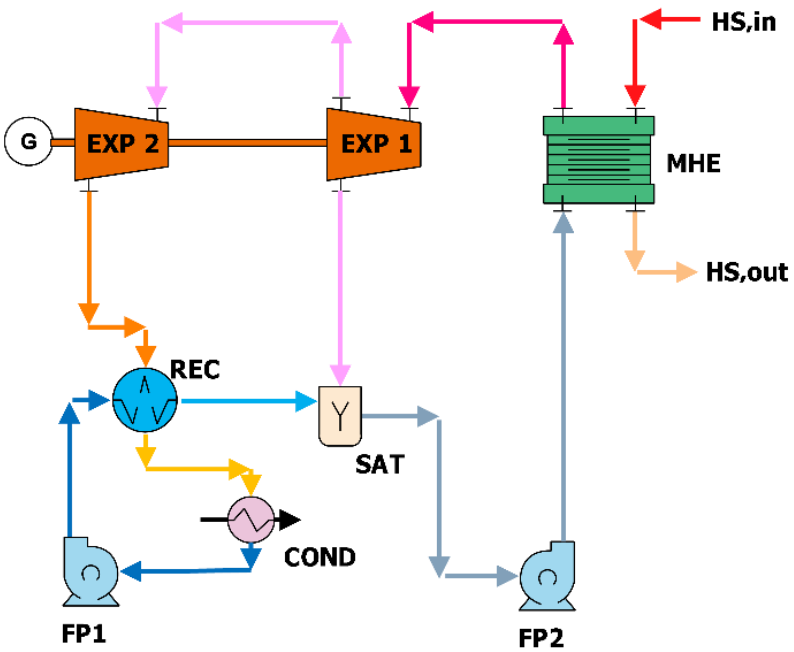

Figure 5. Regenerative and Recuperative Cycle.

The *dual pressure levels* ORC architecture and the *dual fluid scheme* have been investigated by Shokati et al., 2015.

In the *dual pressure levels scheme* (see Figure 6), the high and low pressure evaporators (HPEVA and LPEVA) and preheaters (HPPH and LPPH) are fed by the heat source fluid. In this cycle, the working fluid that leaves the condenser (COND), is pressurized in the low pressure feed pump (LPFP) and enters the LPPH. Here, the WF at medium pressure receives the heat from the HS fluid. Afterwards, it exits LPPH as saturated liquid at medium pressure. This liquid is splitted into two portions: the first one flows into the high pressure feed pump (HPFP), the HPPH and the HPEVA, then enters the high pressure turbine stage (HPEXP). The other portion enters the LPEVA and exits as saturated vapor at medium pressure. The working fluid portion that leaves the HPEXP and the one coming from the LPEVA is firstly joined in a mixer (MIX). The medium pressure vapor expands in the low pressure turbine (LPEXP) and then enters the condenser (COND). The cycle loop starts again because the LPFP sucks the WF from the condenser hotwell. In this configuration the heat source fluid passes through the following heat exchangers: HPEVA, HPPH, LPEVA and LPPH.

The dual fluid ORC is also equipped with a high and a low pressure preheater (HPPH and LPPH) and a high and a low pressure evaporator (HPEVA and LPEVA). The scheme is depicted in Figure 7. The cycle is composed by two loops and in each loop there is a different organic fluid. As an example, the first organic fluid can be isopentane (in Figure 7, red continuous line) while the second one can be isobutane (blue dotted line). The first fluid exiting from the high pressure feed pump (HPFP) enters the high pressure preheaters (HPPH) and evaporator (HPEVA). At the HPEVA outlet section the fluid is at the saturated vapor condition. Then, it expands in the high pressure turbine (HPEXP) and enters the lower pressure evaporator (LPEVA) where it heats the second working fluid. The fluid is then

sucked by the HPFP and the cycle is closed. The second fluid leaves the LPEVA at the saturated vapor state and enters the low pressure turbine (LPEXP) where it is expanded to the condensation pressure. At the condenser (COND) outlet, the fluid is sucked by the low pressure pump (LPFP) and sent, firstly, to the low pressure preheater (LPPH) and then to the LPEVA.

The heat source medium (in Figure 7, black continuous line), firstly, heats the first fluid in the HPEVA and in the HPPH; then, enters the LPPH where it heats up the second fluid.

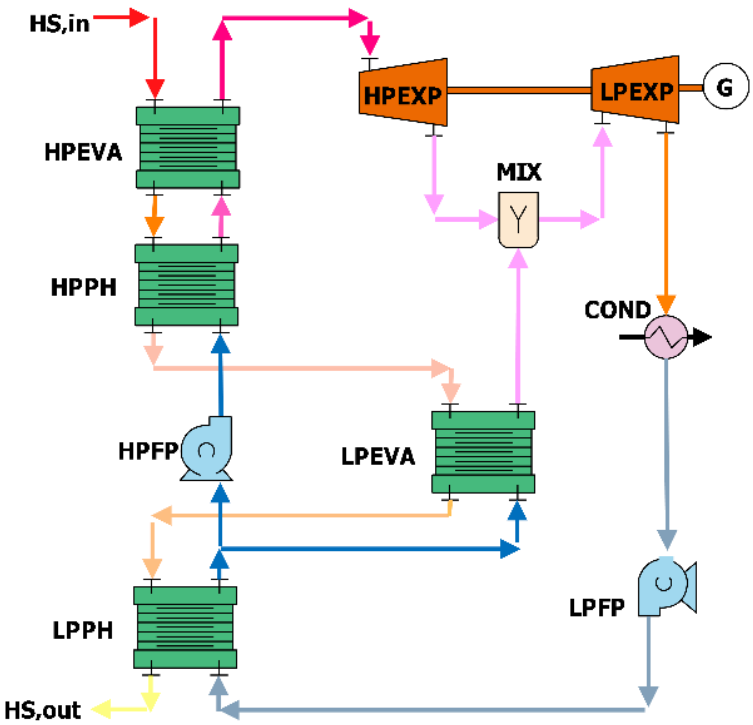

Figure 6. Dual pressure levels scheme.

In the plant schemes depicted in Figures 2-7, the heat source medium and the ORC WF streams exchange heat directly but, if the ORC medium is a flammable substance and the heat source temperature is relatively high (T < 300°C), an intermediate thermal oil loop needs to be incorporated to avoid risky contacts between the HS medium and the organic fluid. In this way, also flammable organic media can be adopted.

In addition, all the proposed cycles can be subcritical or transcritical. The adoption of a transcritical or supercritical cycle, which means an evaporation pressure higher that the critical one, guarantees better cycle efficiency (close to 8%), higher heat exchanger efficiency but also requires specific materials and safety precautions.

Note that, at the time of writing, transcritical cycles and layouts characterized by turbine extraction or dual pressure levels or dual fluids plant are not yet commercially available but are currently being studied mainly in the form of prototypes or proof of concepts.

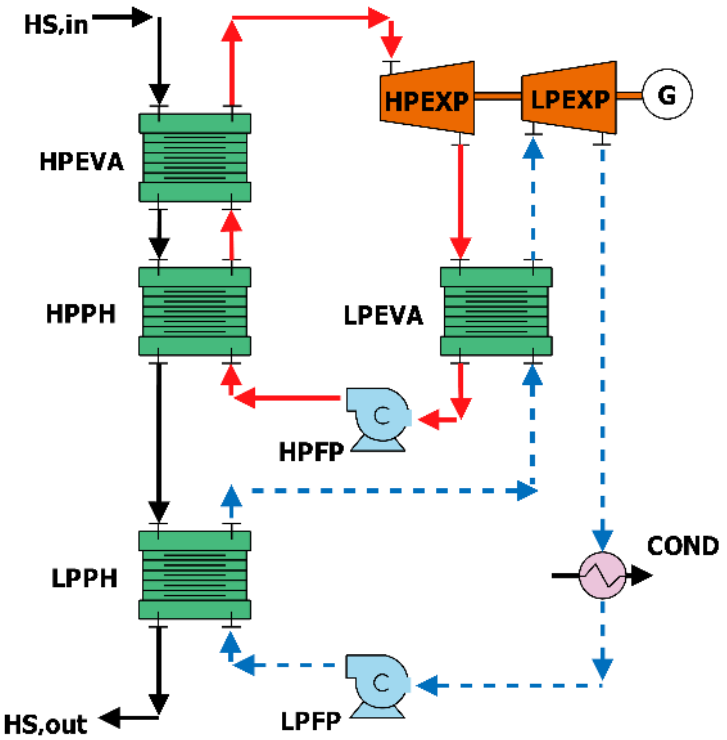

Figure 7. Dual fluid scheme.

3. ORCs and Renewable Heat Sources

Being the aim of the present chapter to analyze different Organic Rankine Cycle applications with respect to the nature of the heat source, in the following section an in-depth review of the state of the art of ORCs which convert renewable sources heat into power is presented. Firstly, the ORC-biomass fed system is deeply analyzed taking into account both direct and indirect combustion methods. Then, ORCs coupled with geothermal and solar energy and Ocean Thermal Energy Conversion using ORC turbo generators have been analyzed. Finally, the use of Organic Rankine Cycles to recover waste heat is discussed.

3.1. ORC-Biomass Fed System

Biomass is the fourth largest energy source in the world and contributes to nearly 14% of the world's raw energy demand (Mao et al., 2015). In the European Union, the use of biomass has increased since the middle of the 1990s due to high subsidies and CO_2 emission regulation. As an example, in 2008, biomass covered 3.5% and 2.7% of the EU and North America energy share, respectively, while it still supplies most of the energy needs in developing countries such as Nepal (97%), Bhutan (86%), Nigeria (85%), Kenya (76%) and Cote d'Ivoire (75%) (Demirbas et al., 2009).

Biomass is the result of natural organic processes and its availability is relatively large: therefore, its exploitation and conversion into heat and/or power is a good option especially due to the significantly lower cost in comparison to conventional fossil fuels.

In general, biomass resource includes wood and wood waste, agricultural crops, aquatics plants, algae and agriculture, animal, municipal and food industry wastes.

Wood is derived from trees while wood wastes are available as sawdust, board ends, bark, etc. Cotton stalks, wheat and rice straw, maize and jowar cobs, rice husks, etc. are classified as agricultural waste while sugar cane and sugar beets, grains, cassava, sunflower, jatropha curcus, etc. are crops sown for energy purposes.

The use of biomass as renewable energy source is really convenient because it allows meeting various energy needs including electricity generation, space and process heating and vehicle motion. To this purpose, several studies have been carried out to estimate biomass potential, how the governmental policies can support its sustainable development and where it can be used for electricity generation (Long et al., 2013). These researches have pointed out that biomass is characterized by low energy density therefore it is well suited for decentralized, medium- and small-scale combined heat and power systems for two reasons: on the one hand, biomass based systems can reduce fuel transportation costs if used on site, on the other hand, it is difficult to find a large end-user requiring the heat produced in a large-scale combined heat and power system.

The production of power from biomass can occur through external combustion (e.g., by means of Organic Rankine Cycle) or internal combustion after gasification, pyrolysis or transesterification (e.g., internal combustion engine). The internal combustion is characterized by higher efficiency than the external one but it needs complicated and problematic fuel cleaning systems. For this reason, the use of external combustion is preferred and for these reasons ORC units are particularly suitable for biomass applications.

3.1.1. Biomass Direct Combustion

A typical plant is made up by a Biomass Fired Thermal Oil Heater and an Organic Rankine Cycle unit. The use of an intermediate oil loop is needed to transfer the heat from the hot gases to the power cycle avoiding risky contact between the hot fluid and the organic medium and preventing fluid overheating (Lecompte et al., 2015). In addition, the thermal oil loop guarantees larger inertia and lower sensitivity to load variations, lower pressure in the boiler and simpler and safer control and operation of the plant. Typical values of the thermal oil temperature are in the range 150°-310°C: values that guarantee a long oil life.

Being the pure and simple electricity generation cost not competitive in the actual energy market, the plant needs to be a combined heat and power (CHP) unit in order to ensure the profitability of the investment. Therefore, the ORC unit produces electrical energy via the electric generator coupled with the expander while the hot water for district heating and/or other thermal processes is recovered from the condenser. As said, these plants are mainly decentralized units driven by the heat demand.

Due to technical problems related to the heat transportation for long distances, the plant thermal power is limited to 6-10 MW, corresponding to an electric power of 1-2 MW. Note that, in this power range, conventional steam cycles are not cost-effective due to the high pressures and temperatures required for their optimal performance. In addition, compared to the SRC, the Organic Rankine Cycle technology offers automatic and continuous working, no

corrosion problems, lower pressures and temperatures, easy start up, reliability and good efficiency at design point and during part-load operations.

A simplified scheme of the biomass CHP unit is depicted in Figure 8.

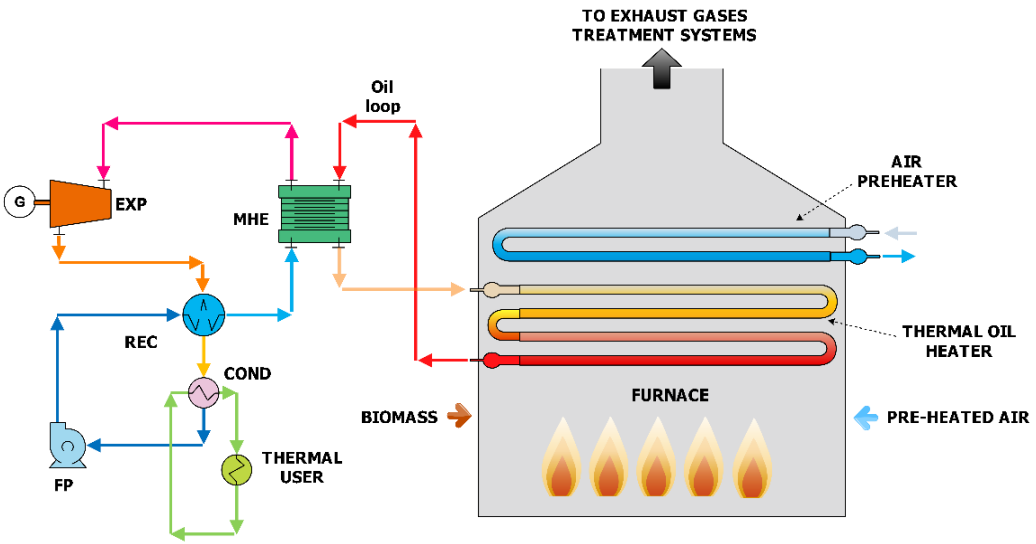

Figure 8. Scheme of a biomass power plant.

The heat generated by the biomass combustion is transferred from the flue gases to the thermal oil which is used to preheat, evaporate and, if needed, superheat the ORC working fluid at a temperature slightly lower than 300°C. The working medium is then expanded, passes through the recuperator to preheat the liquid coming from the feed pump and is finally condensed at a temperature between 60° and 120°C to satisfy the user's heat needs.

The ORC electrical efficiency ranges between 6 and 17% while the system overall efficiency ranges between 80 and 85%.

The cost of a commercial ORC module is estimated at 1600-2765 €/kW_{el} while the electricity production cost ranges between 9 and14 c€/kWh_{el} depending on the biomass price.

In literature, several studies on ORCs coupled with biomass boilers are available. As an example, Bini and Manciana, 1996, presented a comparison between a CHP unit based on ORC turbo generator and a Stirling engine. They concluded that the ORC maximum temperature is limited by the fluid thermal stability and that it is really difficult to efficiently implement a Stirling engine. Therefore, despite the lower efficiency, it is easier and more cost effective to build an ORC than a Stirling engine.

Obernberger et al., 2002, describe and evaluate the performance of the 1 MW_{el} ORC plant installed in Lienz. The plant started operation in autumn 2001 and covers the heat demand of approximately 70% of the Lienz buildings. The plant consists of two biomass boilers, an ORC turbo generator, a solar collector panel and an oil-fired boiler which has to be used during peak hours. The investigation showed that the plant has an electric efficiency of 18% and supplies 60000 MWh/year of heat (to Lienz city) and produces 7200 MWh/year of electricity.

Drescher and Bruggemann, 2007, presented a procedure to select suitable working fluids for ORC fed by biomass boiler. For biomass plants operating with a maximum working fluid

temperature of 300°C, a suitable pressure is in the range 0.9 to 1.5 MPa and the highest efficiency is reached with alkybenzenes fluid family.

An energetic and economic investigation of the ORC applications has been presented in (Schuster et al., 2009) while the technical and economic aspects of biomass fueled CHP plant based on ORC turbo generators feeding a DHN have been analyzed in (Duvia et al., 2009; Tanczuk and Ulbrich, 2013) and monitored in (Prando et al., 2015).

An extensive literature review concerning the development of small and micro scale biomass-fueled CHP systems has been performed in (Dong et al., 2009) while a survey of existing small-scale CHP plants in Sweden and Finland has been discussed in (Salomon et al., 2011).

Algieri and Morrone, 2014, investigated the energetic performance of a biomass ORC for domestic CHP generation and evaluated the possibility of installing the system in the Italian residential sector while Hao et al., 2011, also evaluated the energetic performance of a 2 kW_{el} cogenerative ORC unit for residential purposes.

Finally, Branchini et al., 2013, presented a systematic comparison of biomass ORC configurations by means of comprehensive performance indexes. They concluded that the most suitable configuration for ORC fed by biomass is the recuperative one.

In conclusion, despite the works available in literature and the large number of plants installed throughout the world, technical data on existing plants are very scarce. However, it can be said that these plants are economically viable, able to supply heat and power with a good efficiency and can contribute to CO_2 emissions reduction.

3.1.2. Biomass Gasification

The main competing technology for electricity or combined heat and power production from solid biomass is gasification. In this case, the solid biomass is not burned into a boiler furnace but is transformed into a gas (called "syngas") essentially composed by H_2, CO, CO_2 and CH_4. The gas produced by the gasifier is firstly treated and filtered to eliminate solid particles, and then is burned in an internal combustion engine (ICE).

In order to increase the plant overall efficiency, the heat content of the exhaust gases exiting from the ICE and/or the heat extracted from the gas cleaning system and/or the heat coming from the ICE cooling water can be recovered with an ORC to generate electricity or heat and power. This solution increases the plant costs but boosts the system installed power.

A scheme of a cogeneration system with gasification unit and an ICE coupled with an ORC is shown in Figure 9.

The ORC turbo generator can be a recuperative cycle if the size of the ICE is relatively big (higher than 300-400 kW_{el}) otherwise the ORC basic scheme is usually employed.

In literature, different opinions about the gasification technology maturity can be found. For example, Quoilin et al., 2011b, estimate that a plant based on the biomass combustion coupled with the ORC technology has an investment cost 75% lower and a maintenance cost 200% lower than a gasification system while Schuster et al., 2009, assert that ORC plants are the only proven technology for decentralized applications producing power up to 1 MW_{el} from solid fuels like biomass. In addition, as underlined by Vélez et al., 2012, there are several uncertainties regarding the estimation of the installation time, the plant costs, the system performance and the plant reliability.

For these reasons and being biomass fired boilers coupled with ORCs a well-known technology, there are no commercially available gasification plants coupled with ORCs but only few demonstration units have been set up.

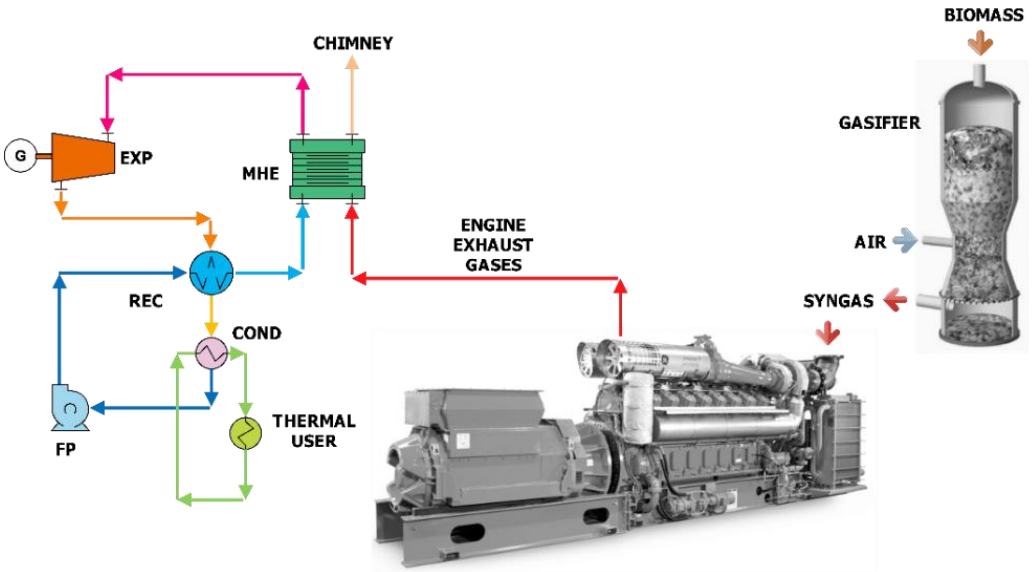

Figure 9. Scheme of a gasifier coupled with an internal combustion engine and an ORC turbo generator.

3.1.3. Biomass Anaerobic Digestion

The anaerobic digestion of biomass produces the so called biogas fuel. As for the gas produced by the biomass gasification, the biogas needs to be introduced into an internal combustion engine to produce work. The heat released by the ICE is partially used to maintain the digester required temperature. However, as in gasification plants, a remarkable amount of waste heat is available at medium and low temperature: the exhaust gases exiting from the ICE, the heat extracted from the gas cleaning system and the heat of the engine cooling water.

The insertion of an ORC unit boosts the plant electricity production because the waste heat can be converted into electricity or heat and power. A plant scheme is depicted in Figure 10. Theoretically, the ORC installation can abate the electricity production cost from 13.16 c€/kWh to 5.65 c€/kWh (Schuster et al., 2009).

Regarding biogas plants coupled with ORCs, several investigations have been carried out and presented in literature. For example, Schulz et al., 2007, and Niemczewska, 2012, suggest applying the ORC technology to biogas plants with an output power exceeding 300 kW_{th} and where there is no heat demand. They also remark that about 20% of the thermal energy from the associated CHP generation is available for the ORC process. In practice, they recommend to use the ORC without a heat application.

Kane et al., 2007, propose to increase the electrical efficiency of a small biogas engine with a bottoming cycle based on scroll expander Organic Rankine Cycle while Saravia et al., 2012, studied the possibility of retrofitting an existing ICE fed with landfill biogas with on

ORC. In the first case the ICE was a 200 kW_{el} biogas engine while the second plant was equipped with 16 ICE modules, each one with a nameplate power of 1059 kW_{el}.

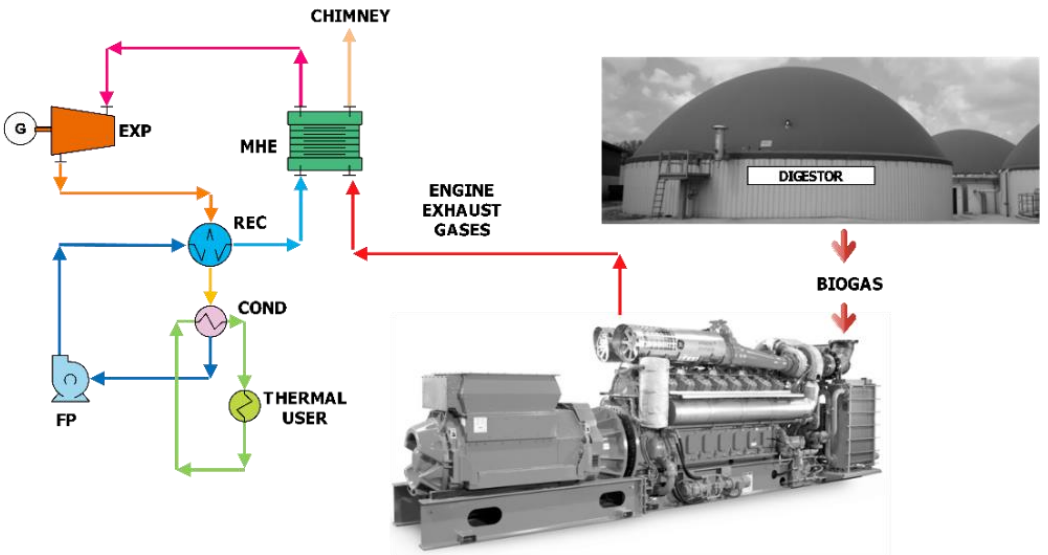

Figure 10. Scheme of a biogas plant.

The energetic performance of an ORC system fed by the heat generated from the integrated aerobic/anaerobic treatment of organic waste has been analyzed by Di Maria et al., 2014 while the greenhouse gas reduction potential that can be achieved by recovering with an ORC unit the waste heat released from a biogas engine has been evaluated by Uusitalo et al., 2016.

Finally, Meinel et al., 2014, propose an innovative two-stage ORC configuration to recover the ICE waste heat. The ICE is fed with biogas from a biomass digestion plant while the heat is recovered from the exhaust gases at 490°C and 1 bar. Despite the slightly higher constructive complexity, the analysis shows an increment of the thermodynamic efficiency in comparison to the conventional ORC scheme.

As pointed out in the previous section, ORCs which recover biogas fed ICEs waste heat are not commercially available and only few demonstration units are in operation.

3.1.4. Waste Heat Recovery from Internal Combustion Engines

As presented in the previous sections, investigations on ORCs which recover the waste heat released by ICEs fed with biogas, gasification fuel or other biofuels are really few. However, several researchers have analyzed the possibility of inserting an ORC unit to recover the ICE waste heat in both automotive and stationary applications. But, in many cases they do not take into account the fuel type burnt into the ICE because the ORC unit performance is not directly affected by this parameter.

Most of these researches are theoretical investigations/simulations (Bombarda et al., 2010; Shu et al., 2014)) while only few are experiments (Boretti, 2012). In addition, many of the engines are fed by traditional fuels (mainly Diesel and natural gas) because the objectives are to improve the fuel conversion efficiency and increase the engine power in order to reduce

the fuel consumption. For a clear overview of Organic Rankine Cycles which recover the internal combustion engines waste heat, see (Sprouse and Depcik, 2013).

3.2. ORC and Geothermal Energy

Geothermal energy is the thermal energy generated and stored in the Earth. It is considered to be a clean, abundant and renewable energy source because the heat is continually restored by the natural heat production.

Barbier, 2012, estimates that the Earth total potential is about $4 \cdot 10^{13}$ W: a value three times higher than the world total consumption. However, technical and economic reasons restrict the sites where the geothermal resource can be exploited. Indeed, in 2008, there were 504 geothermal plants in operation in 27 countries with an installed capacity of about 10 GW, but, only 373 MW are based on the ORC technology (DiPippo, 2012).

Depending on the geological formation, the geothermal energy can be classified either by the temperature level (high (> 180°C), medium (100°-180°C) and low temperature (< 100°C)) or by the heat transfer mode (dry rock, steam and pressurized water) while geothermal power units can be grouped as: dry steam, single-flash, double-flash and binary cycle plants.

Double-flash and dry-steam plants are characterized by temperatures in the range 240° to 320°C and 180° to 300°C while single flash and binary cycles work with temperature between 200°C and 260°C or 125°C and 165°C, respectively.

Single and Double-flash cycles have a utilization efficiency of 30-35% and 35-45% respectively. The highest utilization efficiency can be reached with dry-steam units (50-65%) while the lowest with binary geothermal plants (25-45%).

All these plant configurations are characterized by moderate complexity and medium-high investment costs.

When the geothermal site produces dry steam or a mixture of steam/brine with temperatures higher than 200°C, the best conversion method is the direct injection of the fluid into a turbine in open cycle with or without fluid re-injection (Vélez et al., 2012) while for lower temperatures the use of an ORC is the best way to produce electricity or heat and power. Usually these plants are binary plants: the most widely adopted type of geothermal unit for low temperature sources.

Figure 11 depicts the typical geothermal ORC plant scheme.

The geothermal fluid extracted from one or more production wells is used to heat the ORC working medium. After that, it is re-injected via injection wells. The ORC turbo generator is usually a non-recuperative unit in order to reduce the plant complexity and the equipment costs.

The first geothermal unit was installed in Italy in 1904-1905 and was an experimental test rig while the first commercial unit was built in Larderello (Italy) with a power of 250 kW_{el}.

The first binary geothermal plant was installed in Paratunka (Russia) and started the production in 1967. The ORC working fluid was R12 while the geothermal heat source was water at a temperature of 81°C. The plant design power was 680 kW_{el}.

Another example is the Neustadt-Glewe (Germany) plant. The ORC unit has a rated power of 210 kW_{el}, is fed by water at 98°C while the working fluid is perfluoropentane which works in a single-stage turbine.

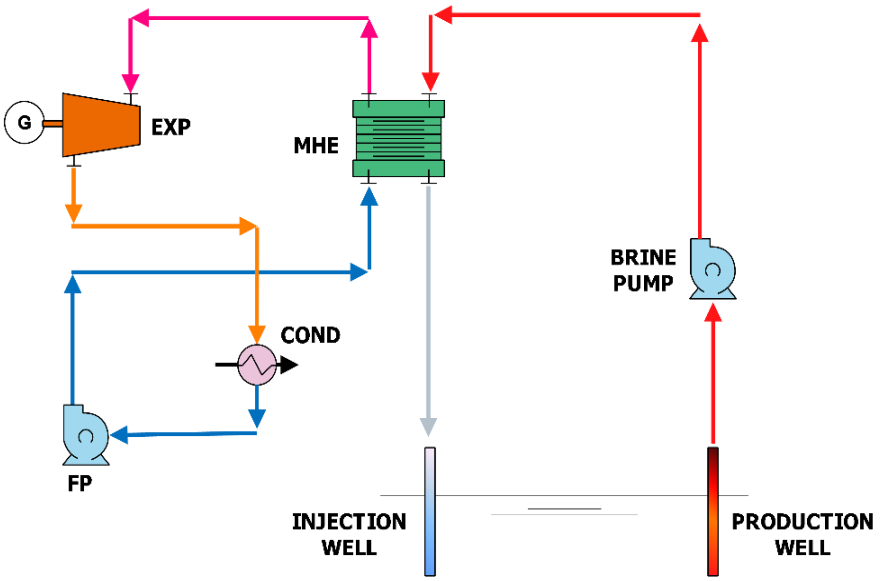

Figure 11. Scheme of a geothermal binary plant.

In literature many authors have carried out studies and researches about not only the feasibility and operation of geothermal ORC plants, but also their integration with fossil fuels, biomass boilers, etc.

For example, DiPippo, 2012, and Franco and Villani, 2009, evaluated the optimal geothermal resource utilization considering the first and the second law efficiency. They found a first law efficiency in the range 5-15% and a second law efficiency of 20-54%.

Following these suggestions, several researchers conducted theoretical investigations on ORC fluid selection as a function of the first or the second law efficiency. However, as remarked by Shengjun et al., 2011, fluids with high thermal or exergetic efficiency cannot ensure from technical and economic viewpoint.

For this reason, numerous studies have been dedicated to fluid selection using different criteria. Pure fluids and mixtures have been tested in sub-critical and transcritical configurations but, until now, no one has found a unique criterion to optimally select the working medium. This is due to the wide range of flow rates and temperatures available in the geothermal sites.

Also economic investigations have been performed during the years. Heard et al., 1990, estimated the installation costs of these plants variable in the range 1000-4000 €/kW_{el} while Lukawski, 2010, predicted a drop in the geothermal power generation cost from 15 c€/kWh to 4-8 c€/kWh in the period 2005-2020. This uncertainty is mainly justified by the different temperatures of the geothermal source.

Therefore, further research needs to be done in order to evaluate the plant feasibility and reliability.

In conclusion, ORC plants fed by geothermal wells are nowadays a proven technology in the range from high to low temperatures and are commercially available with power from 300 kW_{el} to 1200 kW_{el}. However, there is the need of standardizing the production to reduce the plant costs.

3.3. ORCs in Solar Applications

Compared to the actual energy demand or the other renewable energy sources (geothermal, wind, ocean and biomass), direct solar radiation has an enormous potential. Anyhow, we should also consider that biomass, ocean thermal, hydropower and wind energies themselves are derived forms of solar energy. Therefore, several investigations have been performed to estimate solar potential and how to use it. For example, in (IPCC, 2011) the theoretical potential of the solar energy is estimated at $3.9 \cdot 10^6$ EJ/year.

The conversion of solar energy into mechanical energy and/or electricity or heat is possible by means of direct or indirect conversion technologies.

Photovoltaic systems directly convert solar energy into electricity while solar thermal power technologies (such as linear or punctual collectors) track the sun, reflect the radiation onto a collector and use it to heat a fluid at different temperature levels.

There are three main concentrating solar power technologies commercially available: parabolic dish, solar tower and parabolic trough.

Punctual concentration technologies like parabolic dishes and solar towers operate with high concentration factors and temperatures (higher than 300°C). Therefore, the most appropriate cycles to exploit the generated heat are steam cycles, combined cycles or Stirling engines, while parabolic trough collectors work at lower temperature and are suitable for ORC applications. Note that for temperature lower than 80°C the generated heat is used for domestic hot water and space heating while power generation systems based on the ORC technology work with temperature between 80°C and 300°C.

ORCs solar power units consist of a solar field, a storage tank and the ORC module. A scheme is depicted in Figure 12.

The sun's rays are reflected by mirrors in order to concentrate the solar energy and then heat up a fluid. Generally speaking, this fluid is a heat transfer medium which is then used in the ORC main heat exchanger to preheat, evaporate and, if needed, superheat the Organic Rankine Cycle working fluid. The ORC turbo generator can be a recuperative unit or a non-recuperative one. Solar energy is unpredictable and intermittent: so a storage tank is needed to assure the plant operation for some hours when the solar radiation is not available (night or cloudy weather).

In small-scale ORC power plants, it is fundamental to reduce components costs and system complexity, therefore the ORC working fluid is directly heated up into the solar collectors.

Up to now, several theoretical investigations have been performed on ORC solar plants with power from one kW up to a few MW but very few plants are available in the market.

In Arizona (USA) a 1 MW_{el} concentrating solar ORC plant is in operation since 2006 (Tchanche et al., 2011). The plant is owned by Arizona Public Service while Solargenix and ORMAT provided the solar collects and the ORC unit, respectively. The ORC working fluid is n-Pentane while the cycle efficiency is 20.7%. As pointed out by Quoilin et al., 2013, the overall solar to electricity efficiency is 12.1% at design condition.

The first world micro-scaled concentrated solar power (CSP) plant was built in Kona desert (Hawaii, USA) and started operation in 2009. It has an installed capacity of 2 MW and a cost of approximately 20 million dollars. The ORC unit manufacturer is ElectraTherma Inc. while the parabolic trough collectors have been supplied by Alanod Aluminium-Veredlung.

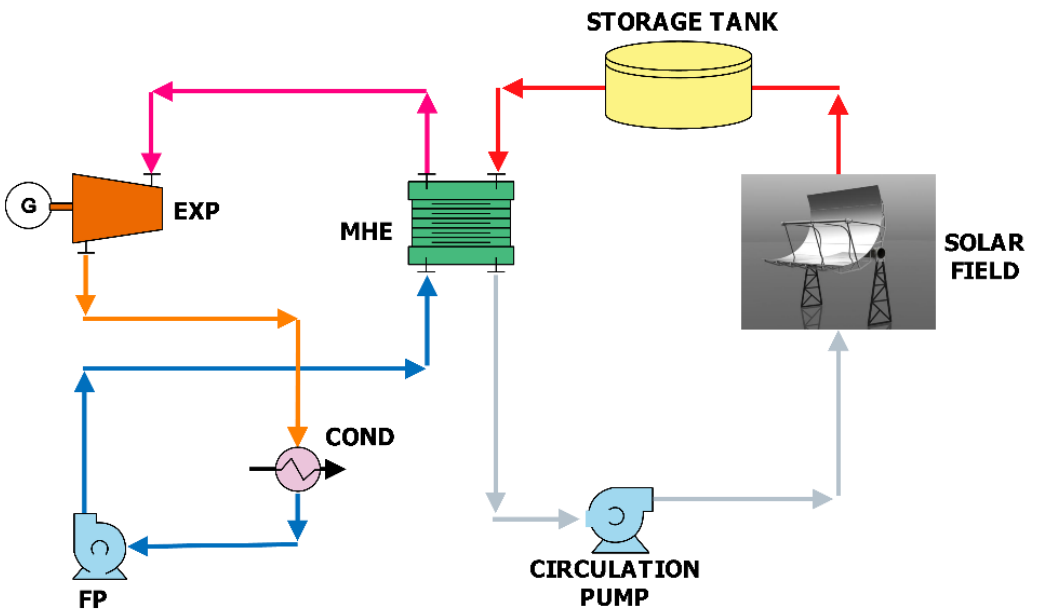

Figure 12. Scheme of a solar ORC plant.

The CSP plant supplies 500 kW of electricity to the national grid, is managed by the Hawaii Electric Light Company (HELCO) and can provide enough clean solar thermal power for more than 250 Hawaii homes. In addition, the plant will reduce the state's oil import by 2000 barrels a year and carbon emissions by 6000 tons over 30 years (National Energy Laboratory, 2009).

Small off-grid ORC solar power plants are also under investigation due to their capability of feeding small and isolated local grids in developing countries. An example is the plant installed in Lesotho by STG International.

Other technologies are being investigated:

- Solar pond power plants consisting of a salt gradient solar pond and an ORC.
- Solar ORCs coupled with reverse osmosis desalination systems.
- Duplex-Rankine cooling systems.
- Hybrid systems like the one proposed by Kane et al., 2003, in which solar collectors, two superposed ORCs and a diesel engine are integrated.

In conclusion, ORCs producing electricity or heat and power from solar units have a great potential but, at the time of writing, several additional investigations need to be done before reaching their commercial viability.

3.4. Ocean Thermal Energy Conversion Using ORC Turbo generators

Oceans cover over 70% of the planet surface and could be utilized as a source of virtually unlimited renewable energy. Obviously, the oceans thermal energy is provided by the sun

because oceans water acts as a natural solar receiver and heat storage unit. In practice, the energy coming from the sun is absorbed and stored in a seawater surface layer with a thickness of about 50-100 m and with an approximate temperature in the range between 26°C and 31°C (typical temperature of tropical regions).

Considering that the temperature falls gradually from the sea level to the ocean bottom, at a depth of 800-1000 m the temperature is 2-7°C. Therefore, a power cycle which uses the temperature difference between the cold deep water and the warm surface water to produce useful work, which can be in the form of electricity, is a possible energy conversion method.

To this purpose, numerous research works have been conducted with the aim of finding an efficient Ocean Thermal Energy Conversion (OTEC) method and, actually, there are five possible cycles for OTEC: open, closed and hybrid OTEC cycle, Kalina cycle and Uehara cycle (Tchanche et al., 2011). The minimum admissible temperature difference between the cold and hot layer is about 20°C. Therefore, only tropical regions are suitable for OTEC plants.

The closed OTEC cycle was the first proposed in 1881 by D'Arsonval while the first open OTEC cycle was proposed, built and tested by George Claude in the period 1920-1930. Since the 1970s, Japan is the principal contributor to the development of OTEC power cycle technologies but the potential market has been identified in over 50 countries such as India, Korea, Hawaii, etc.

Among the five possible configurations, the most adopted cycle is the closed one. It is an Organic Rankine Cycle because the heat source temperature is really low, then water cannot be used. A working fluid having a low-boiling point (-30°C) is employed (ammonia, propane, etc.) and a configuration with an evaporator, a turbine, a pump and a condenser is usually adopted. The warm surface water is used to evaporate the ORC working fluid while the deep cold water is employed to condense the working medium coming from the turbine. The condensed fluid is then pumped back to the evaporator to close the cycle.

A typical OTEC cycle efficiency is about 3-5% (Tchanche et al., 2011). This really low value is due to the very low energy grade of the heat source.

Despite the really low efficiency, several investigations have been conducted. As an example, Wu and Burke, 1998, developed a computer tool to optimize the closed-cycle OTEC system configuration using Refrigerant-12 as working fluid and choosing as objective function the specific power (the power per unit total heat exchanger surface area) of the heat engine. The specific power was calculated and an upper bound was determined after the manipulation of the boiler and condenser pressure.

Odum, 2000, proposed an energy analysis of the Taiwan OTEC system using the energy evaluation method. Due to the large investment, results suggest that the system is not likely to become economically acceptable in Taiwan.

Nevertheless, Yeh et al., 2005, developed a computer tool to evaluate the performance of an OTEC system installed in Taiwan Ocean. Parameters like pipe length, pipe diameter, warm and cold seawater temperature, mass flow rate of seawater have been considered to obtain the generated net power. The difference in seawater temperature between the surface and the deep ocean (eastern Taiwan) considered for the analysis was around 20°C for the entire year. Fujita et al., 2012, performed a description of the potential of Ocean Thermal Energy Conversion to produce not only clean energy but also potable water, refrigeration, and aquaculture products. In Faming et al., 2012, an energy and exergy analysis of the OTEC system has been presented in order to select the most suitable working fluid. Results show

that ammonia is a good choice from the net power output viewpoint. From the exergy loss viewpoint, the larger scale ORC should choose the better performance heat exchanger to decrease the exhaust loss, which accounts for a large proportion of exergy loss of ORC in OTEC plant. Finally, Yoon et al., 2014a, firstly performed an efficiency comparison of subcritical OTEC power cycle using various working fluids; then they suggested the use of R717 to design a high-efficiency power cycle (Yoon et al., 2014b).

Starting from the above survey, it is possible to conclude that OTEC is receiving attention all over the world because it might be a promising energy conversion system. But, at the moment, OTEC is characterized by low efficiency and high investment costs. For these reasons and being the estimated OTEC potential for electricity generation in the range of 3-5 TW, the development of multi-purposes OTEC plants able to provide electricity, fresh water refrigeration, air conditioning and so on might be a valid alternative to conventional single purpose unit.

3.5. Waste Heat Recovery

The waste heat is defined as the heat generated during combustion, a chemical or a thermal process and released to the environment. An example is the heat released as hot exhaust gases by an internal combustion engine or a gas turbine or the hot air exiting from an industrial oven. Obviously, waste heat is not a renewable energy source because, usually, it is generated from fossil fuels. However, this very big loss of energy increases the production costs and releases large quantities of pollutants. These pollutants can be chemical products, such as CO_2, NO_x, SO_x, etc., or heat. The rejected heat can modify the aquatic or earth equilibrium causing negative effect on biodiversity (Bundela and Chawla, 2010). Therefore, recovering the waste heat can help mitigate these pollution sources but also can be useful to generate additional electricity or heat and power.

Numerous studies have been conducted in order to identify the involved industrial processes and the potential of such waste heat.

Aluminum, Copper, Glass, Iron and Steel industries, cement and building material industry, food and beverage processing industry, pulp and paper industry, petroleum and chemical industry are characterized by high energy demand but also high rejected heat at high, medium and low temperature.

As an example, Bailey and Worrell, 2005, estimated that USA can generate $750MW_{el}$ from waste heat while 500 MW_{el} and 3000 MW_{el} can be produced by Germany and Europe, respectively.

Obviously, the state (solid, liquid or gas), the mass flow rate and the temperature of the flows significantly influence the waste heat recovery unit type, efficiency and cost. Usually, waste heat sources can be grouped with respect to the temperature level: high (> 650°C), medium (230-650°C) and low (< 230°C) (Tchanche et al., 2011).

Especially in the medium to low temperature applications, the ORCs have demonstrated their ability to recover the waste heat with simple plant layout (mainly the schemes depicted in Figure 2 and 3), acceptable efficiency and reasonable costs. As for the cases presented in previous sections, the open literature is full of works regarding ORCs which recover waste heat from gas turbines, cars, trucks and ships engines or industrial processes.

Therefore, it is possible to assert that ORCs are a very important technology to recover waste heat and perform fuel saving and environmental protection.

4. ORC COMPONENTS AND MANUFACTURERS

Turboden, ORMAT and Maxxtec are the first three ORC leading companies in terms of installed units but, all around the world, there are many emerging companies which build low capacity units for micro CHP or for internal combustion engines/gas turbines waste heat recovery.

As pointed out by Quoilin et al., 2013, there is a large variety of ORC modules which can be categorized according to the unit size, the type of technology and of the target application.

These are key factors to choose the kind of application and select the suitable components, in particular the expanders.

Several types of expansion machines are available on the market:

- Turbines: axial, radial, impulse, reaction and multi-stage.
- Positive displacements units: screw, piston and vane expanders and Wankel engines.

For low power ORC units, radial and axial turbines are characterized by low efficiency and high manufacturing costs, therefore different type of machines need to be employed.

Being a good expansion device characterized by high efficiency throughout a wide range of operation, low vibration and noise levels and, obviously, low purchasing cost, several investigations suggest to adopt axial turbines in MW-size ORC units and scroll and screw expanders in kW size units. However further research activities need to be done in order to better design and manage scroll and screw expanders. On the contrary, pumps and heat exchangers units are well known components.

Other aspects as ORC system design and optimization or system dynamics and control need to be better investigated both theoretically and experimentally.

CONCLUSION

The wide panorama of ORC applications has brought a large number of scientific papers and technical applications throughout the world. Many researchers have conducted theoretical and experimental activities, related to the exploitation of the possible heat sources, the kind of plants to be matched with the ORCs, the final product to be obtained (electricity or heat). The characteristics of the ORCs have been deeply studied, to select the most convenient layout of the plants, the optimization of the organic fluid selection, etc.

Organic Rankine Cycles coupled with Biomass Fired Thermal Oil Heaters are the most widespread application due to their capability of producing both electricity and thermal power while recovering the waste heat is the most promising and safe way to mitigate pollution sources and increase energy efficiency in industries. ORC plants fed by geothermal wells or fluids heated up by solar collectors are nowadays proven technologies but they need a standardized production to reduce the plant costs and become competitive, while OTEC

plants might be a promising energy conversion system. Therefore, more generally, there are a very big number of possible applications; some of them can be considered as mature technologies, some others are promising or in the demonstration phase; at last, some of them seem to have scarce practical possibilities; but the scientific and technical knowledge will advance and might be able to offer unexpected results in the future.

In conclusion, the ORCs technologies show a very interesting potential in the present energetic scenario, which will be more and more dominated by the need to decrease the use of non renewable sources, increase the use of renewable and improve the energy saving by means of suitable recovering techniques.

REFERENCES

Algieri, A. and Morrone, P. 2014. "Energetic analysis of biomass-fired ORC systems for micro-scale combined heat and power (CHP) generation. A possible application to the Italian residential sector." *Applied Thermal Engineering* 71(2), 751-759.

Bailey, O., and Worrell, E. 2005. Clean energy technologies: A preliminary inventory of the potential for electricity generation. Report of the Lawrence Berkeley National Laboratory.

Bao, J. and Zhao, L. 2013. "A review of working fluid and expander selections for Organic Rankine Cycle." *Renewable and Sustainable Energy Reviews* 24, 325.

Barbier, E. 2002. "Geothermal energy technology and current status: an overview." *Renewable and Sustainable Energy Reviews* 6(1), 3-65.

Benato, A., Stoppato, A., Pierobon, L., and Haglind, F. 2014. "Dynamic performance of a combined gas turbine and air bottoming cycle plant for off-shore applications." In Proceedings of the ASME 2014 12th Biennial Conference on Engineering Systems Design and Analysis.

Bini, R., and Manciana, E. 1996. "Organic Rankine Cycles turbo generators for combined heat and power production from biomass." In Proceedings of 3rd Munich Discussion Meeting-Energy Conversion from Biomass Fuels Current Trends and Future Systems, pp. 22-23.

Bombarda, P., Invernizzi, C. M., and Pietra, C., 2010. "Heat recovery from Diesel engines: A thermodynamic comparison between Kalina and ORC cycles." *Applied Thermal Engineering* 30(2), 212-219.

Boretti, A. 2012. "Recovery of exhaust and coolant heat with R245fa Organic Rankine Cycles in a hybrid passenger car with a naturally aspirated gasoline engine." *Applied Thermal Engineering* 36, 73-77.

Branchini, L., De Pascale, A., and Peretto, A. 2013. "Systematic comparison of ORC configurations by means of comprehensive performance indexes." *Applied Thermal Engineering* 61(2), 129-140.

Bundela, P., and Chawla, V. 2010. "Sustainable development through waste heat recovery." *American Journal of Environmental Sciences* 6(1), 83-89.

Cavazzini, G., and Dal Toso, P. 2015. "Techno-economic feasibility study of the integration of a commercial small-scale ORC in a real case study." *Energy Conversion and Management* 99, 161-175.

Chys, M., Van Den Broek, M., Vanslambrouck, B., and De Paepe, M. 2012. "Potential of zeotropic mixtures as working fluids in Organic Rankine Cycles." *Energy* 44(1), 623-632.

Demirbas, M. F., Balat, M., and Balat, H., 2009. "Potential contribution of biomass to the sustainable energy development." *Energy Conversion and Management* 50(7), 1746-1760.

Di Maria, F., Micale, C., and Sordi, A. 2014. "Electrical energy production from the integrated aerobic-anaerobic treatment of organic waste by ORC." *Renewable Energy* 66, 461-467.

DiPippo, R. 2012. "Geothermal power plants: principles, applications, case studies and environmental impact." Butterworth-Heinemann.

Dong, L., Liu, H., and Riffat, S. 2009. "Development of small-scale and micro-scale biomass-fuelled CHP systems - a literature review." *Applied thermal engineering* 29(11), 2119-2126.

Drescher, U., and Bruggemann D. 2007. "Fluid selection for the Organic Rankine Cycle (ORC) in biomass power and heat plants." *Applied Thermal Engineering* 27(1), 223-228.

Duvia, A., Guercio, A., and Rossi, C. 2009. "Technical and economic aspects of biomass fuelled CHP plants based on ORC turbogenerators feeding existing district heating networks." In Proceedings of 17th European Biomass Conference, Hamburg, Germany, June, pp. 2030-2037.

European Parliament and Council of the European Union. 2009. Directive 2009/28/EC.

Faming, S., Yasuyuki, I., Baoju, J., and Hirofumi, A. 2012. "Optimization design and exergy analysis of Organic Rankine Cycles in Ocean Thermal Energy Conversion." *Applied Ocean Research* 35(0), 38-46.

Farrell, W. M. 1988. "Air cycle thermodynamic conversion system."

Franco, A., and Villani, M. 2009. "Optimal design of binary cycle power plants for water-dominated, medium temperature geothermal fields." *Geothermics* 38(4), 379–391.

Fujita, R., Markham, A. C., Diaz, J. E. D., Garcia, J. R. M. et al. 2012. "Revisiting Ocean Thermal Energy Conversion." *Marine Policy* 36(2), 463-465.

Ghazikhani, M., Passandideh-Fard, M., and Mousavi, M. 2011. "Two new high-performance cycles for gas turbine with air bottoming." *Energy* 36(1), 294-304.

Hao, L., Yingjuan, S., and Jinxing, L. 2011. "A biomass-fired micro-scale CHP system with Organic Rankine Cycles (ORC) thermodynamic modelling studies." *Biomass and Bioenergy* 35(9), 3985-3994.

Heard, C., Fernàndez, H., and Holland, F. 1990. "Development in geothermal energy in Mexico - part twenty-seven: The potential for geothermal Organic Rankine Cycle power plants in Mexico." *Heat Recovery Systems and CHP* 10(2), 79-86.

Helm, D. 2014. "2030 Framework for Climate and Energy Policies." Available on: www.ec.europa.eu.

Hung, T.C. 2001. "Waste heat recovery of Organic Rankine Cycle using dry fluids." *Energy Conversion and Management* 42(5), 539-553.

IPCC. 2011. IPCC special report on renewable energy sources and climate change mitigation.

Kalina, A. 1982. "Generation of energy by means of a working fluid, and regeneration of a working fluid." *EP Patent* App. EP19, 810,302,177.

Kane, E.H.M., Favrat, D., Gay, B., and Andres, O. 2007. “Scroll expander Organic Rankine Cycle (ORC) efficiency boost of biogas engines.” In ECOS 2007, Volume 2, pp. 1017-1024. Università degli Studi Di Padova.

Kane, M., Larrain, D., Favrat, D., and Allani, Y. 2003. “Small hybrid solar power system.” *Energy* 28(14), 1427-1443.

Kim, Y. M., Kim, C. G., and Favrat, D. 2012. “Transcritical or supercritical CO_2 cycles using both low- and high-temperature heat sources.” *Energy* 43(1), 402-415.

Lecompte, S., Huisseune, H., Van den Broek, M., Vanslambrouck, B., and De Paepe M. 2015. “Review of Organic Rankine Cycles (ORC) architectures for waste heat recovery.” *Renewable and Sustainable Energy Reviews* 47, 448-461.

Long, H., Li, X., Wang, H., and Jia, J. 2013. “Biomass resources and their bioenergy potential estimation: A review.” *Renewable and Sustainable Energy Reviews* 26, 344-352.

Lukawski, M. 2010. “Design and optimization of standardized Organic Rankine Cycle power plant for European conditions.” Master’s Thesis, University of Iceland and the University of Akureyri, Akureyri, Iceland.

Maloney, J., and Robertson. R. 1953. Report CF-53-8-43. Technical report, ORNL, OAK Ridge, TN.

Mao, G., Zou, H., Chen, G., Du, H., and Zuo, J. 2015. “Past, current and future of biomass energy research: A bibliometric analysis.” *Renewable and Sustainable Energy Reviews* 52, 1823-1833.

Meinel, D., Wieland, C., and Spliethoff, H. 2014. “Effect and comparison of different working fluids on a two-stage Organic Rankine Cycle (ORC) concept.” *Applied Thermal Engineering* 63(1), 246-253.

National Energy Laboratory. 2009. http://www.power-technology.com/ projects/.

Niemczewska, J. 2012. “Characteristics of utilization of biogas technology.” *Nafta-Gaz* 68(5), 293-297.

Obernberger, I., Thonhofer, P., and Reisenhofer, E. 2002. “Description and evaluation of the new 1000 kWel Organic Rankine Cycle process integrated in the biomass CHP plant in Lienz, Austria.” *Euroheat and Power* 10, 1-17.

Odum, H.T. 2000. “Emergy evaluation of an OTEC electrical power system.” *Energy* 25(4), 389-393.

Pezzuolo, A., Benato, A., Stoppato, A., and Mirandola, A. 2016. “The ORC-PD: A versatile tool for fluid selection and Organic Rankine Cycle unit design.” *Energy* 102, 605-620.

Prando, D., Renzi, M., Gasparella, A., and Baratieri, M. 2015. “Monitoring of the energy performance of a district heating CHP plant based on biomass boiler and ORC generator.” *Applied Thermal Engineering* 79(0), 98-107.

Quoilin, S. 2011a. “Sustainable energy conversion through the use of Organic Rankine Cycles for waste heat recovery and solar applications.” *Ph.D. Diss*, University of Liege.

Quoilin, S., Broek, M. V. D., Declaye, S., Dewallef, P., and Lemort, V. 2013. “Techno-economic survey of Organic Rankine Cycle (ORC) systems.” *Renewable and Sustainable Energy Reviews* 22, 168-186.

Quoilin, S., Declaye, S., Tchanche, B. F., and Lemort, V. 2011b. “Thermo-economic optimization of waste heat recovery Organic Rankine Cycles.” *Applied Thermal Engineering* 31(14-15), 2885-2893.

Salomon, M., Savola, T., Martin, A., Fogelholm, C. J., and Fransson, T. 2011. "Small-scale biomass CHP plants in Sweden and Finland." *Renewable and Sustainable Energy Reviews* 15(9), 4451-4465.

Saravia, J.R., Galaz, J.R.V., Villena, A.C., and Ortiz, J.N. 2012. "Technical and economical evaluation of landfill-biogas fired combined cycle plants." *Distributed Generation and Alternative Energy Journal* 27(3), 7-25.

Schulz, W., Heitmann, S., Hartmann, D., Manske, S., Peters-Erjawetz, S., Risse, S. et al. 2007. "Utilization of heat excess from agricultural biogas plants." Technical Report. Bremen (Germany): Bremer Energie Institut, Universitat Bremen, Institut fur Umweltverfahrenstechnik.

Schuster, A., Karellas, S., Kakaras, E., and Spliethoff, H. 2009. "Energetic and economic investigation of Organic Rankine Cycles applications." *Applied Thermal Engineering* 29(8–9), 1809-1817.

Shengjun, Z., Huaixin, W., and Tao, G. 2011. "Performance comparison and parametric optimization of subcritical Organic Rankine cycle (ORC) and transcritical power cycle system for low-temperature geothermal power generation." *Applied Energy* 88(8), 2740-2754.

Shokati, N., Ranjbar, F., and Yari, M. 2015. "Exergoeconomic analysis and optimization of basic, dual-pressure and dual-fluid ORCs and Kalina geothermal power plants: A comparative study." *Renewable Energy* 83, 527-542.

Shu, G., Li, X., Tian, H., Liang, X., Wei, H., and Wang, X. 2014. "Alkanes as working fluids for high-temperature exhaust heat recovery of Diesel engine using Organic Rankine Cycle." *Applied Energy* 119, 204-217.

Smith, I. K. 1993. "Development of the Trilateral Flash Cycle system. Part 1. fundamental considerations." *Proceedings of The Institution of Mechanical Engineers Part A: Journal of Power and Energy* 207(A3), 179-194.

Smith, I.K. and da Silva, R.P.M. 1994. "Development of the Trilateral Flash Cycle system. Part 2: Increasing power output with working fluid mixtures." *Proceedings of the Institution of Mechanical Engineers, Part A: Journal of Power and Energy* 208(2), 135-144.

Sprouse, C., and Depcik, C. 2013. "Review of Organic Rankine Cycles for internal combustion engine exhaust waste heat recovery." *Applied Thermal Engineering* 51(1), 711-722.

Tanczuk, M., and Ulbrich, R. 2013. "Implementation of a biomass-fired co-generation plant supplied with an ORC (Organic Rankine Cycle) as a heat source for small scale heat distribution system - a comparative analysis under Polish and German conditions." *Energy* 62, 132-141.

Tchanche, B. F., Lambrinos, G., Frangoudakis, A., and Papadakis G. 2011. "Low-grade heat conversion into power using Organic Rankine Cycles - A review of various applications." *Renewable and Sustainable Energy Reviews* 15(8), 3963-3979.

Tchanche, B. F., Pétrissans, M., and Papadakis, G. 2014. "Heat resources and Organic Rankine Cycle machines." *Renewable and Sustainable Energy Reviews* 39, 1185.

Tchanche, B. F., Quoilin, S., Declaye, S., Papadakis, G. and Lemort, V. 2010. "Economic feasibility study of a small scale Organic Rankine Cycle system in waste heat recovery application." *Proceedings of the ASME 10th Biennial Conference on Engineering Systems Design and Analysis*, 2010, VOL 1, 249-256.

Uehara, H., Ikegami, Y., and Nishida, T. 1994. "Performance analysis of otec using new cycle with absorption and extraction process." *In Proceedings of Oceanology International*, Volume 6, pp. -.

Uehara, H., Ikegami, Y., Mitsumori, T., Sasaki, K., and Nagami R. 1999. "The experimental research on ocean thermal energy conversion using the Uehara cycle." *In Procedings of International OTEC/DOWA Conference*, Imari, Japan, pp. 132-141.

Uusitalo, A., Uusitalo, V., Gronman, A., Luoranen, M., and Jaatinen-Varri, A. 2016. "Greenhouse gas reduction potential by producing electricity from biogas engine waste heat using Organic Rankine Cycle." *Journal of Cleaner Production* 127, 399-405.

Vélez, F., Segovia, J. J., Martìn, M.C., Antolìn, G., Chejne, F., and Quijano, A. 2012. "A technical, economical and market review of Organic Rankine Cycles for the conversion of low-grade heat for power generation." *Renewable and Sustainable Energy Reviews* 16(6), 4175-4189.

Venkatarathnam, G., and Timmerhaus, K.D. 2008. "Cryogenic mixed refrigerant processes." Springer.

Wali, E 1980. "Optimum working fluids for solar powered Rankine-cycle cooling of buildings." *Solar Energy* 25(3), 235-241.

Wang, J., Sun, Z., Dai, Y., and Ma S. 2010. "Parametric optimization design for supercritical CO_2 power cycle using genetic algorithm and artificial neural network." *Applied Energy* 87(4), 1317-1324.

Wu, C., and Burke, T. 1998. "Intelligent computer aided optimization on specific power of an OTEC Rankine power plant." *Applied Thermal Engineering* 18(5), 295-300.

Yamaguchi, H., Zhang, X. R., Fujima, K., Enomoto, M., and Sawada, N. 2006. "Solar energy powered Rankine cycle using supercritical CO_2." *Applied Thermal Engineering* 26(17-18), 2345-2354.

Yang, Y., Yang, L., Du, X., Zhou, Y., and Guo C. 2013. "Supercritical CO_2 Rankine cycle using low and medium temperature heat sources." *ASME 2013 7th Int. Conf. on Energy Sustainability Collocated with the ASME 2013 Heat Transfer Summer Conf. and the ASME 2013 11th Int. Conf. on Fuel Cell Science, Engineering and Technology, ES2013.*

Yeh, R.-H., Su, T.-Z., and Yang, M.-S. 2005. "Maximum output of an OTEC power plant." *Ocean Engineering* 32(5), 685-700.

Yoon, J.I., Son, C.H., Baek, S.M., Kim, H.J., and Lee, H.S. 2014a. "Efficiency comparison of subcritical OTEC power cycle using various working fluids." *Heat and Mass Transfer* 50(7), 985-996.

Yoon, J.I., Son, C.H., Baek, S.M., Kim, H.J., and Lee, H.S. 2014b. "Performance characteristics of a high-efficiency R717 OTEC power cycle." *Applied Thermal Engineering* 72(2), 304-308.

Zhang, X., He, M., and Zhang, Y. 2012. "A review of research on the Kalina cycle." *Renewable and Sustainable Energy Reviews* 16(7), 5309-5318.

Zhao, L. and Bao, J. 2014. "Thermodynamic analysis of Organic Rankine Cycle using zeotropic mixtures." *Applied Energy* 130, 748-756.42.

In: Renewable Energy Systems
Editor: Sandip A. Kale
ISBN: 978-1-53610-423-3

Chapter 12

RENEWABLE ENERGY TECHNOLOGIES IN NIGERIA: CHALLENGES AND OPPORTUNITIES FOR SUSTAINABLE DEVELOPMENT

Sunday O. Oyedepo* and Philip O. Babalola
Department of Mechanical Engineering, Covenant University, Ota, Nigeria

ABSTRACT

Access to substantial quantity and quality energy infrastructures is essential to rapid and sustainable economic development. Availability of modern energy services directly contributes to economic growth and poverty reduction through the creation of wealth. With its fast growing population, energy need per person, poor technology and fast growing urbanization, Nigeria has been one of the countries with fast growing modern energy (electricity) needs in the world over the last two decades. Development and economic growth continue to affect the growing demand of energy consumption in Nigeria. The crucial challenge faced by power sector in Nigeria currently is the issue of sustainability. The acute electricity supply hinders the country's development, notwithstanding the availability of vast natural resources in the country. Nigeria is endowed with abundant energy resources but the existing electric energy infrastructures are unable to meet the energy demands of teeming population. There is imbalance in energy supply and demand in the country. Over the period of 2000 to 2014, there was an average of about 2.35 billion kWh of energy gap between energy production and energy consumption. Also, the highest electricity consumption per capita so far recorded was 156 kWh in 2012. This makes Nigeria one of the countries with the lowest electricity consumption on a per capita basis in the world. Nigeria is blessed with abundant renewable energy sources that can promote economic growth and provide sufficient capacity to meet up with the future electricity demand. In view of this, this article presents a critical review on the current energy scenario in Nigeria and explores the alternative energy like solar, wind, biomass and mini-hydro energy to ensure reliability and security of energy supply in the country. This paper as well evaluates the progress made in renewable energy (RE) development in Nigeria with the roadmaps for future implementation. In conclusion, the adoption of renewable energy technologies in a

* E-mail: sunday.oyedepo@covenantuniversity.edu.ng.

decentralized energy manner, especially for rural communities in hybrid and in stand-alone applications is considered to improve electricity supply and enhance the overall economic development.

Keywords: sustainable energy, renewable energy technologies, decentralized energy system, economic growth, poverty reduction, energy infrastructures

1. INTRODUCTION

During the last few years the 'energy issue' has been assuming a more and more important role among any other choice, strategy and policy concerning human survival and development. Modern societies strongly depend on reliable, affordable and sustainable energy supplies. In fact, energy is an obligatory input for most production processes and other economic activities and an essential component of way of life. Increased access to modern energy services is vital for social and economic development (Oyedepo, 2014).

At present, majority of energy resources in the world are derived from fossil fuels (such as natural gas, oil and coal) which inevitably leads to the continuing depletion of energy resources and emerging of adverse environmental impacts (Lorenzini et al. 2010). Hence, development and deployment of clean, renewable energy is imperative in the economic and environmental interest for every country. Renewable energy has an important role to play in meeting future energy needs and achieving sustainability. However, its diffusion and deployment is slow in the past decade due to low fossil fuel prices and barriers in the energy market. Rigorous methods are needed to accelerate the development and utilization of renewable energy, and to increase its contribution to the current energy supply mixes.

The need of developing countries to enhance their renewable energy applications will present economic opportunities for trading-based cities. The use of renewable energy in developing countries like Nigeria is at present very limited, although their potential is believed to be significant.

Due to various financial and technical constraints, renewable energy remains untapped in Nigeria. Nigeria continues to be heavily dependent on fossil fuels. The detrimental impacts on the environment and, the financial burden placed on the economy, through the current inefficient use of these fossil fuels, need to be addressed through the application of appropriate technologies, national energy policies and management measures. Nonetheless, the social and economic development and poverty alleviation are the overriding priorities of Nigeria. The energy requirements for the urgently needed socioeconomic development in this country could be provided by renewable energy (RE) sources. Thus, in order to promote renewable energy technologies (RETs) in Nigeria, more effective and responsive policies are required that would cater for immediate needs of people (Mohammeda et al., 2013).

A country experiencing energy poverty can be said to be a situation where its citizens lack electric power to meet even their basic needs such as lighting and cooking. In this situation, a large number of people in the developing countries like Nigeria are negatively affected by their very low consumption of energy use, while some use dirty polluting fuels and others spend excessive time to obtain fuel in order to meet their basic needs (Emodi and Boo, 2015). According to the Energy Poverty Action Initiative of the World Economic Forum

(IEA, 2007), "Access to energy is fundamental to improve the quality of life and is a key imperative for economic development."

Poor access to energy in Nigeria obviously translates into increased poverty, poor economic performance, limited employment opportunity and complicated prospects for institutional development. The high growth rate of the population is an indication that the country's energy demand will continue to rise, similar to how the increase in global population and industrial transformation of the 20thcentury tremendously increased energy demand (Mohammeda, 2013). The energy crisis situation in Nigeria has considerably affected the public users of electricity. This phenomenon has undeniably compelled the majority of households in both rural and urban segments of the country to significantly depend on combustible RE sources especially for domestic heating and cooking. Fuel wood and charcoal are widespread energy sources commonly used in Nigeria. Universally accessible energy services in the form of renewable energy resources that are adequate, affordable, reliable, of good quality, safe and environmentally benign are therefore a necessary condition for sustainable development and poverty reduction in the country.

The prime objectives of this study are to: (i) review energy resources in Nigeria and present condition of power sector (ii) review the potentials and utilization of renewable energy sources (solar, wind, small hydro and biomass) in Nigeria (iii) examine factors mitigating against development of renewable energy technologies in Nigeria (iv) assess the roles of renewable energy technologies as means of sustainable development in Nigeria.

2. NIGERIAN ENERGY SCENARIO

2.1. An Overview of Power Sector in Nigeria

Electricity as an essential commodity for modern people is very important for the future development of the society. This good must be supplied on a continuous basis in order to cover the daily requirements. To this end, effective performance and high availability factor of power generation industry (Power Sector) are of great importance towards achieving quality and reliable supply of electricity. Continuous access to quality energy infrastructure is an essential ingredient for sustained economic growth and development. Inadequate supply of electricity has the capability to retard development of industries, small scale businesses, hospitals and establishment of other infrastructural facilities in the urban and rural settlements (Oyedepo, et al., 2012).

Power Sector is a basic constituent for the development of worldwide economy; its evolution is based on making quality compatible with energy service, as it is the only means to lay the foundation of a stable sharp and economic growth. According to the Ministry of Economy (2002), the Power sector constitutes an essential part of the economic activity of a country being a dynamic element of the same, as well as, it supposes an undeniable strategic value to the rest of the sectors of the economy. For that reason, the power provision in optimal conditions of security, quality and price is not to be waived objective in the definition of the power policy of a country.

One of the ways of meeting the growing energy demand in a developing country like Nigeria is to have a suitable and sustainable means of power generation. Unfortunately,

Nigeria's power sector has been experiencing enormous challenges due to obsolete equipment, inadequate generation and transmission capacities, and high aggregate technical and commercial losses. These challenges stem from decades of neglect, mismanagement and inadequate funding. The problems worsened as a result of massive increase in demand of electricity due to economic and population growth. Lack of electricity has forced about 62% of Nigerians to rely on wood fuel for their entire energy needs resulting in massive deforestation in the country (Babanyara and Saleh, 2010; Eleri, et al., 2012; Zubairu et al., 2015). The dependence on firewood has also constitutes a major indoor pollution hazard and has caused the death of about 79,000 Nigerians due to smoke inhalation in 2011 (Eleri and Onuvae, 2011). According to a study by the World Health Organization in 2013, the death caused by smoke inhalation from fire wood used by women reached 98,000 (Emodi and Boo, 2015).

In the past two decades, the power demand in Nigeria has been on the increase while available generating capacity remained largely static or even showing a decreasing long-term trend. The consequence of this has been load shedding in order to ensure system stability (equilibrium between available generation and demand relatively met) (Oyedepo, 2014b).

Table 1 shows the performance indicators for Nigeria's electricity supply industry between 1999 and 2005. During this period, the average plant availability was about 50% significantly short of international standards of over 95%. Moreover, the power sector witnessed a low availability in 2001 as the available capacity stood at 1, 750 MW due to only about 24% installed units were functional (Adegbulugbe, 2007).

Majority of the existing fleet of power plants in Nigeria is a mix of plants and were built over 25 years ago. These old thermal power stations suffer considerably from poor maintenance, hence, the available generating capacity was just under 6,200 MW in 2012 and has risen to 6 840 MW in 2015 (Werner and Faruk, 2015). However, unavailability of gas, breakdowns, water shortages and grid constraints severely limit the power plant performance, which means that despite an increase in the available installed capacity over the last years (see Table 2), only between 3000 MW to 4 500 MW are actually being generated (the highest peak generated ever in Nigeria was 4,517.6 MW on December 23, 2012). Up to 2 700 MW of power generation capabilities are regularly lost due to gas shortage, up to 500 MW are lost due to water management, while several hundred megawatts are regularly lost due to line constraints. The poor performance of the power plants has led to acute shortage of electricity across the country with power outages of several hours per day.

Table 1. Performance Indicators for Nigeria's Electricity Supply Industry: 1999 – 2005

Year	Average Plant Availability (%)	Capacity Factor(%)	Load Factor (%)
2000	30.0	32.0	75.7
2001	27.7	32.5	68.3
2002	42.5	36.9	76.3
2003	46.2	39.8	92.0
2004	47.5	44.6	95.8
2005	44.4	41.5	90.6

Source: Adegbulugbe, 2007.

Table 2. Electricity Generation Profile (2007 to 2014)

Year	Average Generation Availability (MW)	Maximum Peak Generation (MW)	Maximum Daily Energy Generated (MWh)	Total Energy Generated (MWh)	Total Energy Sent out (MWh)	Per Capita Energy Supply (kWh)
2007	3781.3	3599.6	77,322.3	22,519,330.5	21,546,192.2	155.3
2008	3917.8	3595.9	86,564.9	18,058,894.9	17,545,382.5	120.4
2009	4401.8	3710.0	82,652.3	18,904,588.9	18,342,034.7	122.0
2010	4030.5	4333.0	85,457.5	24,556,331.5	23,939,898.9	153.5
2011	4435.8	4089.3	90,315.3	27,521,772.5	26,766,992.0	165.8
2012	5251.6	4517.6	97,781.0	29,240,239.2	28,699,300.8	176.4
2013	5150.6	4458.2	98,619.0	29,537,539.4	28,837,199.8	181.4
2014	6158.4	4395.2	98,893.8	29,697,360.1	29,013,501.0	167.6

Source: NERC, 2014

Generating plant availability in Nigeria is low and the demand – supply gap is crippling. Grid power is unreliable and insufficient to meet growing demand, resulting in frequent load-shedding and other outages. This has as well limited majority of Nigerians' access to clean and modern energy services. Moreover, the acute electricity supply hinders the country's development, notwithstanding the availability of vast natural resources in the country (Udoudoh and Umoren, 2015).

Figure 1 shows the historic development of electricity generation in Nigeria and of the selected peer countries. It is observed that Nigeria performed worst of the five countries in terms of absolute electricity generation. Over a 20 year period, there was an increase of 93% in mainline generating capacity in Nigeria. By contrast, Indonesia ramped up its electricity production by 372% and Bangladesh even by 451%. As a result, Bangladesh generated almost twice as much electrical energy in 2012 as Nigeria did (Werner and Faruk, 2015).

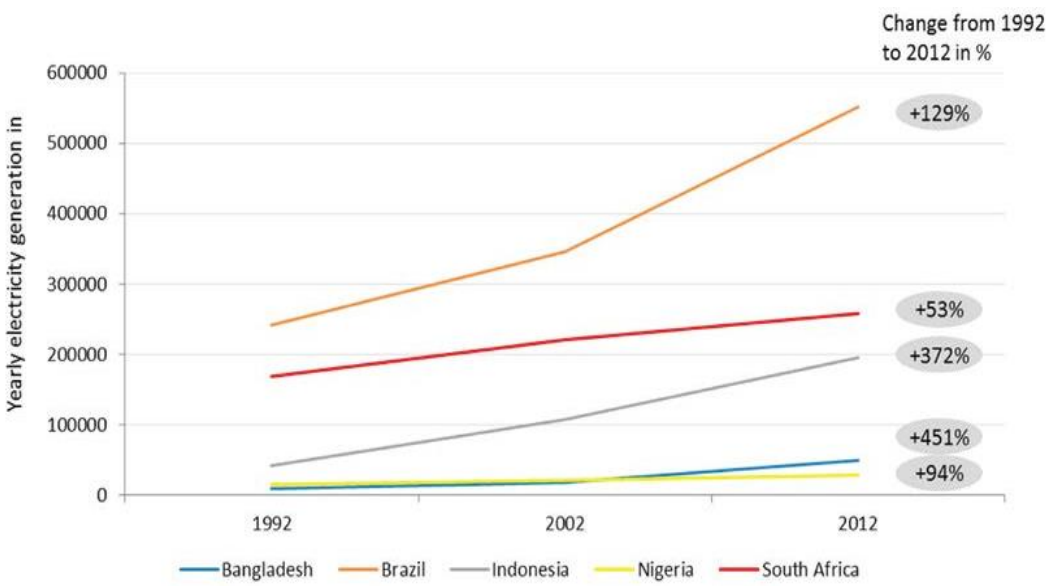

Source: IEA (2013).

Figure 1. Electricity Generation (GWh) in Nigeria and Peer Countries since 1992.

The country's electricity consumption per capita as at 2012 was 12 watts/person which is very low compared with most countries in the world like Brazil with 268 watts/person, Spain 645 watts/person and South Korea 1,038 watts/person in the same year (Usman and Abbasoglu, 2015).

Presently, Nigeria depends on its aged hydro plant installments and petroleum reserves for electricity generation. Majority of power plants in the country run on fossil fuel (natural gas and petroleum products)(Table 3) and whenever there is shortages of the fossil fuel due to vandals the power generation drops. Based on this fact, there is need for alternative renewable sources of fuel for our power plants for 100% supply cannot be over emphasized. The adoption of renewable energy technologies in a decentralized energy manner, especially for rural communities and in stand-alone applications, will improve electricity supply and enhance the overall economic development (Ajao, et al., 2009).

Table 3. Existing Nigerian Power Plant Fleet as at 2015

Power Station	Type	Year Completed	Installed Capacity (MW)	Installed Available Capacity (MW)	Capacity (MW) as at May 2015
AES	SCGT	2001	270	267	0
Afam IV - V	SCGT	1982	580	98	0
Afam VI	SCGT	2009	980	559	523
Alaoji NIPP	CCGT	2015	335	127	110
Delta	SCGT	1990	740	453	300
Egbin	Gas Fired Steam Turbine	1985	1320	931	502
Geregu	SCGT	2007	414	282	138
Geregu NIPP	SCGT	2012	434	424	90
Ibom Power	SCGT	2009	142	115	92
Ihovbor NIPP	SCGT	2012	450	327	225
Jebba	Hydro	1986	570	427	255
Kainji	Hydro	1968	760	180	181
Okpai	CCGT	2005	480	424	391
Olorunsogo	SCGT	2007	335	244	232
Olorunsogo NIPP	CCGT	2012	675	356	87
Omoku	SCGT	2005	150	0	0
Omotosho	SCGT	2005	335	242	178
Omotosho NIPP	SCGT	2012	450	318	90
River IPP	SCGT	2009	136	166	0
Sapele	Gas Fired Steam Turbine	1978	900	145	81
Sapele NIPP	SCGT	2012	450	205	116
Shiroro	Hydro	1989	600	480	350
Odukpani	SCGT	2013	561	70	0
Total			*12067*	*6840*	*3941*

Key: SCGT – Simple Cycle Gas Turbine, CCGT – Combined Cycle Gas Turbine.
Source: NERC 2015.

Nigeria projects that by the year 2020, the country's generation capacity would be in excess of 40GW (40,000MW), and the energy mix will constitute 69% thermal generation; 17% hydro; 10% coal; and about 4% of renewable (www.nipc.gov.ng).

Presently, most of the power received by Nigerian electricity consumers is on-grid power supplied by the Distribution Companies (DISCOs). Inadequate transmission infrastructure is among the constraints the on-grid power generation has over the years. The existing transmission system is only capable of delivering about 5,300MW (out of the total installed capacity of 12,522MW) of power to DISCO trading points. This is as a result of Nigeria's current weak transmission infrastructure which is majorly radial, which means that it's a single path of transmission with a power source at one end. This implies that any fault in the path could potentially lead to a collapse of the transmission network. The issue with transmission has been estimated to reduce the power generation capacity by a total of about 263MW. Although, the Transmission Company of Nigeria plans to upgrade the transmission system to a capacity of 11,000MW by 2020 (subject to adequate funding and completion of projects planned for implementation); the transmission infrastructure in its current state, without an upgrade and improved technology, is unable to accommodate the estimated increase in generation by 2020. Hence, there is need for decentralized renewable energy system in the country (Werner and Faruk, 2015).

2.2. Electricity Access in Nigeria

Electricity access is low in Nigeria which is the largest economy in Africa in terms of GDP and population (Emodi and Yusuf, 2015). At present, only 10% of rural households and 40% of the country's total population have access to electricity (Oseni, 2012). Among those who have access, a comparable number receive electricity services that are below the standards of quantity and reliability expected of an efficiently performing sector. The situation is significantly different at different geopolitical zones. Table 4 shows distribution of households without electricity access in the different geo-political zones of Nigeria (in Percentage). From Table 4, it is observe that the lack of electricity access is more severe in the northern parts of Nigeria with the North-East geopolitical zone having 71.6%.

Table 4. Distribution of households without electricity access in the different geo-political zones of Nigeria (in Percentage)

North-West	%	North-Central	%	North-East	%	South-West	%	South-East	%	South – South	%
Jigawa	56.5	Benue	72.0	Adamawa	71.4	Ekiti	15.2	Abia	33.3	Akwa-Ibom	38.3
Kaduna	42.4	Kogi	48.1	Bauchi	58.5	Lagos	0.3	Anambra	38.3	Bayelsa	36.9
Kano	56.2	Kwara	38.5	Borno	77.3	Ogun	20.4	Ebonyi	68.1	Cross-River	46.3
Katsina	59.7	Nassarawa	70.6	Gombe	55.4	Ondo	41.9	Enugu	48.5	Delta	46.3
Kebbi	54.4	Niger	56.6	Taraba	88.8	Osun	33.9	Imo	12.6	Edo	15.2
Sokoto	69.5	Plateau	71.3	Yobe	78.0	Oyo	38.8	Rivers	21.7	Zamfara	77.1
Average	59.4	Average	59.5	Average	71.6	Average	25.1	Average	40.2	Average	34.1

Source: NBS (2009).

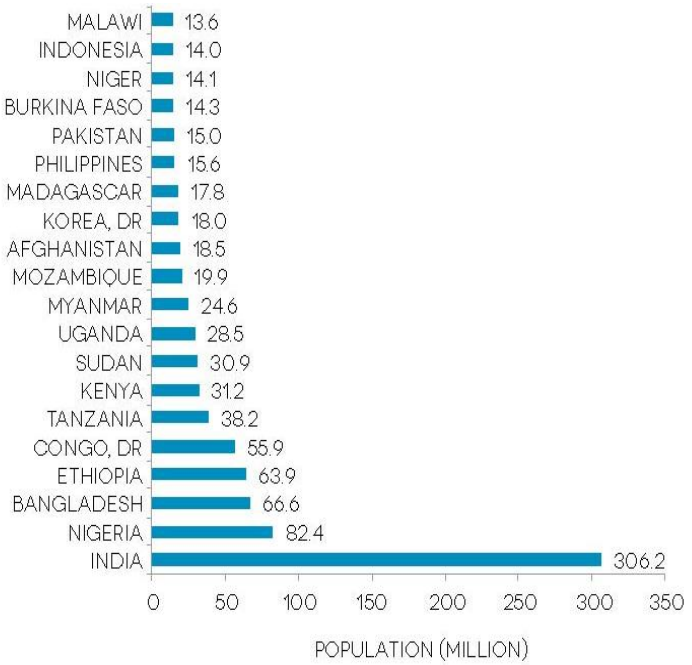

Source: World Bank Global Electrification Database, 2012; WHO - Global Household Energy Database, 2012.

Figure 2. The 20 countries with the highest deficit in access to electricity in 2010.

A report released by the World Bank and some foreign organizations has shown Nigeria taking the ignominious position of the second worst country with high electricity access deficit. The report states that 82.4 million Nigerians lack access to electricity. In an assessment of the worst 20 countries in the world, Nigeria came second to India with a population of 306.2 million people with lack of access to electricity (Figure 2). Unfortunately, while India, China, Indonesia, Pakistan, Bangladesh, Brazil, Philippines are moving very fast to resolve the challenge ahead of the Sustainable Energy for all by 2030, Nigeria is lagging with an annual increase in the access to electricity at the rate of 1.8 percent (Sustainable Energy for All Initiative, 2012).

Electricity access is more than just a connection to a distribution network; it requires that electricity is provided adequately as demanded and in a reliable, affordable manner. The provision of adequate and reliable electricity service on demand requires a balanced, planned expansion of generation capacity and transmission and distribution (T&D) for delivering electricity securely and efficiently, based on the location of generation plants and load centers, and coordinating with off-grid options where feasible. Policies and regulation are needed to achieve this, both to facilitate the large capital investments needed to bridge the access gap and to ensure that electricity services are financially viable and affordable for all, especially the poor (Heider et al., 2015).

There is no doubt that the present power crisis afflicting Nigeria will persist unless the government diversifies the energy sources in domestic, commercial, and industrial sectors and adopts new available technologies to achieve sustainable development through energy security while at the same time combat the challenges of global warming (Emodi and Ebele,

2016). In diversifying energy sources that is sustainable, effective utilization of renewable energy (RE) in decentralized form becomes the best option. Globally, there has been upward trend in the utilization of renewable energy in the generation of modern energy (electricity) (Oseni, 2012).The level of utilization of Nigeria's RE resources requires serious attention to salvage the country from a looming energy crisis.

2.3. Energy Resources in Nigeria

Energy resources of a country refer to the stock of materials and resources from which energy can be drawn with given present know- how. Energy resources are among the most important assets of any nation. It is a well-known fact that high rate of industrial growth is a function of the amount of energy available and the extent to which that energy is utilized (Shaaban and Petinrin, 2014).

Nigerian energy resources are categorized into conventional and non-conventional forms. The conventional energy resources consist of coal, crude oil, natural gas and hydroelectric power and lignite. The non-conventional energy resources in Nigeria include solar, nuclear fuels, geothermal, biomass, oil shales, tar sand, wind and tidal from sea (Nwanya, 1998). Table 5 and Figure 3 show the energy resources potential in Nigeria and the geographical distribution of these energy resources. From Table 5, it is seen that Nigeria is endowed with an abundant supply of natural energy sources, both fossil and renewable. These diverse resources are available all over the country. Figure 3 provides a general indication of regions in Nigeria with high potential for selected energy resources**.** If these resources are properly harnessed and effectively managed, Nigeria would have been among the richest energy generation in the world. Unfortunately, some of these resources are yet to be tapped while the maximum utilization of others is not in view, thus making energy a major concern and priority in the country. Hence, rapid growth in the energy need above generation levels and poor access have therefore always been the result of resources underutilization and a major constraint to economic growth.

Energy plays a double role in Nigeria's economy: as an input into all economic activities and as the mainstay of Nigeria's foreign exchange earnings through the export of crude oil and, more recently, from increasing natural gas exports. Nigeria's economy is heavily dependent on the oil sector and now on gas too, since both together account for 90 - 95% of export revenues, over 90% of foreign exchange earnings and nearly 80% of government revenues. The majority of Nigeria's exports of crude are destined for markets in the United States and Western Europe with Asia becoming an increasingly important market of late (Oyedepo, 2013).

The Nigeria National Petroleum Corporation (NNPC) revealed that Nigeria's oil production in 2014 stood at 2.5 million barrels per day (bbl/day) making it the 13th largest producer of crude oil in the world. It also holds the 9th largest natural gas reserves in the world. However, its gas-dominated electricity grid still experiences frequent collapses due to inadequate gas supply and obsolete infrastructures.

Many indigenous researchers have looked into the availability of renewable energy resources in Nigeria with a view to establishing their viability in the country. In this regard, the potential of generating electricity through the following renewable energy resources in Nigeria such as solar energy, wind energy, hydropower and biomass has been established and

confirmed feasible(Adaramola and Oyewola, 2011; Agbetuyi et al., 2012, Oji et al., 2012, Ladan, 2009). For example, Nigeria's annual average daily solar radiation is about 5.535 kWh/m^2/day, varying between 3.5 kWh/m^2/day and7.0 kWh/m^2/day at the coastal areas in the south and at the northern boundary respectively.

Table 5. Nigeria's energy reserves/potentials as at 2006

Resources	Reserves	Reserves (Billion ton)	% Fossil
Crude oil	33 billion bbl	4.488	31.1
Natural gas	4502.4 billion m^3 (159 trillion scf)	3.859	26.7
Coal and Lignite	2.7 billion tones	1.882	13.0
Tar Sands	31 billion bbl oil equivalent	4.216	29.2
Sub Total (Fossil Fuels)		*14.445*	*100.0*
Hydropower (Large scale)	10,000 MW		
Hydropower (Small scale)	734 MW	Provisonal	
Fuelwood	13,071,464 (Forest land)	Estimate	
Animal waste	61 million tones/yr	Estimate	
Crop residue	83 million tones/yr	Estimate	
Solar radiation	3.5 – 7.0 kWh/m^2-day	Estimate	
Wind	2 – 4 m/s (annual average	Estimate	

Source: Renewable Energy Master Plan (2006).

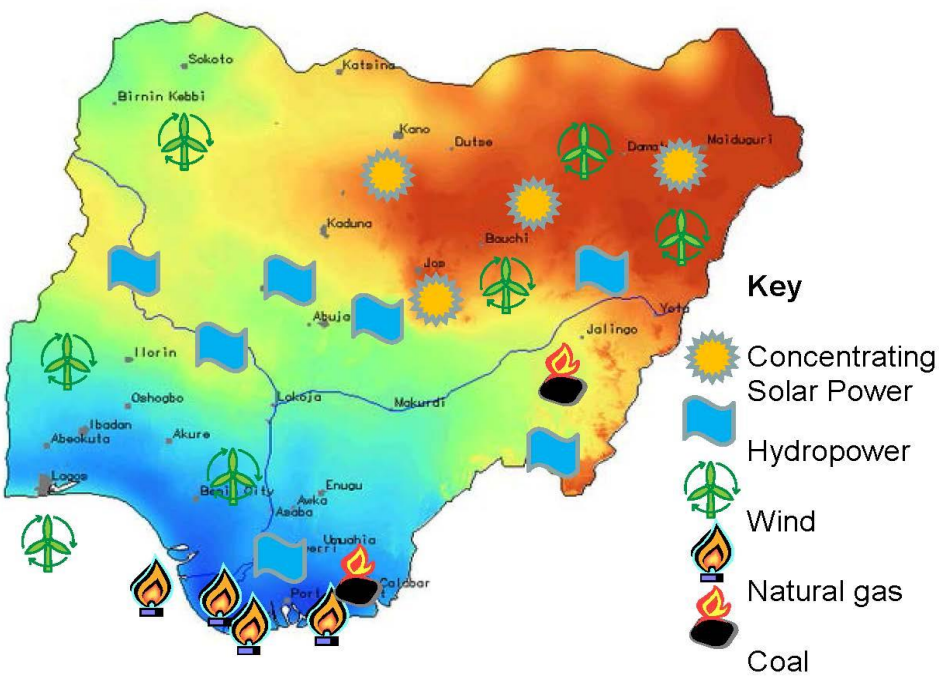

Figure 3. Diversity of geographic distribution of Nigeria's portfolio of energy sources.

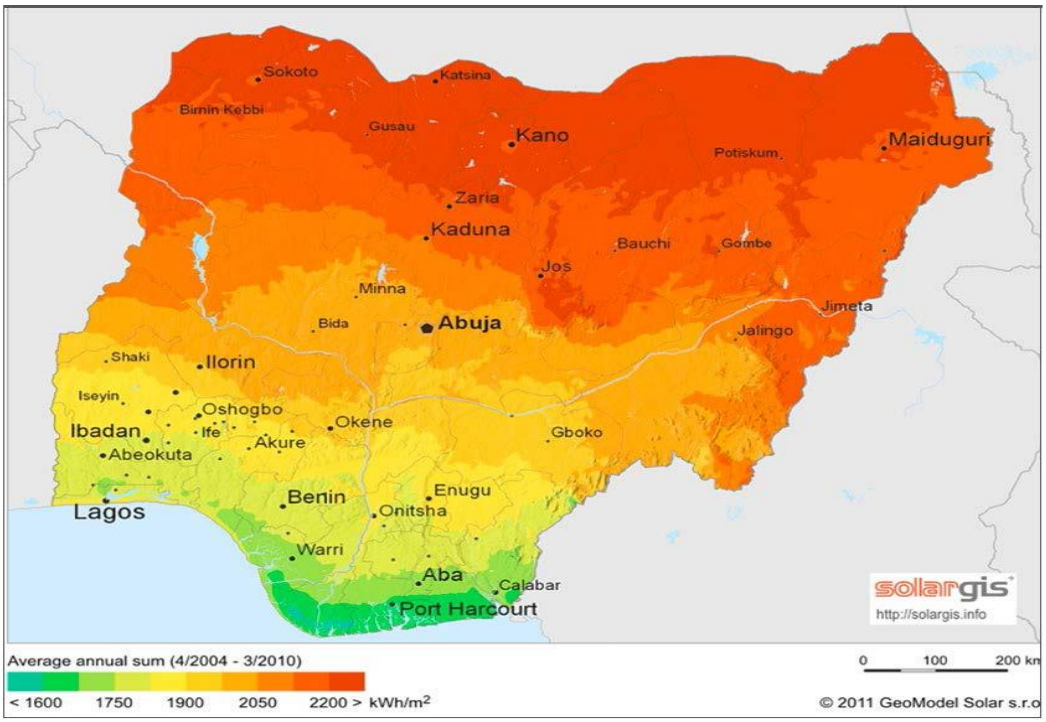

Figure 4. Solar Irradiation Levels of Global Horizontal Irradiation (GHI) in Nigeria.

Nigeria has a potential for electricity production from Solar PV technology in the range of 207,000 GWh per year if theoretically only 1% of the land area (e.g., 920 km² = 920 x 10^6 m²) were covered with state-of-the-art poly-crystalline PV modules, with an electricity yield of 1,500 Wh/Wp per year. This figure is tenfold the total electricity production of Nigeria in 2011. As can be seen from the map in Figure 4, the best potential for large-scale solar power plants (preferably PV) lies in the northern part of the country. Long-term annual average global horizontal irradiation (GHI) values in the northern states ranges from 2,000 to 2,200 kWh/m². This high solar irradiation is comparable to very high-yield sites in southern Spain, northern Africa, Australia and Latin America. The south of Nigeria has less potential for solar energy as it is often cloudy and has a longer rainy season.

The World Bank recommends in this context that off-grid solutions be developed using renewable energy sources, commenting that "PV and hybrid systems are already economically competitive for many off-grid applications. Gasoline and diesel generators produce power at levelised cost of energy (LCOE) between US$ 0.23 and $0.42/kWh. The cost of electricity from PV and hybrid PV-wind diesel systems are in the range of $0.30/kWh and $0.22/kWh, respectively. As the costs of renewables continue down the learning curve, and fossil fuel prices in Nigeria revert to global market prices ("export parity"), the economic advantages of renewables will become ever greater." It proposes that solar PV in particular be used for water pumping and irrigation (IEA, 2014).

Wind energy resource in Nigeria is available at an annual average speed of 2.0 m/s near the coast to 5.0 m/s at the height of 10 m in northern parts of the country. The Ministry of Science and Technology has carried out wind energy resource mapping (Lahmeyer; 2005).

This wind mapping project indicated wind speed of up to 5 meters per second in the most suitable locations, which reveals only a moderate and local potential for wind energy.

The highest wind speeds can be expected in the Sokoto region, the Jos Plateau, Gembu and Kano/Funtua. The stations at Maiduguri, Lagos and Enugu also indicated fair wind speeds, sufficient for energy generation by wind farms. Apart from these sites, other promising regions with usable wind potential are located on the Nigeria western shoreline (Lagos Region) and partly on the Mambila Plateau. The calculations indicate the highest energy yield at the coastal area of Lagos, followed by the Sokoto area and the Jos Plateau. The computed 3D wind map is shown in Figure 5. To date, the Federal Ministry of Power reports that an off-shore wind mapping is being undertaken (Vincent – Akpu, 2012). However, no details about this have been disclosed. Such information would beneficial for further investigation of the potential of wind power in Nigeria. There are two larger wind farm projects ongoing at present, namely 10 MW in Katsina, and 100 MW in Plateau State. As regards the 100 MW wind-power farm outside Jos, due diligence has been completed on the application for a license to operate. The owner reports that a provisional Independent Power Producer (IPP) license has been obtained from the National Electricity Regulatory Commission (NERC) acknowledging that JBS Wind Power Limited has met all regulatory requirements to commence operation. The smaller 10 MW Katsina pilot wind farm is being built by a French company on behalf of the Federal Ministry of Power (FMP) and is about to be completed (FMP, 2015).

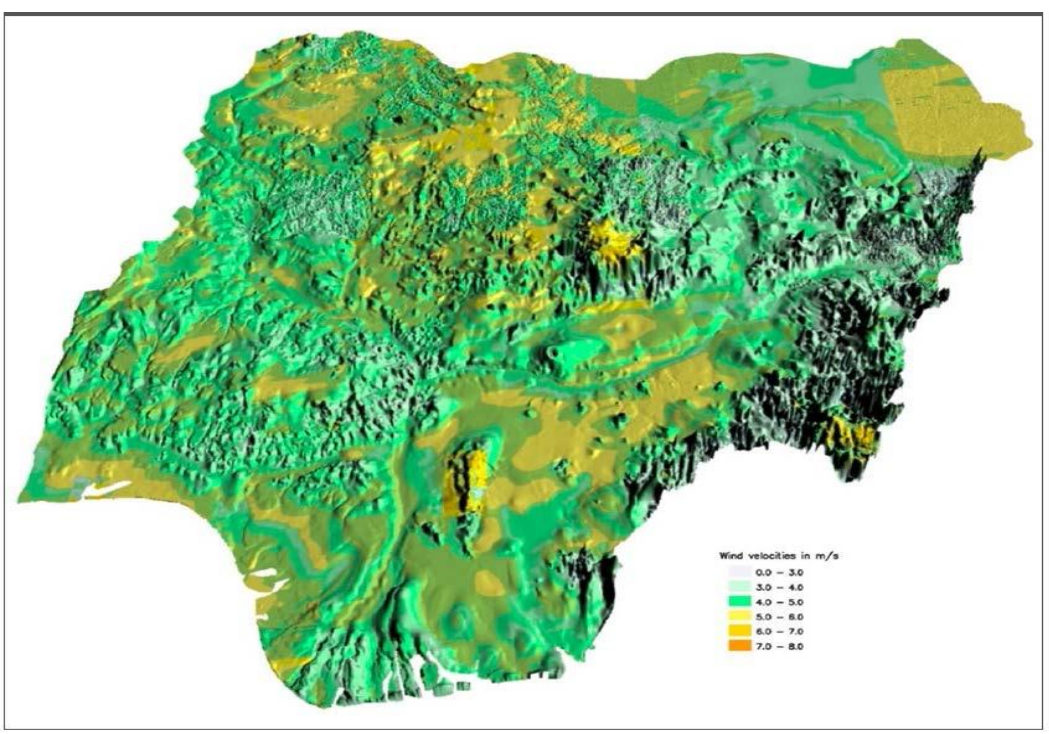

Source: Ministry of Science and Technology, Nigeria 2005.

Figure 6. 3D Wind Map of Nigeria 80 m above the Ground.

Nigeria ranked ninth in hydropower potential in Africa with technical hydropower energy at 32,450 GWh/yr. As at 2001, only 21.5% (6986 GWh/yr) of the hydro potential was used. Currently there are 1.9 GW hydropower capacity installed in 3 large power plants (Kainji: 760 MW; Jebba: 570 MW; Shiroro: 600 MW), although only roughly half of it is operational (NERC, 2012). A World Bank reference scenario following Federal Government of Nigeria (FGN) plans and feedback from stakeholders suggests hydropower utilization could be increased to 7.2 GW by 2035 (World Bank, 2013). The ECN estimates the large hydro potential even at 11 250 MW and the small hydro potential at 3 500 MW (ECN, 2013). In spite of this huge potential, hydropower capacity in Nigeria still remains underexploited. Current hydropower generation is about 14% of the nation's hydropower potential and represents some 30% of total installed grid connected electricity generation capacity of the country (Oyedepo, 2012).

Figure 7 shows flow patterns vary considerably between wet and dry season. The large seasonal variation (some rivers only showing 5 to 10% of flow in the dry season) may significantly restrict the economical viable potential for hydropower in the country. This is particularly true for run-of-river plants typically applied for small and mini hydro power. It must be observed here that Small Hydropower (SHP) has gained rapid consideration in both the developed and developing economies of the world because of its inherent advantages like in-excessive topography problems, reduced environmental impact, minimal civil works and the possibility for power generation alongside with irrigation, flood prevention, navigation and fishery.

In recent studies, hydropower potential sites are distributed in 12 States and in the river basin. However, SHP potential sites exist in virtually all parts of Nigeria. There are over 278 unexploited sites with total potentials of 734.3 MW (Essan, 2003). So far about eight (8) small hydropower station with aggregate capacity of 37.0 MW has been installed in Nigeria by private company and the government**.** Some around Jos Plateau, where there is 2MW Station at Kwall fall on N'Gell river (river Kaduna) and 8MW station at Kurra fall, which was developed by a private company (NESCO) more than 75 years ago. The technically exploitable small hydro power (SHP) capability in Nigeria is high but underutilized. The SHP development programme in the last year has been able to assess additional 22 potential sites for developments.

A cost comparison between small-scale hydro power plants and diesel generators for rural electrification clearly indicates the cost effectiveness of the former. It will therefore be useful for the country if more attention is paid to the exploitation of small scale hydro resources for power generation.

Studies by indigenous researchers (Ladan, 2009; Simonyan and Fasina, 2013; Ogwueleke, 2009; Agbro and Ogie, 2012; Agba et al., 2010) revealed that the country has high potential for bioenergy development because roughly 74 million ha of Nigeria's total land (98 million ha) is arable and about 60% of the arable land is lying idle.

In view of the increasing demands for electricity in the country, alternative off-grid renewable energy solutions are needed to diversify power generation from the vast supply of renewable biomass materials. Nigeria, as an agrarian economy has ample opportunity to bridge the electricity demand-supply gap by utilizing its abundant biomass resources such as agricultural residues (Garba and Zangina, 2015). The biomass resources of Nigeria can be identified as wood biomass, forage grasses and shrubs, residues and wastes (forestry, agricultural, municipal and industrial) as well as aquatic biomass.

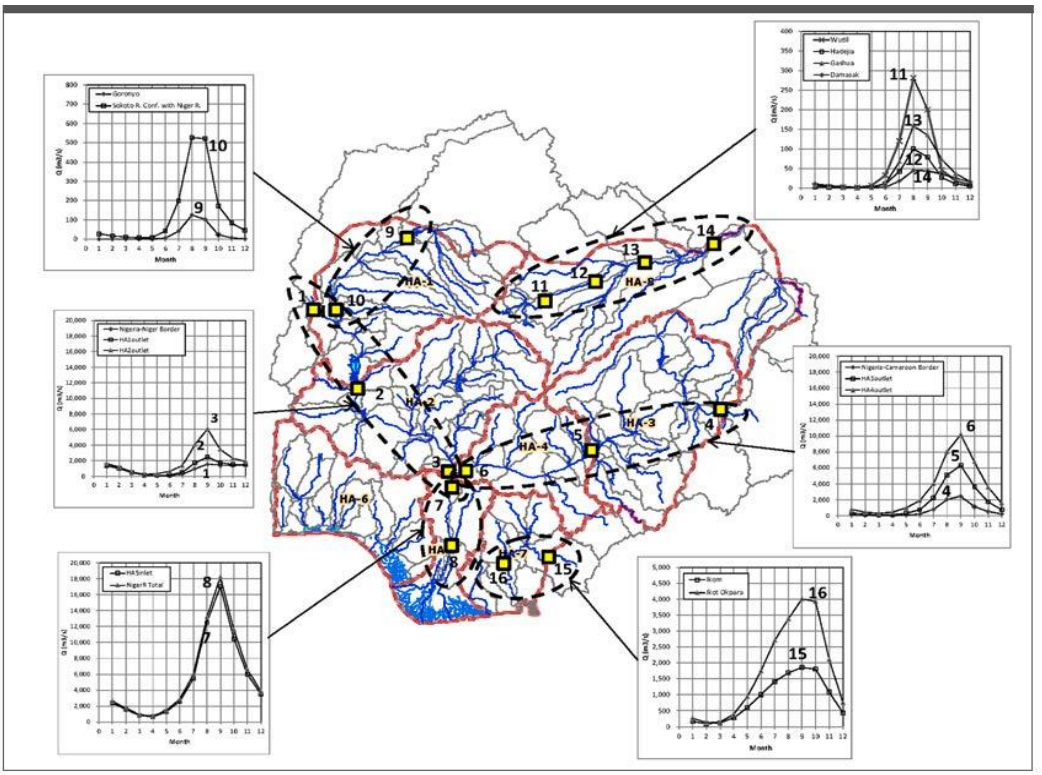

Figure 7. Hydro Potential: Seasonal Flow Pattern at Representative Points.

From the perspective of available land and wide range of biomass resources, Nigeria has significant potential to produce biofuels and even become an international supplier. Bioenergy feedstock is not only abundant in Nigeria, it is also widely distributed. Nigeria is the largest producer of cassava in the world. Nigeria could also become a major player in the biofuel industry given the enormous magnitude of various waste/residues (agricultural, forestry, industry and municipal solid) available in the country.

The country well-endowed with abundant biomass energy resources, which are not being utilized adequately. Putting the huge quantities of biomass resources, mostly in the form of agricultural residues and wastes, which are currently disposed by burning or dumping, to energy production could potentially increase the energy supply thereby increasing energy mix and balance in Nigeria. There are also environmental benefits of reducing greenhouse gas emissions by generating electricity from biomass as well as supply of electricity in the rural areas (Pereira et al., 2012; Simonyan and Fasina, 2013). There exist a great opportunities for exploitation of different types of biomass in Nigeria with an estimated 2.01 EJ (47.97 MTOE) biomass residues and wastes available to be exploited annually.

For energy purposes, Nigeria is using 80 million cubic meters (43.4×10^9 kg) of fuel wood annually for cooking and other domestic purposes. The energy content of fuel wood that is being used is 6.0×10^9 MJ out of which only between 5 and 12% is the fraction that is gainfully utilized for cooking and other domestic uses (Ajao et al., 2009).

According to assessment carried out by World Bank (2013), it was expected that by 2015 conversion of biomass-to-power could deliver as much as 1,643 GWh/year, with the figure

rising to 13,140 GWh/year by 2035. Unfortunately, to date, there has been little mention of any plans to establish large biomass power plants, for example along the model developed in Brazil for sugarcane plantations, where the crushed fibers (bagasse) are used as the feedstock to great effect. This is even more surprising given the prevalence of academic literature demonstrating the biomass potentials on the ground in Nigeria.

3. SUSTAINABLE ENERGY TECHNOLOGY(SET) DEVELOPMENT

Sustainable development may be broadly defined as living, producing, and consuming in a manner that meets the needs of the present without compromising the ability of future generations to meet their own needs. The aim of sustainable development is to achieve improvement in quality of life, including improving standards of living in less developed countries while safeguarding the ecological processes upon which life depends (Oyedepo, 2012). In this context, the concept of sustainable energy technology (SET) refers to the energy technology that is capable of providing energy to meet consumers' needs (demands) at an affordable cost on a long-term basis without disturbing (compromising) ecological balance (Ali, 2011). That means SET is environment-friendly and cost-effective. However, the viability of SET adoption depends on the socio-economic and technical background of rural dwellers in Nigeria.

Reliable energy supply is essential in all economies for lighting, heating, communications, industrial equipment, transport, etc. Purchases of energy account for 5 to10% of gross national product in developed economies. However, in some developing countries, fossil fuel imports (i.e., coal, oil, and gas) may cost over half the value of total exports; such economies are unsustainable, and an economic challenge for sustainable development. World energy use increased more than ten-fold during the 20^{th} century, predominantly from fossil fuels and with the addition of electricity from nuclear power. In the 21^{st} century, further increases in world energy consumption may be expected, largely due to rising industrialization and demand in previously less developed countries, aggravated by gross inefficiencies in all countries. Whatever the energy source, there is an overriding need for efficient transformation, distribution, and use of energy (Twidell and Weir, 2015).

Thus energy sustainability is considered to involve the sustainable use of energy in the overall energy system. This system includes processes and technologies for the harvesting of energy sources, their conversion to useful energy forms, energy transport and storage, and the utilization of energy to provide energy services such as operating communications systems, lighting buildings and cooking. Thus, energy sustainability goes beyond the search for sustainable energy sources, and implies sustainable energy systems, i.e., systems that use sustainable energy resources, and that process, store, transport and utilize those resources sustainably (Oyedepo, 2015).

Sustainable energy technologies are necessary to save the natural resources avoiding environmental impacts which would compromise the development of future generations (Oyedepo, 2013). Delivering sustainable energy will require an increased efficiency of the generation process including the demand side. In attaining sustainable development, increasing the energy efficiencies of processes utilizing sustainable energy resources plays an

important role. The utilization of renewable energy offers a wide range of exceptional benefits (Hepbasli, 2008).

As a complementary measure, development of renewable energy resources in Nigeria is important to promote economic growth, protect ecosystems and provide sustainable natural resources. Furthermore, renewable energy resources development in developing countries like Nigeria will promote poverty reduction, improve education quality, maternal health, gender equality, and aim at combating child mortality, AIDS and other diseases which would be in line with the Millennium Development Goals (United Nations, 2006). Moreover, the sustainable energy technologies often reduce or avoid greenhouse gases (GHGs) emissions, such projects would also address the climate change issue (Doukas et al., 2009; Karakosta et al., 2012). However, these kinds of practices are, unfortunately, rare in the country. Notwithstanding, with effective policy formulation by government and private partnership involvement in renewable energy technologies, there is guarantee of sustainable national development in Nigeria.

3.1. Challenges for Sustainable Energy Technology Development in Nigeria

Needs and availability of raw material are sadly not always guarantors of technology development. This is true in this case for sustainable energy development in Nigeria. The following are recognized potential challenges to the development of sustainable energy technology in the country:

- *Lack of related technical skill*: Historically, a major reason for failed renewable energy system projects in Nigeria has been the absence of know-how transfer of the new technology to individuals in the communities that received them. The executors of new technology often overlook the need for local technical training, maintenance service expertise development, user education and awareness. Renewable energy technician training will be absolutely necessary for any renewable energy project to be successful. Builders will need education in renewable energy construction techniques and the public psyche will need to be shifted to adapt their lifestyles to a changing energy system.
- *Uncertainty of finance sources*: Renewable energy technology is still expensive at its current stage of development, even to governments. For rural communities and individuals, the cost of owning a self-sponsored renewable energy system is simply cost prohibitive. Short of a donor-developed project by an NGO, an innovative financing approach will be needed to implement a renewable energy based infrastructure in the rural communities where the need is the greatest.
- *Orderly implementation of the new energy systems*: This is important in order to cut down on sloppy projects and ―quackery. Typical of any newly introduced social apparatus, the excitement of new energy technology coupled with the yearning of citizens for a steady power supply is attracting a myriad of ―quacks into the renewable energy development business. One of the greatest impediments to adoption of the new energy system will be disappointed citizens who are burnt with

failed renewable energy projects executed by illegitimate businesses wanting only to make a profit.

- Poor resource management and lack of commitment by various levels of government to invest in energy development are also real challenges that may mitigate a successful implantation of any sustainable energy technology. When resources are transformed and managed properly they are capable of providing fountains of prosperity. However, when mismanaged, they are equally capable of producing mountains of misery to the society.

4. RENEWABLE ENERGY TECHNOLOGIES DEPLOYMENT

Renewable energy technologies (RETs) can be deployed to produce marketable energy by converting natural phenomena into useful forms of energy. These technologies use the sun's energy and its direct and indirect effects on the earth (solar radiation, wind, falling water and various plants, i.e., biomass), gravitational forces (tides), and the heat of the earth's core (geothermal) as the resources from which energy is produced. These resources have massive energy potential, however, they are generally diffused and not fully accessible, most of them are intermittent, and have distinct regional variability (Bazmia and Zahedia, 2011). Nowadays, significant progress is made by improving the collection and conversion efficiencies, lowering the initial and maintenance costs, and increasing the reliability and applicability.

The potential role of renewable energy technologies (RETs) in transforming global energy use, with a focus on sustainable development and increasing the welfare and health of the rural poor, is enormous. Renewable energy sources, such as biomass, biogas, wind, solar, mini-hydro, geothermal, can provide sustainable energy services, using a mix of readily available, indigenous resources with potential to result in minimal local environmental damage or net emissions of GHGs. A transition to renewables-based energy systems looks increasingly desirable and possible because the costs of solar and wind power systems have dropped substantially in the past three decades. Most forecasts indicate that costs of renewably produced electricity should continue to decline, while the price of oil and gas continues to fluctuate. If social and environmental costs are included in the estimation of electricity costs, RETs become still more attractive (Kuku, 2009).

The objectives of harnessing renewable energy (RE) as primary energy source are focus on provision of sustainable energy to the economically subjugated fraction of the society, combat energy shortage, encourage the development of rural infrastructure and provide clean energy from the perspective of the Kyoto directive towards global decarbonization. The popularity of RE development can be directly allied to the growing trend of environmental concern and the rapidly depleting reserves of conventional energy resources due to the aggressive utilization. These emergent concerns call for a viable alternative solution to the contemporary environmental challenges and the energy crisis scenario through sustainable means (Albadi and El-Saadany, 2010).

The increasing energy demand, the rapidly depleting fossil fuel reserves and the environmental problems associated with the use of fossil fuel have necessitated the development of alternative energy sources - renewable energy sources (such as wind energy,

solar energy, hydro power etc) for electricity generation in Nigeria. It is reported that the electricity generation in Nigeria as at 2015 was less than 5,000 MW due to fluctuations in the availability and maintenance of production sources, leading to a shortfall in supply (Zubairu et al., 2015). However, analyses of available renewable energy resources data for selected cities have confirmed a high prospect of renewable energy resources in Nigeria. Several studies on renewable sources of energy have also been performed.

The Nigerian Energy Commission and the Solar Energy Society of Nigeria have been tasked with generating a standalone solar-powered solution for the remote rural dwellers. The country is looking towards further development of the hydropower resources and other renewable energies such as wind, solar and biomass to close the generation shortfall and foster the economic growth. The level of utilization of Nigeria's RE resources requires serious attention to salvage the country from a looming energy crisis (Shaaban and Petinrin, 2014).

Since the early 2000, Nigeria has identified RE as an additional source to improve electrical power generation. Presently, RE is being developed for empowering the local economies, but the RE incorporation to the national grid is yet to be implemented at a greater scale (Abdullahi et al., 2015). Nigeria is among the developing countries that are slowly striving to include RE in their future energy development. Amongst the reasons for the slow uptake in RE are high capital cost of initial financial investment as well as lack of adequate knowledge regarding the benefits of RE.

As stated earlier, in Nigeria, there is high solar irradiation and excellent wind speed that can be effectively utilized for electricity generation. To maximally benefit from these, there is a greater need for good leadership and good governance.

Many experts now argue that technologies such as solar, wind, and small-scale hydropower are not only economically viable but also ideal for rural areas. Renewable energy technologies (RETs) are cost-competitive with conventional energy sources in applications such as solar water heating, off-grid electrification with solar photovoltaics (PV), small-scale biomass power generation, biofuels, grid-connected and off-grid wind power, small hydropower, geothermal power, and methane utilization from urban and industrial waste (Painuly, 2001).

4.1. Development of Renewable Energy Technologies in Nigeria

In Nigeria as in other developing nations, the demands for sustainable energy are increasing due to population and developmental growth. But the available infrastructures for providing and extending these required energy especially to rural areas have continued to diminish and have become grossly inadequate in recent times. The realization of this fact have necessitated the need for the nation to identify and promote the development and utilization of other renewable energy sources such as wind, small or mini hydropower sources to augment the existing ones for the socio-economic development of the unreached rural areas of Nigeria (Otuna et al., 2012).

Recently, modern and efficient technologies have been used to develop and adopt devices for the utilization of renewable energy resources by the following Research Centers of the Energy Commission of Nigeria:

- Center for Energy Research and Development, Obafemi Awolowo University, Ile-ife, Osun State;
- Centre for Energy Research and Training, Ahmadu Bello University, Zaria, Kaduna State;
- National Centre for Energy Research and Development, University of Nigeria, Nsukka, Enugu State;
- Sokoto Energy Research Center, Usman Dan-Fodio University, Sokoto, Sokoto State.

The Centers at Ile-Ife and Zaria work on peaceful application of Nuclear Science and Technology while those at Nsukka and Sokoto work on solar energy and other renewable energy sources.

Raw materials used for some of these devices have more than 90% local contents. Some of these appliances include:

- Solar Crop Dryers (such as the 2 tone capacity Rice Solar Dryer at Agbani, Enugu State and 2 tone capacity Forage Solar Dryer at National Agricultural Production Research Institute, Ahmadu Bello University, Zaria, Kaduna State), which can be used to process agricultural products such as rice, maize, pepper, tomatoes, cocoa, tea, and coffee;
- Solar Water Heaters for providing hot water in hotels and hospitals for bathing and washing, such the 1000 liter capacity Solar Water Heater at the maternity ward of Usman Dan-Fodio University Teaching Hospital, Sokoto, Sokoto State;
- Solar PV Water Pumping for clean potable water, such as the 7.2k Wp Solar PV Plant at Kwalkwalama in Sokoto, the 2.85kWp Solar PV Plant at the centre for mentally-ill Destitutes at Itumbuzo in Abia State and the 5.00kWp Solar PV Plant at Comprehensive Health Centre in Laje, Ondo State;
- Biogas Plants for cooking gas and bio-fertilizer, such as the $20m^3$Biodigester at Ifelodun Cooperative Farm at Agege, Lagos State, the $10m^3$ biogas plant at Achara in Enugu State and the $30m^3$ biogas plant at Zaria Prison in Kaduna State; and 5kWp wind power plant at Sayya Gidan Gada in Sokoto State;
- The Energy Commission of Nigeria, the defunct Power Holding Cooperation of Nigeria and MTN-Nigeria are collaborating with the World Bank on a bio-fuel for rural electrification project in Nigeria. The bio-fuel is to be sourced from Jatropha Plant or any economically viable energy crop on a long term basis. Similarly, the Energy Commission of Nigeria signed another MOU with Green Shield of Nigeria (a registered NGO with diversed interest in alternative energy sources etc) to produce bio-diesel as a renewable energy for domestic and commercial uses in Nigeria, using Jatropha plant.
- The Renewable Energy Programme office, Adamawa State Government and Green Carbon Afrique is developing sugarcane based biofuel plants in Girei and Demsa Local Government Areas of Adamawa State covering 2,000 hectares of plantations. This initiative is to produce sugar for local use and export, ethanol and ultimately electricity. This integrated project is being replicated in ten states of the country.

- Currently, rice production and processing in Nigeria is typically undertaken by small local farmers using basic processing technology. Typical issues limiting economies of large-scale rice production include lack of access to improved technologies, the high costs of energy for parboiling, and lower output quality (post processing). However, working in conjunction with Carbon Quest and Adamawa State, the Renewable Energy Programme office is establishing an integrated "Rice Processing and Power Generating Facilitator", to the economic benefit of the investing state, garnering the advantages of large-scale rice production and self-generated power from the rice husks.

As pointed above, there have been a number of pilot projects in renewable energy in Nigeria. However, so far very few initiatives have been scaled up or replicated. In the following section we highlight some of the key challenges that practitioners have identified in facilitating local energy provision in low-income communities in Nigeria.

4.2. Barriers to Penetration of Renewable Energy Technologies in Nigeria

Despite technological developments and economic viability for several applications, renewable energy sources have been tapped only to a small fraction of its potential in Nigeria. This is due to the existence of several types of barriers to the penetration of renewable energy. Among these barriers are:

4.2.1. Policy and Regulatory Barriers

The focus of national policy has consistently been on centralized conventional sources of electric power. Several incentives were established to promote investments in conventional power generation. Subsidizing grid power has so far penalized investments in alternative energy solutions. This lack of a level playing field for all energy sources and technologies has constituted a formidable barrier to the growth of alternative electricity services.

Until lately, the defunct Power Holding Company of Nigeria (PHCN) was the only entity legally permitted to produce and distribute electricity. Under the 2005 Act, independent power producers are permitted to operate, however, the legal framework for successfully implementing PPA is still evolving. The perception of significant regulatory risks by potential investors and financial institutions compound the challenges faced by potential renewable electricity investors. Moreover, guaranteed access to the grid is an important element of an investment decision to embark on grid-connected power projects. At present, a non-discriminatory open access to the national electricity grid, for renewable power, is not assured.

4.2.2. Financing and Investment Barriers

In 2011, the government approved electricity prices of between N4/Kwh and N6/Kwh for single-phase consumers; between N6/Kwh and N8/Kwh for industrial users; and between N8/Kwh and N12/Kwh for the highest demand users, but the cost of electricity production was N10 per Kwh. This pricing regime discouraged the entry of profit oriented private investors (Bello, 2013). The existing law or absence of enabling legislation has been a greater

deterrent to private investment than the tariffs. Renewable energy projects have high initial costs. This affects the overall cost of energy produced per kWh. Investors will not be favorably disposed to wind, small hydro or power from cogeneration plants if they will not make profit by selling the electricity. Average electricity tariff in Nigeria is put at about N6.75 per KW-h (approximately 5 cents per kWh). Average cost of typical sources of renewable power for mini hydro is 5-10 cents; solar PV: 20-40 cents; biomass power: 5-12cents; wind power: 6-10 cents. Without adequate financial incentives market entry will be difficult.

Nigeria has no significant manufacturing capacity for components of renewable energy technologies. The existing capacity in solar PV and small hydro plants is limited. Significant supply chain constraints include long project implementation periods, high import tariffs, bottle-necks in the customs clearing of goods and the issue of corruption.

4.2.3. Technological Barrier

As noted in the 2005 National Renewable Energy Master Plan supplies and servicing for renewable electricity projects are not readily available in Nigeria. Therefore, potential IPPs may face significant logistical challenges in procuring equipment and maintenance support for renewable electricity projects.

Beyond the local availability of supplies, there are significant gaps in the capacity for manufacture and maintenance of system components such as small hydro and wind turbines. In most cases, the choice and design of turbines are site-specific. With no local turbine manufacturers available in Nigeria, this adds to project complexity and costs. The simple fact that the project will be dependent on manufactures of the turbines for spares and major maintenance presents a major technical challenge. To compound these barriers, these projects are often located in remote areas and therefore face significant challenges in attracting competent and qualified manpower for operations.

4.2.4. Limited Public Awareness

There is limited public awareness of the potentials of renewable electricity in meeting some of the energy and development challenges facing the country. The inadequacy of awareness creates a market distortion which results in higher risk perception for potential renewable electricity projects. The general perception is that these forms of energy technologies are not mature and only suited for niche markets.

4.2.5. Standards and Quality Control

A major constraint to the development of the renewable energy market in Nigeria is the poorly established standard and quality control of locally manufactured and imported technologies. Creating quality assurance is a precondition for building consumer confidence and in growing the market for renewable energy. Two important dimensions to issues of quality include the perception of potential users, poorly developed regime for standards setting, testing and certification as well as professionalism among operators.

4.2.6. Inadequate Resource Assessment

The growth of the renewable power industry will depend to a large extent on the availability of a solid resource database. Reliable and up-to-date sources of data will assist investors in making decisions on renewable electricity in the country.

4.2.7. Intermittency of Resource Availability

An underlying barrier affecting all renewable electricity resources is the intermittency of their availability. The challenge of energy storage and system management presents a major challenge and adds to the complexity and costs of renewable electricity.

The Policy Guideline establishes a framework to address the above barriers. It creates measures that enable market expansion and private sector participation in renewable electricity business. It further facilitates grid-connected and off-grid operations as well as increased role for renewable electricity in rural electrification.

4.3. Decentralized Renewable Energy Systems

Energy will always be at the forefront of growth and development. Nigeria's renewable energy potentials are too promising to be ignored. With projections estimating Nigeria's fossil fuel reserves to be depleted to an uneconomical point by 2050 (Shaaban and Petinrin, 2014), more than ever the time to pay close attention to decentralized renewable energy generation is now.

Today, renewables are seen not only as sources of energy, but also as tools to address many other pressing needs, including: improving energy security; reducing the health and environmental impacts associated with fossil and nuclear energy; mitigating greenhouse gas emissions; improving educational opportunities; creating jobs; reducing poverty; and increasing gender equality.

Presently, most of the power received by Nigerian electricity consumers is central (on-grid) power supplied by the Distribution Companies (DISCOs). On-grid power generation has over the years had its constraints, some of which are: unavailability of gas, inadequate transmission infrastructure, liquidity issues in the Nigerian Electricity Supply Industry (NESI), non-completion of Nigerian Integrated Power Project (NIPP) Plants etc. It is imperative to note that whilst the issues raised above are being resolved, Nigeria has to look at viable solutions for increasing access to electricity in the country through decentralized energy system.

The use of decentralized renewable electricity is a promising way to meet the demand for basic energy needs in Nigeria, especially among the rural dwellers. Such systems – which include, for example, solar home systems, small wind and mini-hydro, and portable solar lanterns – do not require installation of costly transmission lines and are becoming increasingly affordable to improved economies of scale as a result of the growing number of users and technical improvements. In addition, decentralized systems are more likely to be manufactured and/or repaired locally and are hence, less dependent on foreign technical assistance, strengthening the sustainability of rural livelihoods (Oyedepo, 2014).

Considering Nigeria's plans to increase generation capacity in the coming years and the low level of access to electricity in the rural areas; there is need for significant investments in

decentralized (off-grid) energy system generation. Among the prospects of decentralized energy system solutions in Nigeria include the following:

4.3.1. Potential to Grow Industrial Clusters and Small Cottage Industries

Most industrial clusters and some small cottage industries require uninterrupted power supply to function optimally. The power supplied could be generated through fully decentralized renewable power plants or embedded within distribution networks. This could potentially transform the economy of these areas; increase profitability for the existing businesses; create jobs; and breed a crop of customers who are willing to pay for electricity supplied. In view of this, the Manufacturers Association of Nigeria (MAN) has identified about 28 clusters for mini-grid modular plants ranging from 5 to 50MW in areas including Ogun and Lagos States (www.thisdaylive.com).

4.3.2. Opportunity to Expand and Refurbish Distribution Networks of the DISCOs

In line with the NERC Regulation for Independent Electricity Distribution Networks, 2012 (IEDN Regulations), decentralized renewable generation plants require Independent Electricity Distribution Networks (IEDNs) to supply electricity to end users, save for eligible customers upon declaration by the Minister of Power, who can be supplied to directly. This creates opportunities for investors who may wish to create off-grid projects with their own IEDN. This could potentially be a win-win situation for DISCOs who could either collaborate with developers to expand or refurbish their network; add to their number of paying customers; or acquire the developer assets given the right regulatory framework.

4.3.3. Opportunity to Collaborate with State Governments

Many state governments are looking to partner with investors to develop more decentralized (off grid) projects than on-grid projects. This may be to avoid regulatory constraints (as a result of the fact that most laws, regulations, and agencies for on-grid projects are controlled by the federal government) which state governments may experience when executing on-grid projects. It must, however, be noted that whilst these constraints may be minimal with off-grid projects, they cannot be totally avoided, as NERC, being the regulator of the power sector still has the power to issue off-grid licenses and generally regulate the power sector. Notably, the Lagos State Government has initiated some Independent Power Projects (IPPs) to provide electricity to its own establishments, including schools, ministries, hospitals, and courts. As at July, 2015, the state had commissioned five IPPs with an accumulated capacity of 47.5MW.

4.3.4. Access to Other Fuel Alternatives

Most of the power plants in Nigeria are gas fired thermal plants. Given the current constraints with gas, decentralized renewable power plants are able to take advantage of diverse and hybrid fuel sources like renewables (solar, wind, biomass) and because the power is not generated on grid, transmission constraints with renewables are eliminated. This would be particularly more useful in areas where there is limited gas supply, e.g., the northern part of Nigeria where solar, wind, and hydro sources are prevalent.

4.3.5. Considerable Insulation from the Issues within the NESI

Given Nigeria's considerable power requirements, decentralized energy system solutions within a cluster of customers willing and able to pay present available investment opportunity for power developers. This is particularly because their investment would be insulated from the current liquidity issues in the NESI.

4.3.6. Opportunity for Rural Electrification

Decentralized energy system solutions are also useful in Nigeria in view of some topographical or geographical challenges in the rural areas which have made it uneconomical to extend the grid to such areas. Rural electrification in Nigeria is currently in a weak and dilapidated state; hence there is a dire need for investments. It is expected that many rural electrification projects will spring up this year. A priority for the renewable energy agency (REA) should be the sustainable development of rural mini-grids that are targeted towards the economic development of these rural communities so that the communities can learn the culture of paying for electricity.

4.4. Policies and Renewable Energy Resources Initiatives

To deploy renewable energy sources for economic growth in Nigeria requires committed political will and plans with set target, time lines and incentives legal and appropriate institutional frame works.

In addition to this, well – formed, comprehensive and coherent energy policies are essential in guiding towards efficient utilization of renewable energy resources. It must be emphasized however that the existence of an energy policy, while crucial, does not guarantee responsible management of a country's energy resources. Nigeria currently has no comprehensive Renewable Energy Policy. There was brief mention of renewable energy technologies in the 2003 National Energy Policy, but it was not detailed enough to give proper guidance for implementing a national renewable energy programme. The Energy Commission of Nigeria in November 2005 (ECN 2005) drafted a National Renewable Energy Master Plan (REMP), in line with the goals laid down by the National Energy Policy, the National Policy on Integrated Rural Development, the Millennium Development Goals (MDGs) and the National Economic Empowerment and Development Strategy (NEEDS).

The overall objective of the REMP is to articulate a national vision, targets and a road map for addressing key development challenges facing Nigeria through the accelerated and exploitation of renewable energy. It classifies renewable energy targets into three levels according to the time frame for implementation: Short term (2005-2007); Medium term (2008-2015); and Long term (2016 – 2025). Therefore the whole plan spans across a period of 20 years, by which time new renewable energy sources are expected to be contributing 10 percent of the nation's energy supply.

The REMP comprises six different activities to be implemented within six different programmes:

- Framework Programme for Renewable Energy Promotion
- Nigerian Solar Programme

- Nigerian Small Hydro Programme
- Nigerian Wind Programme
- Nigerian Biomass Programme
- New Energy Research and Development Programme

One shortcoming of the REMP is that it does not advocate a separate rural renewable energy programme. It does acknowledge that renewable energy is a viable tool for fostering rural empowerment and development, but it does not fully capitalize on the unique opportunity presented for rural development by renewable energy technologies.

The REMP is useful at the present stage of renewable energy in Nigeria, but it should not be viewed as a substitute for a National Renewable Energy Policy. Indeed, the REMP makes provision for the review of policy and regulatory instruments within the Framework Programme for Renewable Energy Promotion. The Framework Programme is in fact designed to address every one of the likely barriers to implementation of renewable energy. This means that any piece of research done to eliminate any of the barriers will contribute to strengthening the Framework Programme laid out by the REMP. This is extremely significant, as the Framework Programme provides the general context within which each of the other specific programmes will work smoothly.

The objectives of the REMP are laudable, but government is already falling behind on its plans. The deadline for reaching the short term goals (2007) is past, and not many of the set tasks have been accomplished as yet. The projected electricity supply from all sources (conventional and renewable) by 2007 was 7000 megawatts, with 56 megawatts to be supplied by renewable energy sources. Today actual figures are much lower. Total electricity generation in the country is just above 4000 megawatts. The proportion of the total generated by renewables is not officially known, but it is very negligible.

5. RECOMMENDATIONS FOR THE WAY FORWARD IN ACHIEVING SUSTAINABLE ENERGY

Based on the benefits of renewable energy systems, the following recommendations are suggested key in moving forward on large-scale deployment of renewable energy technologies in Nigeria:

5.1. Establishing a Legal and Regulatory Framework

All the objectives listed in the Power Sector Reform programme, if fully implemented, will help solve the energy poverty issue in Nigeria. NERC must monitor the activities of all participants in the electricity market and ensure that all rules, regulations, and codes are enforced in a fair, transparent and equitable way. It is also crucial to institutionalize and improve the relevant legal and administrative framework, including establishing a serious commitment to developing and enforcing standards, regulations and codes for Renewable Energy Technologies and Systems (RET/RES). NERC also has to ensure that each energy sector decision will be in the public interest.

5.2. Adoption of Feed – in Tarrifs Scheme

Several countries have adopted feed-in tariffs, public competitive bidding (tendering), tax incentives, and quotas to drive deployment of renewable energy system. The use of public competitive bidding has gained momentum in recent years, with Brazil, El Salvador, Peru, and Uruguay issuing tenders in 2013 for more than 6.6 GW of renewable electric capacity. Japan for example implemented the solar Feed in Tariff (FIT) scheme that began in November 2009 and this has played an essential role in the recent strong growth in solar PV installations. According to the program, utilities are required to purchase surplus solar electricity for ten years at a fixed rate of JPY48 (USD 0.60)/kWh— almost twice as high as the market price of electricity—for residential PV installations below 10 kW(Wei-Ming et al., 2014). The FIT program has been very successful; according to Ministry of Economy Trade and Industry (METI) (2014), the annual surplus solar electricity purchased by the utilities reached 1.4 billion kWh in 2010. At the end of 2011, Japan had the third largest solar PV capacity in the world after Germany and Italy, with an installed capacity of 4.9 GW (European Photovoltaic Industry Association, 2012). Nigeria can take a cue from this.

5.3. Fiscal Support

The provision of fiscal incentives can address financial barriers to the development of renewable (Emodi and Ebele, 2016). Fiscal support can come in various forms which may be from tax exemptions on imported RE equipment, to tax holidays on generation incomes (KPMG, 2011). Some tax incentive policies includes; import duty/excise duty concession, VAT concession, tax credit, production tax concession, and tax holiday on generation income. Furthermore, environmental taxes have proved to be an effective fiscal support in some countries. An example is observed in Denmark which was one of the first European Union countries to implement an environmental tax. Since 1992, Denmark energy consumers have been charged a CO_2 tax and some of the revenue generated goes to generators of electricity from renewable energy (Fouquet and Johansson, 2005). Another country is Sweden which used the same approach and this added in the expansion of biomass. This made energy from fossil fuel such as coal very expensive (Joelsson, 2011).

5.4. Regular Evaluation of Existing Energy Policy and Plans

The government should plan to review, periodically assess and evaluate the existing National Energy Policy, Renewable Energy Master Plan, Solar PV Master Plan, Energy Master Plan, and Renewable Electricity Master Plan.

5.5. Increased National Awareness

In order to create awareness of new energy sources, research into Renewable Energy Technologies and Systems should be promoted nationally, as should news about their

development, uses, deployment and dispersal. Disseminating information about new energy sources, drawing up public awareness strategies and Consumer Consultation Services will also be important.

5.6. Investment and Private sector Involvement

Speeding up DE deployment in Nigeria requires huge investment that exceeds the current capability of the domestic private sector. So far, foreign investment capital and national foreign exchange earnings have funded energy sector investment. Introducing new market incentives, along with fiscal and regulatory measures at the national and local Government levels, could encourage more private investment in the power sector. In addition, feed-in tariffs (see glossary) could stimulate the private sector to invest in DE technology and make DE viable.

5.7. Technological and Environmental Support

In order to support the development of RE, the technological and environmental support needs to be explored. For technological aspect, R&D support comes in mind. Most R&D programs are typically in the form of grants or loans and sometimes provided with no expectations of financial gains. However, it is very important that the particular R&D program receiving the funds for the R&D develops patentable technologies. In Australia, the government competitive grant scheme called the Renewable Energy demonstration Programs (REDP) was used to support the development of commercial RE projects and mini-grid project (Hogg and O'Regan, 2010). The German Federal Ministry of Economic Cooperation and Development (BMZ) commissioned the Renewable Energy Support Programme for ASEAN (RESP-ASEAN) to enable the sharing of expertise and policies in order to improve framework conditions for RE in ASEAN countries. This produced corresponding guidelines for bioenergy projects in Indonesia bioenergy project and Philippines solar project (ASEAN-RESP, 2015).

5.8. Renewable Portfolio Standards

Considered as the least-cost option for RE development in many countries, RPS has a reputation for bringing down the cost of RE technologies and it creates a competitive market. The RPS system has shown in many countries to be a sustainable policy to RE generators since the government will compensate them for their extra costs through subsidies. This option if considered by the Nigerian government has the potential to create a RE market in Nigeria that will be very competitive since Nigeria have the market and large RE resource potential. However, the Nigerian government should ensure the flexibility of targets and adjust it on the short-term bases. The government should also take note of regional imbalance in pricing as some locations may have higher RE resource potential than others, while some may have the problems of electricity transmission and distribution.

5.9. International Cooperation

Developing international cooperation is important, especially in the areas of developing local RETs and RES manufacturing capacity and Smart Grid systems that can enable grid stability when RE electricity is injected.

5.10. Education and Training

The government, together with educational institutions, should establish education and training in RETs and RES to develop the skills and knowledge of technicians, engineers, administrators, and other key staff.

CONCLUSION

This study examines the appropriateness of utilizing available renewable energy sources in Nigeria, namely solar energy, wind energy, small hydro power and biomass in form of decentralized energy system to provide electricity in rural areas. Decentralized energy system has been shown to offer substantial advantages over conventional power generation in Nigeria. This remains true across a range of areas, including the environment, the economy, efficiency, security and reliability, as outlined in this paper.

Current energy policy is not suitable for sustainable economic growth in Nigeria. Since current centrally managed systems have completely failed to address the nation's energy problem, a decentralized energy system based on possible future re-structuring of a Federal Nigeria is discussed. Only decentralized energy systems in which users are involved in planning, development, construction, operation, and maintenance, are sustainable in the long-term. Decentralized energy projects are small in size but more efficient, and can avoid major environmental, social disturbances, and foreign investment associated with large-scale centrally managed energy systems.

The economic and social opportunities that sustainable energy systems can bring are significant attractions for various private and federal organizations in Nigeria to invest aggressively in the new systems. However, an orderly adaptation process to the new energy system must be followed. This includes:

a) Identification of solar powered electric energy, small hydro-power system and biogas generation through biomass technology development as systems enterprises that will create maximum benefit at the grassroots level in both the rural and urban communities of Nigeria;
b) Prioritization of the need to modify the current energy generation and distribution monopoly in Nigeria and allow decentralized investment and development of sustainable energy systems;
c) Creation of a triad joint research synergy between a foreign research institution, two or more research institutions in Nigeria and a renewable energy development

professional who will bring about the execution and implantation of research results into practice;

d) Identification of the distributed social infrastructures that will benefit from the identified sustainable energy sources; and
e) Developments of financing models that will help stimulate sustainable energy development and make it affordable to citizens.

REFERENCES

Abdullahi A. M, Asan V. W, Firdaus M. S, Ibrahim A. M, Abu B. M and Norhidayah M. Y(2015), 'An assessment of renewable energy readiness in Africa: Case study of Nigeria and Cameroon', *Renewable and Sustainable Energy Reviews* 51: 775–784.

Adegbulugbe, A.O (2007), *Balancing the Acts in the Power Sector: The Unfolding Story of* 188 *Nigeria Independent Power Projects*, Presented at the 2007 27th USAEE/IAEE North American Conference, at http://www.usaee.org/usaee2007/submissions/Online Proceedings/AS%20Momodu%20Paper.doc (last visited on 29 April 2009).

Adaramola, M.S., Oyewola, O.M., (2011), 'Wind speed distribution and characteristics in Nigeria', *ARPN J. Eng. Appl.* Sci. 6 (2), 82–86.

Agba A.M., Ushie M.E., Abam F.I., Agba M.S., Okoro J (2010), Developing the Biofuel Industry for Effective Rural Transformation, *European Journal of Scientific Research;* Feb2010, Vol. 40 Issue 3, p441.

Agbetuyi, A.F., Akinbulire, T.O., Abdulkareem, A., Awosope, C.O., (2012), 'Wind energy potential in Nigeria', *International Electrical Engineering Journal* 3 (1), 595 – 601.

Agbro, E. and Ogie, N (2012)"A Comprehensive review of Biomass Resources and Biofuel Production Potentials in Nigeria," in: *Research Journal in Engineering and Applied Sciences*, Vol. 1, No. 3, 2012 pp. 149-55.

Ajao, K.R, Ajimotokan, H.A and Popoola, O.T (2009), 'Electric Energy Supply in Nigeria, Decentralized Energy Approach', *Cogeneration and Distributed Generation Journal,* Vol. 24 (4): 34 – 50.

Albadi M.H and El-Saadany E.F (2010), 'Overview of wind power intermittency impacts on power systems', *Electric Power Systems Research* 80: 627 - 632.

Ali, E (2011), 'The Transfer of Sustainable Energy Technology to Developing Countries: Understanding the Need of Bangladesh', *Energy Science and Technology* Vol. 1, No. 1, pp. 94 – 109.

ASEAN-RESP (2015) Renewable energy in South-East Asia, Available: https://www.giz.de/en/worldwide/16395.html.

Bazmia, A.A and Zahedia, G (2011), 'Sustainable energy systems: Role of optimization modeling techniques in power generation and supply—A review', *Renewable and Sustainable Energy Reviews* 15:3480 – 3500.

Bello, S.L (2013), '*Evaluating the Methodology of Setting Electricity Prices in Nigeria'*, International Association for Energy Economics, 4th Quarters, 31 – 32.

Doukas, H., Karakosta, C. and Psarras, J. (2009) 'RES technology transfer within the new climate regime: a 'helicopter' view under the CDM', *Renewable and Sustainable Energy Reviews*, Vol. 13, No. 5, pp.1138–1143.

Energy Commission of Nigeria (ECN) (2013): *Renewable Energy Master Plan* (2013), Abuja, Nigeria.

Eleri, E. O. and Onuvae, P. (2011). Low-Carbon Africa: Leapfrogging to Green Future: Low Carbon Nigeria. Retrieved July 18, 2015, from www.christainaid.org.uk/resources/policy/climate/low-carbon-africa.aspx.

Eleri, E. O., Ugwu, O., and Onuvae, P. (2012). *Expanding access to pro-poor energy services in Nigeria. Abuja*, Nigeria: International Center for Energy, Environment and Development.

Emodi, N. V. and Boo, K. J. (2015). Sustainable Energy Development in Nigeria: Overcoming Energy Poverty. *International Journal of Energy Economics and Policy*, 5(2), 580-597.

Emodi, N.V and Boo, K (2015), 'Sustainable Energy Development in Nigeria: Overcoming Energy Poverty', International Journal of Energy Economics and Policy, 5(2), 580-597.

Emodi, N.V and Yusuf, S.D (2015), 'Improving Electricity Access in Nigeria: Obstacles and the Way Forward', *International Journal of Energy Economics and Policy*, Vol. 5, No. 1, pp.335-351.

Emodi, N.V and Ebele, N.E (2016), 'Policies Promoting Renewable Energy Development and Implications for Nigeria, British Journal of Environment and Climate Change', 6(1): 1-17.

Emodi, N.V and Ebele, N.E (2016), 'Policies Promoting Renewable Energy Development and Implications for Nigeria', *British Journal of Environment and Climate Change*, 6(1): 1-17.

Esan, A.A (2003), Preparedness on Development Green Energy for Rural Income Generation-Nigeria's Country Paper UNIDO, INSHP/IC SHP, Hangzhou, China June 19-23, 2003.

European Photovoltaic Industry Association, (2012), Global Market Outlook for Photovoltaics until 2016. Available at ⟨http://www.epia.org/home/⟩(Last visited on 30.06.2014).

Federal Ministry of Power (FMP)(2015), Federal Ministry of Power: National Renewable Energy And Energy Efficiency Policy (NREEEP) for the Electricity Sector (May 2015), Abuja, Nigeria.

Fouquet D and Johansson T (2005), Energy and environmental tax models from Europe and their link to other instruments for sustainability: policy evaluation and dynamics of regional integration. In Presentation at the Eighth Senior Policy Advisory Committee Meeting, Beijing, China. 2005;18.

Garba, N.A and Zangina, U (2015), 'Rice straw and husk as potential sources for mini-grid rural electricity in Nigeria', *Int. Journal of Applied Sciences and Engineering Research*, Vol. 4, Issue 4, 523 – 530.

GIZ (2015), *Hydro Power Potential Assessment for Partner States*, Abuja, Lagos.

Heider, C, Taylor – Dormond, M, Gaarder, M, Atur, V and Jammi, R (2015), World Bank Group Support to Electricity Access, FY2000–FY2014, World Bank.

Hepbasli, A (2008), 'A key review on exergetic analysis and assessment of renewable energy resources for a sustainable future', *Renewable and Sustainable Energy Reviews* 12:593–661.

Hogg K and O'Regan R (2010), Renewable energy support mechanisms: An overview. PricewaterhouseCoopers LLP, Globe Law and Business.

IEA. (2007), *Energy Poverty Action Initiative,* Brochure. Paris, France: International Energy Agency.

IEA (2013), *Key World Energy Statistics,* Paris, France.

IEA (2014), *World Energy Outlook,* Paris, France.

Joelsson J (2011), *On Swedish bioenergy strategies to reduce CO_2 emissions and oil use;* 2011.

Karakosta, C., Doukas, H. and Psarras, J. (2008) 'A decision support approach for the sustainable transfer of energy technologies under the Kyoto Protocol', *American Journal of Applied Sciences*, Vol. 5, No. 12, pp.1720–1729.

Karakosta, C, Flamos, A and Doukas, H (2010), 'Sustainable energy technology transfers through the CDM? Application of participatory approaches for decision making facilitation', *Int. J. Environmental Policy and Decision Making*, Vol. 1, No. 1, pp. 1 – 16.

KPMG (2011), Taxes and Incentives for Renewable Energy. Energy and Natural Resources; 2011.
Available:https://www.kpmg.com/Global/en/IssuesAndInsights/ArticlesPublications/Documents/Taxes-Incentives-Renewable-Energy-2011.pdf.

Kuku, T.A (2009), Renewable Energy for Sustainable Socio-Economic Development of the Nation, Nigeria, Keynote paper presented at the International Conference/Workshop on Renewable Energy, an option to Nigeria Energy Challenges, Covenant University, Ota, 13th to 17th July, 2009.

Ladan, M., 2009, 'Policy, legislative and regulatory challenges in promoting efficient and renewable energy for sustainable development and climate change mitigation in Nigeria', In: Proceedings of the 2nd Scientific Conference of Assellau, University of Nairobi Nairobi. ABU Press, 23–25 Mar 2009. Nairobi, Kenya.

Lahmeyer (2005), Wind Energy Resource Mapping and Related Works Project, Lahmeyer, International, 2005, *Bad Vilbel*, Germany.

Lorenzini, G, Biserni, C and Flacco, G (2010), Solar Thermal and Biomass Energy, WIT Press. Ashurst Lodge, Ashurst, Southampton, SO40 7AA, UK.

Ministry of Economy (2002), Planning of the sectors of electricity and gas development of the networks of transport 2002–2011. Madrid: Secretary of State of Energy, Industrial Development and of the Small and Medium Company. Main directorate of Power Policy and Mines.

Ministry of Economy Trade and Industry (METI), 2014. New Strategic Energy Plan, METI, Japan.

Mohammeda, Y.S, Mustafa, M.W, Bashir, N and Mokhtar, A.S (2013), 'Renewable energy resources for distributed power generation in Nigeria: A review of the potential', *Renewable and Sustainable Energy Reviews* 22: 257–268.

NBS (2009), *Social Statistics in Nigeria,* Abuja: National Bureau of Statistics.

NERC (2012), Nigerian Electricity Regulatory Commission Regulations for Embedded Generation 2011 (January 2012).

NERC (2015), Order No. NERC/REG/3/2015, ''Amended Multi Year Order Tariff (MYTO) – 2.1 for the period April 1st, 2015 to December 2018, Abuja, Nigeria.

Nigerian Minister of Power, Works and Housing (2016), Opportunities for off-grid solutions in the Nigerian power sector, www.nipc.gov.ng (Accessed 6/30/2016).

Nnaji, C.E., Uzoma, C.C. and Chukwu, J.O (2010), 'The Role of Renewable Energy Resources in Poverty Alleviation and Sustainable Development in Nigeria', Continental *J. Social Sciences* 3: 31 – 37.

Nwanya, S.C (1998), *Modelling Energy Pattern in the Industrial Sector of Nigeria,* M.Sc Project, University of Nigeria, Nsukka, Nigeria, pp 1 – 79.

Ogwueleke T (2009), Municipal Solid Waste Characteristics and Management in Nigeria, *Iranian Journal of Environmental Health Science and Engineering,* 2009, Vol. 6, No. 3, pp. 173-180.

Oseni, M.O (2012), 'Improving households' access to electricity and energy consumption pattern in Nigeria: Renewable energy alternative', *Renewable and Sustainable Energy Reviews* 16 3967– 3974.

Otuna, J.A, Onemano;J.A and Alayande, A.W (2012), 'Assessment of the Hydropower Potential of Kangimi Reservoir in Kaduna State Nigeria', Nigerian Journal of Technology (NIJOTECH) Vol. 31, No. 3, pp. 300 – 307.

Oyedepo, S.O (2012), 'On energy for sustainable development in Nigeria', Renewable and Sustainable Energy Reviews 16:2583– 2598.

Oyedepo, S.O(2013),'Energy in Perspective of Sustainable Development in Nigeria', *Sustainable Energy, Vol. 1, No. 2, 14-25.*

Oyedepo, S.O (2014), Development of Small Hydropower: A Pathway towards Achieving Sustainable Energy Development, In: Rupert, C.E (Ed.) *Hydropower Types, Development Strategies and Environmental Impacts,* Nova Science Publishers, Inc., New York: 67 – 119.

Oyedepo, S.O (2014b), Thermodynamic Performance Analysis Of Selected Gas Turbine Power Plants In Nigeria, PhD Thesis, Covenant University, Nigeria, pp 1 – 282.

Oyedepo, S.O (2014), 'Towards achieving energy for sustainable development in Nigeria', *Renewable and Sustainable Energy Reviews* 34: 255–272.

Oyedepo, S.O, Adaramola, M.Sand Paul, S.S (2012), 'Analysis of wind speed data and wind energy potential in three selected locations in south-east Nigeria', *International Journal of Energy and Environmental Engineering,* 3:7, pp 1 – 11, http://www.journal-ijeee.com/content/3/1/7.

Painuly, J.P (2001), 'Barriers to Renewable Energy Penetration: A Framework for Analysis', *Renewable Energy* 24: 73–89.

Pereira E. G, Da Silva J. N, De Oliveira J. L and Machado C. S (2012), 'Sustainable energy: A review of gasification technologies', *Renewable Sustainable Energy Review.* 16:4753-4762.

Renewable Energy Master Plan (2006).

Shaaban, M and Petinrin, J.O (2014), 'Renewable energy potentials in Nigeria: Meeting rural energy needs', *Renewable and Sustainable Energy Reviews* 29: 72 – 84.

Simonyan, K.J. and Fasina, O (2013), Biomass resources and bioenergy potentials in Nigeria," in: *African Journal of Agricultural Research,* Vol. 8(40), Oct. 2013, pp. 4975 – 89.

Sustainable Energy for All Initiative (SE4ALL)(2012). *In Support of the Objective to Achieve Universal Access to Modern Energy Services by 2030*. Technical Report of Task Force 1: New York. http://www.sustainableenergyforall.org/about-us.

Twidell, J and Weir, T (2015), Renewable Energy Resources (3rd Ed.), *Routledge, Taylor and Francis Group, 711 Third Avenue, New York, NY 10017.*

Usman, Z. G and Abbasoglu, S (2015), 'An Overview of Power Sector Laws, Policies and Reforms in Nigeria'**,** Asian Transactions on Engineering Volume 04 Issue 02: 6 – 12.

Udoudoh, F. Pand Umoren, V. E (2015), 'An Appraisal of Public Electricity Performance and its Implications on Economic Development in Nigeria', *Sacha Journal of Environmental Studies* Volume 5 Number 1, Pp. 63-73.

United Nations (2006), *The millennium development goals report*, United Nations, New York.

Vincent-Akpu, I.(2012), 'Renewable Energy Potentials in Nigeria,' in: IAIA12 Conference Proceedings Energy Future The Role of Impact Assessment, 32nd Annual Meeting of the International Association for Impact Assessment, 27 May – 1 June 2012, Porto – Portugal.

Wei-Ming C, Hana K and Hideka Y (2014), 'Renewable energy in eastern Asia: Renewable energy policy review and comparative SWOT analysis for promoting renewable energy in Japan, South Korea, and Taiwan', *Energy Policy* 74: 319 – 329.

Werner, D and Faruk Y.Y (2015), An Overview with a Special Emphasison Renewable Energy, Energy Efficiencyand Rural Electrification, 2nd Edition, June 2015, Nigerian Energy Support Programme (NESP), Federal Secretariat Complex Shehu Shagari Way, Maitama, Abuja, Nigeria, pp 1 – 152.

World Bank (2013), *Low-Carbon Development Opportunities for Nigeria*, Raffaello Cervigni., John Allen Rogers, and Max Henrion, (eds.), (International Bank for Reconstruction and Development/The World Bank, Washington, 2013), Washington, USA.

Zubairu G. U, Serkan A, Neyre T. E and Murat F(2015), 'Transforming the Nigerian Power Sector for Sustainable Development', *Energy Policy* 87: 429–437.

ABOUT THE EDITOR

Sandip A. Kale is working as Associate Professor in Mechanical Engineering Department, Trinity College of Engineering and Research, Pune affiliated to Savitribai Phule Pune University India from 2010. He also handles responsibilities as Dean, Research in the institute. He has completed his Ph.D. and Master's Degree from Pune University. He has more than 15 years industrial, academic and research experience. He has published more than forty research papers in various conferences and journals. He has worked as Guest Editor for publishing many special issues. He has worked as an Editor for an edited book "Renewable Energy and Sustainable Development" published by Nova Science Publishers, USA. He is an author of a first book published on Multi-rotor Wind Turbine. He has worked as Conference Chair for three international conferences and one national conference. He is working as Editorial Board member and reviewer for many international journals. His basic research areas are wind and solar energy, renewable energy and composite materials. Now a day he is also working in the field of Internet of Things.

E-mail: sakale2050@gmail.com

INDEX

A

abatement, 196
Abeokuta, 67, 71, 76, 80, 83
access, 25, 105, 107, 226, 227, 229, 231, 232, 233, 244, 246, 254, 256
acid, 65, 66, 164, 165, 171, 172
actual output, 88
actuation, 161
adaptation, 252
adhesives, 73
administrators, 252
adsorption, 76
advancements, 2, 43
adverse effects, 73, 76
aesthetic, 76
Africa, 2, 36, 37, 231, 235, 237, 253, 254
agencies, 247
agricultural produce, 68, 69, 71, 80, 81, 82
agricultural sector, 81
agriculture, 208
air mass, 4, 5, 22, 42
air temperature, 23
alcohols, 200
aldehydes, 200
algae, 208
algorithm, vii, 85, 86, 88, 89, 90, 91, 97, 98, 145, 198, 224
alternative energy, 225, 241, 243, 244
Altitude, 5, 10, 11, 12, 13, 14, 15, 36, 54
aluminium, 33
amines, 200
ammonia, 197, 198, 217, 218
amplitude, 134, 135, 140
anaerobic digestion, 195, 211
annealing, 58
annual rate, 40
ANOVA, 85, 87
anti-reflection coating, 60, 62, 65
apex, 8
aquaculture, 217
arithmetic, 109
Arrays, 22, 35
ASEAN, 251, 253
Asia, 113, 233, 257
assessment, 102, 108, 109, 110, 144, 145, 147, 148, 149, 161, 232, 238, 253, 254
assets, 233, 247
atmosphere, 3, 4, 8, 41, 42, 71
atoms, 54, 55
attachment, 89
Austria, 222
average temperature, 5, 67, 80
awareness, 2, 240, 245, 250
Azimuth, 9, 11, 12, 36

B

bacteria, 71
band gap, 42, 45, 46, 47, 53, 56, 57, 58, 61, 65, 66
Bangladesh, 229, 232, 253
barriers, 29, 226, 244, 245, 246, 249, 250
base, 102, 184
basic needs, 226
basic research, 259
batteries, 56
Beijing, 254
bending, 149
benefits, 2, 166, 238, 240, 242, 249
benign, 227

Bhutan, 207
bias, 89
binary blends, 168, 171, 179
biodegradability, 164
biodiesel, v, viii, 163, 164, 165, 166, 167, 168, 170, 171, 172, 173, 174, 175, 176, 177, 178, 179, 180, 182, 184, 192, 193
biodiversity, 218
bioenergy, 222, 237, 251, 255, 256
biofuel, 163, 238, 243, 253
biogas, 211, 212, 222, 223, 224, 241, 243, 252
biomass, 54, 182, 195, 196, 197, 198, 207, 208, 209, 210, 211, 212, 214, 215, 220, 221, 222, 223, 225, 227, 233, 237, 238, 241, 242, 245, 247, 250, 252
blends, 163, 165, 166, 167, 168, 170, 172, 174, 175, 176, 177, 178, 180
Blocking Diodes, 34, 35, 36
boilers, 209, 211, 214
Brazil, 230, 232, 239, 250
bulk materials, 46
Bypass Diodes, 33, 34, 35

C

CAD, 149, 150
cadmium, 30
calcium, 47
Cameroon, 253
campaigns, 103
candidates, 39, 46, 199
carbon atoms, 47
carbon dioxide, 41, 164
carbon emissions, 216
carbon monoxide, 182, 187
carbon nanotubes, 55
case studies, 103, 114, 220, 221
casting, 46, 54, 76, 106
catalyst, 182, 184
CDM, 253, 255
ceramics, 66, 193
certification, 245
challenges, viii, 228, 232, 240, 241, 244, 245, 248, 255
Characteristics of a Solar Cell, 19
characteristics of PV modules, 1
chemical characteristics, 164
chemical industry, 218
chemical properties, 193
chemical reactions, 188
chemical stability, 199, 202
Chicago, 83
child mortality, 240
Chile, 68
China, 232, 254
chromosome, 90
cities, 226, 242
citizens, 226, 240, 253
classification, 140
clean energy, 217, 241
cleaning, 7, 14, 15, 208, 210, 211
climate, 40, 73, 82, 106, 221, 240, 253, 254, 255
climate change, 40, 82, 106, 221, 240, 255
clusters, vii, 101, 102, 103, 108, 110, 113, 114, 247
CO2, 41, 106, 111, 196, 198, 207, 210, 218, 222, 224, 250, 255
coal, 3, 40, 54, 226, 231, 233, 239, 250
coated engine, 181, 184, 185, 186, 187, 188, 189, 190, 191, 192
coatings, 181
cogeneration, 196, 210, 245
collaboration, 105
combustion, 164, 181, 182, 183, 184, 185, 189, 190, 192, 193, 197, 207, 208, 209, 210, 211, 213, 218, 219, 223
commercial, 29, 34, 40, 43, 47, 49, 202, 209, 213, 216, 220, 228, 232, 243, 251
commodity, 227
communication systems, 106
communities, 226, 230, 240, 244, 248, 252
comparative analysis, 223
compatibility, 202
competitors, 39, 43, 68, 196
complexity, 43, 196, 200, 212, 213, 215, 245, 246
composition, 4, 165
compounds, 42, 88
compression, 183, 192, 193
computer, 119, 127, 217, 224
condensation, 199, 200, 201, 206
conditioning, 218
conductivity, 40, 57, 60, 74, 202
conductor, 47
conference, 259
configuration, 197, 199, 202, 203, 205, 210, 212, 217
Congress, 37, 68
connectivity, 107
constituents, 170
construction, 32, 67, 71, 72, 75, 76, 86, 97, 102, 115, 240, 252
consulting, 109
consumption, 2, 49, 85, 117, 196, 213, 225, 226, 230, 231, 239, 244, 246, 250
containers, 70

contamination, 69, 81, 193
Continental, 256
control, vii, 69, 72, 98, 99, 102, 115, 116, 119, 121, 122, 123, 124, 125, 126, 141, 142, 143, 144, 145, 155, 208, 219, 245
convection, 70, 71, 83
convergence, 148, 155
cooking, 68, 70, 226, 227, 238, 239, 243
cooling, 46, 68, 182, 186, 210, 211, 216, 224
cooperation, 252
copper, 30
correlation, 97, 165, 166, 167, 169, 170, 172, 174, 175, 176, 177
corrosion, 209
corruption, 245
cost, vii, 30, 43, 45, 46, 47, 48, 49, 57, 68, 69, 81, 103, 104, 116, 127, 148, 165, 198, 202, 208, 209, 210, 211, 214, 215, 218, 219, 235, 237, 239, 240, 242, 244, 251
cotton, 172, 179, 182
Council of the European Union, 196, 221
covering, 56, 68, 73, 243
CPI, 101, 102, 103, 108, 109, 111, 113
crises, 68, 148
critical value, 196
crop, 67, 70, 69, 71, 73, 76, 80, 81, 208, 243, 247
crude oil, 233
crystal structure, 47
crystalline, vii, 24, 28, 29, 31, 32, 33, 34, 35, 39, 40, 42, 43, 235
CTA, 110, 111, 112, 113
culture, 248
curricula, 2
customers, 119, 247, 248
cycles, viii, 184, 189, 196, 197, 198, 206, 208, 213, 215, 217, 220, 221, 222

D

damping, 127, 135, 139
danger, 69, 70
data distribution, 97
database, 246
decentralized energy system, 226, 246, 247, 248, 252
decomposition, 199
deficiencies, 2, 70, 232
deforestation, 228
deformation, 147
degradation, 46, 47, 48
dehydration, 69
Delta, 230, 231
Denmark, 250
density and viscosity of biodiesel, viii, 163, 165, 170, 177, 179
density values, 168, 170, 171, 172, 173, 174
Department of Energy, 21, 37
deposition, 5, 61, 62, 66, 165
deposits, 182
deprivation, 103
depth, 103, 199, 207, 217
developed countries, 182, 239
developing countries, vii, 2, 207, 216, 226, 239, 240, 242
developing economies, 237
deviation, 15, 16, 115, 133, 134, 139, 140, 173
diamonds, 29
diesel engines, 182, 193
diesel fuel, 178, 180, 181, 182, 183, 184, 185, 186, 187, 188, 189, 190, 191, 192, 193
differential equations, 115, 119, 126, 127
diffusion, 226
digestion, 212
diodes, 33, 34, 35, 36
diseases, 240
dispersion, 87
distillation, 68
distributed load, 155
distribution, 7, 41, 50, 58, 86, 94, 97, 105, 111, 119, 156, 157, 158, 223, 231, 232, 233, 234, 239, 247, 251, 252, 253
district heating, 208, 221, 222
DOI, 36, 144
drying, 67, 68, 69, 70, 71, 72, 73, 76, 79, 80, 81, 82, 83
drying chamber, 71, 72, 73, 76, 81
dumping, 238
durability, vii, 182
dynamic load, 147
dynamic simulation, 116, 127, 145
dynamic viscosity, 169

E

early labor, 49
earnings, 233, 251
East Asia, 253
ecological processes, 239
economic activity, 227
economic development, 225, 226, 227, 230, 242, 248
economic growth, 2, 182, 225, 226, 227, 233, 240, 242, 248, 252
economic performance, 227

economic problem, 90
economies of scale, 246
education, 37, 240, 252
educational institutions, 252
educational opportunities, 246
Egypt, 114
Eigen values, 147, 155
Eigen vectors, 147, 149
El Salvador, 250
electric capacity, 250
electric circuits, 16
electric current, 19
electrical conductivity, 57
electrical properties, 66
electricity, 2, 5, 11, 16, 35, 40, 45, 53, 54, 55, 56, 68, 85, 116, 117, 118, 119, 196, 197, 198, 208, 209, 210, 211, 213, 215, 216, 217, 218, 219, 220, 224, 225, 227, 228, 229, 230, 231, 232, 233, 235, 237, 238, 239, 241, 242, 243, 244, 245, 246, 247, 248, 249, 250,251, 252, 254, 255, 256
electrodes, 40, 56, 58, 66
electromagnetic, 8, 127, 132, 138, 139
electrons, 19, 29, 40, 54, 55
emission, 59, 164, 181, 183, 184, 186, 187, 191, 192, 193, 207
employability, 164, 177
employment, 227
empowerment, 249
encoding, 90
endurance, 193
energy consumption, 40, 116, 196, 225, 239, 256
energy density, 208
energy efficiency, 114, 196, 219
energy infrastructures, 225, 226
energy input, 70
energy security, 232, 246
energy supply, 68, 81, 225, 226, 238, 239, 248
engineering, 2, 45, 47, 192, 221
England, 193
entropy, 200
environment, 39, 81, 106, 107, 112, 163, 218, 226, 239, 252
environmental impact, 202, 221, 226, 237, 239, 246
environmental protection, 196, 219
enzymes, 71
equilibrium, 218, 228
equipment, 54, 71, 200, 202, 213, 228, 239, 245, 250
erosion, 199
ester, viii, 164, 171, 172, 181, 182, 183, 184, 192, 193
ethanol, 182, 243
ethers, 200
Europe, 218, 254
European Commission, 196
European Parliament, 196, 221
European Union, 116, 207, 250
evacuation, 104
evaporation, 200, 201, 206
evolution, 49, 90, 227
excitation, 115, 119, 122, 127, 128, 132, 135, 139, 140, 141, 142
exciton, 46
execution, 253
exercise, 76
experimental condition, 61
expertise, 1, 240, 251
exploitation, 115, 122, 126, 195, 197, 198, 208, 219, 237, 238, 248
exports, 233, 239
extraction, 204, 206, 224

F

fabrication, 42, 45, 46, 49, 58, 66
Factors Affecting the Performance of Solar Cells, 25
farmers, 81, 244
farms, 86, 101, 102, 104, 105, 107, 108, 109, 113
federal government, 237, 247
Feed In Tariff, 105
feedstock, 238, 239
fibers, 239
field emission scanning electron microscopy, 59
fill factor, 21, 22
films, 30, 53, 55, 56, 57, 58, 60, 61, 62, 65, 66
filtration, 66, 165
financial incentives, 245
financial institutions, 244
financial performance, 107
finite element method, viii
Finland, 210, 223
first generation, 42
fitness, 90, 92
flat plate collectors, 70
flavour, 73
flexibility, 43, 49, 251
flora, 106
flora and fauna, 106
fluctuations, 126, 134, 135, 138, 140, 147, 242
flue gas, 209
fluid, 164, 170, 172, 176, 197, 199, 200, 201, 202, 203, 204, 205, 206, 207, 208, 209, 213, 214, 215, 217, 219, 220, 221, 222, 223

fluid extract, 213
fluorine, 56, 57
food, vii, 67, 68, 69, 70, 71, 72, 73, 75, 76, 80, 81, 82, 208, 218
food industry, 208
food spoilage, 81
force, 148, 151, 153, 154, 155, 170, 176
forecasting, 86, 97, 98
foreign exchange, 233, 251
foreign investment, 251, 252
formation, 58, 165, 182, 188, 213
formula, 12, 13, 15, 25, 94, 172
fouling, 193
France, 145, 255
friction, 164
fruits, 69, 70, 73
fuel cell, 37
fuel consumption, 181, 185, 213
fuel prices, 182, 226, 235
funding, 228, 231, 251
fusion, 3

G

gallium, 30
gasification, 195, 208, 210, 211, 212, 256
GDP, 231
GEF, 37
gender equality, 240, 246
genes, 90
geo-political, 231
germanium, 58
Germany, 2, 37, 40, 213, 218, 221, 223, 250, 255
GHG, 106, 111, 196
glass substrates, 53, 56, 58, 59, 61, 65
global economy, 49
global warming, 40, 232
glycerol, 182
governance, 242
government revenues, 233
governments, 240, 247
grain boundaries, 42
grants, 251
graph, 28, 63, 187, 188
grasses, 237
grassroots, 252
gravitational force, 241
gravity, 148
Greece, 115, 117, 119
greenhouse, 71, 196, 212, 238, 240, 246
greenhouse effect, 71, 73
greenhouse gas, 196, 212, 238, 240, 246
grids, 55, 196, 216, 248
gross national product, 239
growth divergence, 89
growth rate, 227
growth temperature, 58, 59
guidance, 248
guidelines, 103, 251

H

harvesting, 58, 239
Hawaii, 215, 216, 217
health, 81, 240, 241, 246
heat loss, 74, 75, 76, 182, 186, 192
heat release, 189, 190, 192, 211, 218
heat transfer, 182, 199, 202, 213, 215
height, 102, 126, 148, 151, 152, 153, 157, 235
hemisphere, 13, 15, 42
high strength, 148
homes, 56, 216
hotels, 56, 243
House, 106
housing, 72
hub, 102, 126, 141
human, vii, 226
humidity, 69, 86
hybrid, vii, 31, 40, 97, 98, 115, 119, 124, 140, 148, 217, 220, 222, 226, 235, 247
hydrocarbons, 182, 188, 197, 198, 200
hydroelectric power, 233
hydrophobicity, 58
hydroxyl, 182

I

ICE, 210, 211, 212
Iceland, 222
ideal, 15, 34, 242
IEA, 116, 117, 144, 227, 229, 235, 255
illumination, 40
Impact Assessment, 257
improvements, 49, 103, 246
incidence, 42, 53, 54
incompatibility, 182
incomplete combustion, 164, 188
India, 39, 53, 83, 101, 102, 113, 114, 147, 153, 163, 178, 181, 183, 192, 217, 232, 259
indirect effect, 241
indium, 30, 56, 57, 58, 66

individuals, 240
Indonesia, 229, 232, 251
induction, 143, 144, 145
industrial sectors, 232
industrial transformation, 227
industrialization, 107, 239
industries, 9, 30, 31, 39, 43, 46, 47, 48, 69, 86, 109, 114, 196, 198, 218, 219, 227, 228, 238, 246, 247
inequality, 98
inertia, 91, 121, 123, 132, 148, 208
infrastructure, 227, 231, 240, 241, 246
institutions, 2, 109
insulation, 75, 182
insulators, 54
integrated circuits, 54
integration, 2, 214, 220
interface, 57, 62
International Bank for Reconstruction and Development, 2, 37, 257
International Energy Agency (IEA), 30, 255
international standards, 22, 32, 228
Intervals, 98
investment, 39, 104, 113, 116, 198, 200, 208, 210, 213, 217, 218, 232, 242, 244, 246, 248, 251, 252
investors, 105, 244, 246, 247
ions, 58
Iran, 85, 86, 114
Iraq, 53
Ireland, 97
Irradiance, 2, 8, 22, 23, 25, 27, 28, 35, 42, 50
Irradiation, 2, 7, 8, 9, 22, 28, 35, 235, 242
irrigation, 235, 237
IRS, 25
ISC, 19, 20, 21, 25, 27
isobutane, 205
isolation, 34
isopentane, 205
issues, 102, 103, 163, 244, 245, 246, 248, 259
Italy, 195, 213, 250

J

Japan, 217, 224, 250, 255, 257
joints, 76

K

Kenya, 7, 207, 255
Korea, 217
Kyoto Protocol, 196, 255

L

landscape, 106, 122, 141
Latin America, 235
laws, 16, 168, 247
legislation, 244
legume, 81
lens, 68
liberalization, 196
lidar, 103
life cycle, 106
light, 3, 4, 5, 19, 41, 42, 46, 47, 56, 57, 61, 66, 198
light emitting diode (LED), 46
light scattering, 61
liquidity, 246, 248
loans, 251
low temperatures, 164, 178, 197, 201, 214
LRA, 142, 143
lubricating oil, 182
lying, 172, 237

M

magnet, 15
magnetic field, 15
Magnetic North, 15, 16
magnetization, 140
magnitude, 128, 135, 138, 155, 156, 157, 159, 161, 164, 238
majority, 81, 226, 227, 229, 233
Malaysia, 83
management, 5, 108, 226, 228, 246, 248
manipulation, 217
manpower, 245
manufacturing, 28, 30, 43, 48, 49, 54, 106, 219, 245, 252
mapping, 235, 236
market incentives, 251
market share, 42
marketing, 68
mass, 4, 29, 42, 68, 79, 80, 90, 156, 159, 161, 164, 165, 167, 201, 202, 217, 218
material handling, 68
materials, vii, 30, 31, 39, 40, 42, 46, 47, 53, 54, 55, 56, 57, 58, 64, 65, 67, 69, 70, 71, 72, 75, 81, 181, 182, 184, 202, 206, 233, 243, 259
matrix, 89, 109, 120, 121, 140, 141, 181, 184
matter, 164
measurement, 7, 8, 107, 108, 122, 126, 142, 183
meat, 69

media, 206
MEG, 46
melt, 54
mercury, 68, 76
metal ions, 58
metals, 72
meter, 75, 183
methanol, 182
methodology, 101, 103, 108, 109, 113
Mexico, 221
MGDM network, 85
MGDM-GA method, 85
MGDM-PSO method, 85
microcrystalline, 30, 42, 58, 62
microstructure, 59
microwaves, 3
migration, 107
mixing, 68, 165, 166, 168, 198
MMA, 126, 141, 143
modeling, vii, 1, 2, 23, 25, 85, 108, 116, 102, 161, 221, 253
models, viii, 35, 86, 97, 98, 119, 144, 149, 163, 165, 170, 172, 177, 179, 253, 254
modifications, 47, 164, 196
Modules, vii, 1, 2, 5, 13, 14, 15, 16, 17, 18, 19, 22, 23, 28, 29, 30, 31, 32, 34, 35, 37, 42, 43, 46, 54, 212, 219, 235
Modules and Arrays, 22
moisture, 47, 48, 67, 68, 69, 71, 79, 80, 81
moisture content, 68, 69, 71, 79, 80
mold, 71
mole, 165
molecular mass, 182
molecular weight, 58, 170, 202
molecules, 164, 166, 170, 176
momentum, 176, 250
Monocrystalline Solar Cells, 29
morphology, 58, 59
multi-criteria approach, 101, 102, 103, 113
Multicrystalline Solar Cells, 29
multilayer films, 66
multiple regression, 88
multiple regression analysis, 88
mutation, 90

N

nanocrystals, 46
nanometer, 58
nanostructured materials, 45
nanotechnology, 2
nanotube, 56
National Aeronautics and Space Administration (NASA), 37
national policy, 244
natural gas, 68, 212, 226, 230, 233
natural resources, 225, 229, 239, 240
Neem kernel oil, vi, viii, 181, 183, 184, 192
neglect, 228
Nepal, 207
neural network, vii, 85, 86, 87, 89, 90, 91, 94, 97, 98, 99, 198, 224
neural networks, 89, 98
neurons, 87, 88, 89, 94, 95
neutrons, 3
Nigeria, vi, viii, 67, 71, 207, 225, 226, 227, 228, 229, 230, 231, 232, 233, 234, 235, 236, 237, 238, 239, 240, 242, 243, 244, 245, 246, 247, 248, 249, 250, 251, 252, 253, 254, 255, 256, 257
nitrogen, 188, 191
nitrous oxide, 41
NOCT, 19, 22, 23, 25, 32, 33
non-focusing collectors, 70
North America, 207, 253
NPL, 178
NREL, 44, 45, 46
nuclei, 3
nuisance, 107

O

obstacles, 13
obstruction, 76
oceans, 3, 216
officials, 101, 102, 109
oil, viii, 3, 40, 54, 68, 171, 172, 173, 174, 175, 176, 177, 179, 181, 182, 183, 184, 192, 193, 206, 208, 209, 216, 226, 233, 234, 239, 241, 255
oil production, 233
Oklahoma, 36
opacity, 188, 189
operations, 94, 96, 97, 102, 209, 245, 246
opportunities, viii, 226, 238, 247, 252
optical properties, 57, 62, 66
optimal performance, 208
optimization, 86, 90, 91, 94, 97, 98, 99, 108, 114, 164, 198, 200, 219, 222, 223, 224, 253
optimum temperature, 67, 73
orbit, 12, 36
organic compounds, 199

Organic Rankine Cycle, vi, 195, 196, 197, 198, 199, 207, 208, 211, 213, 215, 217, 219, 220, 221, 222, 223, 224
oxidation, 188
oxygen, 68, 182, 188

P

Pacific, 83, 113
Pakistan, 232
parallel, 16, 17, 18, 19, 22, 23, 24, 25, 34, 35
parity, 30, 235
participants, 249
path analysis, 98
PCM, 82
Peak Sun Hours, 7, 8, 9
peelings, 67, 68, 80, 81
performance evaluation, v, vii, 67, 82, 101, 102, 113
performance indicator, 102, 103, 104, 107, 108, 109, 110, 228
performance measurement (PM), 182, vii
permit, 76
Peru, 250
PES, 98
pests, 69
PET, 66
petroleum, 163, 164, 176, 177, 218, 230, 233
phase transitions, 201
Philippines, 232, 251
phosphorous, 55
photons, 46, 54
photovoltaic, v, vii, 1, 2, 5, 16, 19, 22, 23, 32, 35, 36, 37, 39, 40, 42, 46, 50, 53, 54, 55, 56, 57, 70, 215, 250, 254
physical properties, viii, 163, 164, 165, 172, 177
physics, 40, 155, 161, 166
pitch, 122, 148, 161
plants, 2, 86, 109, 117, 195, 196, 202, 208, 209, 210, 211, 213, 214, 215, 217, 218, 219, 221, 223, 228, 230, 232, 237, 241, 243, 245, 247
platform, 25
playing, 244
PNA, 141
point defects, 42
polar, 9
polarity, 34
policy, 226, 227, 240, 248, 249, 251, 252, 254, 257
pollutant, 106, 218
pollution, 196, 218, 219, 228
Polycrystalline or Multicrystalline Solar Cells, 29
polymer, 31, 40, 46, 58
polymers, 56
polythene, 71
polyurethane, 67, 71
poor performance, 228
population, 90, 225, 227, 228, 231, 232, 242
portfolio, 102, 234
Portugal, 257
poverty alleviation, 107, 226
poverty reduction, 225, 226, 227, 240
POWER, 128
Power Characteristic of a Solar Cell, 20
power generation, 3, 40, 53, 54, 86, 97, 98, 102, 104, 162, 214, 215, 223, 224, 227, 228, 230, 231, 237, 242, 244, 246, 252, 253, 255
power plants, 145, 196, 197, 199, 215, 216, 221, 223, 228, 230, 235, 237, 239, 247
preparation, 57, 93, 184
preservation, 70, 82
prevention, 237
primary data, 101
principles, 66, 221
prior knowledge, 86
private investment, 245, 251
private sector, 246, 251
probability, 86, 90
producers, 117, 244
production costs, 218
professionalism, 245
profit, 241, 244
profitability, 208, 247
project, 5, 9, 99, 236, 240, 243, 245, 251
propagation, 89
propane, 217
prosperity, 241
protection, 34, 196
protons, 3, 55
prototypes, 161, 198, 206
public awareness, 245, 251
public interest, 249
publishing, 259
pulp, 218
pumps, 219
pure water, 184
purity, 42, 54
PV cell modelling, 1
PV cell module and array, 1
PV Cells, 19
pyrolysis, 208

Q

quality assurance, 245
quality control, 245
quality of life, 227, 239
quality standards, 166
quantification, 86
quantum dot, vii, 39, 46, 57
questionnaire, 101, 102, 113
quotas, 250

R

radiation, 2, 3, 4, 5, 7, 8, 9, 14, 15, 35, 37, 40, 41, 42, 50, 70, 72, 74, 81, 198, 215, 234, 241
radius, 46, 141, 151
ramp, 25
random numbers, 91
rate of change, 170, 177
raw materials, 30
REA, 248
reality, 29
recombination, 42
recommendations, 249
recovery, viii, 128, 195, 196, 198, 218, 219, 220, 221, 222, 223
reflectivity, 3, 57
Reform, 249
regeneration, 221
regional integration, 254
regression analysis, 165
regression method, 168, 170
regulations, 247, 249
regulatory framework, 247
regulatory requirements, 236
rejection, viii, 181, 182, 192, 193
reliability, 86, 105, 199, 209, 210, 214, 225, 231, 241, 252
renaissance, 40
renewable energy, 1, vi, vii, viii, 2, 5, 36, 37, 39, 40, 41, 50, 51, 54, 68, 81, 82, 83, 103, 114, 116, 117, 143, 144, 145, 148, 161, 162, 163, 178, 192, 195, 198, 208, 213, 215, 216, 218, 221, 223, 225, 226, 227, 230, 231, 233, 234, 235, 237, 240, 241, 242, 243, 244, 245, 246, 248, 249, 250, 251, 252, 253, 254, 255, 256, 257, 259
renewable energy sources (RES), vii, 39, 40, 54, 68, 81, 116, 117, 118, 119, 143, 144, 145, 148, 195, 198, 215, 221, 225, 227, 235, 241, 242, 243, 244, 248, 249, 252, 253
renewable energy technologies (RETs), vi, viii, 103, 116, 225, 226, 227, 230, 240, 241, 242, 244, 245, 248, 249, 250, 252
repetitions, 91
reputation, 251
requirements, 39, 58, 83, 101, 201, 202, 226, 227, 248
research institutions, 252
researchers, vii, viii, 2, 47, 54, 172, 195, 200, 201, 202, 212, 214, 219, 233, 237
reserves, 230, 233, 234, 241, 246
residue, 183, 184, 234, 237, 238
resistance, 17, 19, 21, 23, 24, 25, 56, 57, 59, 66, 164
resolution, 86, 183
resource management, 241
resource utilization, 214
resources, 68, 103, 105, 110, 148, 163, 164, 196, 222, 223, 225, 226, 227, 233, 237, 238, 239, 240, 241, 242, 246, 248, 254, 255, 256
response, 22, 104, 152, 153, 183
revenue, 104, 107, 109, 112, 198, 250
reverse osmosis, 216
rice husk, 208, 244
risk, 69, 81, 108, 199, 244, 245
rodents, 69
rods, 58, 65
Romania, 145
room temperature, 45, 47
rotation axis, 148
roughness, 58, 151, 153
rules, 249
rural areas, 238, 242, 246, 248, 252
rural development, 249
Russia, 213

S

safety, 32, 106, 164, 202, 206
SAR, 107, 112
saturation, 24, 25, 200, 202
sawdust, 208
scattering, 4, 8, 41
scientific papers, 219
scope, 25, 47, 48, 145
sea level, 8, 217
search space, 90
security, 144, 225, 227, 252
seed, 171, 172, 173, 179, 182
Selecting Diodes, 35
selenium, 40
semiconductor, 25, 40, 46, 54, 55

sensitivity, 30, 47, 172, 208
sensor, 183
services, 225, 226, 227, 229, 231, 232, 239, 241, 244, 254
settlements, 227
shade, 13
shape, 76, 148, 151
shoreline, 236
shortage, 228, 241
shortfall, 242
signals, 25, 122
silicon, vii, 5, 28, 29, 30, 31, 35, 40, 42, 43, 45, 46, 54, 55, 57, 58, 62, 66
simulation, 2, 23, 25, 35, 98, 115, 116, 119, 127, 134, 139, 144, 145, 200, 212
social infrastructure, 253
society, 227, 241
sodium, 184
sodium hydroxide, 184
software, 5, 94, 115, 149, 161
Solar Altitude, 12, 14
solar cells, vii, 18, 21, 23, 25, 28, 29, 30, 31, 34, 35, 39, 40, 42, 45, 46, 47, 53, 54, 56, 57, 58, 59, 60, 61, 62, 63, 65, 66
solar collectors, 215, 216, 219
solar cookers, 70
solar dryer, 68, 69, 70, 71, 73, 76, 77, 78, 79, 80, 81, 82, 83, 243
solar energy, vii, 1, 2, 5, 8, 35, 36, 39, 40, 45, 47, 50, 53, 54, 55, 56, 58, 65, 66, 67, 68, 69, 70, 81, 83, 114, 195, 198, 207, 215, 224, 233, 235, 242, 243, 252, 259
Solar Radiation, 2, 3, 4, 5, 7, 9, 15, 35, 36, 37, 40, 41, 42, 50, 70, 72, 81, 215, 234, 241
solar system, 1, 2, 3, 5, 22, 72
solid state, 47
solidification, 164
solution, 14, 46, 54, 58, 66, 69, 90, 119, 127, 148, 210, 241, 242
South Africa, 67, 83
South Asia, 114
South Korea, 230, 257
Spain, 2, 86, 94, 230, 235
species, 90
specific gravity, 178
specific heat, 199
specifications, 22, 34, 183
spin, 58, 59
stability, 47, 48, 49, 57, 144, 228, 252
stakeholders, 101, 237
standard of living, 81
Standard Test Conditions (STC), 5, 19, 22, 32, 33
state, 68, 74, 82, 102, 127, 128, 132, 138, 195, 197, 198, 200, 203, 206, 207, 216, 218, 231, 232, 235, 243, 244, 247, 248
Static load, 147
steel, 30, 67, 71, 72, 73, 76, 148, 161
stock, 233
storage, 54, 68, 70, 71, 81, 82, 83, 117, 119, 196, 215, 217, 239, 246
stress, 147, 149, 154, 155, 156, 157, 159, 161
stroke, 181, 183
structural defects, 42
structure, 48, 57, 62, 63, 65, 89, 90, 108, 124, 151, 152, 153, 155, 159, 182, 199, 252
substrate, 30, 48, 53, 56, 58, 61, 62, 65, 66
succession, 16
sugar beet, 208
sugarcane, 239, 243
Sun, 3, 7, 8, 9, 10, 12, 15, 50, 69, 70, 82, 83, 182, 193, 224
sunlight, vii, 39, 40, 42, 45, 49, 54, 55, 56, 70, 73
Sunpath Diagram, 9, 10, 11, 35, 36
supplier, 5, 18, 238
supply chain, 245
surface area, 217
surface layer, 217
surface tension, 164
surplus, 46, 48, 54, 55, 250
survival, 226
sustainability, 225, 226, 239, 246, 254
sustainable development, vi, viii, 69, 113, 208, 220, 225, 227, 232, 239, 241, 248, 255, 256, 257, 259
sustainable economic growth, 252
sustainable energy, 36, 50, 98, 113, 114, 220, 221, 222, 223, 224, 226, 232, 239, 240, 241, 242, 249, 252, 253, 254, 255, 256
Sweden, 210, 223, 250
synthesis, 46

T

Taiwan, 217, 257
tar, 72, 76, 233
target, 58, 119, 219, 248
tariff, 245
Task Force, 256
tax incentive, 250
taxes, 250
technical assistance, 246
technical efficiency, 113
technician, 2, 240

techniques, 46, 58, 61, 88, 162, 178, 220, 240, 253
technological developments, vii, 244
technology, vii, 1, 2, 30, 31, 34, 39, 40, 42, 43, 45, 46, 47, 48, 49, 69, 83, 102, 103, 116, 117, 195, 196, 197, 198, 208, 210, 211, 213, 214, 215, 216, 217, 219, 220, 222, 225, 226, 227, 231, 232, 235, 239, 240, 241, 242, 244, 245, 251, 252, 253, 255, 256
technology transfer, 253, 255
temperature, viii, 5, 22, 23, 24, 25, 27, 28, 30, 33, 35, 41, 42, 57, 58, 66, 67, 68, 71, 73, 76, 77, 78, 79, 80, 86, 163, 165, 166, 167, 168, 169, 170, 172, 174, 175, 176, 177, 179, 180, 182, 183, 184, 186, 188, 195, 196, 197, 198, 199, 200, 201, 202, 206, 208, 209,210, 211, 213, 215, 217, 218, 221, 222, 223, 224
ternary blends, 166, 167, 168, 172, 179
test procedure, 184
testing, 22, 32, 67, 76, 93, 94, 105, 111, 245
texture, 53, 58, 61
thermal energy, 46, 70, 170, 195, 198, 211, 213, 216, 224
thermal stability, 53, 58, 66, 209
thermodynamic cycle, 197
Thin Film Cells, v, 28, 30, 31, 36, 53, 57, 58, 61, 63, 65
thin films, 30, 42, 54, 55, 56, 57, 58, 59, 60, 63, 65, 66
Third World, 37
tides, 241
Tilting Solar Modules, 14
time frame, 248
time series, 86, 98
tin, 55, 56, 57
tin oxide, 55, 56, 57
titanate, 47
tones, 234
total energy, 8, 182
tourism, 107
toxicity, 53, 58, 199
tracks, 14
training, 2, 89, 90, 91, 93, 94, 240, 252
transesterification, 164, 181, 182, 184, 208
transformation, 115, 119, 239
transient analysis, 116
transmission, 62, 119, 228, 231, 232, 246, 247, 251
transparency, 49, 56, 60
transparent conductive films, 53, 55, 56, 58, 66
transportation, 46, 68, 71, 164, 182, 196, 208, 239, 255
treatment, 57, 58, 212, 221
tunneling, 99
turbulence, 148, 152

U

uncoated engine, 181, 183, 185, 186, 187, 188, 189, 190, 191, 192
uniform, 81, 91, 94, 97
United Kingdom, 37, 82
United Nations, 240, 257
United States (USA), 5, 33, 68, 83, 215, 218, 233, 257, 259
urban, 161, 227, 242, 252
urbanization, 225
Uruguay, 250
USGS, 120, 122, 127, 141

V

vacuum, 42, 201
valence, 40
valve, 192
vapor, 199, 200, 202, 203, 205
variables, 87, 88, 115, 121, 122, 127, 128, 131, 132, 134, 135, 137, 138, 139, 140, 170
variations, 7, 19, 20, 115, 121, 126, 134, 152, 208
varieties, 80
VAT, 250
VAWT, 147, 148, 149, 162
vector, 86, 87, 88, 89, 90, 91, 98
vegetable oil, 164, 182, 193
vegetables, 69, 73, 81
vehicles, 182, 196
velocity, 86, 90, 91, 104, 105, 110, 114, 115, 119, 121, 122, 123, 125, 126, 127, 128, 132, 134, 135, 139, 140, 141, 142, 147, 153, 159
vibration, 219
viscosity, viii, 58, 163, 164, 165, 167, 168, 169, 170, 172, 174, 175, 176, 177, 178, 179, 180, 181, 182, 185, 187, 188, 189, 190, 191, 199, 202
vision, 248
voiding, 239
volatility, 181, 190

W

Washington, 37, 257
waste, viii, 175, 176, 177, 195, 196, 198, 207, 208, 211, 212, 213, 218, 219, 220, 221, 222, 223, 224, 234, 238, 242

waste heat, viii, 195, 196, 198, 207, 211, 212, 213, 218, 219, 220, 222, 223, 224
waste heat recovery, vi, viii, 195, 196, 198, 212, 218, 219, 220, 221, 222, 223
water, 3, 4, 41, 58, 68, 70, 181, 182, 183, 184, 186, 196, 197, 198, 199, 200, 202, 208, 210, 211, 213, 215, 217, 218, 221, 228, 235, 241, 242, 243
water shortages, 228
wavelengths, 46
weak grid, v, 115, 116, 119, 126, 135, 139, 145
welfare, 81, 241
wells, 213, 214, 219
West Africa, 22
Western Europe, 233
wide band gap, 56
Wind Energy Conversion System, 116, 144
wind farm, vii, 85, 86, 94, 96, 98, 101, 102, 103, 104, 105, 106, 107, 108, 109, 110, 111, 112, 113, 114, 236
wind power, v, vii, 85, 86, 87, 93, 94, 96, 97, 98, 104, 107, 119, 140, 144, 145, 236, 241, 242, 243, 245, 253
wind speed, 5, 86, 97, 98, 105, 111, 122, 126, 127, 147, 148, 151, 152, 153, 236, 242, 256
wind turbines, 86, 101, 102, 103, 107, 113, 114, 145, 148, 161, 162, 245
windows, 54, 56, 65
wood, 67, 69, 71, 72, 74, 75, 76, 208, 227, 228, 237, 238
wood waste, 208
working conditions, 200
World Bank, 2, 37, 232, 235, 237, 238, 243, 254, 257
World Health Organization WHO, 228, 232
worldwide, 5, 119, 227, 253

Y

yeast, 71
yield, 7, 14, 16, 45, 46, 123, 188, 235, 236

Z

zinc oxide, 56
ZnO, vii, 53, 57, 58, 64, 65, 66